Development of RNA silencing as a novel disease control strategy to protect pines from Dothistroma needle blight

A thesis presented in the partial fulfilment of the
requirements for the degree of
Master of Science (MSc)
in Genetics
at Massey University, Manawatu,
New Zealand

Ashleigh M. Mosen

2022

Abstract

Pinus radiata, the main commercial forest species grown in New Zealand, is one of many pine species worldwide that are susceptible to Dothistroma needle blight (DNB), caused by the fungus *Dothistroma septosporum*. New methods are needed to help manage and control this disease over current control measures such as fungicide spraying, pruning, and thinning. RNA silencing is a radical new approach to directly combat pathogens. Due to the success of many studies in controlling agricultural and horticultural crops, by exogenously applying dsRNA molecules targeting virulence genes, this has raised the question of whether forest pathogens can also be controlled with this method. RNA silencing has the potential to silence genes specific to a fungal pathogen, rendering it less virulent, and reducing disease symptoms on affected host plants. The aims of this work were to create an RNA spray targeting individual genes specific to *D. septosporum*, and to determine if spray applications of the RNA can reduce pathogen virulence and protect pines from fungal infection. As proof of concept, a spray application of a 737 nt *eGFP*-dsRNA was used to target an enhanced green fluorescent protein gene in *D. septosporum*. Also, 509 nt and 408 nt *DsAflR*-dsRNAs were synthesised targeting two different regions of the dothistromin pathway regulatory protein gene, named *DsAflR* 1-dsRNA and *DsAflR* 2-dsRNA. The *DsAflR* gene is involved in the production of the virulence factor dothistromin. All three dsRNAs were labelled with fluorescein to detect its uptake into cells, which was successful. RNA silencing was detected by reduced gene expression levels *in vitro* for samples treated with *DsAflR* 1-, *DsAflR* 2-dsRNA, as well as the RNAi control *eGFP*. There was a statistically significant reduction in *DsAflR* gene expression by applying *DsAflR* 1-dsRNA to *D. septosporum* grown on agar; however not all the reductions seen for treatment with each respective dsRNA were statistically significant and a lot of variability was observed between replicates. *In planta* silencing trials, in which pine shoots were treated with dsRNA and inoculated with *D. septosporum* spores, revealed reductions in fungal biomass in dsRNA treated samples in some cases, although more replicates are needed to confirm these results. Nevertheless this study has contributed new knowledge for the development of spray applications of dsRNA to reduce DNB disease. It provides a starting point for more research in controlling forest pathogens and could ultimately help to replace existing chemical-based forest management practices. Furthermore, the knowledge gained is applicable to a diverse

range of pathogens and plant hosts, for which this ground-breaking technology holds great promise.

Acknowledgements

The completion of my Master of Science degree would not have been possible without the help of my supervisors, post-docs and members of the plant pathology lab.

In particular, I would like to give a huge thank you to my main supervisor Professor Rosie Bradshaw for her ongoing support and encouragement throughout my studies. Her endless time and effort in helping me with my project has made a significant impact on the ability to finish my Masters degree. I really appreciated her constructive criticism and she played a major role in enabling me to make the best of every opportunity available. I cannot say thank you enough for all that she has done and pushed me out of my comfort zone. Not only is she a very down to earth person but she is a great supervisor who I could rely on and was always willing to help no matter how busy she was and in times where I was very stressed. Thank you for giving me the opportunity to give an oral presentation at the New Zealand Plant Protection Society (NZPPS) 2021 Conference to talk about my exciting project.

To Dr Carl Mesarich, I would like to thank him for all his help as my co-supervisor. In particular, for his input in troubleshooting with my experiments. It was not an easy journey, but he helped me take it one step at a time when things weren't working and provided alternative ideas to try to solve problems. Thank you for supporting me throughout my Masters and I appreciate you taking the time to provide feedback on my thesis.

To members of the plant pathology lab I thank all of you for your support and advice. It was a pleasure to work with all of you and you are a great bunch of people. To my lab mentor Melissa Guo, I thank you for your guidance and support in the lab. Your involvement in my project has made a significant difference. I have learnt so many valuable skills that I will take on board with me in my future career. Thank you for your assistance in lab experiments from the very beginning. Thank you Berit Hassing for joining in on my project later on in the second half of the year and for your patience in helping me with new techniques that I had never done before. Your input in providing alternative ideas was much appreciated. Thanks Hannah McCarthy for showing me

around the lab right from the beginning and for your technical advice along the way. Thank you also for helping with the pine shoot experiment.

To Raoul Solomon and Matthew Savoian (Manawatu Microscopy and Imaging Centre, Massey University), thank you for your help with training for confocal microscopy and Anja Schiemann for teaching me to use the lightcycler for quantitative Reverse Transcription Polymerase Chain Reaction (RT-PCR).

Special thanks to my family for supporting me throughout the course of my Masters degree and in particular for their financial support to even be able to do this course. Thank you for believing in me and giving me that extra push to carry on.

I'd like to acknowledge Massey University for giving me the opportunity to pursue my Masters and providing financial support with scholarships. This includes the Peter Densem Postgraduate Scholarship (2021) and the Massey University COVID-19 Master's Research Bursary (2021). In addition, I would like to thank the New Zealand Institute of Forestry (NZIF) and its foundation for awarding me the Frank Hutchinson Postgraduate Scholarship (2021), the NZPPS for a Research Scholarship (2021) and Rosie Bradshaw for her kind contribution. I would also like to thank Dr Richard Winkworth for taking me on as a Summer student as part of the Summer Scholarship in 2019 and Briana Nelson for mentoring me in the lab. I am very grateful for this amazing experience, as it was from then on that I decided I wanted to carry on with my studies.

Table of Contents

Abbreviations

A	Absorbance
A_{260}	Absorbance at 260 nanometer(s)
A_{280}	Absorbance at 280 nanometer(s)
aa	Amino acid
AB	Aniline blue
AF	Aflatoxin
AflR	Dothistromin pathway regulatory gene
AGO	Argonaute
AGO-PIWI	Argonaute - P-element induced wimpy testis
Amp	Ampicillin
Amp^R	Ampicillin resistant
BLAST	Basic local alignment search tool
BLASTn	Nucleotide database search using a nucleotide query
BLASTp	Protein database search using a protein query
bp	Base pair(s)
˚C	Degrees Celsius
cDNA	Complementary deoxyribonucleic acid
Cf	*Cladosporium fulvum*
cm	Centimetre(s)
CRISPR/Cas9	Clustered regularly interspaced short palindromic repeats and CRISPR-associated protein 9
Ct	Cycle threshold
CTAB	Cetyl trimethylammonium bromide
Cy3	Cyanine 3-UTP
d	Day(s)
DCL	Dicer-like protein(s)
DEPC	Diethylpyrocarbonate
ΔΔCt	Delta delta Ct
DM	Dothistroma medium
DNA	Deoxyribonucleic acid
DNase	Deoxyribonuclease

DNB	Dothistroma needle blight
dNTP	Deoxynucleotide triphosphate
DON	Deoxynivalenol
Ds	*Dothistroma septosporum*
DSM	Dothistroma Sporulation Medium
dsRNA	Double-stranded ribonucleotide
DUF	Domain of unknown function
EDTA	Ethylene diamine tetra-acetic acid
eGFP	Enhanced green fluorescent protein
EtOH	Ethanol
EVs	Extracellular vesicles
Ff	*Fulvia fulva*
FHB	Fusarium head blight
FPKM	Fragments per Kilobase of transcript per million mapped reads
g	Gram
gDNA	Genomic DNA
GFP	Green fluorescent protein
h	Hour(s)
HF	High fidelity
HIGS	Host-induced gene silencing
hph	Hygromycin resistance gene
IPTG	Isopropyl β- d-1-thiogalactopyranoside
JGI	Joint Genome Institute
kb	Kilobase pair
kV	Kilovolt(s)
L	Litre
L1	Linker motif 1
L2	Linker motif 2
LB	Lysogeny Broth
LDH	Layered double hydroxide clay nanosheets
M	Molar
Mb	Megabase
Mg	*Mycosphaerella graminicola*

mg/mL	Milligrams per millilitre
MID	Middle
min	Minute(s)
miRNA	Micro RNA
mL	Millilitre
mm	Millimetre
mM	Millimolar
MQ	MilliQ ultra-purified water
mRNA	Messenger RNA
NCBI	National Centre for Biotechnology Information
NEB	New England BioLabs Inc
ng	Nanogram(s)
nm	Nanometer
ng/µL	Nanogram per microlitre
NRPS	Non-ribosomal peptide synthase(s)
nt	Nucleotide(s)
Ω	Omega
OD	Optical density
OTEs	Off-target effects
p	Probability
PAZ	PIWI-Argonaute-Zwille
PCR	Polymerase chain reaction
PDA	Potato dextrose agar
1/2 x PDA	Half-strength potato dextrose agar
PDB	Potato dextrose broth
PEG	Polyethylene glycol
piRNAs	P-element induced wimpy testis (PIWI)-interacting RNAs
PIWI	P-element induced wimpy testis
PKS	Polyketide synthase(s)
PMMG	Pine Needle Minimal Medium with glucose
pmol	Picomole(s)
ppt	Precipitated

qPCR	Quantitative polymerase chain reaction
qRT-PCR	Quantitative reverse transcription polymerase chain reaction
RdRP	RNA-dependent RNA Polymerase
ref	Reference
RG	Regeneration media
RISC	RNA-induced silencing complex
RNA	Ribonucleic acid
RNAi	RNA interference
RNase	Ribonuclease
ROS	Reactive oxygen species
rpm	Revolutions per minute
RPMK	Reads per million per Kilobase
rSAP	Shrimp alkaline phosphatase
RT	Reverse transcriptase
$	Dollar(s)
SDS	Sodium dodecyl sulphate
sec	Second(s)
SIGS	Spray-induced gene silencing
siRNA	Small interfering RNA
SM	Secondary metabolite(s)
sRNA	Small non-coding ribonucleic acid
ssRNA	Single-stranded ribonucleic acid
tar	Target
TB	Trypan blue
µF	Microfarad
µL	Microliter(s)
µm	Micrometre(s)
µM	Micromolar
µg	Microgram
µg/mL	Microgram per millilitre
U/µL	Units per microlitre
UV	Ultraviolet

V	Volts
WA	Water agar
WT	Wildtype
w/v	Weight/volume ratio
χ^2	Chi-square
$\times g$	Times gravity
X-gal	5-bromo-4-chloro-3-indolyl-β-D-galactopyranoside
Zt	*Zymoseptoria tritici*

List of Figures

List of Tables

Chapter 1: Introduction

1.1 Forests and Forest health

Fungal pathogens pose a huge threat to plants worldwide, often resulting in detrimental effects, such as slower growth or death. In order to counteract pathogen attack an in-depth understanding of the interaction between fungal plant pathogens and their host plants is essential, as well as the development of new methods for better disease control for agricultural, horticultural and forest industries. Forests provide natural resources, such as wood and are vitally important for climate regulation, carbon storage (sequester carbon from the environment - carbon farming) and human health (Boyd et al., 2013). With the forestry industry being the third largest export sector in New Zealand (Goulding, 2016) forest resources provide a significant income of $44.8 billion per year (Rolando et al., 2016). *Pinus radiata* is the most planted commercial tree species in NZ forests. Of the species of trees planted globally, the most dominant species in planted forests in the tropics and Southern hemisphere are *Pinus*, *Eucalyptus* and *Acacia* (Brockerhoff et al., 2013). However, in countries such as Canada, native tree species are planted including *Picea*, *Pinus*, *Cunninghamia* and *Tectona.* These native tree species are typically planted due to their ability to grow under variable environmental conditions and are beneficial since they initially have a fast growth rate (Bauhus et al., 2010).

Plants are subjected to abiotic and biotic stresses, such as changes in temperature which coincide with the changing climate, making trees more susceptible to disease (Allen et al., 2015). This has led to elevated levels of stress and mortality in forest trees and will continue to affect the onset and progression of forest tree diseases caused by pathogens, as shown in the disease triangle modified by Hennon et al. (2020) (Figure 1.1). Increased temperatures are just one of the contributing factors to climate change, with the hottest decade reported worldwide from 2010 to 2019 (Kennedy et al., 2020). It has been reported from the 2015 Forest Resources Assessment (FRA) that 141.6 million hectares of forest land have been impacted by biotic and abiotic stresses in 75 countries from 2003 to 2012 (van Lierop et al., 2015). In fact, losses in forest area are expected to continue globally (Keenan et al., 2015), therefore a global strategy needs to be implemented to protect our forests and prevent exacerbation of disease. Solutions to manage and prevent plant pests and pathogens should be a priority as the “future of forests will be influenced by our ability to respond to damaging pests and the threat to biological invasions.” (Wingfield et

al., 2015). Novel approaches to manage forest diseases are likely to become even more important in the future. Due to the changing climate there may be more severe epidemics in the future, since climatic factors are key drivers of intensified invasions of pathogens. RNA silencing presents a completely novel strategy to control fungal plant pathogens in forests. However, in agricultural systems, RNA silencing is increasingly recognised as an alternative method to using conventional fungicides, and many studies have shown the effectiveness of this approach; for example, to control the broad host-range fungal pathogens *Sclerotinia sclerotiorum* and *Botrytis cinerea* (McLoughlin et al., 2018).

This thesis addresses RNA silencing as a potential solution to manage the forest pathogen *D. septosporum*. Although there are forestry practices employed to manage the spread and severity of Dothistroma needle blight (DNB), a foliar disease of pine (gymnosperm host) by the causal agent *D. septosporum,* there are still outbreaks worldwide.

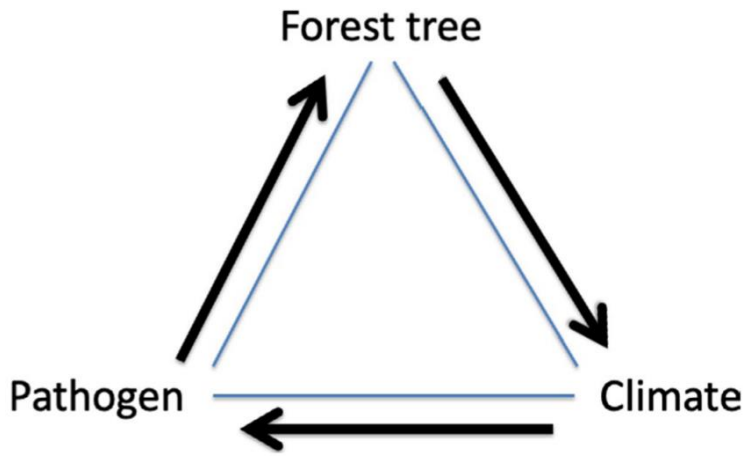

Figure 1.1 Disease triangle illustrating the effects climate change has on favouring pathogens and exacerbating diseases of forest trees. The links between climate, pathogens and forest trees are indicated. Figure adapted from Hennon et al. (2020).

1.1.1 Symptoms and incidence of Dothistroma needle blight disease

The incidence of DNB has increased in the Northern hemisphere since the 1970s (Drenkhan et al., 2016) and there have been serious outbreaks in Canada, UK and other parts of Europe (Bulman et al., 2016). Prior to the 1970s, the disease was prevalent in commercial pine plantations in the Southern hemisphere; for example, the disease was introduced into NZ in the early 1960s (Gilmour, 1967) and inhabits most of the country where suitable hosts are present (Bulman et al., 2004). *D. septosporum* infects over 70 species of pine (Bednářová et al., 2006; Drenkhan et al., 2016). *Dothistroma pini* is

another fungal species which also causes DNB (Barnes et al., 2004) in many pine species, but is not found so frequently as *D. septosporum* and is not present in NZ.

Symptoms of DNB begin with the appearance of yellow-brownish spots that develop into wider bands of brick-red necrotic lesions (Figure 1.2). The lesion colour is a result of the fungus producing a mycotoxin called dothistromin, which is a virulence factor (Kabir et al., 2015a) (see section 1.1.5), although mild disease symptoms are still caused in its absence. Within these red bands, black spots can be seen, which contain fruiting bodies comprising of asexual spores (Bradshaw, 2004). The symptoms of needle dieback generally start at the base of the crown of pine trees and radiate upwards to the top of the tree (Bulman et al., 2016). *D. septosporum* has detrimental effects on pine, killing needles and in severe cases resulting in tree death (Bradshaw, 2004; Gilmour, 1967). However, the severity of disease depends on factors such as host susceptibility, the inoculum level of the fungus, the age of the tree and climatic conditions (Brown & Webber, 2008; Woods et al., 2016). As a result of DNB disease, the growth of trees is affected and needle defoliation usually occurs within the months of September and October (Southern Spring), though on current foliage needle defoliation is prevalent in the warmer months of Summer.

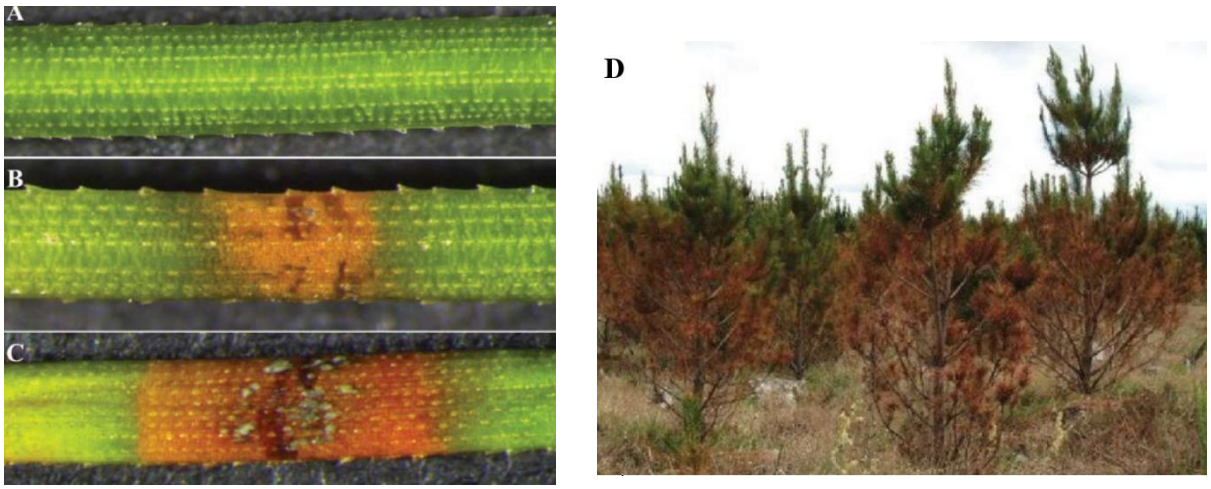

Figure 1.2. Symptoms of Dothistroma needle blight (DNB). (A) Pine needle not infected by *Dothistroma septosporum.* (B) Early symptom of DNB showing a lesion developing on an affected needle and the production of dothistromin. (C) Late stages of infection, indicating the presence of fruiting bodies within the lesion (Kabir et al., 2015b). (D) Dieback of needles in the lower parts of *Pinus radiata* trees. Adapted from Bulman et al. (2008).

1.1.2 Distribution of disease worldwide and species susceptible to disease

The geographic distribution of DNB disease is widespread, showing the capacity for *D. septosporum* to infect pine species in 76 countries (Drenkhan et al., 2016). DNB was first described in 1911 in Russia (Doroguine, 1911), but there were no further accounts of DNB until 1954 in Europe, (Murray & Batko, 1962) and 1955 in Serbia (Krstić, 1958). Throughout the 1960s to 1980s, DNB was reported in other countries within Europe (Figure 1.3), but it was not until the 1990s that there was a dramatic increase in DNB cases in European countries (Brown & Webber, 2008; Villebonne & Maugard, 1999). The disease is prevalent in North America (USA, Canada, Mexico and Jamaica), Central America and South America (Agrentina, Bolivia, Brazil, Chile, Colombia, Ecuador, Peru and Uruguay). DNB has also been reported in 57 African countries, including Ethiopia, Kenya, Malawi, South Africa, Swaziland, Tanzania, Uganda and Zambia. Since the 1960s the disease has also been reported in NZ, Australia and Papua New Guinea (Oceania). DNB is currently still a major problem worldwide, including in NZ (Bulman et al., 2013; Rodas et al., 2016).

A recent population genetics study investigating the origins of *D. septosporum* (Mullett et al., 2021) identified three pathogen clusters, mainly found in North America, Western Europe and Eastern Europe. Within the Eastern European cluster are various subclusters (North-eastern, Central European, Western Asian and Turkish) (Mullett et al., 2021). The North American cluster was genetically distinct and more restricted to certain geographic areas compared to the other clusters. The pathogen likely originated from a central point within North-eastern Europe and Western Asia. The authors proposed that a series of divergence events occurred with the oldest being the Turkish subcluster from the North-eastern European subcluster, and the most recent divergence events being the Central European cluster from the North-eastern European subcluster and then the Western European cluster (Mullett et al., 2021).

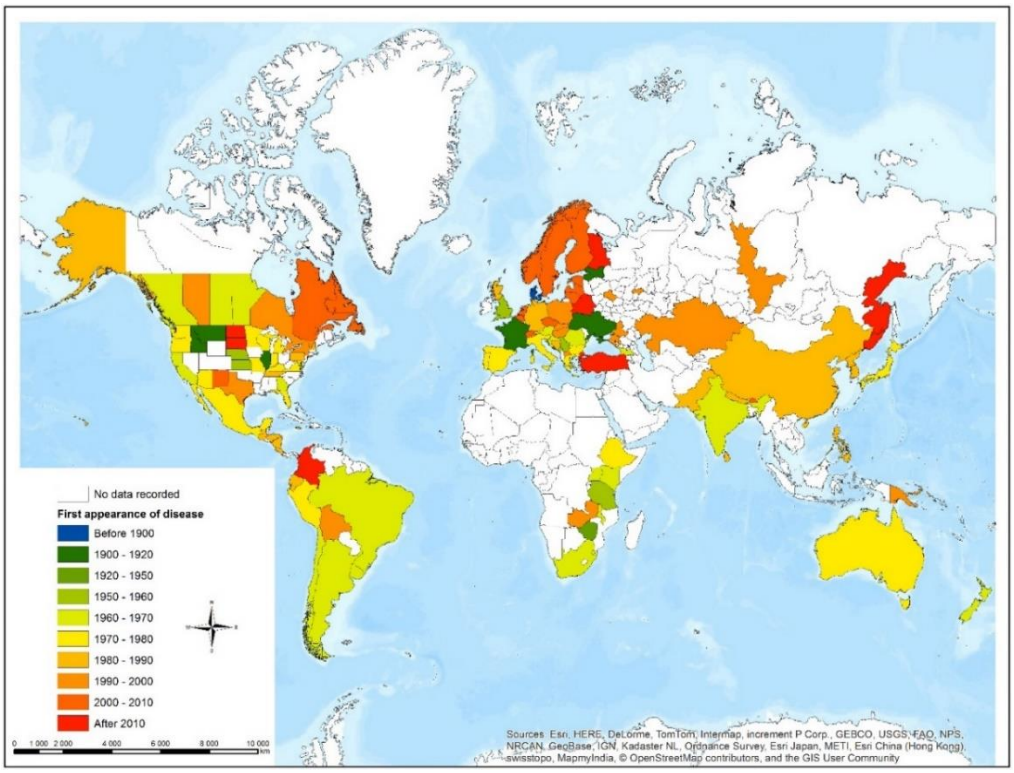

Figure 1.3. World map demonstrating where Dothistroma needle blight (DNB) disease has been reported. Dates of the first recorded appearance of the disease are indicated. Adapted from Drenkhan et al. (2016).

1.1.3 Epidemiology

D. septosporum is a fungus that belongs to the Ascomycetes and exhibits a hemibiotrophic lifestyle upon growth inside its host plant (Kabir et al., 2015b). This foliar pathogen first feeds off living plant tissue, as part of its biotrophic stage, and switches to killing its hosts plant cells in the necrotrophic stage. *D. septosporum* exhibits an asexual lifestyle, however its sexual stage has been reported in some parts of the world (Groenewald et al., 2007). Transmission of DNB disease occurs mainly by rain splash, whereby its spores travel via water droplets to infect other pines.

D. septosporum conidia (asexual spores) germinate on the leaf surface. It has been shown that within this early stage of infection, *D. septosporum* lives as an epiphyte, growing on the surface for a period of approximately two weeks in glasshouse conditions (Figure 1.4A) (Bradshaw et al., 2016; Kabir et al., 2015b). During this time there are no visible signs of damage to pine needles. Runner hyphae are able to penetrate through the host's stomata, leading to successful colonization of the apoplastic space (mesophyll) and eventually early lesion formation in the mid stage of infection (Figure 1.4B). After a few

weeks, *D. septosporum* generates conidia, which erupt from a mature lesion in the needle and initiate transmission of the disease to other pines, repeating the infection cycle (Muir & Cobb, 2005); this is classified as the late stage of infection (Figure 1.4C). The formation of a brown colour on needles is due to the accumulation of dothistromin and necrosis, whereby needles can drop prematurely (Edwards & Walker, 1978).

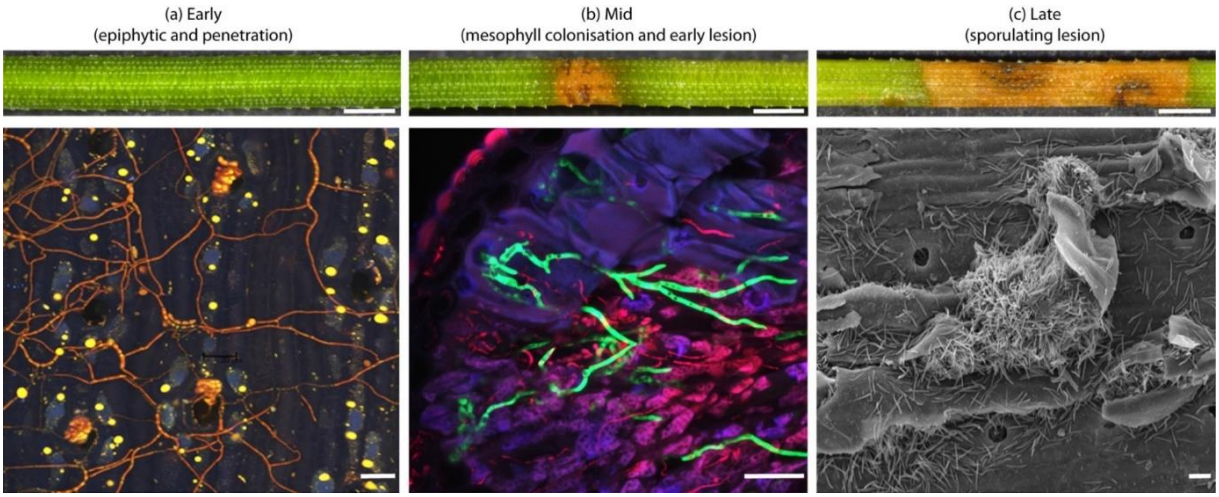

Figure 1.4. Stages of growth of *Dothistroma septosporum* in *Pinus radiata.* (A) Confocal microscopy: The early phase entails the fungal hyphae growing epiphytically, then penetrating through the stomatal pores. No symptoms or lesions are apparent on the needle. (B) Confocal microscopy cross-section of an infected needle: Mid stage of infection *in planta* showing colonization of the host mesophyll by a green fluorescent protein (GFP)-labelled strain of *D. septosporum* (Kabir et al., 2015b); at this stage lesions appear on the pine needle. (C) Scanning electron microscopy: Late stage of infection where fruiting bodies erupt through the mature lesion, allowing the dispersal of spores. Macroscopic (top) and microscopic (bottom) size bars are 1 mm and 20 μm, respectively (Bradshaw et al., 2016).

1.1.4 Dothistromin toxin

Dothistromin toxin, the virulence factor produced by *D. septosporum*, is a secondary metabolite (SM). Fungal SMs are natural products produced by fungi that can play specific roles in the lifestyle of the fungus, such as defence and development, as well as pathogen virulence (Ozturk et al., 2019). Fungi produce many different SMs and these differ with respect to the organism. SMs are classified into categories based on the properties of the core enzymes used for their biosynthesis. These include polyketides, non-ribosomal peptides, and terpenes. For example, polyketide synthases (PKS) and non-ribosomal peptide synthases (NRPS) function as modular enzymes, adding either Acyl-CoA units (PKS extender units) or amino acids (NRPS building blocks) respectively onto the growing chain to build a polymer, which is then modified by other enzymes

(Brakhage, 2013). Most SM genes are clustered (Keller, 2019), but some can have a more complex organisation (Chettri et al., 2013; Rokas et al., 2018).

D. septosporum produces the mycotoxin dothistromin, which is classified as a polyketide and is also a virulence factor. This broad-spectrum toxin is produced *in vitro* and *in planta* (Bassett & Buchanan, 1970). The chemical structure of dothistromin is similar to that of the aflatoxin (AF) precursor versicolorin B (Bradshaw, 2004) (Figure 1.5). Dothistromin plays an important role in DNB disease, as confirmed from studies with dothistromin deficient mutants defective in *PksA* (polyketide synthase) or *HexA* (fatty acid synthase) genes. These knockout mutants either showed no production or reduced levels of dothistromin. Further, there were reduced DNB symptoms on pine, suggesting lower pathogen virulence (Chettri et al., 2013; Kabir et al., 2015a).

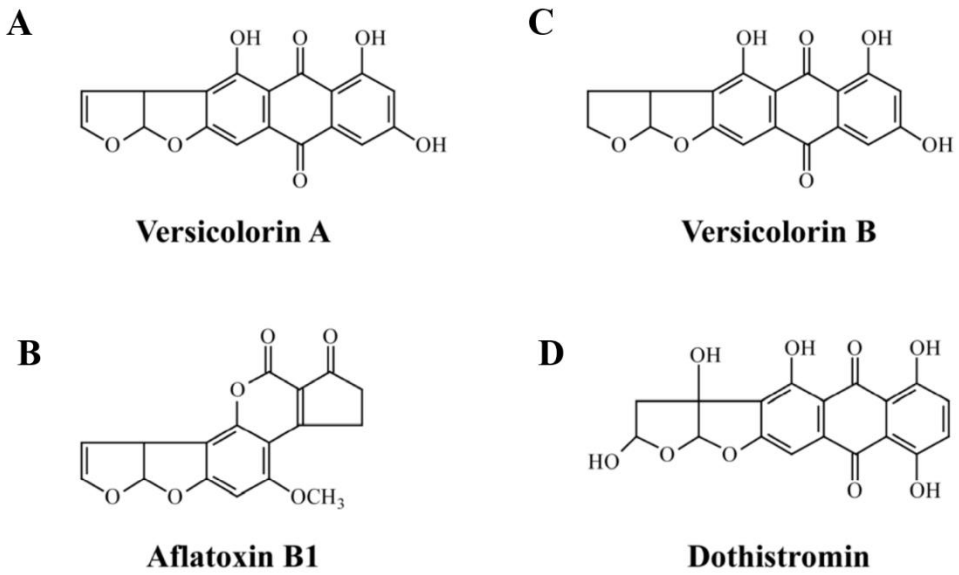

Figure 1.5. Structures of dothistromin and the related compounds versicolorin A/B and aflatoxin. (A) Veriscolorin A. (B) Aflatoxin B1. (C) Versicolorin B. (D) Dothistromin. All compounds show structural similarity. Adapted from Bradshaw (2004).

Despite fungal secondary metabolite genes usually having a clustered arrangement in a genome, genes involved in the synthesis of dothistromin are arranged at separate loci (six in total) on a 1.3-Mb chromosome (Chettri et al., 2013). One of these genes, *DsAflR* (dothistromin pathway regulatory gene), is a key regulator of dothistromin genes and affects the expression of other biosynthetic genes in the pathway; the majority of dothistromin biosynthetic genes are downregulated in *D. septosporum AflR* mutant strains

(Figure 1.6; Chettri et al. (2013)). Therefore, *DsAflR* could be a potential target for gene silencing, as silencing of this gene would be expected to reduce the production of dothistromin, and consequently decrease the virulence of the pathogen.

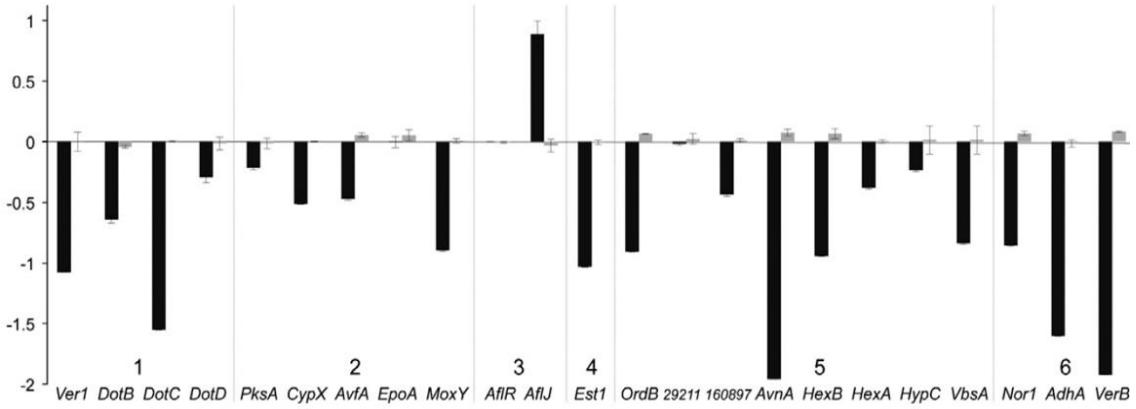

Figure 1.6. Quantitative real-time PCR (qRT-PCR) data indicating the expression of dothistromin genes in *Dothistroma septosporum AflR* (dothistromin pathway regulatory gene) knockout (KO) mutants *in vitro*. Expression data are shown as the $\log_{10}$ x-fold differences of each gene in an *DsAflR* KO mutant (KO1; black bars) and *DsAflR* complementation mutant (CO1; grey bars) compared to the wild type (WT). The numbers 1–6 located at the bottom of the graph indicate the locus number on chromosome 12. Adapted from Chettri et al. (2013).

1.1.5 Factors contributing to Dothistroma needle blight disease

Many factors contribute to the development of DNB disease. High humidity is a requirement for *D. septosporum* to penetrate the stomata and establish disease. Since *D. septosporum* relies on rain splash as its predominant mode of transmission to cause disease, long periods of dry weather can also limit the rate of infection (Gadgil, 1977). Humidity is correlated with temperature and rainfall, which also impact upon the dispersal of spores (Boateng & Lewis, 2015). A lower severity of disease is evident in regions with periods of dry weather, where the temperature is less favourable for *D. septosporum.* In addition, optimal conditions for severe infection include mild temperatures of 16–20˚C, high inoculum levels and a requirement for needles to be moist for over ten hours (Bulman, 1993). However, since DNB disease occurs across a selection of differing climates (tropical to subarctic) (Watt et al., 2009) *D. septosporum* is clearly capable of thriving in a variety of conditions.

In British Columbia (BC) Canada there have been DNB outbreaks since the 1830s (Welsh et al., 2009) and *D. septosporum* has more recently caused widespread damage and

mortality to entire *Pinus contorta* (lodgepole pine) plantations. Woods et al. (2005) distinguished trends in precipitation events, leading to the suggestion that a key driver of DNB epidemics in Canada is wetter summers, leading to increased severity of DNB disease. It has also been suggested that the increased occurrence of DNB disease outbreaks is linked to climate change and El Niño-Southern Oscillation (ENSO) events.

ENSO is a key driver of climatic factors, such as temperature and precipitation (droughts, floods, tropical cyclones), leading to variability in climate (Zebiak et al. (2014); Figure 1.6). Coexistence of El Nino events and DNB epidemics was thought to occur in the late 1990s. For example, around 1997/1998 there was an El Nino event (Cai et al., 2014), which occurred during the time of a major outbreak of DNB in Canada (Woods et al., 2005). Climatic factors, in particular El Niño events, leading to increased precipitation and temperatures, have ultimately affected certain stages of the life cycle of *D. septosporum*, such as those present in Figure 1.7, including spore release and dispersal, germination and infection. This, in turn, results in an increase in incidence and severity of disease.

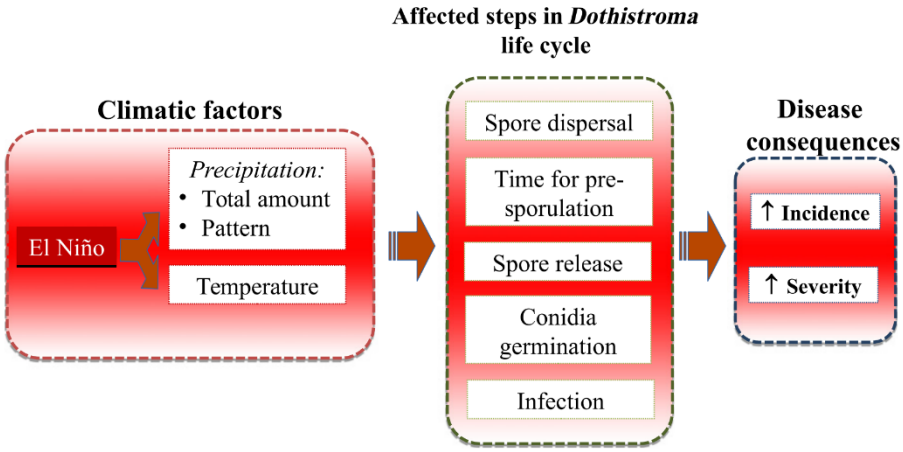

Figure 1.7. Climatic factors influencing the occurrence of Dothistroma needle blight (DNB) outbreaks, by affecting stages of the fungus throughout its life cycle. The increasing incidence and severity of DNB disease has been triggered as a response to climatic factors, such as increased periods of wetness and variable temperatures, which have impacted on the dispersal and germination of spores and hence infection levels. Adapted from Woods et al. (2016).

The choice of host species planted in commercial forests can also influence the disease outcome, as some species of pine have a higher degree of susceptibility to DNB compared

to other species. *P. radiata, Pinus attenuata* and *Pinus ponderosa* are highly susceptible to DNB, though with increasing age *P. radiata* can build up resistance. Pine species with low disease susceptibility include *Pinus patula*, *Pinus taeda* and *Pinus sylvestris* (Drenkhan et al., 2016).

1.1.6 Current DNB control strategies on pine

Current DNB disease management and preventative practices within the forestry industry are aimed at reducing disease levels either by silvicultural methods, chemical control by spraying with fungicides, biological control, or breeding pines with increased resistance to the pathogen. Although, these practices contribute to lowering the inoculum level and reducing the chances of neighbouring trees from being infected, there is a requirement to develop new control strategies to combat pathogen attack.

The spraying of copper fungicides is the predominant method of DNB control in NZ, although it is also employed in some other countries with DNB. Around 70,000 hectares are sprayed per year in NZ, although this only occurs every 2–3 years (Bulman et al., 2016). DNB surveys are completed every year to determine disease levels and to assess if spraying is required. Spraying takes place above Radiata pine forests using aircraft to distribute the fungicide (Bulman et al., 2004). The most effective time to spray is in late spring, when *D. septosporum* is about to begin its infection cycle (Bulman et al., 2004). Chemical control is an effective method of control, as copper acts by killing fungal spores (Bulman et al., 2013) and the copper residues persist on pine needles. This creates a protective barrier, inhibiting establishment of disease (Franich, 1988). In other countries a range of fungicides are used including Benlate (benomyl), Brestan (fentin acetate and maneb), Daconil 2787 (chlorothalonil) and Dyrene (anilazine) (Gibson, 1974). These were used primarily before the 1970s, before the production of more effective copper-based fungicide sprays: copper oxychloride and cuprous oxide (Bradshaw, 2004; Ray & Vanner, 1988).

Silvicultural practices, such as thinning and pruning, are also important in disease management and prevention schemes. Thinning is a forestry practice involving removal of some trees to accommodate areas for the remaining trees to grow and also has the effect of reducing levels of DNB disease (Bulman et al., 2013). Thinning increases air circulation, reducing moisture on foliage, and helps protect against infection from other

trees through wider spacing. Thinning has been successful in reducing the incidence of disease in some countries, such as Britain where copper fungicides are not used in forest areas (Bulman et al., 2016). Pruning involves the removal of heavily infected branches, allowing increased airflow, as well as reduced inoculum (Bulman et al., 2004). It can be effective in suppressing disease levels for one season (Bulman et al., 2008). While it may have some benefits, additional control measures may be needed.

D. septosporum can be controlled through breeding *P. radiata* for increased resistance to DNB disease. Breeding is likely to be successful in countries where there is a clonal population of the pathogen, such as in NZ, where the *D. septosporum* population is predominantly clonal and only one mating type is present (Barnes et al., 2014; Bradshaw et al., 2019). In NZ breeding efforts are centred at the Radiata Pine Breeding Co-operative (Jayawickrama & Carson, 2000). Resistance to DNB refers to pine species that have increased resistance or tolerance to infections caused by *D. septosporum.* The breeding process is costly and time consuming, since it takes seven years for *P. radiata* to reach sexual maturity (Bradshaw, 2004). However, the overall level of disease control likely to be achieved from breeding pines for increased resistance will be improved due to NZ having a relatively small pathogen population, due to the effectiveness of chemical control and also because of the increased tolerance of *P. radiata* to DNB after 15 years of age (Bulman et al., 2013).

Studies of the roles of pathogen effector proteins in plant-pathogen interactions hold great potential for characterising and identifying plant resistance genes for use in breeding programmes and some effector characterisation has been achieved in *D. septosporum* (Guo et al., 2020; Hunziker et al., 2021). Effectors are virulence factors produced by pathogens to allow colonization and growth inside the plant (Lo Presti et al., 2015; Rocafort et al., 2020). Plants can recognise pathogen effectors if they have corresponding immune receptors, with this recognition resulting in defence responses, such as the hypersensitive cell death response (HR) that renders the fungus avirulent (Spoel & Dong, 2012) and prevents the pathogen from growing within plant tissue (Heath, 2000). Plant breeding programmes could be advanced through the use of propagating plants with certain immune receptors, so that they are able to detect known core (conserved) effectors, leading to broad-spectrum resistance. For example, the core effector protein Ecp2-1 is conserved across multiple pathogens and has been identified in *D. septosporum,* where it

appears to play a role in restricting the growth of this pathogen in pine, possibly by eliciting plant defence (Guo et al., 2020). Other candidate *D. septosporum* effector proteins, such as Ds70057, Ds70694, Ds71487, Ds74283 and Ds131885 are able to cause a HR in the non-host plants *Nicotiana benthamiana* and/or *Nicotiana tabacum*, suggesting that they may be able to be recognised by immune receptors in these species. Of interest, one of these candidate effectors, Ds70057, was also able to elicit a HR in *P. radiata* and is a highly expressed candidate effector that is also upregulated during the mid and late stages of DNB disease *in planta* (Hunziker et al., 2021). This suggests that pine has an immune receptor corresponding to this effector, although *D. septosporum* could use the cell death associated with HR as a means of initiating a switch from biotrophy to necrotrophy. Due to this uncertainty, more research is required to answer these questions. It is likely that future outcomes of breeding will be facilitated from molecular studies, such as the identification and use of molecular markers associated with resistance, over traditional procedures such as selecting pines with phenotypic traits. One such study identified resistance genes under positive selection that may respond to *D. septosporum* effectors (Lu et al., 2021) and could have the potential to aid in the development of selective breeding.

Biological control is a potentially useful tactic to apply to the management of DNB disease. An *in vitro* study showed that some *Trichoderma* and *Bacillus* species inhibited growth and exhibited antagonistic activity towards *D. septosporum* (McDougal et al., 2011). In other studies the bacterium *Aneurinibacillus migulanus* was shown to lower the severity of DNB disease in *Pinus contorta* (Alenezi et al., 2016) and various fungal endophytes were tested as biocontrol agents in the pine host *P. ponderosa*. Of these, *Penicillium goetzii* significantly reduced disease severity, while *Bionectria ochroleuca*, *Elytroderma species*, *Hormonema dematioides*, and *Penicillium raistrickii* significantly increased disease severity (Ridout & Newcombe, 2015). Future studies need to be carried out to establish whether biocontrol of foliar pathogens is effective in the forest situation. Nevertheless, biological control has been shown to have some potential.

Despite utilising these disease control strategies to control or prevent DNB, *D. septosporum* continues to cause disease. The discovery of topical applications of RNA, as a tool for managing plant disease in agricultural and horticultural settings, could be a useful additional tool for controlling forest pathogens such as *D. septosporum*.

1.2 RNA silencing

RNA carries out many roles within cells. A major role of some types of RNA is to synthesise proteins from mRNA encoding genetic information, in the process of translation. There are three types of RNAs involved in translation, including messenger RNA (mRNA), ribosomal RNA (rRNA) and transfer RNA (tRNA). RNA also has structural, enzymatic, or regulatory roles. For example, RNA molecules can regulate gene expression to turn specific genes on or off as needed for many processes like development and cellular differentiation (Morris & Mattick, 2014). RNA silencing (also known as RNA interference - RNAi) is a mechanism of gene regulation at the post-transcriptional level, which deploys small non-coding RNAs (sRNAs) to instigate gene silencing. The three key classes of sRNAs are micro RNAs (miRNAs), small interfering RNAs (siRNAs) and P-element induced wimpy testis (PIWI)-interacting RNAs (piRNAs) (Burroughs et al., 2014).

1.2.1 Discovery of RNA silencing

The phenomenon of RNA silencing was revealed in the 1990s by molecular biologists, who introduced transgenes into organisms to overexpress certain genes. Instead of overexpression, genes were knocked down or silenced, preventing protein translation (Burroughs et al., 2014). In one of these studies, extra copies of the chalcone synthase (*CHS*) genes were introduced into petunia flowers via transformation to obtain purple petals (Napoli et al., 1990). The transgenes introduced targeting *CHS* genes were either in sense or antisense orientation. As a result, RNA silencing occurred in the central region of flowers, the abundance of *CHS* mRNA was reduced and pigmentation was completely or partially inhibited in some flowers. This was termed co-suppression or post-transcriptional gene silencing (PTGS) (Cogoni & Macino, 2000). Even though mRNA transcripts were synthesised via transcription of DNA to RNA, there was silencing of the target gene as mRNA transcripts were degraded (Hammond et al., 2001). Scientists later discovered that dsRNA (sense and antisense strands combined) was more efficient at blocking protein translation than single-stranded sense or antisense RNA (Fire et al., 1998). This was confirmed by testing RNAi in *Caenorhabditis elegans*. Antisense mRNA and dsRNA were injected into ovaries expressing *mex-3* mRNA, which is a gene encoding a KH domain (known to interact with RNA) that plays a role in blastomere identity in *C. elegans* embryos (Draper et al., 1996). An *in situ* hybridization study of cells treated with

dsRNA targeting the *mex-3* gene indicated that no *mex-3* mRNA could be detected, in contrast to the untreated or *mex-3* antisense mRNA-treated cells (Fire et al., 1998) (Figure 1.8D). RNAi can be also used to control fungi and was first discovered in 1992 in *Neurospora crassa,* when it was termed 'quelling' (Romano & Macino, 1992).

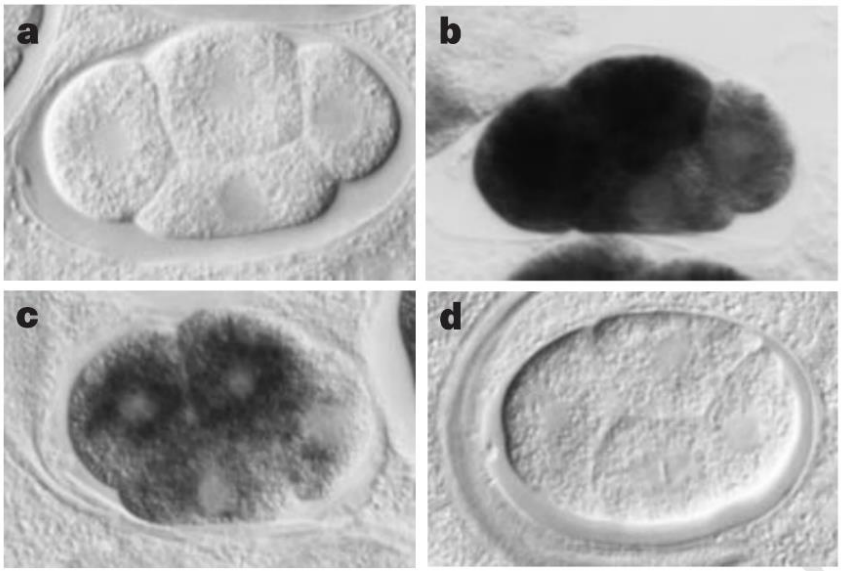

Figure 1.8. RNA interference (RNAi) in *Caenorhabditis elegans* embryos. All interference contrast micrographs shown captured *in situ* hybridisation in embryos. Antisense probes for the *mex-3A* portion of *mex-3* were used to assay distribution of the endogenous *mex-3* mRNA. (A) Embryo serving as a negative control in the absence of the hybridisation probe. No staining was observed. (B) Embryo showing normal distribution of endogenous *mex-3* mRNA (shown by the dark staining). (C) Embryo from a parent injected with *mex-3* antisense RNA, indicating the presence of *mex-3B* mRNA by the dark staining. There appears to be lower levels than wild type (WT). (D) Embryo from a parent injected with *mex-3B* dsRNA, depicting that there was no detection of *mex-3* RNA. Each embryo is approximately 50 µm in length. Adapted from Fire et al. (1998).

1.2.2 Mechanism and approaches to induce RNA interference (RNAi)

RNAi technologies use double-stranded RNA (dsRNA) molecules or hairpin RNAs (hpRNAs) to target and silence specific genes, for example pathogen genes that are important in causing disease. The mechanism involves the production of 21–24 nucleotide (nt) siRNAs from dsRNAs. This occurs in cells as a result of cleavage by RNase III-like enzymes called Dicer or Dicer-like proteins (DCLs). The siRNAs interact with Argonaute (AGO) in an RNA-induced silencing complex (RISC), which separates the sense and antisense strands. The antisense strand (guide strand) remains bound to AGO and binds with the target mRNA. This leads to cleavage of the mRNA, inducing gene silencing. RNA-dependent RNA Polymerases (RdRPs) are recruited by cells to

mediate amplification of the siRNAs (Majumdar et al., 2017) (Figure 1.9). Dicer and/or DCLs, AGO and RDRPs make up the components of the RNAi silencing machinery (Chapter 3, section 3.1).

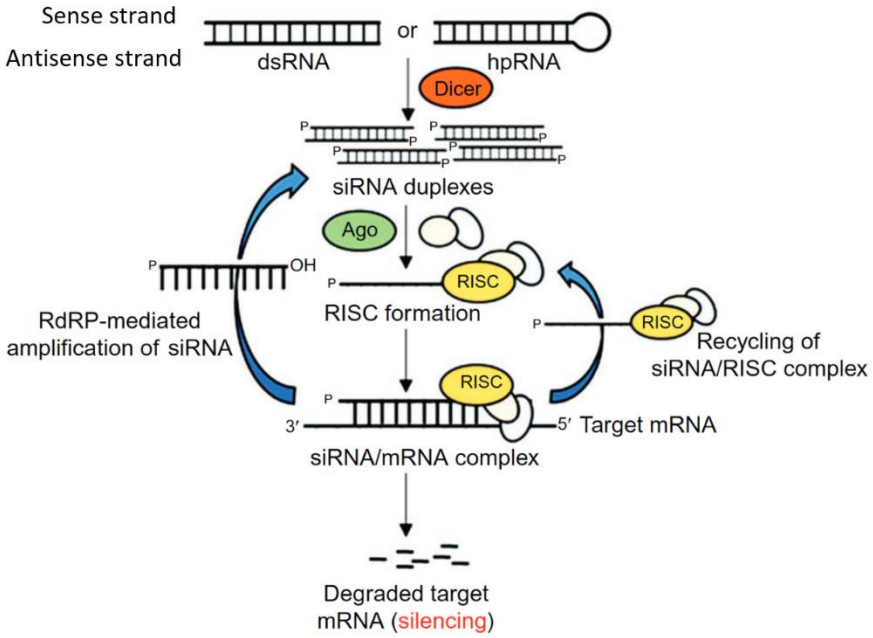

Figure 1.9. General mechanism of RNA silencing. Dicer processes double-stranded RNAs (dsRNAs) or hairpin RNAs (hpRNAs) into small interfering RNA (siRNA) duplexes. These associate with Argonaute (AGO) in an RNA-induced silencing complex (RISC), where the antisense strand RNA binds with AGO. The siRNA/RISC complex binds mRNA with a complementary sequence to the siRNA. The degraded target RNA is effectively silenced. There can also be recycling of the siRNA/RISC complex and RNA-dependent RNA Polymerase (RdRP)-mediated amplification of siRNA. Figure reproduced from Majumdar et al. (2017).

There are two types of RNAi-based approaches to achieve suppression of disease and plant protection: host-induced gene silencing (HIGS) and spray-induced gene silencing (SIGS) (Figure 1.7). HIGS generates transgenic plants that express dsRNAs that can, for example, silence genes within an invading pest or pathogen (insect pest, virus, oomycete, and/or fungal pathogen). HIGS is also used for producing plants with desired traits to enhance their resistance to pathogens, or for applications other than pathogen control. For example, HIGS has been used to study the role of cell wall-related genes, such as those involved in lignin biosynthesis (Wagner et al., 2007), by silencing an enzyme involved in the biosynthesis of methoxylated monolignols called hydroxycinnamoyl - CoA: shikima te hydroxycinnamoyltransferase (HCT) in *P. radiata*. SIGS involves the exogenous application of dsRNAs in the form of an RNA spray, which are taken up into cells. The latter approach eliminates the need to create transgenic plants (Machado et al., 2018).

HIGS and SIGS work in different ways (Figure 1.10). With HIGS, the dsRNAs are processed into siRNAs by the plant and these can be delivered into a fungal pathogen by extracellular vesicles (EVs) via the symplast (Höfle et al., 2020). Genetically modified plants, which express specific dsRNAs, designed to target a specific fungal gene characteristic to the pathogen, are processed into smaller sequences called siRNAs by the plants' DCLs. These siRNAs are responsible for degrading mRNAs within the fungal pathogen, reducing its ability to cause infection (Sang & Kim, 2020). The process of SIGS begins with direct spray application of the dsRNAs onto the plant, which are taken up into EVs in the apoplast and then into the fungus or into the plant itself, where *DCLs* work to chop up the dsRNAs to produce siRNAs (Höfle et al., 2020). Thus there are two different pathways - uptake of dsRNAs is either directly by the fungus itself, or indirectly by the plant before transportation into the fungus - which result in the same outcome, that is, blocking protein translation by reducing mRNA levels of target genes in comparison to endogenous expression (Sang & Kim, 2020).

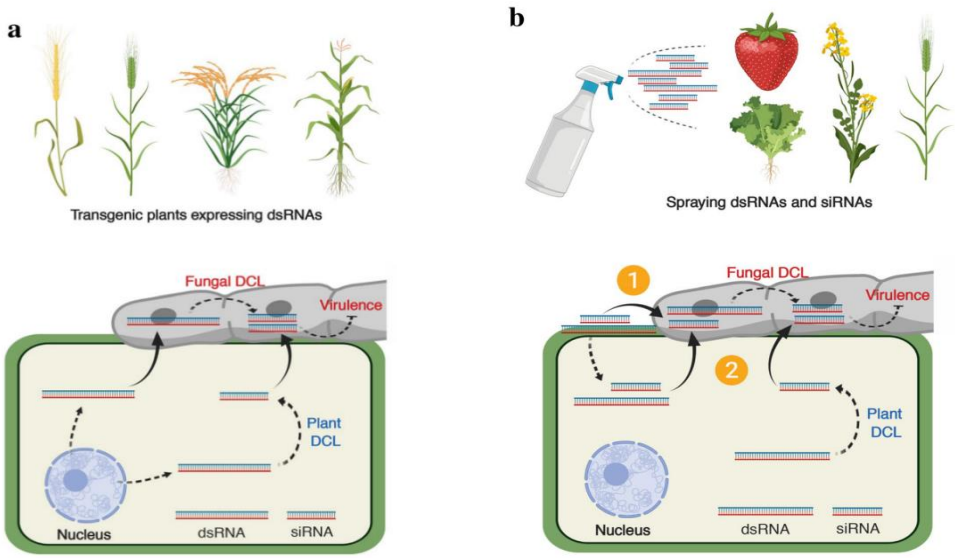

Figure 1.10. Mechanisms of host-induced gene silencing (HIGS) and spray-induced gene silencing (SIGS) to silence genes within fungal plant pathogens. (A) HIGS is where transgenic plants are generated which express sequence-specific double-stranded RNAs (dsRNAs) targeting specific genes, such as those in a fungal pathogen. The dsRNAs are cleaved into small interfering RNAs (siRNAs) by either plant Dicer-like proteins (DCLs) inside the plant or by fungal DCLs in the fungus. Then, these degrade pathogen mRNAs to counteract pathogen virulence. (B) SIGS: dsRNAs targeting pathogen genes are sprayed onto the surfaces of plants (e.g. Strawberry, lettuce, canola, and barley). The fungal pathogen can either directly take up the dsRNAs, or the host plant takes these up first before they or the siRNAs are transferred into the fungus to silence target genes (Sang & Kim, 2020).

1.2.3 Roles of RNA in communication between plants and fungi

Communication between plants and fungi is essential for cross-kingdom RNAi (or bidirectional cross-kingdom RNA trafficking), a mechanism referring to the transfer of siRNAs between pathogens and host plants. Plants can produce host-derived siRNAs, which are taken up by the pathogen from EVs. In turn, the pathogen can also produce siRNAs that can act as effectors to silence genes within the plant (Figure 1.11) (Huang et al., 2019). For example, the effector protein HopT1 from *Pseudomonas syringae* inhibits the activity of its host AGO1 protein (Navarro et al., 2008). It has been suggested that the movement of siRNAs occurs via EVs in the plant, or by transporters in the plasma membrane. However, many knowledge gaps still exist (Majumdar et al., 2017). HIGS and SIGS are relatively new technologies that have come about to control pathogens.

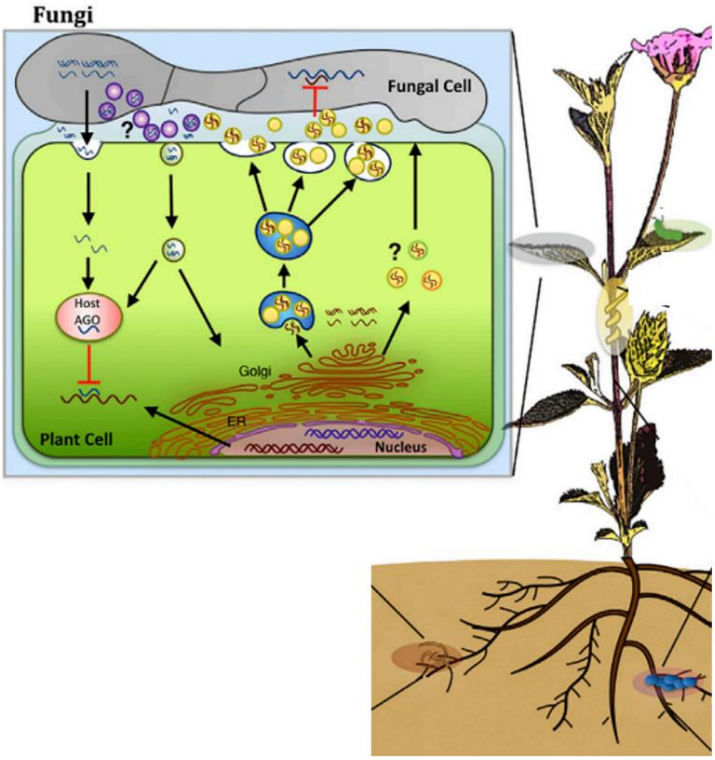

Figure 1.11. Representative schematic diagram of bidirectional RNA trafficking between plants and fungi. The transfer of small interfering RNAs (siRNAs) occurs across two cell types (plant and fungus). siRNAs derived from the host plant are transported into fungal pathogens in secreted extracellular vesicles (EVs) to aid in suppression of fungal virulence genes. siRNAs derived from the fungal pathogen can act as effectors to be transported into the host plant, whereby silencing of host defence genes can be exploited by the pathogen utilising the host Argonaute (AGO) protein, resulting in successful invasion by the fungal pathogen (Huang et al., 2019).

1.2.4 Applications of RNA silencing

RNA silencing technology has been utilised for studying gene functions, the roles of proteins, and their regulation in signalling pathways (Baulcombe, 2004). This molecular tool has also been used for breeding crops to increase nutritional value, through targeting specific metabolites (Koch & Kogel, 2014). RNA silencing has a diverse range of applications, like helping to provide solutions for individuals with food allergies or intolerances. For example, to produce crops that are hypoallergenic, or have reduced autoimmunogenic activity to help individuals with Coeliac disease to consume wheat (gluten)-containing foods (Wen et al., 2012). RNA silencing also has application in transgenic plants with increased resistance through HIGS against insects, nematodes, bacteria and fungi. External applications of RNA by SIGS have been shown to be effective in controlling a wide range of fungal-plant pathogens (Wang & Jin, 2017). There are advantages and disadvantages posed by both silencing technologies. A comparison of features characteristic to HIGS and SIGS is shown in Table 1.1.

Table 1.1. Comparison of features in both host-induced gene silencing (HIGS) and spray-induced gene silencing (SIGS) technologies.

Feature	HIGS[c]	SIGS[c]	Reference
Controls a wide range of fungi	✓	✓	Wang and Jin (2017)
Alternative to using fungicides	✓	✓	Machado et al. (2018)
Highly specific	✓	✓	Machado et al. (2018) Panwar et al. (2016)
Could be overcome by suppression	✓	✓	Machado et al. (2018)
Could provide effective postharvest control	×	✓	Machado et al. (2018)
Involves GMOs[a]	✓	×	Wang and Jin (2017)
Potential for off-target effects	✓	✓	Petrick et al. (2013) Machado et al. (2018)
Instability of RNA	✓	✓	Wang and Jin (2017) Dubelman et al. (2014)
High dsRNA production cost	✓	✓	Machado et al. (2018)
Lack of transformation protocols	✓	N/A	Wang and Jin (2017)
Environmentally friendly	×	✓	Wang and Jin (2017)
Doesn't produce heterologous proteins that could lead to concerns about allergies	×	✓	Machado et al. (2018)
RNAi[b] targets could have a few sequence mismatches and still be effective	✓	✓	Machado et al. (2018)

[a]GMOs = Genetically modified organisms.
[b]RNAi = RNA interference.
[c]Presence or absence of feature specific to HIGS or SIGS. NA = Not applicable.

1.2.5 Applications and examples of host-induced gene silencing (HIGS) to control pathogens

HIGS relies on the production of transgenic organisms and involves expression of hpRNAs or siRNAs (Machado et al., 2018). This RNA-based silencing technology has been successful in controlling many pathogens (Table 1.2). For example, in tobacco HIGS reduced the virulence of *Sclerotinia sclerotiorum,* through targeting the chitin synthase gene of this fungal pathogen (Andrade et al., 2016). Although HIGS may be an effective management strategy to control diseases, it has limitations. There is controversy over the use of genetically modified organisms (GMOs) as transgenic plants are generated. There are also technical limitations of the impact of RNA instability (Wang & Jin, 2017). Other disadvantages include not having transformation protocols for some crop species. HIGS may not be effective in controlling infections post-harvest. The reason for this could be due to limited cross kingdom trafficking of RNA between the plant and fungal pathogen, and low metabolic activities and/or fundamental processes occurring in the plant (Machado et al., 2018). Just as there is selection for resistance by adaptation in the population, allowing stronger individuals to survive (Lee et al., 2010), individuals within the population can also adapt and increase in abundance, so that they are no longer susceptible to HIGS. In this case, there would be strong selection of these individuals with the population, as a survival mechanism to counteract the effects of the silencing technology. Variation may already exist within the population, therefore HIGS may not be effective.

Advantages of HIGS include its high specificity and its potential to establish control, even when there are mismatches in the target sequence. HIGS can be tailored to control more than one pathogen, though careful design is essential to target multiple genes (Machado et al., 2018). A major concern associated with RNA silencing technologies is off-target effects (OTEs), which could have impacts on the host plant and beyond (Roberts et al., 2015). A solution to prevent OTEs is to target genes highly specific to the pathogen. If the targeted genes were similar to those in the plant host or other species, this could greatly impact on the yield or growth of the plant, or disturb the symbiotic balance with beneficial organisms like mycorrhizas, rhizobia and biocontrol species, like *Trichoderma* (Machado et al., 2018).

Pathogens may also acquire a suppression system which could hinder the effects of RNAi. This possibility has been studied in oomycete pathogens (Machado et al., 2018). For example, effector proteins secreted by *Phytophthora infestans* within host cells have been shown to suppress RNA silencing by inhibiting siRNAs produced by plant DCLs (Qiao et al., 2013). Additional research is necessary to investigate whether plant pathogenic fungi are also able to suppress RNAi, by a means of secretion of fungal effectors, or via another mechanism of action (Machado et al., 2018).

Table 1.2. Overview of host-induced gene silencing (HIGS) to control fungal and oomycete pathogens, viruses, and insects.

Fungal pathogen	Host plant	Target gene(s)	Target gene function	Conclusion	Reference
Aspergillus flavus	Maize	*AflR*	Transcription factor involved in aflatoxin biosynthetic pathway	Downregulation of *AflR*, accumulation of lower levels of aflatoxin	Masanga et al. (2015)
A. flavus	Maize	*AflC*	Polyketide synthase involved in aflatoxin biosynthetic pathway	No detection of aflatoxin – *AflC* was effectively silenced	Thakare et al. (2017)
A. flavus	Maize	*Amy1*	Alpha amylase	Reduction in gene expression, fungal colonisation, and aflatoxin production	Gilbert et al. (2018)
Blumeria graminis	Barley	*Avra10*	Avirulence effector protein	Reduced fungal development in the absence of the matching resistance gene *Mla10*	Nowara et al. (2010)
B. graminis f. sp. *hordei*	Barley	*BEC1005*, *BEC1011*, *BEC1016*, *BEC1018*, *BEC1019*, *BEC1038*, *BEC1040*, *BEC1054*	Glucanases, metalloproteases, ribonuclease-like proteins, unknown proteins	HIGS constructs for *BEC1011* and *BEC1054* caused the greatest effect on disease development (60 to 70% decrease)	Pliego et al. (2013)
Fusarium culmorum	Wheat	*FcFgl1*, *FcChsV*, *FcFmk1*, *FcGls1*	β-1,3-glucan synthase, myosin motor domain-containing chitin synthase V, mitogen-activated protein (MAP) kinase, glucan synthase 1	Reduced disease symptoms Enhanced resistance Hyphal cell wall defects	Chen et al. (2016)
Fusarium graminearum	Barley	*CYP51A*, *CYP51B*, *CYP51C*	Three paralogous *CYP51* genes (ergosterol biosynthesis genes)	Growth inhibition and altered fungal morphology	Koch et al. (2013)
F. graminearum	Wheat	*Chs3b*	Chitin synthase 3b	Conferred resistance to Fusarium head blight and Fusarium seedling blight	Cheng et al. (2015)
Fusarium oxysporum	Banana	*ERG11A*, *ERG11B*, *ERG11C*, *ERG6A*, *ERG6B*	Three paralogous *CYP51* genes (ergosterol biosynthesis genes); two C-24 sterol methyltransferase paralogs	Reduced transcript levels and disease symptoms	Dou et al. (2020)

Table 1.2. Continued.

Fungal pathogen	Host plant	Target gene(s)	Target gene function	Conclusion	Reference
Magnaporthe oryzae	Rice	*MoABC1*, *MoMAC1*, *MoPMK1*	ABC transporter, membrane-bound adenylate cyclase, mitogen-activated protein kinase	Inhibited disease development and reduced the transcription of targeted fungal genes	L. Zhu et al. (2017)
M. oryzae	Rice	*MoAP1*	Transcription factor	Inhibited fungal growth, abnormal spores, and decreased pathogenicity	Guo et al. (2019)
Puccinia striiformis f. sp. tritici	Wheat	*PsFUZ7*	MAPK kinase gene	Restricted hyphal development and strong resistance to *P. striiformis*	X. Zhu et al. (2017)
P. striiformis f. sp. tritici	Wheat	*PsCPK1*	Protein kinase A (PKA) catalytic subunit gene	Downregulation of *PsCPK* expression	Qi et al. (2018)
Puccinia triticina	Wheat	*PtMAPK1*, *PtCYC1*, *PtCNB*	MAP kinase, cyclophilin, calcineurin regulatory subunit	Suppressed disease phenotype and reduction in transcript levels	Panwar et al. (2013)
Verticillium dahliae	*Arabidopsis*, tomato	*Ave1*, *Sge1*, *NLP1*	Effector, transcription factor six gene expression 1, necrosis-and ethylene-inducing-like protein	Reduced Verticillium wilt disease in tomato (one out of three silencing constructs) and reduced disease in *Arabidopsis* (2 silencing constructs)	Song and Thomma (2018)
Oomycete					
Phytophthora infestans	Potato	*PiGPB1*, *PiCESA2*, *PiPEC*, *PiGAPDH*	G protein β-subunit,	Hairpin RNA targeting the PiGPB1 resulted in most restricted disease progress.	Jahan et al. (2015)
Insect					
Brown planthopper (BPH, *Nilaparvata lugens*)	Rice	*GST*	Glutathione S-transferase	Significantly retarded relative growth rate of the nymphs and the insect female fecundity. Plants also showed enhanced resistance when attacked by BPH	Yang et al. (2020)

Table 1.2. Continued

Virus	Host plant	Target gene(s)	Target gene function	Conclusion	Reference
Potato virus X (PVX) *Potato virus Y* (PVY) *Solanum tuberosum cv* (*Potato leaf roller virus*) (PLRV)	Potato	*ORF, HC-Pro, CP*	Open reading frame 2 Helper Component Protease gene Coat protein gene	20% of the transgenic plants were immune against all three viruses	Arif et al. (2012)
Cucumber vein yellowing virus (CVYV), *Melon necrotic spot virus* (MNSV), *Moroccan watermelon mosaic virus* (MWMV) and *Zucchini yellow mosaic virus* (ZYMV)	Melon	*Cm-eIF4E*	Eukaryotic translation initiation factors (eIF) of the 4E family	Decreased accumulation of *eIF4E* mRNA and resistance to four viruses	Rodriguez-Hernandez et al. (2012)
Rice gall dwarf virus (RGDV)	Rice	*Pns9*	Viroplasm matrix protein	Transgenic plants had strong and heritable resistance to RGDV infection and did not allow the propagation of RGDV	Shimizu et al. (2012)
Banana bunchy top virus (BBTV)	Banana	*Rep*	Replication initiation protein	Completely resistant to BBTV infection	Shekhawat et al. (2012)

1.2.6 Applications and examples of spray-induced gene silencing (SIGS) to control pathogens

SIGS is another RNAi method that can be used for disease control, which involves spraying plants with an RNA fungicide. The spray contains dsRNAs specific to the pathogen target mRNA (Machado et al., 2018). Studies have acknowledged the success of RNA silencing to control *B. cinerea* and *Fusarium graminearum* (Table 1.3). In *B. cinerea* dsRNAs were produced to target Dicer-like proteins 1 and 2 (*DCL1*/*2*). As a result, there were reduced disease symptoms (Wang et al., 2016). In another study, three cytochrome P450 lanosterol C-14-α-demethylase (*CYP51*) genes were targeted and silenced in *F. graminearum* and shown to be highly effective in protecting barley from

Fusarium head blight (FHB) (Koch et al., 2016). Together, these studies have shown the potential for SIGS in suppressing fungal plant diseases (McLoughlin et al., 2018).

SIGS is a sustainable and environmentally friendly approach to achieving crop protection. Like HIGS, it is also specific so that the dsRNA does not trigger silencing of unintended genes in other pathogens or plants (Machado et al., 2018). SIGS has been shown to be effective in controlling diseases in monocots and dicots (Huang et al., 2019). This strategy is powerful and fast, making it advantageous over other methods of disease control. Unlike fungicides, which have harmful effects on the environment, SIGS will not leave behind toxic residues (Wang & Jin, 2017). SIGS is also likely to be beneficial over HIGS to control infections post-harvest on fruits, leaves, dried seeds, or roots, although experiments need to be conducted to validate post-harvest control and determine the best time to spray (Machado et al., 2018; Majumdar et al., 2017). DsRNA can be taken up directly by the metabolically active pathogen or host plant, whereas there are limited opportunities for cross-kingdom tracking of RNA between two cell types (plant and pathogen) in HIGS and there is also not much activity occurring in the plant (Machado et al., 2018). SIGS could potentially be adapted to spray forests, forest nurseries, and *P. radiata* plantations in NZ and other countries to control DNB and other diseases.

Table 1.3. Overview of spray-induced gene silencing (SIGS) to control fungal pathogens, oomycetes, viruses, and insects.

Fungal pathogen	Host plant	Target gene(s)	Target gene function	Conclusion	Reference
Botrytis cinerea	*Arabidopsis*	*DCL1*	Dicer-like protein 1	Reduced virulence	Wang et al. (2016)
B. cinerea	Lettuce, tomato, strawberry	*DCL2*	Dicer-like protein 2	Reduced virulence	Wang et al. (2016)
B. cinerea	Tomato, strawberry, grape, lettuce, onion and rose	*DCL1*, *DCL2*	Dicer-like proteins 1 and 2	Reduced disease symptoms	Wang et al. (2016)
B. cinerea	*Brassica napus* (canola)	*BC1G_04955* (SS1G_11912 homologue), *BC1G_04775* (SS1G_06487 homologue), *BC1G_01592*, *BC1G_07805* (SS1G_07873 homologue), *BC1G_10306* (SS1G_11912 homologue) *BC1G_01592* (*SS1G_05899* homologue)	Peroxidase, mitochondrial import inner membrane translocase subunit (*TIM44*), pre-40S ribosomal particle, necrosis/ethylene inducing peptide 2	Reduced lesion size	McLoughlin et al. (2018)
Fusarium culmorum	-	*CYP51A*, *CYP51B*, *CYP51C*	Cytochrome P450 lanosterol C-14α-demethylase	Inhibited *F. culmorum* in *in vitro* cultures	Koch et al. (2018)
Fusarium graminearum	Barley	*CYP51A*, *CYP51B*, *CYP51C*	Cytochrome P450 lanosterol C-14α-demethylase	Reduced virulence	Koch et al. (2016)
Gfp-expressing *F. graminearum strain* Fg-IFA65$_{GFP}$	Barley	*Gfp*	Jelly fish green fluorescent protein	No fluorescence in mycelia	Koch et al. (2016)
F. graminearum Dcl-1 mutant Fg-IFA6$_{\Delta dcl\text{-}1}$	Barley	*DCL1*	Dicer-like protein	Heavily infected distal areas of barley leaves.	Koch et al. (2016)
Sclerotinia sclerotiorum	*Canola*	59 target genes including: *SS1G_05899*, *SS1G_07873*, *SS1G_09897*	Cell wall modification, mitochondria, ROS response, protein modification, pathogenicity factors, transcription, splicing, and translation	Significantly reduced fungal lesion formation	McLoughlin et al. (2018)

Table 1.3. Continued.

Insect pest	Host plant	Target gene(s)	Target gene function	Conclusion	Reference
Caterpillar	*Arabidopsis thaliana Solanum lycopersicum* (Tomato)	*DCL2*, *PolIV*	Dicer-like protein 2, polymerase	Showed inherited resistance over 2 generations through a mechanism of DNA methylation	Rasmann et al. (2012)
Caterpillar	*Arabidopsis* mutants defective in jasmonate perception or siRNA biogenesis	*COI1*, *DCL2*, *DCL3*, *DCL4*, *NRPD2A*, *NRPD2B*	Coronatine insensitive 1, dicer-like proteins, nuclear RNA, polymerase d2a, nuclear RNA Polymerase d2b	No inherited resistance	Rasmann et al. (2012)
Diabrotica virgifera virgifera LeConte (western corn rootworm)	Transgenic corn plants	-	Essential genes	Larval stunting and mortality, reduction in feeding damage	Baum et al. (2007)
Leptiotarsa decemlineata (Potato beetle)	*Solanum tuberosum* (Potato)	*actin*	Gene is important for cellular processes	Inhibited larval growth	San Miguel and Scott (2016)
L. decemlineata	Potato	V-ATPase A and V-ATPase E orthologs	Vacuolar-type H^+ ATPases	Larval mortality	Baum et al. (2007)
Schmidtea mediterranea (Planarian-flatworm)	-	astacin-like MP (B10), arrestin E30, H.108.3a	Metalloproteinases	Inhibited gene expression	Newmark et al. (2003)
Oomycete					
Hyaloperonospora arabidopsidis	*A. thaliana*	*CesA3*	Cellulose synthase A3	Suppressed infection	Bilir et al. (2019)
Virus					
Tobacco Mosaic Virus (TMV)	*Nicotiana tabacum L cv. Xanthi* (Tobacco)	*TMV p126*	Silencing suppressor and coat protein genes	50-65% resistance to virus	Konakalla et al. (2016)
Bacteria					
Erwinia amylovora	Apple	*DspE*-interacting kinases	Host enzymes	Resistance to infection	Boureau et al. (2006)

1.2.7 Uptake of dsRNA into fungal cells

For RNAi-based plant protection strategies to be successful in silencing fungal genes, uptake of the potent dsRNA molecule has to occur. It was shown that dsRNA uptake may occur at the tips of hyphae, where hyphal elongation occurs (Figure 1.12) (Wytinck, Manchur, et al., 2020). In this study (Wytinck, Manchur, et al., 2020), confocal imaging revealed accumulation of eGFP fluorescence at hyphal tips and it was shown that the region behind the hyphal tip displayed a greater reduction in eGFP fluorescence in an *eGFP*-expressing strain of *S. sclerotiorum.* This suggested that the hyphal tip could be the site for dsRNA uptake, or alternatively where dsRNA localises, to induce an RNAi effect (Wytinck, Manchur, et al., 2020). The region behind the hyphal tip is known as an endocytic collar, which acts to recycle excess membrane from exocytosis. As hyphae elongate to accommodate growth expansion of the fungal cell wall, it is easy for extracellular materials to come into contact with the endocytic collar. Among filamentous fungi, this region is where endocytosis occurs (Steinberg, 2014). The same authors (Wytinck, Manchur, et al., 2020) also demonstrated that the dsRNA uptake mechanism in *S. sclerotiorum* was through clathrin-mediated endocytosis (CME; Figure 1.12B) (Šečić & Kogel, 2021; Wytinck, Sullivan, et al., 2020). It is thought that the process of CME occurs in a similar way to in insects, where dsRNAs first bind to receptor proteins located on the cell surface and then interact with clathrin, as well as AP2, which is an adapter protein complex, to induce invagination of the membrane forming a vesicle. This vesicle matures into a late endosome where dsRNA is released to reach its destination in the cytoplasm to induce processing of the dsRNAs to be silenced (degraded). However, it remains unknown exactly when the dsRNA is released, and raises questions as to how it is moved throughout cells (Wytinck, Sullivan, et al., 2020). To validate whether CME participates in dsRNA uptake, the same authors Wytinck, Sullivan, et al. (2020) carried out *in vitro* liquid culture tests with dsRNA targeting *eGFP* in *S. sclerotiorum* and analysed whether dsRNA uptake occurred in hyphae in the presence of chlorpromazine, a chemical inhibitor of CME that "prevents the formation of clathrin-coated pits at the site of vesicle invagination by translocation of clathrin from the plasma membrane to intracellular vesicles" (Vercauteren et al., 2010). No reduction in *eGFP* fluorescence was observed, suggesting that dsRNA was not taken up, indicating a role for CME in dsRNA uptake in *S. sclerotiorum* (Wytinck, Sullivan, et al., 2020).

1.2.7.1 Mechanisms and barriers to overcome

Although dsRNA molecules need to be taken up into cells effectively, in order to achieve RNA silencing, there are many obstacles that need to be crossed, such as physical and biochemical barriers. Physical barriers are the requirement for dsRNA uptake through the hyphal cell wall and plasma membrane in fungi in the case of SIGS, where fungal or plant uptake can firstly take place, or if the dsRNA is taken up by the plant it has to pass through the waxy cuticle, cell wall and plasma membrane (Bennett et al., 2020). Biochemical barriers include nucleases (RNases), which have the ability to degrade dsRNA (Figure 1.12A).

The fungal cell wall is comprised of chitin, polysaccharides and glycoproteins, whereas the plasma membrane is comprised of lipids with proteins (Riquelme et al., 2018). In turn, the plant cell wall consists of cellulose, hemicelluloses, pectin and biopolymers, which act as a protective barrier (Bennett et al., 2020). The plant cuticle also acts as a barrier due to its waxy coated surface, which is a lipophilic film surrounding the epidermis of leaves. It plays a role in preventing dehydration of plant surfaces (Schreiber, 2005). High pressure spaying of dsRNAs has been implemented in studies to address the issue of absorption of dsRNA by the plant. For example, the effects of abrasion and flooding on movement of fluorescently labelled RNAs in *N. benthamiana* and tomato plants has been tested by Bennett et al. (2020) to determine if this improved penetration of the RNA through the plant cuticle. It was found that by spraying abrasive particles (<700 kPa), such as celite or alumina, in combination with the RNA or after application of the RNA, there appeared to be an improvement in RNA uptake.

RNA molecules need to be able to withstand degradation from potential extracellular nucleases, which presents as yet another barrier to suppression of fungal target genes using SIGS (Šečić & Kogel, 2021). dsRNA uptake can either be indirect (EVs) or direct (from the environment). The destination of dsRNA silencing within fungal hyphae is the cytoplasm, therefore it has to bypass the plasma membrane, either by CME or via EVs (Figure 1.11). The use of nanoparticles to protect dsRNA from being degraded has been studied and shown to improve the efficacy of dsRNA uptake (see Figure 1.12D).

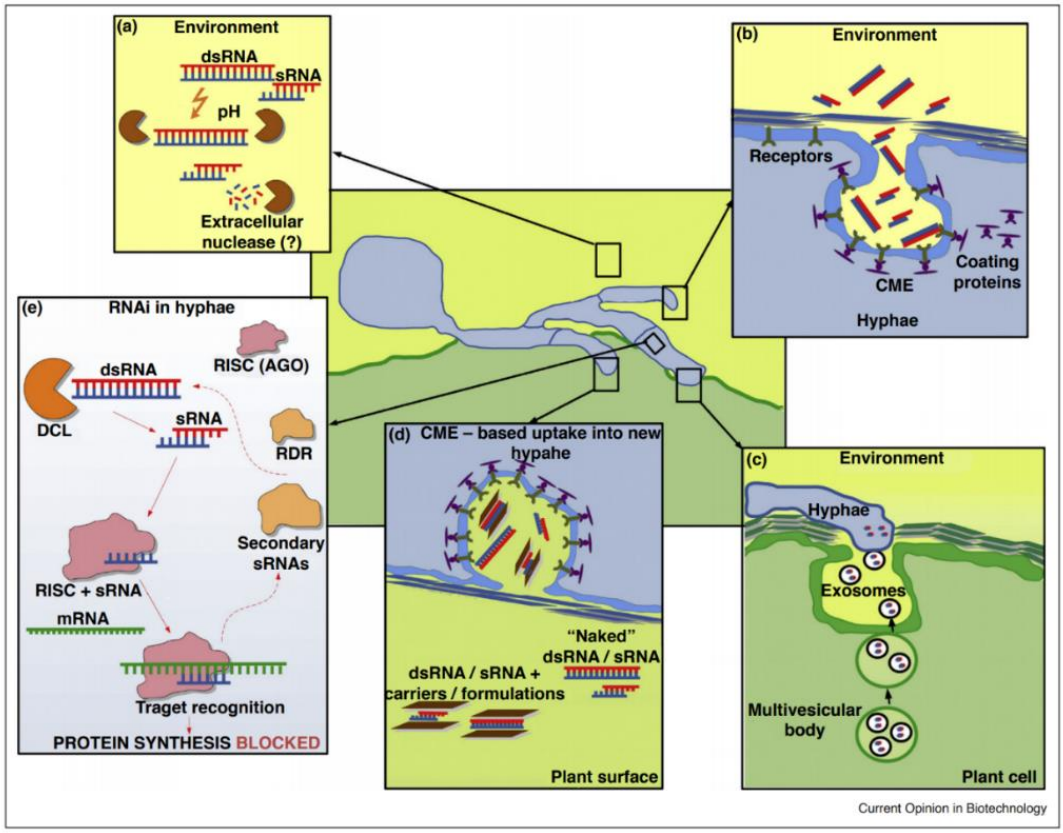

Figure 1.12. Diagram depicting the different ways for double-stranded RNA (dsRNA) to be taken up and their processing in fungi. There are a number of hurdles that must be overcome for successful delivery and processing of dsRNA. (A) Within the environment the dsRNA can potentially get degraded by extracellular nucleases, thus compromising its stability. (B) The dsRNA molecules have to be delivered into the cytoplasm either by clathrin-mediated uptake (CME) or (C) by extracellular vesicles (EVs) from plant cells to be delivered into the cytoplasm. (D) Formulations and carriers aim to increase the longevity and stability of dsRNA. (E) Finally the dsRNA must be processed by components of the RNA interference (RNAi) machinery, so that RNA silencing can be achieved. Image retrieved from Šečić and Kogel (2021).

1.3 Hypothesis, aims and objectives

The notion of RNA silencing to control fungal pathogens has been explored by plant biologists to counteract crop losses, but there has been very little focus on using this tool to control forest pathogens. Using *D. septosporum* as a model fungal pathogen that causes disease in pines, the focus of this project was to use SIGS to reduce the virulence of *D. septosporum* and lessen the effects of the disease when pine hosts are under attack. To address the potential for RNA-based silencing technology to attempt to control a forest pathogen, the following aims and objectives were pursued:

Hypothesis:

RNA silencing using exogenous spray applications of RNA can reduce the virulence of *D. septosporum* in infecting its host plant *P. radiata.*

Objective 1:

Identify the best pathogen target genes for RNA silencing trials.

This will be achieved by conducting an extensive literature search to help identify what genes have been successfully targeted and silenced in other fungal species, and to search for pathogen genes with predicted or known functions, such as virulence factors, in the *D. septosporum* genome. A list of candidate gene targets for *D. septosporum* will be generated and their *in planta* expression data will be assessed to help determine which genes would be ideal to target for RNAi. The candidate genes will be checked for the presence of OTEs in the *D. septosporum* genome and also other fungal species, using the *D. septosporum* target gene sequences as queries against other fungal species, to ensure specificity of the target sequence.

Objective 2:

Make RNA silencing constructs and dsRNA for each of the specific targets.

To facilitate the development of RNAi for controlling *D. septosporum* by SIGS, constructs will be generated by Polymerase Chain Reaction (PCR) amplification of the target genes *DsAflR* (dothistromin pathway regulatory protein) and *eGFP* (enhanced green fluorescent protein). The amplicons will be cloned in a plasmid vector and used as templates for dsRNA synthesis. The *eGFP*-dsRNA will serve as a control, as there will be a visual decrease in fluorescence if this gene has been silenced.

Objective 3:

Determine the effects of RNA silencing on *Dothistroma septosporum* gene expression *in vitro.*

To determine if the dsRNA is delivered into fungal cells, the dsRNA will be labelled with a fluorophore (Cy3; cyanine 3-UTP). Confocal microscopy analyses will be conducted to detect successful uptake of the labelled dsRNA. Once dsRNA uptake is established the effects of applying different concentrations of dsRNA to *D. septosporum* mycelium cultures will be trialled to optimise maximum knockdown of the target genes. The mRNA transcript levels of *DsAflR* and *eGFP* will be measured at different intervals post inoculation of dsRNA using qRT-PCR to analyse changes in mRNA transcript abundance between dsRNA-treated and untreated samples.

Objective 4:

Determine the effects of RNA silencing on *Dothistroma septosporum* gene expression and virulence *in planta* (*Pinus radiata*).

To further investigate the significance of silencing *DsAflR* and *eGFP, in planta* assays will be carried out in the host plant *P. radiata.* Disease symptoms will be monitored in combination with fungal biomass and target gene expression to determine if the pathogen shows reduced *DsAflR* or *eGFP* gene expression and supressed virulence.

Through performing research to investigate RNA silencing as a potential control measure for disease management and prevention, I aim to provide a starting point for further research so that RNA silencing can be adapted and optimised to field applications in the forest. This will be the first study to provide a blueprint for controlling other forest pathogens using SIGS technology.

Chapter 2: Materials and Methods

2.1 Biological material

All fungal and bacterial strains used in this study are listed in Table 2.1. Plasmid vectors are listed in Table 2.2.

2.1.1 *Escherichia coli*

The DH5α strain of *Escherichia coli* was used for the propagation and maintenance of plasmids.

2.1.2 *Dothistroma septosporum*

The NZE10 (ICMP 24376) isolate of *D. septosporum* from New Zealand was used for all fungus-related work in this study. The genome of this isolate has been sequenced (de Wit et al., 2012) and was annotated by the Joint Genome Institute (JGI). The genome sequence and gene/protein annotations were accessed through the JGI MycoCosm database (https://mycocosm.jgi.doe.gov/Dotse1/Dotse1.home.html).

2.1.3 *Pinus radiata*

Pinus radiata shoots were used as plant material in this study for *in planta* silencing trials. All shoots were obtained from Scion (Rotorua, New Zealand) and were clones of genotype S6 (Doth susceptible 6) produced by tissue culture. These clonal shoots without roots were grown from embryo cotyledon tissue under sterile conditions and maintained in glass jars containing LPch agar (LP medium containing 5g of activated charcoal) (Hargreaves & Reeves, 2014). Each jar contained seven microshoots (shoots 1–7), which served as replicate shoots in this study (Hargreaves & Reeves, 2014; Hunziker et al., 2021).

Table 2.1. Fungal and bacterial strains used in this study.

Biological material	Plasmid transformed	Relevant characteristics/genotype	Reference	Fluorescence[2]
Fungi				
Dothistroma septosporum NZE10	-	Wildtype New Zealand isolate (ICMP 24376)	de Wit et al. (2012)	N/A
FJT172 (transformant 1)	pPN82[1]	Constitutive eGFP-expressing *D. septosporum* NZE10	This study	Bright
FJT173 (transformant 2)	pPN82[1]	Constitutive eGFP-expressing *D. septosporum* NZE10	This study	Very bright
FJT174 (transformant 5)	pPN82[1]	Constitutive eGFP-expressing *D. septosporum* NZE10	This study	Bright
FJT175 (transformant 7)	pPN82[1]	Constitutive eGFP-expressing *D. septosporum* NZE10	This study	Very bright
FJT176 (transformant 8)	pPN82[1]	Constitutive eGFP-expressing *D. septosporum* NZE10	This study	Bright
FJT177 (transformant 10)	pPN82[1]	Constitutive eGFP-expressing *D. septosporum* NZE10	This study	Bright
Bacterium				
Escherichia coli DH5α	-	– φ80lacZΔ M15 Δ (*lacZYA-argF*) *U169 recA1 endA1 hsdR17* (rK– mK+) *phoA supE44* λ- *thi–1 gyrA96 relA1*	(Taylor et al., 1993); Invitrogen	N/A

N/A = not applicable.

[1]Plasmid containing the *eGFP* (enhanced green fluorescence protein)-encoding gene was prepared previously by Tanaka et al. (2006). See Appendix 7.5.2 for plasmid map (Figure A7.4).

[2]Based on the degree of fluorescence, transformants were grouped into two categories: very bright fluorescence and bright fluorescence. Transformants 2 and 7 were verified by polymerase chain reaction (PCR) to check the integration of the *eGFP* gene into the *D. septosporum* genome and were eGFP strains used for further experiments (Appendix section 7.6).

Table 2.2. Plasmid vectors used in this study.

Plasmid	Relevant characteristics/purpose	Selective antibiotic	Reference
pICH41021	pUC19 with *Bsa*I sites removed, Amp^R; *lacZ* complementation	Ampicillin	Kindly provided by S. Marillonet
pR239 (pPN82)	pBS EGFP *hph Pgpd*	Ampicillin	Tanaka et al. (2006)
pR223 (pBC-hygro)	Vector for fungal transformation; contains *hph* resistance gene	Hygromycin	Silar (1995)
pICH41021::*DsAflR* 1 sense	dsRNA construct for *DsAflR* 1 sense	Ampicillin	This study
pICH41021::*DsAflR* 1 antisense	dsRNA construct for *DsAflR* 1 antisense	Ampicillin	This study
pICH41021::*DsAflR* 2 sense	dsRNA construct for *DsAflR* 2 sense	Ampicillin	This study
pICH41021::*DsAflR* 2 antisense	dsRNA construct for *DsAflR* 2 antisense	Ampicillin	This study
pICH41021::*eGFP* sense	dsRNA construct for *eGFP* sense	Ampicillin	This study
pICH41021::*eGFP* antisense	dsRNA construct for *eGFP* antisense	Ampicillin	This study

Amp^R = resistance to ampicillin.
eGFP = enhanced green fluorescent protein gene.
Hph = hygromycin resistance gene.
DsAflR is a dothistromin pathway regulatory gene in *Dothistroma septosporum.*
Plasmid maps are located in Appendix 7.5.

2.2 Culturing *Dothistroma septosporum*

2.2.1 Growth on solid media

D. septosporum was routinely grown on either Dothistroma medium (DM), Dothistroma Sporulation Medium (DSM) or Pine Needle Minimal Medium with glucose (PMMG) (McDougal et al., 2011). Recipes for these media are in Appendix 7.1.1 and culturing took place in a Class II Biohazard cabinet (BH2000 Series, model BHA120). For point inoculations, a small piece of mycelium (4 mm x 4 mm) was taken from an actively growing edge of a colony using a sterilised scalpel and transferred to an agar plate. For spreading inoculum across agar plates containing a sterile cellophane membrane, a 4 mm plug of *D. septosporum* mycelium was ground with a sterile micropestle in 400 µL of MilliQ ultra-purified water (MQ), then 100 µL of ground mycelia were spread onto each plate. The plates were wrapped with Parafilm™ M (Bemis Neenah, WI) and incubated at 22˚C for 7–10 days (d). Strains were sub-cultured regularly every 3–4 weeks and plates were stored at 4˚C until required. For long term storage, glycerol stocks were made

containing small pieces of mycelium in 30% glycerol, snap frozen in liquid nitrogen and kept at -80˚C.

For growing *D. septosporum* spores from an e*GFP*-expressing transformant (FJT175), a 4 mm x 4 mm piece of mycelium was grown on DM as above. After 10 d of growth, ground mycelium was spread onto a DSM plate (Appendix 10.1.3) and grown for a further 10 d. Sterile MQ water (3 mL) was added to the agar plate and left to stand for 10 min. Spores were released by carefully scraping the surface of colonies using a sterile glass spreader and filtered through a nappy liner (Johnson and Johnson) into a sterile 15 mL Falcon tube (CELLSTAR®, Greiner bio-one). The spore suspension (200 µL) was spread onto PMMG plates (Appendix 10.1.4) and incubated for 9 d to obtain spores as above. The concentration of spores was determined using a haemocytometer (Weber Scientific, Middlesex England) and phase contrast polarised light microscope (Olympus CX41). The spore suspension was diluted to a final concentration of 5 x 10^6 spores/mL to use as inoculum for the *in planta* pathogenicity tests on pine shoots in glass jars (section 2.12).

2.2.2 Growth in liquid media

For growth of *D. septosporum* in liquid media, 100 µL of ground mycelium, prepared as in section 2.2.1, were inoculated into 125 mL flasks containing 25 mL of DM broth (Appendix 10.1.2), sealed with cotton wool and tinfoil. The mycelium was grown for 6–7 d on an orbital shaker (New Brunswick Scientific, NJ, USA) at 200 rpm (revolutions per minute) before harvesting. For the purposes of isolating RNA, the mycelium was harvested by filtration through a sterile nappy liner, weighed to give aliquots of approximately 0.5 g, wrapped in tinfoil and snap frozen in liquid nitrogen, then stored at -80˚C until required.

2.3 Culturing *Escherichia coli* and generation of competent cells

Cultures of *Escherichia coli* were grown overnight for 12–16 h at 37˚C on Lysogeny Broth (LB) agar medium (Appendix 10.2.1) or in LB broth (Appendix 10.2.2) with shaking at 220 rpm on a Classic series C10 platform shaker (New Brunswick Scientific) for the propagation of plasmids. For blue-white selection of recombinant plasmids on LB agar, ampicillin (Sigma Aldrich, Steinheim, Germany) was added at a final concentration of 100 µg/mL, Isopropyl β-d-1-thiogalactopyranoside (IPTG; inducer of β-galactosidase)

at 100 µM and 5-bromo-4-chloro-3-indolyl-β-D-galactopyranoside (X-gal; substrate for β-galactosidase) at 20 µg/mL.

Competent *E. coli* cells for transforming various constructs by electroporation were prepared as follows. DH5α cells from a glycerol stock were streaked onto an LB agar plate without antibiotics. The following day, a single colony was inoculated into 5 mL LB medium and incubated overnight at 37˚C on a platform shaker at 200 rpm. Then, two 2 L flasks, each containing 400 mL of LB medium, were inoculated with 5 mL of overnight culture, and incubated at 37˚C (at 200 rpm) until an optical density (OD_{600}) of between 0.65 and 0.75 was reached using an Amersham BioSciences Ultrospec 3100 pro Spectrophotometer. The cultures were then poured into 4 pre-cooled sterile 400 mL Centrifugation Polypropylene Bio bottles (Thermo Fisher Scientific, USA) and left on ice for 30–40 min. The cultures were collected by centrifugation at 5,000 rpm (4,696 × *g*) for 20 min at 4˚C in a Heraeus Megafuge 16R centrifuge (Thermo Fisher Scientific, USA). The supernatant was poured off and ~250 mL of ice-cold 10% glycerol was added to each centrifuge bottle. The cells were resuspended by gently swirling on ice, then four wash steps were performed. Firstly, the cells were collected by centrifugation at 5,000 rpm (4,696 × *g*) for 20 min at 4˚C, the supernatant poured off and glycerol added as before to resuspend the cells. These steps were repeated three times, except the centrifugation step was for 15 min instead of 20 min. After the last wash, the cell suspension was pooled into one bottle, collected by centrifugation again, the supernatant poured off and the cell pellet resuspended in 1 mL glycerol. Aliquots (50–100 µL) of the competent cells were transferred into pre-chilled sterile 0.6 mL tubes and snap frozen in liquid nitrogen, then stored at -80˚C until required.

2.4 Polymerase chain reaction (PCR)

2.4.1 Primers

PCR primers were designed using Geneious v9.1.8 software (https://www.geneious.com/) (Kearse et al., 2012) and synthesised by Integrated DNA Technologies (IDT; Coraville, IA, USA). Primer stocks were diluted to either 200 µM or 100 µM using sterile MQ water and stored at -20˚C, then further diluted to make 10 µM working stocks as needed. All primers used in this study are shown in Table 2.3.

2.4.2 Standard Polymerase Chain Reactions (PCRs)

PCRs were set up on ice in 0.2 mL PCR tubes (AXYGEN) and carried out in an Eppendorf Gradient Mastercycler® (Eppendorf, Hamburg, Germany). Standard PCRs were performed in 25 µL volumes, unless otherwise stated, with standard Taq DNA Polymerase (New England BioLabs Inc., USA) used as per the manufacturer's instructions. Plasmid or genomic DNA (gDNA; extracted as in section 2.5) was used as template DNA for PCR, diluted to 10 ng/µL, and 1µL was used in the reaction. An example of a reaction set up and PCR programme is shown in Table 2.4. The annealing temperature was optimised according to the melting temperature of the primers.

Table 2.3. Polymerase Chain Reaction (PCR) primers used in this study.

Type of primer	Lab ref	Primer/Probe Sequence (5'-3')	Product size (bp)
Colony PCR & sequencing			
M13 LacZ rev	27	GCGGATAACAATTTCACACAGG	
M13 LacZ fwd	28	GCCAGGGTTTTCCCAGTCACGA	Various[1]
dsRNA synthesis			
DsAflR - RNAi-1-For1*	2268	TAATACGACTCACTATAGGGAGACGGACGGACT TCGCACGCCAC	509
DsAflR - RNAi-1-Rev1*	2269	CCCATGTCGGACACCGAGG	
DsAflR - RNAi-1-For2*	2270	TAATACGACTCACTATAGGGAGACCCATGTCGG ACACCGAGGTG	509
DsAflR - RNAi-1-Rev2*	2271	CGGACGGACTTCGCACGCCAC	
DsAflR - RNAi-2-For1*	2272	TAATACGACTCACTATAGGGAGACAAACATCGA TTTGTCAATG	408
DsAflR - RNAi-2-Rev1*	2273	GTGCGGCTGCGAGGTCGACC	
DsAflR - RNAi-2-For2*	2274	TAATACGACTCACTATAGGGAGAGTGCGGCTGC GAGGTCGAC	408
DsAflR - RNAi-2-Rev2*	2275	CAAACATCGATTTGTCAATGACC	
T7_eGFP_fwd_sense_AM*	2347	TAATACGACTCACTATAGGGAGAGTGAGCAAGG GCGAGGAGCTG	737
eGFP_rev_sense_AM*	2348	CTTGTACAGCTCGTCCATGCC	
T7_eGFP_fwd_anti_AM*	2349	TAATACGACTCACTATAGGGAGACTTGTACAGC TCGTCCATGCC	737
eGFP_rev_anti_AM*	2350	GTGAGCAAGGGCGAGGAGCTG	
Amplifying fragment for RNAi[3]			
pICH41021_backbone_rev_XbaI	2353	AGTCGACCTGCAGGCATGCAAG	
pICH41021_backbone_fwd_SacI	2354	CGAATTCACTGGCCGTCG	Various[2]
Verification of *GFP*			
GFP GG for	1952	GGTCTCGTTCGGAATGGTGAGCAAGGGCGAGGA	
GFP GG rev	1953	GGTCTCAAAGCTTACTTGTACAGCTCGTCCATGC	720
qRT-PCR[4]			
Gfp_F_exp1	2399	CGACAACCACTACCTGAGCA	82
Gfp_R_exp1	2400	GAACTCCAGCAGGACCATGT	
AflR_F_exp1	2401	ACAAGTCGACGAGCTTCTGG	94
AflR_R_exp1	2402	TGCTGCATTTCACCTTCGATG	
TEF1_F_exp3	2450	CGTGACATGAGACAGACCG	102
TEF1_R_exp3	2451	CTTGGCAGCCTTGACGG	
Dicer_F_exp1	2437	CAAGAACCCGCGAGAGTACC	87
Dicer_R_exp1	2438	TTGCCAGATCCAGTGTCGAG	
qPCR[5]			
pksA64	2458	CTGTCTTCCTCGACCTGTT	102
pksA164	2459	AAGCACACCTGGAAAGAATGA	
CAD918	2462	CAGCAAGAGGATTTGGACCTA	101
CAD1019	2463	TTCAATACCCACATCTGATCAAC	

T7 promoter sequences are underlined.

*All primers used for amplifying the RNAi fragment to be cloned in the pICH41021 vector were phosphorylated at the 5'-end.

[1]See section 2.9.6 for sizes of PCR products.

[2]See section 2.10.1 for sizes of PCR products.

[3]RNAi = RNA interference.

[4]qRT-PCR = Quantitative Reverse Transcription Polymerase Chain Reaction.

[5]qPCR = Quantitative Polymerase Chain Reaction.

Table 2.4. Example of a standard Polymerase Chain Reaction (PCR) setup and cycling conditions.

Component	25 µL reaction	Final concentration
10X Standard Taq reaction buffer	2.5 µL	1X
10 mM dNTPs	0.5 µL	200 µM
10 µM forward primer	0.5 µL	0.2 µM
10 µM reverse primer	0.5 µL	0.2 µM
Template DNA	1 µL	10 ng
Taq DNA Polymerase	0.125 µL	1.25 units/50 µl PCR
MQ water	19.875 µL	-

Cycle step	Temp	Time	Cycles
Initial denaturation	95˚C	5 mins	1
Denaturation	95˚C	30 sec	
Annealing	45-68˚C	60 sec	30
Extension	68˚C	1 min/kb	
Final extension	68˚C	5 min	1
	4˚C	hold	

2.4.3 High fidelity Polymerase Chain Reaction (PCR)

For amplifying DNA inserts for cloning into plasmid vectors, a high fidelity (HF) DNA Polymerase enzyme (Phusion HF DNA Polymerase; NEB) was used to facilitate amplification with few sequence errors. PCRs were performed as per the manufacturer's instructions (refer to section 2.9.2 for reaction setup).

2.4.4 Colony Polymerase Chain Reaction (PCR)

For *E. coli* colony PCR analyses (section 2.9.6), small samples of cells from the transformants were added directly to the PCR by touching a single colony with a sterile pipette tip and transferring to a PCR tube. Standard PCR was carried out, except an initial heating step for 5 min at 95˚C was used to release plasmid DNA from the cell, serving as a template for the amplification reaction.

2.4.5 Agarose gel electrophoresis

PCR products were resolved on 0.8–1.5% agarose gels (Gold Bio, St Louis, USA; Appendix 7.3.1) at 80-100 Volts (V) until the loading dye (Appendix 7.3.1) had migrated about 3/4 of the length of the gel. A small volume (2 µL) of a 1 kb plus DNA size marker (NEB) was run in a single lane on the gel to determine the size of PCR products. DNA in the gels was stained with ethidium bromide (10 mg/mL) for 15 min on an orbital shaker

(Orbit LS Labnet) at 85 rpm and gels were then transferred to a Universal Hood IITM (Bio-Rad, USA) for UV visualization and imaging. Gel photos were processed using Image Lab™ software.

2.4.6 Purification of DNA from agarose gels

In cases where multiple PCR amplicons were obtained on agarose gels, the required bands were cut from the gel using a scalpel on a Dark Reader transilluminator (Clare Chemical Research) and transferred to a sterile microcentrifuge tube. The DNA was purified using a QIAquick Gel Extraction Kit (Qiagen, Hilden, Germany) according to the manufacturer's instructions. In contrast, where single PCR amplicons were obtained, the DNA was purified using Sepharose™ (Sigma-Aldrich, Steinheim, Germany), especially for those subjected to cloning in plasmid vectors (section 2.9).

2.5 Isolation of genomic DNA (gDNA) from *Dothistroma septosporum* and *Pinus radiata*

A cetyltrimethylammonium bromide (CTAB) method (Doyle & Doyle, 1987) was used for extracting gDNA from *D. septosporum* with a few alterations. Fungal cultures were grown on DM agar plates containing a layer of sterile cellophane for 10 d at 22˚C. The mycelium was transferred to a sterile 1.5 mL tube and ground with a micro-pestle. However, for isolating high quality gDNA, grinding mycelium in a mortar and pestle with liquid nitrogen was required. To each of the samples, 600 µL of 2% CTAB (Appendix 7.2.2) and 2 µL of RNase (20 mg/ml) were added, mixed by inversion, then incubated for 10 min at 37˚C in an ACCUBLOCK digital dry bath (Labnet International Inc), followed by a further 30–40 min at 65˚C. After cooling the samples to room temperature, 600 µL of chloroform was added and mixed to help separate proteins from the DNA and allow for separation of cellular components into aqueous and organic phases. The tubes were centrifuged for 5 min at 13,000 rpm (16,249 × *g*) in a Heraeus Biofuge Pico benchtop microcentrifuge and the aqueous phase that contained gDNA was transferred to a new sterile tube. To obtain cleaner gDNA, another 600 µL of chloroform was added and the extraction repeated. To each tube, 600 µL of isopropanol was added, mixed and left for 20 min in the -20˚C freezer. After a brief spin at 8,500 rpm (6,947 × *g*) for 5 min to pellet the precipitated DNA, the isopropanol was decanted off. To wash the gDNA, 600 µL of cold 70% ethanol was added, and the gDNA collected by centrifugation at 8,500 rpm

(6,947 × *g*) for 5 min, decanted and repeated a further time. Traces of ethanol were removed, and the DNA pellet left to air-dry in a TPE Labrocare® Fume Cupboard for 10-15 min. Finally, the DNA was resuspended in 50 µL of TE buffer (Appendix 7.2.2).

For extracting gDNA from infected *P. radiata* needles and whole shoots, the above protocol was followed using pine needle tissue ground in a sterile mortar and pestle. An extra step was included after the first chloroform step, which was the addition of 100 µL of a 1:1 ratio of phenol chloroform. The sample was centrifuged in a in a Heraeus Biofuge Pico benchtop microcentrifuge at 13,000 rpm (16,249 × *g*) for 5 min, then the aqueous phase transferred to a new tube and a further 100 µL of chloroform added as above. After centrifuging and transfer of the aqueous phase, the rest of the Doyle and Doyle (1987) procedure was followed, beginning with the addition of isopropanol.

2.5.1 Quantification of DNA

DNA concentration and quality were determined using a Nanodrop™ (DeNovix DS-11, Thermo Fisher Scientific, USA). The requirements for high quality DNA were that the absorbance ratio at 260 nm and 230 nm (A260:A230) should be ≥ 1.8 and the absorbance ratio at 260 nm and 280 nm (A260:A280) ≥ 1.5. Either MQ water or the buffer used to elute the DNA was used to blank the spectrophotometer before measuring.

2.6 Isolation of RNA and quantitative Reverse Transcription Polymerase Chain Reaction (qRT-PCR)

2.6.1 Isolation of RNA from *Dothistroma septosporum* NZE10 and eGFP strains

High quality RNA was extracted for qRT-PCR to assess relative changes in mRNA transcript levels of the target genes after addition of the dsRNA. TRIzol reagent (Invitrogen, Carlsbad, CA, USA) was used to isolate RNA from *D. septosporum* mycelium (Chomczynski & Sacchi, 1987). Mycelia were harvested and snap frozen in liquid nitrogen (as in section 2.2.2), then ground to a fine powder in a mortar and pestle using liquid nitrogen in a TPE Labrocare® Fume Cupboard. After, 2 mL of TRIzol was added, mixed to form a paste and thawed before transferring to an RNase-free 2 mL microcentrifuge tube (AXYGEN). The samples were centrifuged at 3,500 × *g* for 10 min

at 4˚C in a Heraeus Megafuge 16R centrifuge. The supernatant was split into two new RNase-free 2 mL tubes for each sample (1 mL in each) and 0.2 mL of chloroform was added per 1 mL of TRIzol. The sample was mixed by inversion and incubated at room temperature for 3 min, then centrifuged at 3,500 × *g* for 10 min at 4˚C. The clear upper aqueous phase that contained the RNA was transferred to a new tube and 0.5 volume of isopropanol was added, mixed thoroughly, and incubated on ice for 20 min. The sample was centrifuged again as above, and the supernatant discarded. The RNA pellet was washed with 1 mL of ice-cold 70% ethanol (RNA-grade, diluted with DEPC-treated water) and centrifuged. The ethanol was discarded and the RNA pellet air-dried for 10 min. Then the pellet was dissolved with 40 µL of DEPC-treated water (Invitrogen, Carlsbad, CA, USA) and the RNA stored at -80˚C.

2.6.2 Check for gDNA contamination and DNase treatment of RNA

Before using the RNA to synthesise cDNA, the RNA was first checked for gDNA contamination and quality on a 0.8% agarose and 0.3% SDS gel (Appendix 7.3.2). The gel tank, comb and gel tray were washed with DEPC-treated water to inactivate RNases. A small volume of RNA (1–2 µL) was loaded onto the gel with 1 µL of 6X gel loading dye (as used for DNA gels; Appendix 7.3.1) and run at 85 V for ~45-50 min, or until the loading dye migrated more than half of the length of the gel. RNA or DNA in the gel was stained for 15 min in ethidium bromide (10 mg/mL; RNase-free) (Appendix 7.3.2) and visualised in a Universal Hood IITM (Bio-Rad, USA). To ensure that the RNA was free of contaminating DNA, it was treated with a TURBO DNA-free^{TM} kit (Invitrogen) as per the manufacturer's instructions.

2.6.3 Precipitation of RNA and synthesis of cDNA for quantitative Reverse Transcription Polymerase Chain Reaction (qRT-PCR)

To increase the concentration and reduce the volume of RNA to be used for making complementary DNA (cDNA), the RNA was precipitated by adding 10 M lithium chloride (Appendix 7.2.3) to the RNA to make a final concentration of 2.5 M lithium chloride. The mixture was incubated at -20˚C for 30 min, then centrifuged at 13,300 rpm (19,776 × *g*) in a Heraeus Megafuge 16R centrifuge for 15 min at 4˚C. The supernatant was discarded, the RNA pellet washed with 200 µL of ice-cold 70% ethanol (RNase-free) and centrifuged at 13,300 rpm (19,776 × *g*) for 15 min at 4˚C. The ethanol was discarded

and the RNA pellet air-dried for 10 min, before resuspending the RNA in 12 µL of RNase-free TE buffer (Appendix 7.2.3).

cDNA was synthesised using a QuantiTect Reverse Transcription kit (Qiagen, Hilden, Germany), according to the manufacturer's instructions. For this, 1 µg of RNA was used for cDNA synthesis and to increase the yield of cDNA the reverse transcription reaction was incubated for 30 min at 42˚C, rather than 15 min. The cDNA was stored at -20˚C to be used for qRT-PCR. cDNA was checked for gDNA contamination by PCR using primers that flank an intron (Table 2.3, *TEF1α* qRT-PCR primers).

2.7 Quantitative Reverse Transcription Polymerase Chain Reaction (qRT-PCR) for gene expression analyses.

2.7.1 Primer design

The sequences of primers used for qRT-PCR are shown in Table 2.3 and were designed using Primer3 software (Untergasser et al., 2012). Primers used for amplification of target genes for dsRNA synthesis and gene expression determination by qRT-PCR are shown in Appendix Chapter 5, section 7.8 (Tables A7.5-A7.8 and Figures A7.23-A7.26). The following parameters were manually set: PCR product size: 80–150 bp, primer size: 18–20 bp, Tm (melting temperature) 58˚C (min); 60˚C (optimum); 61˚C (max). After generating primer sets, the positions of primers were checked in Geneious v9.1.8 to see where they bound on the sequence of the gene and primers were avoided that had runs of G's and C's in the primer sequence. To ensure that the primers were unique to the *D. septosporum* genes, the sequences were analysed in JGI (Grigoriev et al., 2012) using BLASTn to ensure they would only bind to the target gene within the *D. septosporum* genome. Standard PCR (section 2.4.2) was first carried out to test that the primers amplified each of the expected fragments from the cDNA template before being used for qRT-PCR.

2.7.2 Quantitative Reverse Transcription Polymerase Chain Reaction (qRT-PCR) cycling conditions

Reactions were performed for relative quantification of gene expression using a LightCycler 480 III (Roche, Penzberg, Germany) and analysed using LightCycler ® 480

SW v1.5.1 (Roche). Each PCR consisted of 5 µL of 2X sensiFAST SYBR No-ROX Mix (Meridian BioScience), 0.5 µL of 10 µM each forward and reverse primer, 1 µL template cDNA (eGFP or wildtype (WT) strain) and the final volume was made up to 10 µL with 3 µL of sterile MQ). After, 1 µL of the appropriate cDNA was added (Table 2.5), the 96-well plate (LightCycler 480 multiwell plate 384, Roche) was secured with sealing foil and briefly centrifuged for 2 min at 2,000 rpm ($568 \times g$) in a Heraeus Megafuge 16R centrifuge to collect the contents in the bottom of the wells. Controls with no template DNA were used. The cycling conditions were: 1 cycle of pre-amplification at 95˚C for 2 min. This was followed by 40 cycles of amplification, beginning with denaturation at 95˚C for 5 sec, annealing at 60˚C for 10 sec and extension at 72˚C for 20 sec. For melting curve analysis, the cycling conditions were 1 cycle of heating to 95˚ for 10 sec, 65˚C for 1 min and heating to 97˚C with a continuous acquisition mode at a ramp rate of 0.11˚C/sec (Table 2.5). The samples were subjected to one cooling cycle at 40˚C for 10 sec with a ramp rate of 1.5˚C/sec before taking the plate out of the LightCycler.

Table 2.5. Quantitative Reverse Transcription Polymerase Chain Reaction (qRT-PCR) setup and cycling conditions.

Component	Volume (µL)	Final concentration
2X sensiFAST SYBR No-ROX Mix	5 µL	1X
10 µM forward primer	0.5 µL	500 nM
10 µM reverse primer	0.5 µL	500 nM
MQ	3 µL	-
Template (gDNA)	1 µL	-
Total	**10 µL**	

Programme	Cycle number	Temp	Time	Ramp rate (˚C/s)
Pre-amplification	1 cycle	95˚C	2 min	4.4
Quantification	40 cycles	95˚C	5 sec	4.4
		60˚C	10 sec	2.4
		72˚C (single)	20 sec	4.4
Melting curve	1 cycle	95˚C	10 sec	4.4
		65˚C	1 min	2.2
		97˚C	continuous	0.11
Cooling	1 cycle	40˚C	10 sec	1.5

2.7.3 Generation of a standard curve

For generating a standard curve, a qRT-PCR run was implemented using a 5-fold dilution series of the WT and eGFP cDNA respectively for each of the primer sets. This was done to determine the efficiencies of amplification for each set of primers. Each sample was analysed in triplicate and the MQ water negative control in duplicate. The efficiency was calculated from the slope of the standard curve using the following formula: $10^{(-1/\text{slope})}$. Standard curves and melt curves for each target gene and the reference genes are provided in Appendix Chapter 5, Figures A7.27-A7.28, as well as the regression line equations, correlation coefficient and efficiency of genes for each standard curve (Table A7.5).

2.7.4 Gene expression analyses for suppression of target genes

Relative quantification was performed to determine if there was a reduction in abundance of messenger RNA (mRNA) transcripts as a result of treatment with the dsRNA. Expression of each of the target genes was normalised to the *D. septosporum* NZE10 housekeeping gene *DsTEF1α* (translation elongation factor 1 alpha) (Chettri et al., 2018). A standard curve was run for a second housekeeping gene beta-tubulin 1 (*DsTub1*) (Chettri et al., 2018), but was disregarded in further analyses as the primer amplification efficiency was poor. Samples were analysed in duplicate and expressed as normalised ratios (as below with the following equation). Analysis of treatments relative to control samples was calculated using the ΔΔCt method. Ct values above 35 cycles were disregarded in analyses, therefore 35 cycles was set as the threshold unless otherwise indicated. The following formula (below) was used for calculations:

$$2^{-\Delta\Delta Ct}$$

Ct stands for cycle threshold, which is the cycle number at which the fluorescence, produced as a result of amplification of the PCR product, exceeds the background level of fluorescence.

ΔCt is the difference in Ct values for the target gene and the housekeeping gene for a given sample (ie. ΔCt = Ct (target gene) – Ct (reference gene)).

ΔΔCt is the difference between the ΔCt values of the treated sample and the untreated/control sample (ie. ΔΔCt = ΔCt (treated sample) – ΔCt (untreated/control sample)).

Target gene refers to the gene of interest (either *DsAflR* or *eGFP*).
Reference gene is *DsTEF1α*.
Treated samples refer to *D. septosporum* mycelium samples treated with dsRNA.
Control samples are those not treated with the dsRNA (untreated – water control).

Although RNA was extracted from three replicates, due to lack of time the qRT-PCR data shown in results section 5.2.1 (Table 5.1) only represent two biological replicates. T-tests were conducted (type 2 equal variance) in Excel using ΔCt values (target – reference).

2.8 Transformation of *Dothistroma septosporum*

Transformation of *D. septosporum* was carried out using the GFP plasmid pR239 (Table 2.2) (Tanaka et al., 2006), in order to make an *eGFP*-expressing control strain that could be used for targeting *eGFP* with dsRNA. A protoplast-based approach was utilised for *D. septosporum* transformation (Bradshaw et al., 1997) (Figure 2.1), using the procedure by Yelton et al. (1984) to prepare protoplasts.

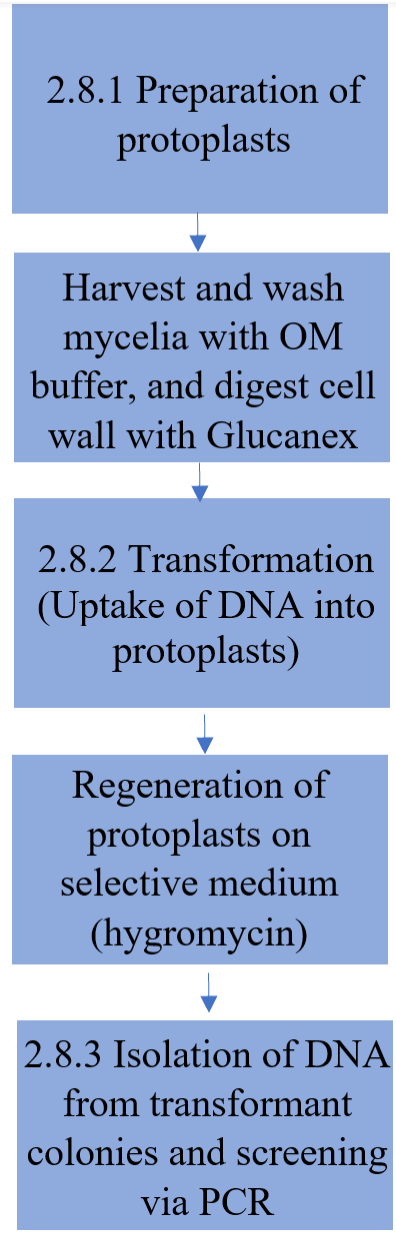

Figure 2.1. Flow chart of the procedure for protoplast transformation. (2.8.1) Protoplasts were prepared for transformation by harvesting mycelia and washing with OM buffer. Glucanex was added to digest the *D. septosporum* cell wall. (2.8.2) The DNA was taken up by the protoplasts. Protoplasts were plated and left to grow and penetrate through the layers of RG agar to form colonies on the selective media. (2.8.3) For screening selected transformants gDNA was isolated from fungal colonies and used as template for PCR to verify insertion of the *GFP* gene.

2.8.1 Preparation of protoplasts

D. septosporum was grown on DM agar plates with cellophane for 6–7 d at 22˚C as in section 2.2.1. Freshly grown mycelium was ground with a micropestle in sterile MQ water and 100 µL was inoculated into 125 mL flasks containing DM broth (Appendix 7.1.1). The mycelia were grown at 22˚C with shaking at 160 rpm (on a G10 GYROTORY shaker, New Brunswick Scientific) for a further 6–7 d. Sterile nappy liners inserted into a funnel were used to collect the mycelia by filtration. The mycelia were washed three times with sterile water and once with OM buffer (Appendix 7.2.1), transferred to autoclaved 125 mL flasks, then filter-sterilised Glucanex® 200G (Novozymes; Appendix 7.2.1) (10 mg/mL in OM buffer) added to digest the fungal cell wall. The flasks were incubated for 12–16 h at 30˚C with shaking at 80 rpm, then the presence of protoplasts determined using an Olympus CX41 microscope. The protoplasts were filtered through a nappy liner to remove mycelial debris and transferred to sterile corex tubes. Following this, 2 mL of ST buffer (Appendix 7.2.1) was overlaid on top of the protoplast solution and centrifuged using a Heraeus Megafuge 16R centrifuge for 5 min at 5,000 rpm (4,696 × *g*) to form a milky layer at the interface between the Glucanex solution and the ST buffer. The protoplasts at the interface and in the upper layer were transferred into corex tubes, washed with 5 mL STC buffer and centrifuged at 5,000 rpm (4,696 × *g*) for 5 min. Three subsequent washes were repeated before protoplasts were resuspended in 0.5 mL of STC buffer. To estimate the concentration of the protoplasts, a sample was diluted 100-fold in STC buffer and examined using a haemocytometer. For transformation, the stock was diluted to a concentration of 1.25 x 10^8 protoplasts/mL and kept on ice.

2.8.2 Transformation with enhanced green fluorescent protein (*eGFP*)

Both circular and/or linearised plasmids can be transformed into *D. septosporum* (Chettri, 2014). For transformation, the plasmid pR223 (hygromycin control) was linearised with *Hind*III (NEB), while pR239 (*eGFP*) remained circular.

A total of 5 µg DNA (circular or linear plasmid) for transformation was concentrated down to 5 µL using a Savant SVC 100H Speed Vac Concentrator (with RH 40-11 rotor) and added to 80 µL of 1.25 x 10^8 protoplasts/mL and 20 µL of 40% PEG (Appendix 7.2.1) on ice. A protoplasts-only (no DNA) tube was prepared as a negative control, as well as a positive control tube of protoplasts with pR223 (pBC-hygro), which contains a hygromycin (*hph*) gene. All tubes were vortexed briefly and left on ice for 30 min before

adding a further 900 µL of 40% PEG, mixing and incubating at room temperature for 20 min. To a 50 mL Falcon tube, 100 µL aliquots of the reaction mixture were added and mixed with 3.5 mL of molten 0.8% Regeneration Media (RG; Appendix 7.1.3) (with no antibiotic), which had been kept at 50˚C. This was then overlaid onto pre-poured RG plates and incubated at 22˚C overnight. The following day, 5 mL of molten 0.8% RG containing hygromycin B (Invitrogen, Carlsbad, CA, USA) at a final concentration of 70 µg/mL was overlaid onto the plates for selection of the transformants. In total, there were plates containing protoplasts with and without selection to obtain the viable cell count, a positive control plate with hygromycin as selection to give the transformation frequency, and 10 plates of *eGFP* for the sample transformation. Colonies appeared after 2–3 weeks.

2.8.3 Isolation of gDNA from transformant colonies and screening via Polymerase Chain Reaction (PCR)

To determine whether there was integration of the eGFP plasmid into the genomes of selected transformants, colonies were purified on RG containing hygromycin using a flamed sterile loop to generate single isolated colonies. After two rounds of purification, the hygromycin-resistant transformants were then characterised by PCR to confirm that *eGFP* was integrated into the genome to generate a strain of *D. septosporum* expressing eGFP. gDNA was extracted from transformants using the CTAB method as described previously (Section 2.3.1) and PCR was carried out using *GFP* primers to amplify a 720 bp product (Table 2.3). Also, for verification of successful transformants, colonies were visualised for GFP fluorescence under a fluorescence microscope (Leica MZ10F; Leica Microsystems, NZ) and images processed using Leica Software Application Suite LAS v3.8.

2.9 Construction of target gene templates for *in vitro* dsRNA synthesis

2.9.1 Gene target region and primer design

To design effective dsRNAs for gene silencing within *D. septosporum,* the choice of genes and the specific target regions were important parameters to consider. Candidate genes were chosen as outlined in Chapter 3, section 3.1, based on previously published studies of gene silencing and of known virulence genes in *D. septosporum*. The dsRNAs

were designed to target at least 400 base pairs (bp) of sequence and constructed using a MEGAScript RNAi kit (Invitrogen, Carlsbad, CA, USA), as per the manufacturer's instructions. This kit was chosen as it had been used in published gene silencing studies and can produce sufficient high quality dsRNA (https://www.thermofisher.com/order/catalog/product/AM1626#/AM1626). Generation of the dsRNA templates involved a plasmid cloning strategy that produced high quality plasmid DNA templates for dsRNA synthesis and consisted of a series of steps (sections 2.9.2 to 2.9.7) as shown in Figure 2.2. Separate DNA templates were prepared for each strand of RNA (sense and antisense) for each of the target genes. To amplify target genes, a T7 promoter sequence (Figure 2.3) was incorporated at the 5' end of the primers for the strand to be transcribed by the T7 RNA Polymerase (MEGAScript RNAi kit). Primers were phosphorylated to allow for the PCR product to be ligated into a dephosphorylated plasmid vector. The primer sequences are listed in Table 2.3 (section 2.4.1) and a schematic diagram is provided in Appendix 7.5.1 showing the positions of the primers. Primers were designed to generate PCR products of 509 bp in length for *DsAflR* 1 (*DsAflR* RNAi-1), 408 bp for *DsAflR* 2 (*DsAflR* RNAi-2) and 737 bp for *eGFP*.

2.9.2 Amplification of *DsAflR* 1, *DsAflR* 2 and *eGFP* templates

To amplify the target regions for dsRNA templates, high fidelity (HF) PCRs were performed. The target gene sequences were amplified from *D. septosporum* NZE10 gDNA for *DsAflR* and from the plasmid pPN82 (Tanaka et al., 2006; Appendix Figure A7.4) for *eGFP*, using target-specific primers (Table 2.3). The 20 µL reaction mixture was set up on ice and included 4 µL of 5X Phusion HF buffer (NEB), 0.4 µL of 10 mM dNTPs (NEB), 1 µL of each of the forward and reverse primers (10 µM), 1 µL of template DNA, 0.2 µL of Phusion HF DNA Polymerase (NEB) and 12.4 µL of MQ water. PCRs were run in an Eppendorf Gradient Mastercycler® using the following PCR programme: 1 cycle of initial denaturation at 98˚C for 30 sec, 30 cycles of heating to 98˚C for a further 10 sec, cooling to 55˚C for 30 sec and heating to 72˚C for 30 sec per kb. For a further 10 min, there was one cycle of final extension at 72˚C. PCR products were resolved on a 1% agarose gel (Appendix 7.3.1) to confirm there was a single band of product for each of *DsAflR* 1, *DsAflR* 2 and *eGFP* (as in section 2.4.5). Then, PCR products were purified to remove salts by applying to a Sepharose™ matrix (Sigma-Aldrich, Steinheim, Germany) according to the manufacturer's instructions. The matrix was set up using 150 µL of Sepharose™ 4B (with bead diameter 45–165 µm; Sigma-Aldrich, Steinheim, Germany)

in a 0.6 mL tube (with small drainage hole made with a needle) inserted into a 1.5 mL microcentrifuge tube. Centrifugation at 2,000 rpm (385 × *g*) in a Heraeus Biofuge Pico benchtop microcentrifuge for ~6 min was required to remove excess water. The Sepharose matrix in the 0.6 mL tube was transferred to a new 1.5 mL tube and the PCR products transferred to the matrix and drawn through by 2 min of centrifugation as above.

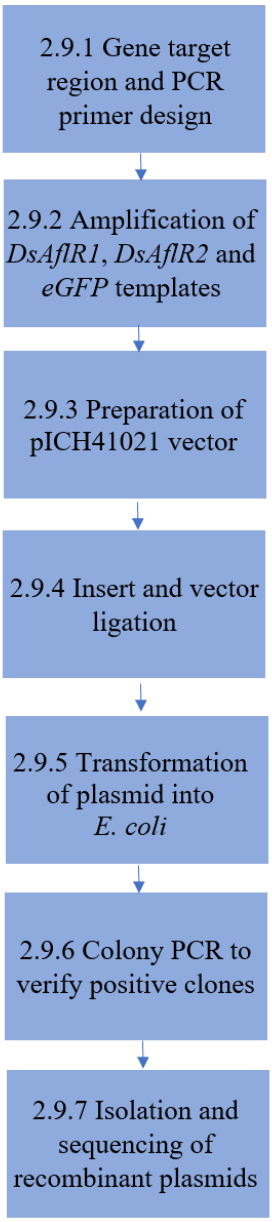

Figure 2.2. Cloning strategy for producing plasmid templates. The section numbers in which the methods are described are given. (2.9.1) Identification of the gene target region and design of primers for PCR amplification. (2.9.2) Templates for each of the target genes were amplified to produce single PCR products. (2.9.3) The plasmid pICH41021 was prepared for cloning the PCR products by digesting and dephosphorylating the plasmid. (2.9.4) Ligation of PCR product into the vector. (2.9.5) Tranformation of the construct into *Escherichia coli*. (2.9.6) Verification of positive clones. (2.9.7) Extraction of plasmid and sequencing.

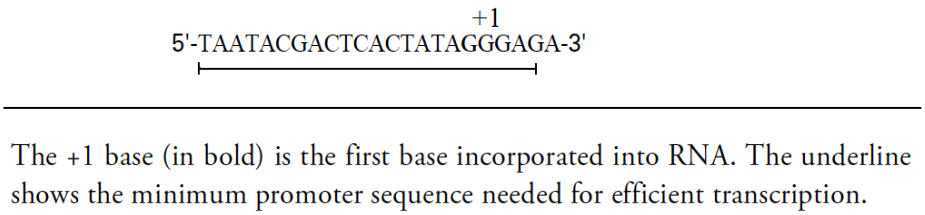

Figure 2.3. T7 Polymerase promoter : Minimal sequence. (ThermoFisher, https://www.thermofisher.com/order/catalog/product/AM1626#/AM1626).

2.9.3 Preparation of the pICH41021 vector

For cloning the RNAi fragment into a destination vector, the plasmid pICH41021 (Table 2.2) was used. The pICH41021 plasmid was digested with the restriction enzyme *Sma*I (20,000 U/mL; NEB), in a 50 µL reaction containing 6.5 µL pICH41021 (1.5 µg), 1.5 µL *Sma*I, 5 µL 10X CutSmart™ buffer (NEB) and 37 µL MQ water. The reaction was incubated at 25˚C for 1 h on an ACCUBLOCK digital dry bath, then the enzyme heat-inactivated at 65˚C for 20 min. The digest was resolved on a 1% agarose gel alongside uncut plasmid, to determine if *Sma*I-treated pICH41021 was fully digested to give a single linear band. Dephosphorylation was necessary to prevent the linearised plasmid from re-circularising. The 60 µL reaction mix consisted of 40 µL of *Sma*I-cut pICH41021 plasmid, 1 µL of rSAP enzyme (shrimp alkaline phosphatase; NEB), 6 µL of 10X CutSmart™ buffer (NEB) and 13 µL of MQ water. After 30 min at 37˚C, the temperature was raised to 65˚C for 5 min to inactivate the enzyme.

The cut and dephosphorylated plasmid was applied to a Sepharose™ matrix (as described above) to remove salts, which could interfere with transformation of the plasmid into electrocompetent *E. coli* cells (section 2.9.5). The entire 60 µL of *Sma*I-cut dephosphorylated pICH41021 plasmid was pipetted onto the Sepharose matrix and centrifuged for 1 min at 2,000 rpm (385 × *g*) in a Heraeus Biofuge Pico benchtop microcentrifuge. The concentration of plasmid was determined using a Nanodrop™.

2.9.4 Insert and vector ligation

In order to ligate the PCR products into the *Sma*I-cut pICH41021 vector, a ligation reaction was set up using T4 ligase and a molar ratio of 3:1 insert to vector. The amount of insert required for ligation to 50 ng of vector was 28.43 ng for *DsAflR* 1 (509 bp), 22.78 ng for *DsAflR* 2 (408 bp) and 41.16 ng for *eGFP* (737 bp). PCR products were diluted to 10 ng/µL to use for the ligation. To PCR tubes, 2 µL of 10X T4 DNA ligase buffer

(400,000 U/mL; NEB) was added, 1 µL of T4 DNA ligase (NEB), 50 ng of vector (*Sma*I-cut dephosphorylated pICH41021), the appropriate amount of PCR product as listed above, and MQ water to a final volume of 20 µL. *Sma*I-cut dephosphorylated pICH41021 (ligase treated but with no insert) and pICH41021 (uncut plasmid) were used as controls. Ligation reactions were incubated overnight at 4˚C, then the enzyme was heat inactivated at 65˚C for 10 min. Samples were applied to a Sepharose matrix as described above and 1–2 µL of the cleaned samples were transformed into competent cells.

2.9.5 Transformation of plasmid into *Escherichia coli*

Transformation of the *E. coli* strain DH5α was performed via electroporation (Dower et al., 1988) to enable identification and cloning of recombinant pICH41021 vectors containing the PCR products to use as templates for *in vitro* synthesis of dsRNA. Electrocompetent cells, prepared as described previously (section 2.3), were taken out of the -80˚C freezer and thawed on ice and 0.2 cm electroporation cuvettes (Bio-Rad, USA) were pre-cooled on ice. To 50 µL of electrocompetent *E. coli* cells, 1–2 µL of the ligation reactions or plasmid controls were added and transferred to a cuvette. A Micropulser™ (Bio-Rad, USA) was set to "Ec2" for bacteria (25 µF, 2.5 kV and 200 Ω) for electroporation. Immediately after electroporation, 1 mL of LB medium was added to recover the cells, the mixture transferred to a 1.5 mL microcentrifuge tube and incubated at 37˚C on an orbital shaker for 1 h. After incubation, 50–100 µL volumes were plated onto selective LB agar plates (ampicillin 100 µg/mL; X-gal 20 µg/mL and IPTG 100 µM; Appendix 7.1.2) and sealed with tinfoil (ampicillin is light sensitive). Plates were incubated overnight (up to 16 h) at 37˚C for the growth of ampicillin-resistant colonies containing the plasmid.

2.9.6 Colony Polymerase Chain Reaction (PCR) to verify positive clones

Colony PCR was carried out to determine the presence or absence of insert DNA in plasmid constructs and to confirm that the recombinant plasmids had the correct-sized inserts (Table 2.6). The 25 µL reaction mixture consisted of 2.5 µL of 10X Standard Taq reaction buffer (NEB), 0.5 µL of 10 µM dNTPs (dATP, dCTP, dGTP, dTTP) (NEB), 0.5 µL of 10 µM M13 LacZ fwd primer, 0.5 µL of 10 µM M13 LacZ rev primer, 0.125 µL Taq DNA Polymerase (NEB), DNA from a single colony (section 2.4.4) and made up to 25 µL with MQ water. The following PCR programme was run: initial denaturation for 5

min at 95˚C, 30 cycles beginning with denaturation at 95˚C for 5 min, annealing at 55˚C for 60 sec, followed by extension for 1 min per kb at 68˚C. The annealing step was optimised according to the melting temperature of the primers and the extension time adjusted to the size of the amplicon to minimise non-specific amplification. Lastly, there was a final extension for 5 min at 68˚C. PCR products were visualised as in section 2.4.5.

Table 2.6. Polymerase Chain Reaction (PCR) screening of *Escherichia coli* colonies and plasmid sequencing to confirm integration of the insert.

Plasmid used	Type of primer	Primer sequence (5'-3')	Product size (bp)	Insert confirmed by sequencing
pICH41021	M13 LacZ fwd M13 LacZ rev	GCCAGGGTTTTCCCAGTCACGA GCGGATAACAATTTCACACAGG	555	*DsAflR* 1 sense
pICH41021	M13 LacZ fwd M13 LacZ rev	GCCAGGGTTTTCCCAGTCACGA GCGGATAACAATTTCACACAGG	555	*DsAflR* 1 antisense
pICH41021	M13 LacZ fwd M13 LacZ rev	GCCAGGGTTTTCCCAGTCACGA GCGGATAACAATTTCACACAGG	656	*DsAflR* 2 sense
pICH41021	M13 LacZ fwd M13 LacZ rev	GCCAGGGTTTTCCCAGTCACGA GCGGATAACAATTTCACACAGG	656	*DsAflR* 2 antisense
pICH41021	M13 LacZ fwd M13 LacZ rev	GCCAGGGTTTTCCCAGTCACGA GCGGATAACAATTTCACACAGG	737	*eGFP* sense
pICH41021	M13 LacZ fwd M13 LacZ rev	GCCAGGGTTTTCCCAGTCACGA GCGGATAACAATTTCACACAGG	737	*eGFP* antisense

2.9.7 Isolation and sequencing of recombinant plasmids

Colonies that tested positive in colony PCR assays were streaked onto LB agar (Appendix 7.1.2) containing ampicillin, X-gal and IPTG to generate homogeneous colonies from which plasmids could be extracted. Plates were wrapped in tinfoil and incubated at 37˚C overnight. The following day, an overnight culture was prepared in 5 mL of LB medium containing 5 µL ampicillin (100 µg/mL). The medium was inoculated with a single colony by touching the surface of a white colony with a p200 pipette tip and ejecting the tip into the liquid. The culture was incubated overnight at 37˚C on an orbital shaker at 220 rpm. Plasmids were extracted using a Plasmid DNA Mini kit (OMEGA Bio-tek), as per the manufacturer's instructions.

To confirm that the sequence for each RNAi construct was correct, each of the selected recombinant plasmids were sequenced from both ends of the insert by the Massey Genome Service (Massey University, Palmerston North) using an ABI 3730 DNA Analyzer (Applied Biosystems, Foster City, CA). The requirements for sequencing were 250–625 ng of plasmid template and 4 pmol of primers. The final reaction volume was 20 µL, which included 0.4 µL of a 10 µM primer (one primer per sequencing reaction), 1–2 µL of plasmid and MQ water in a 0.2 mL PCR tube. The primers used for sequencing reactions were the same as those used for colony PCR (see Table 2.5).

Sequencing analysis was performed in Geneious v9.1.8 using the ABI files, and multiple alignments of the forward and reverse sequences were performed against the reference/consensus sequence. A search for restriction enzyme sites (*Sac*I and *Xba*I) downstream of the T7 promoter sequence was done to determine the orientation of the fragment that was ligated into the vector and which enzyme was appropriate to use for linearising the plasmid prior to dsRNA synthesis. Plasmid maps are located in Appendix 7.5.3.

2.10 *In vitro* production of dsRNAs

2.10.1 Preparation of plasmid template

In order for the T7 RNA polymerase to efficiently transcribe the target region from the T7 promoter sequence and terminate transcription at the end of that region, the plasmid was linearised downstream of the inserted gene target. It was vital that there was no circular plasmid present in the template as the initiation of *in vitro* transcription is a rate-limiting step, therefore "even a small amount of circular plasmid in a template yield will generate a large proportion of transcript."(https://www.thermofisher.com/document- connect/document- connect.html?url=https%3A%2F%2Fassets.thermofisher.com%2FTFS- Assets%2FLSG%2Fmanuals%2Fcms_072987.pdf). A 100 µL linearisation reaction was prepared for each plasmid template containing 2 µg of plasmid DNA. The reaction mix also contained either 2 µL of *Xba*I (20,000 U/mL) (NEB) or *Sac*I (10 U/µL) (Roche), depending on which enzyme recognition site was downstream of the insert, as well as 10 µL 10X CutSmart™ Buffer (NEB) or 10 X SuRE/Cut™ Buffer A (Roche). To make up the volume to 100 µL, MQ water was added to each reaction, mixed and incubated at

37˚C for 1 h. The enzyme was then heat-inactivated at 65˚C for 20 min. To confirm that cleavage was successful, 2 µL of loading dye was added to 5 µL of each plasmid digest and resolved on a 0.8% agarose gel, along with an uncut plasmid control. Single bands with expected sizes of 3.4 kb, 3.2 kb and 3.1 kb for plasmid templates (both sense and antisense) *eGFP*, *DsAflR* 1 and *DsAflR* 2 respectively were analysed.

To proceed with the transcription reaction, it was important to purify the DNA. This was done by adding 1/20 volume of 0.5 M EDTA (RNase-free; Appendix 7.2.3), 1/10 volume of 3 M NaOAc (RNase-free; Invitrogen, Carlsbad, CA, USA) and 2 volumes of 100% ethanol (RNA-grade). After mixing, the tubes were kept at -20˚C for 15 min. To pellet the DNA, the tubes were centrifuged at 13,000 rpm (16,249 × *g*) in a Heraeus Biofuge Pico benchtop microcentrifuge. The supernatant was discarded and the DNA pellet resuspended in 10 µL of RNase-free TE buffer (Appendix 7.2.3). Purified plasmids prepared using this method are referred to as ethanol-precipitated plasmids throughout this thesis. In one trial, the DNA was treated with Proteinase K (50 µg/mL; Sigma Aldrich, Steinheim, Germany) and sodium dodecyl sulphate (SDS), followed by phenol/chloroform and ethanol precipitation (according to the manufacturer's instructions for the MEGAScript RNAi kit; Invitrogen, Carlsbad, CA, US). However, because of the low amount of DNA recovered after precipitation, these additional steps were eliminated for further template DNA preparations.

To test whether gel-purified plasmid DNA would be a suitable template for dsRNA synthesis, the template was prepared as follows for use in the transcription reaction. Linearised plasmids were resolved on a thin 0.8% agarose gel and the bands extracted using a QIAquick Gel Extraction Kit according to the manufacturer's instructions. Linearised plasmids were then PCR amplified to generate enough sense and antisense template (1 µg of each) for dsRNA synthesis. Primers used for amplification are listed in Table 2.3 (pICH41021 backbone primers). Here, 1 µg of the purified linearised plasmids were concentrated down to 4 µL using a Savant SVC 100H Speed Vac Concentrator to reduce the volume for the transcription reaction.

As an alternative option to gel-purification, the dsRNA template fragments were synthesised by Twist BioScience (Decode Science) with T7 promotor sequences

included. The linear fragments were provided at 1,000 ng (powder) and suspended at 100 ng/µL in DEPC-treated water (Invitrogen, Carlsbad, CA, USA). Due to these smaller templates having a larger molar amount of DNA per ng, in contrast to larger templates (linearised plasmids), the amounts of Twist fragments used in transcription reactions were adjusted to account for there being no plasmid DNA present in these templates. An example calculation is provided in Appendix 7.5.4.

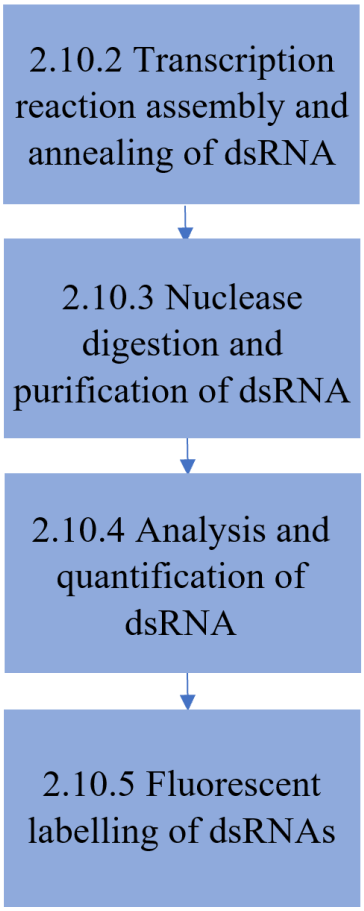

Figure 2.4. Outline of the steps required for synthesis of the dsRNA *in vitro*. The section numbers in which the methods are described are given. (2.10.2) Assembly of the transcription reaction to produce dsRNA. (2.10.3) Nuclease digestion to remove the presence of DNA and any single-stranded RNA, followed by purification to clean the dsRNA. (2.10.4) Quantification of dsRNA and agarose gel electrophoresis. (2.10.5) Cy3 labelling of dsRNA. After each of the various steps a 0.5 µL aliquot was run on a non-denaturing agarose gel to check the dsRNA.

2.10.2 Transcription reaction assembly and annealing of RNA

dsRNA was synthesised using a MEGAScript™ RNAi kit (Invitrogen, Carlsbad, CA, US), then purified and analysed according to the manufacturer's instructions (Figure 2.4). For *in vitro* transcription, a 20 µL reaction was set up on ice as recommended for

producing dsRNA ≥400 nt in length. Different DNA templates (as outlined in section 2.10.1) were used to compare the efficiency of transcription and the yield of dsRNA produced. These included (1) gel-extracted plasmid, (2) plasmids also purified by ethanol precipitation and (3) commercially synthesised fragments (Twist BioScience). The positive control supplied with the kit was used for the first attempt at RNA synthesis and also a mixed template control was included (see Table 2.7). To an RNase-free PCR tube, 4 µL of the sense template (1 µg or equivalent) and 4 µL of the antisense template DNA (1 µg or equivalent) were added along with the following reagents from the Invitrogen MEGAScript RNAi kit: 2 µL of 10X T7 reaction buffer, 2 µL of each of the ribonucleotides (ATP, CTP, GTP and UTP) and 2 µL of T7 enzyme mix. The final volume was made up to 20 µL with nuclease-free water. For the positive control, 2 µL of linear template DNA was used in the reaction. The tubes were incubated at 37˚C for RNA synthesis. The mixed template control had 1 µg of ethanol-precipitated eGFP plasmid (3 µL of each sense and antisense) and 1 µg of positive control template (2 µL). Trials were performed to optimise the efficiency of transcription for each of the templates by increasing the incubation times (Table 2.7).

Since the T7 promoter was on separate molecules, annealing of the sense and antisense strands of RNA was needed after the transcription reaction, to ensure as much of the dsRNA was formed as possible. The RNA was incubated at 75˚C for 5 min and cooled to room temperature for 1 h to allow for annealing of the RNA to produce dsRNA. This step was not required for the positive control, since both RNA strands were hybridised during the reaction, as they were made from a single template containing opposing T7 promoters (two) flanking the transcription region. This may be because of the closer proximity of synthesis of the sense and antisense strands, such that the annealing could occur more efficiently compared to dsRNA generated from two separate templates.

Table 2.7. Amount of DNA and incubation times used for each of the different DNA templates to be transcribed to make RNA.

Target gene	Template DNA used	µg DNA[1]	pmol DNA[1]	Incubation time (h)
eGFP	EtOH ppt plasmid[2]	1	0.4	4
eGFP	Gel-purified plasmid[2]	1	0.4	4
eGFP	EtOH ppt plasmid[2]	1	0.4	6
eGFP	Synthesised fragment	0.2	0.44	6
Positive control	Linear fragment with opposing T7 promoters	1	0.3	2
Mixed template (positive control and *eGFP*)	Linear fragment EtOH ppt plasmid[2]	0.5 µg of each[3]	0.3 0.4	4
DsAflR 1	EtOH ppt plasmid[2]	1	0.5	16
DsAflR 1	Synthesised fragment	0.2	0.5	16
DsAflR 1	Synthesised fragment	0.2	0.5	6
DsAflR 2	EtOH ppt plasmid[2]	1	0.5	16
DsAflR 2	Synthesised fragment	0.1	0.5	16
DsAflR 2	Synthesised fragment	0.1	0.5	6

[1]Both the sense and antisense templates were added in a single reaction (20 µL total volume) and the amounts of DNA shown here are representative of each individual template (sense or antisense), not the combined amount of the two templates. A smaller amount of synthesised fragment (Twist BioScience) was used, as it lacked plasmid DNA. Refer to Appendix section 7.5.4.1 for an example calculation.

[2] Sodium acetate and ethanol-precipitated linearised plasmid (EtOH ppt plasmid).

[3]0.5 µg of sense and 0.5 µg of antisense plasmids were used for each plasmid template (positive control – 1 µg and *eGFP* – 1 µg) to give 2 µg in total.

2.10.3 Nuclease digestion and purification of dsRNA

To digest residual template DNA and any single stranded RNA (ssRNA) that did not anneal in the annealing step, DNase/RNase treatments were performed. A 50 µL reaction was set up on ice with the remaining transcribed and annealed RNA mixture (after running 0.5 µL aliquots on a gel to check the RNA after each step (section 2.10.4)), and the following reagents as in the MEGAScript RNAi kit: up to 50 µL of nuclease-free water, 5 µL of 10X digestion buffer, 2 µL of DNase I (2 U/µL), and 2 µL of RNase. The

nuclease digestion reaction was incubated at 37˚C for 1 h. The treated dsRNA was then purified to remove proteins and nucleic acid fragments by adding the following: 10X binding buffer (MEGAScript RNAi kit), 150 µL of nuclease-free water (MEGAScript RNAi kit) and 250 µL of 100% RNA-grade ethanol (total volume of 500 µL). The dsRNA binding mix was transferred to a filter cartridge and centrifuged in a Heraeus Biofuge Pico Benchtop microcentrifuge Centrifuge (13,000 rpm; 16,249 × *g*) for 2 min. The flowthrough was discarded from the collection tube, the bound dsRNA on the filter washed with 500 µL of wash solution and drawn through by centrifugation as before. A second wash was repeated and residual wash solution removed by centrifuging for a further 30 sec. The dsRNA was recovered in 50 µL of elution solution (MEGAScript RNAi kit) (pre-heated to 95˚C), centrifuged for 2 min and eluted in another 50 µL to recover any remaining RNA.

2.10.4 Analysis and quantification of dsRNA

To analyse the integrity of the dsRNA, samples were resolved on a 1% non-denaturing agarose gel (Appendix 7.3.2). A 0.5 µL aliquot of the RNA was diluted 10-fold with RNase-free TE buffer (Appendix 7.2.3) and 3.5 µL of this was loaded onto the gel. The gel was run at 80 V for ~40 min, or until the bromophenol blue dye had migrated just over 3/4 of the way through the gel. Afterwards, RNA in the gels was stained in 1% ethidium bromide (10 mg/mL; Appendix 7.3.2) for 15 min and visualised in a Universal Hood II^{TM} (Bio-Rad, USA). The concentration of dsRNA was determined using a Nanodrop^{TM}. RNA samples were diluted 10-fold in TE buffer (Appendix 7.2.3) before measuring absorbance (A_{260} and A_{280}) with TE buffer as the blank.

2.10.5 Fluorescent labelling of the dsRNAs

To determine if the dsRNA was delivered into fungal cells, it was labelled with Cy3 using the protocol for labelling long-dsRNA from the Silencer siRNA Labelling kit (AM1632, Invitrogen, Carlsbad, Ca, USA). A 50 µL reaction was assembled in a 1.5 mL tube wrapped in foil (to limit exposure to light) containing 40 pmol of dsRNA, and the following reagents supplied from the siRNA kit: 5 µL of 10X labelling buffer, 5 µL of loading dye, made up to 50 µL with nuclease-free water (see Table 2.8 for an example of the labelling reaction). The reaction was incubated at 37˚C in the dark for 1 h in an Innova 42 Incubator Shaker (New Brunswick Scientific). To precipitate the dsRNA, 5 µL of 5 M NaCl and 125 µL of cold 100% RNA-grade ethanol were added, mixed thoroughly, and

incubated at -20˚C for 30 min. After incubation, the RNA was centrifuged at 4˚C for 20 min at 13,300 rpm (19,776 × *g*) in a Heraeus Megafuge 16R centrifuge. The supernatant was discarded, the RNA pellet was washed with 100 µL of 70% ethanol (RNase-free) and centrifuged at 13,300 rpm (19,776 × *g*) in a Heraeus Biofuge Pico benchtop microcentrifuge for 5 min at room temperature. The supernatant was discarded, the tube briefly re-spun and traces of ethanol removed, before air-drying the RNA pellet for 5-10 min. The labelled RNA was resuspended in 20 µL of nuclease-free water and the absorbance of the RNA and dye was measured using an Implen NanoPhotometer (IMPLEN GmbH, Munich, Germany). The NanoPhotometer was blanked with 200 mM MOPS (pH7.5; Appendix 7.2.3) as instructed in the siRNA kit manual, then absorbance of the labelled RNA (diluted 10-fold) was measured at 260 nm (RNA) and 550 nm (dye). To determine if the labelling reaction was successful, the base:dye ratio was calculated as in the instruction manual, which indicated the proportion of nucleotides labelled with the Cy3 probe. In first instances where the labelling of each of the dsRNAs was carried out, the final labelled dsRNA products were analysed on a 1% non-denaturing agarose gel (RNase-free; Appendix 7.3.2) as in section 2.10.4.

Table 2.8 Example of labelling reaction of enhanced green fluorescent protein gene (*eGFP*)-dsRNA.

Reagent	Volume to add (µL)
Nuclease-free water	3.3
10X Labelling Buffer	5
eGFP-dsRNA **(40 pmol)**	36.7*
Cy3 Labelling Reagent	5
Total	**50**

*****The concentration of *eGFP*-dsRNA was 514.77 ng/µL. Refer to Appendix 7.5.4.2 for determining how much purified dsRNA was required for labelling 40 pmol.

2.11 Microscopy and *in vitro* assays with synthesised dsRNAs

2.11.1 Confocal microscopy analyses and *in vitro* dsRNA trials

Several different methods were developed for testing the effects of dsRNA application to *D. septosporum* cells. Firstly, a trial experiment was conducted using the *eGFP*-dsRNA and *DsAflR* 1-dsRNA at a single concentration over 72 h and mycelium was collected for RNA extractions at the 72 h time point. Secondly, an experiment with the *DsAflR* 1- and *DsAflR* 2-dsRNAs was devised using different concentrations applied in 24 h intervals

for up to 72 h. Initial experiments were also run to determine what medium (water agar (WA), DM or PDA) was suitable for *D. septosporum* growth for microscopy imaging and for extracting RNA for qRT-PCR analyses. Thin sections of mycelium were used to obtain flat hyphal growth for confocal microscopy and 3 mm^2 mycelium plugs for *in vitro* assays from which RNA could be extracted for qRT-PCR.

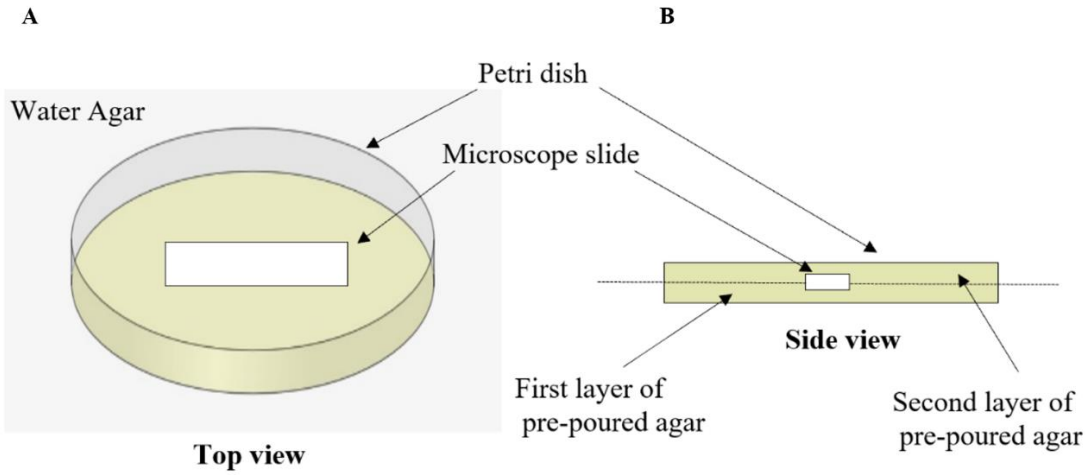

Figure 2.5. Schematic diagram of water agar (WA) media with microscope slides for growing *Dothistroma septosporum* to obtain flat hyphal growth for use in confocal microscopy. (A) Front view of agar medium with a microscope slide wedged in between the first and second layers of pre-poured agar. (B) Side view.

For monitoring the uptake of *eGFP*-dsRNA in *eGFP*-expressing hyphae (*eGFP* strain – FJT175) via confocal microscopy, a small piece of mycelium (2 mm x 2 mm) was extracted from the edge of an eGFP colony (grown on DM agar) and inoculated onto WA plates that had been prepared on sterile microscope slides (as in Figure 2.5 above). Mycelium was grown for 7 d to allow for flat surface growth of the fungus on the agar before transferring 2 mm x 2 mm pieces of mycelium to three individual wells of a 12-well plate (Nunclon Delta surface plates; ThermoScientific, Denmark) containing 0.5 mL of Potato Dextrose Broth (PDB; Appendix 7.1.4) and 0.5 µL of ampicillin (100 µg/mL) to inhibit bacterial growth. Labelled dsRNA (500 ng) or water (untreated control) was mixed with SILWET L-77 (kindly provided by Tim Worn; Polymers International Ltd) at a final concentration of 0.03% then added to each well. The plate was sealed with Parafilm™ M (Bemis Neenah, WI) and wrapped with foil (to prevent photobleaching of the fluorescent label), then incubated at 22˚C with shaking at 100 rpm in an Innova 42 Incubator Shaker (New Brunswick Scientific) for 72 h.

After 24 h, samples were prepared for confocal microscopy on sterile microscope slides with water as mounting fluid. Imaging was carried out at the Manawatu Microscopy and Imaging Centre, Massey University using a confocal (Super Resolution; SR) microscope (LSM900, Leica Microsystems). For analysing the localisation of the Cy3 probe in hyphae (i.e. to detect dsRNA uptake), fluorescence was measured with an excitation wavelength of 550 nm and an emission wavelength of 570 nm (Table 2.9) (40 x oil immersion objective). GFP fluorescence was also measured in each of the samples (excitation wavelength 488 nm, emission wavelength 509 nm) to examine if there were any differential changes in fluorescence intensity, as a direct result of application of the dsRNA. GFP fluorescence and labelled dsRNA was examined after 48 and 72 h for any suppression effect in terms of a decrease in GFP fluorescence. All images were acquired using Zeiss Zen 3.1 (blue edition) software (Carl Zeiss; www.zeiss.com/microscopy) and were later processed in ImageJ (Rueden et al., 2017).

To monitor the uptake of the *DsAflR* 1- and *DsAflR* 2-dsRNAs via confocal microscopy, the same protocol as above was followed, except different concentrations of Cy3-labelled dsRNA (0 ng, 500 ng and 2000 ng for *DsAflR* 1 and 0 ng, 500 ng and 1000 ng for *DsAflR* 2) were added to each well (6 wells in total with three mycelium plugs in each) to make a final volume of 500 µL. Six wells were used for confocal microscopy, whereas the other six were reserved for RNA extractions. After 24, 48 and 72 h a thin piece of mycelium (with agar scraped off) was transferred to microcentrifuge tubes with 100 µL of staining solution (trypan blue and aniline blue, AB20/TB20) (Appendix section 7.2.3) (Hoffmeister et al., 2020) and incubated in the dark for 2–4 h before transferring to a microscope slide with a drop of water and coverslip for imaging (see Table 2.9 below for the wavelengths of each channel).

Table 2.9. Wavelengths used for confocal microscopy analyses.

Channel	Excitation wavelength (nm)	Emission wavelength (nm)	Visible or UV range
Cy3	550	570	Visible
eGFP	488	509	Visible
Brightfield	400	593	Visible
Aniline Blue (AB)	405	450-495*	Visible
Trypan Blue (TB)	561	593-625*	Visible

*Emission wavelengths for AB and TB have a range in which the dyes are emitted.

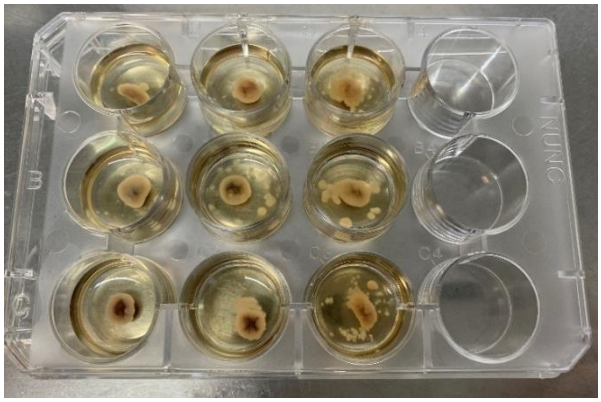

Figure 2.6. Example of a 12-well *Dothistroma septosporum* culture plate setup for *in vitro* trials with dsRNA. Note that this photograph was taken after four days (d) of incubation before adding *eGFP*-dsRNA. The small bits of mycelium are growth from the main mycelium plug, which have broken off from incubating the culture on a shaker.

For examination of the effect of dsRNA treatment on the expression of the target gene *eGFP*, in *D. septosporum* (*eGFP* strain – FJT175), 3 mm^2 mycelium plugs taken from DM agar or half-strength PDA (1/2 x PDA, Appendix 7.1.4) were transferred to six individual wells (three biological replicates for each) in 12-well plates (Nunclon Delta surface plates; ThermoScientific, Denmark) containing 2 mL of PDB (Appendix 7.1.4) and 2 µL of ampicillin (100 µg/mL) to inhibit bacterial growth. The mycelium was grown for 4 d at 22˚C. After, fluorescently labelled *eGFP*-dsRNA (500 ng) or water (untreated control) was mixed with 0.03% SILWET-L77 and incubated for 72 h (Figure 2.6). This method was named the 12-well plate method. An additional method was also explored for application of *eGFP*-dsRNA. Aliquots of dsRNA (total of 5 µL of dsRNA mixed with SILWET L-77) were directly applied to the surface of mycelium plugs grown on either DM agar or 1/2 x PDA and was termed the agar plate method (Figure 2.7). For this method, three 3 mm^2 mycelium plugs were taken from a *Dothistroma septosporum* culture plate (DM or 1/2 x PDA) and transferred to a fresh agar plate of the same medium,

containing three holes premade in the agar with a cork borer (Figure 2.7). Cy3-labelled dsRNA was added (mixed with SILWET as above) and plates were incubated for 72 h as for trials using the 12-well plate method. After 72 h, mycelium plugs were harvested from the 12-well plates and agar plates, wrapped in foil, snap frozen in liquid nitrogen and either stored at -80˚C or used at the time for RNA extractions. The RNA was then used for qRT-PCR (section 2.6). EGFP fluorescence was not quantified during these *in vitro* assays, but various methods were trialled. These included use of a ZOE fluorescent cell imager (Bio-Rad, USA) and a fluorescence microscope (Olympus SZX16 Stereomicroscope) (Figures not shown). For *in vitro* trials with the *DsAflR* 1-dsRNA the same procedures were followed as for *eGFP*-dsRNA trials (12-well plate and agar plate methods), except the mycelium used for inoculum was only grown on DM. An attempt to determine the effects of silencing the target gene *DsAflR* was made by applying different amounts of *DsAflR* 1-dsRNA (0 ng, 500 ng and 2000 ng) to *D. septosporum* cultures in 12-well plates. Mycelium plugs (grown on DM) were harvested from each well at 0, 24, 48 and 72 h, snap frozen in liquid nitrogen and stored at -80˚C until required for RNA extractions.

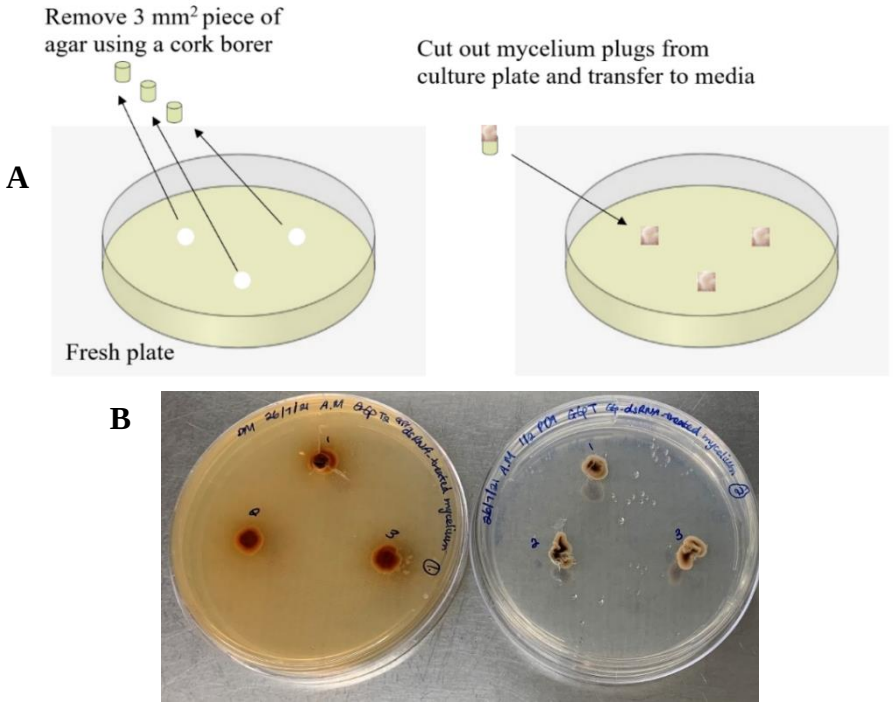

Figure 2.7. Agar plate method for application of dsRNA. (A) The agar plate method involved transferring three 3 mm^2 mycelium plugs from a *Dothistroma septosporum* culture plate (Dothistroma Medium or half-strength Potato Dextrose Agar) to a fresh agar plate of the same medium containing three holes premade in the agar with a cork borer. (B) Growth of *D. septosporum* mycelium on DM (left) and 1/2 x PDA (right), ready for dsRNA to be added.

For the time-course experiment with different amounts of *DsAflR* 2-dsRNA added to *D. septosporum* mycelium in 12-well plates, the method described previously was used. Each well had either 0 ng, 500 ng or 1000 ng and/or 2000 ng of *DsAflR*-dsRNA in 2 mL of PDB with SILWET-L77 at a final concentration of 0.03% (6 wells in total with three mycelium plugs in each). After 24, 48 and 72 h mycelium were harvested as above for RNA extractions.

2.12 Plant pathogenicity assays

2.12.1 Measuring plant:fungal biomass ratio

To estimate the effect of dsRNA treatment on *D. septosporum* infection of pines, plant pathogenicity tests were carried out and the fungal biomass estimated by qPCR. Eight jars, each containing seven clonal *P. radiata* shoots provided by Scion (section 2.1.3) were subjected to various treatments. These included (1) water (untreated control), (2) *eGFP*-dsRNA, (3) *DsAflR* 1-dsRNA and (4) *DsAflR* 2-dsRNA. Each treatment was applied to two jars. These clonal shoots are very expensive, therefore only two jars were used for each treatment and the shoots (numbered 1-7 from different jars) were the replicates. An extra jar provided served as a no dsRNA treatment control, which was sprayed with *D. septosporum* spores only. For spray application 20 µL of each fluorescent dsRNA (*eGFP*, *DsAflR* 1 and *DsAflR* 2) was diluted with DEPC-treated water to a final volume of 1 mL. Within this 1 mL solution, prepared on ice in 1.5 mL nunc tubes (screw top with round bottom; ThermoScientific), 1µL of ampicillin (100 µg/mL; (Sigma) was added to prevent bacterial contamination and 0.3 µL of SILWET-L77 (final concentration of 0.03%) to help with efficient uptake of the dsRNA into the plant. The water control solution also had ampicillin and SILWET-L77. RNA solutions or water were sprayed onto the shoots using a hand sprayer (soaked beforehand in ethanol overnight to minimise contamination and drawn through with DEPC-treated water to remove residual ethanol) in a Biohazard cabinet. To prevent carryover of aerosols from the dsRNA solutions, one treatment was done at a time. Two h after dsRNA inoculation, the jars were sprayed with *eGFP*-labelled *D. septosporum* (FJT175) spores grown as in section 2.2.1. One jar of each replicate was sealed immediately with a sterile petri dish lid and Parafilm™ M (Bemis Neenah, WI), whilst the second jar was left to dry for 10-15 min before sealing. This was done as moisture is needed to germinate spores and the optimum drying time had not been

tested in this type of pathogenicity assay prior to conducting this experiment. Pine microshoots were incubated in a 22˚C controlled growth room and monitored for up to 5.5 weeks for the formation of lesions. At 4.5 weeks needles were sampled from one jar of each of the treatments that had been sealed immediately after inoculation during the experimental setup. The other jar (air dried) was left unopened for comparison and sampled at 5.5 weeks. To check for needles that had fluorescent lesions after 4.5 and 5.5 weeks post-inoculation, shoots were transferred from the sampled jars into a sterile petri dish in a Class II Biohazard cabinet (as in Figure 2.6) and dissected to pull off the individual needles from the stem. Needles were counted and separated based on three different categories: (1) green (alive/healthy) needles, (2) brown (dead/dried) needles and (3) needles with brown necrotic lesions. Dead/dried needles were discarded and t-tests (type 2 equal variance (unpaired)) were performed in Excel using the percentage of needles with eGFP lesions from the individual replicate shoots. Chi-square tests (χ^2) were also performed using numbers of needles with eGFP lesions (Appendix Table A7.11) calculated using the following formula:

$$\chi^2 = \sum \frac{(O-E)^2}{E}$$

Where O = the observed number in a class
E = the number expected in a class that had the sample conformed exactly to the hypothesis.
Σ = summation function

Expected values were calculated based on the hypothesis that there were no significant differences between the number of needles with eGFP DNB lesions between dsRNA-treated and untreated pines. Probability values were determined for the χ^2 values from a probability table, with 1 degree of freedom. If the probability was high, the hypothesis was accepted and if it was 0.05 or less, the hypothesis was rejected (meaning there are differences).

Needles showing visible lesions were transferred to Corning® square bioassay dishes (Sigma-Aldrich, Steinheim, Germany) (Figure 2.8), sealed and photographed under UV using an Olympus SZX16 Fluorescence Stereo Microscope (without opening the plate) to determine if the lesions fluoresced green. Of those sampled, those that had fluorescent lesions were counted and collected for DNA extractions by wrapping them in tinfoil, snap

freezing in liquid nitrogen and storing at -80˚C. Also, remaining whole shoots were removed from the jars and harvested for DNA extractions. All needles and whole shoots were freeze-dried overnight in a Dura-Dry MP freeze-dryer (FTS model; Kinetics Thermal Systems, NY, USA) before extracting gDNA the following day. gDNA was extracted using the 2% CTAB method (section 2.5) for qPCR analyses to estimate the amount of fungal biomass present within the needle lesions. Standard curves and melt curves for the fungal target gene (*DsPksA*) and the pine reference gene (*CAD*) are provided in Appendix Chapter 5, Figures A7.29, as well as the regression line equations, correlation coefficient and efficiency of genes for each standard curve (Table A7.5).

A **B**

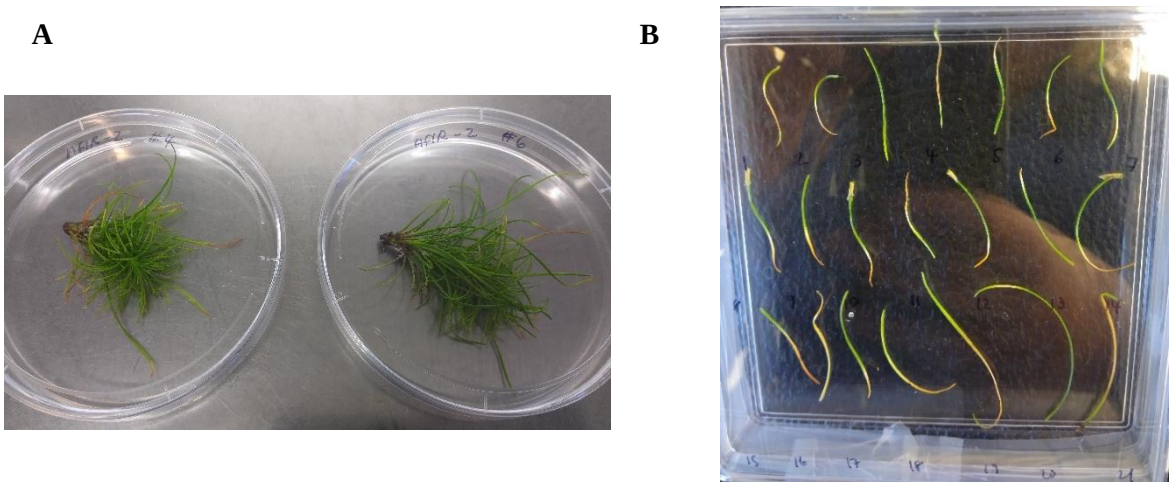

Figure 2.8. Example of pine shoots and needles in petri dish plates. (A) Dissecting whole pine shoots. (B) Arrangement of needles containing lesions in square plate to check for fluorescent lesions.

Biomass quantification was performed using qPCR in a LightCycler 480 III instrument (Roche). The assay utilised by Chettri et al. (2012) to detect the *D. septosporum* target gene polyketide synthase A (*pksA*) and *P. radiata* reference gene cinnamyl alcohol dehydrogenase (*CAD*) was followed, using sequence-specific primers. Standard curves were firstly run for each primer set (*pksA* and *CAD*) with pure gDNA (fungal (eGFP strain) or pine gDNA) serially with MQ to give seven 5-fold dilution points for the regression curve (1000 ng, 200 ng, 40 ng, 8 ng, 1.6 ng, 0.32 ng and 0.064 ng for pine and eGFP *D. septosporum* gDNA). Three technical replicates for each dilution were run for standard curves and two replicates for each DNA sample extracted for infected needle tissue for the assay. The reaction mix consisted of 5 µL of 2X sensiFAST SYBR No-ROX Mix, 0.4 µM of each primer for the target or reference gene, template DNA and MQ water in a 10 µL reaction (Table 2.10). As controls, no template DNA and uninfected

pine DNA templates were included. The cycling programme for SYBR Green consisted of one cycle of pre-amplification at 95˚C for 3 min, 50 cycles of quantification beginning with 5 sec at 95˚C, 10 sec at 60˚C and acquisition at 72˚C for 20 sec, melt curve analysis with one cycle at 95˚C for 10 sec, 65˚C for 1 min and 97˚C with a continuous acquisition mode at a ramp rate of 0.11˚C/sec, followed by cooling at 40˚C for 10 sec to finish (Table 2.10). The number of cycles for quantification was increased to 50 to be able to detect amplification in the lower concentrations. To estimate the amount of fungal biomass in the mixed gDNA samples containing fungal and plant DNA, concentrations of the fungal and pine genes were calculated from the standard curves and the ratios of the fungal *PksA*: pine *CAD* genes then used to estimate the fungal biomass in the plant.

In some of the gDNA samples there was no amplification of the *CAD* and/or *DsPksA* genes so the samples were further purified. For precipitating small volumes of gDNA, TE buffer was added to either 50 µL or 100 µL, transferred to a 0.6 mL microcentrifuge tube and the same volume (50 µL or 100 µL) of choroform/isoamyl alcohol added (24:1 ratio mix). The tubes were inverted, incubated for 3 min at room temperature and centrifuged in a Heraeus Biofuge Pico benchtop microcentrifuge at 13,300 rpm (17,008 × *g*) for 5 min. The upper aqueous phase containing the DNA was transferred to a sterile microcentrifuge tube and 0.1 volumes of 3 M sodium acetate were added, then 2 volumes of cold 100 % ethanol. The gDNA was precipitated overnight for at least 16 h at -20˚C. To pellet the gDNA the tubes were centrifuged for 20 min at 4˚C in a Heraeus Megafuge 16R centrifuge at 13,300 rpm (19,776 × *g*). The supernatant was removed from the tubes and the gDNA washed with either 100-200 µL of cold 70% ethanol and centrifuged for 20 minutes as before. Ethanol was removed from each tube, briefly spun to remove excess ethanol and the pellet air dried at room temperature for 15 minutes. To resuspend the gDNA 10 µL of TE buffer was added and the concentration determined prior to qPCR.

In both cases (tests 1 and 2, before and after re-purification of gDNA, respectively), T-tests were conducted in Excel to determine if differences between pine needles or shoots sprayed with dsRNA had less fungal biomass compared to those treated with water (untreated control) and/or the *eGFP*-dsRNA control.

Table 2.10. Example of reaction set up for quantitative Polymerase Chain Reaction (qPCR) for biomass estimation and the cycling conditions.

For standard curves:

Component	Volume (µL)	Final concentration
2X sensiFAST SYBR No-ROX Mix	5 µL	1X
10 µM forward primer	0.4 µL	400 nM
10 µM reverse primer	0.4 µL	400 nM
MQ	Up to 10 µL	-
Template (gDNA)	1-3.9 µL	1000 ng, 200 ng, 40 ng, 8 ng, 1.6 ng, 0.32 ng, 0.064 ng
Total	**10 µL**	

For actual samples:

Component	Volume (µL)	Final concentration
2X sensiFAST SYBR No-ROX Mix	5 µL	1X
10 µM forward primer	0.4 µL	400 nM
10 µM reverse primer	0.4 µL	400 nM
MQ	Up to 10 µL	-
Template (gDNA)	1-2 µL	-
Total	**10 µL**	

Programme	Cycle number	Temp	Time	Ramp rate
Pre-amplification	1 cycle	95˚C	3 mins	4.4
Quantification	50 cycles	95˚C	5 sec	4.4
		60˚C	10 sec	2.4
		72˚C (single)	20 sec	4.4
Melting curve	1 cycle	95˚C	10 sec	4.4
		65˚C	1 min	2.2
		97˚C	continuous	0.11
Cooling	1 cycle	40˚C	10 sec	1.5

2.13 Bioinformatic analyses to identify *Dothistroma septosporum* gene targets

Bioinformatic tools were used to identify and characterise candidate SIGS gene targets. A list of potential candidates was generated (Chapter 3) and their expression levels *in vitro* and *in planta* were analysed using published transcriptome expression data (Bradshaw et al., 2016). Criteria outlined in a successful SIGS study by McLoughlin et al. (2018) were also considered when selecting the best gene candidates.

Genes which are components of the RNA silencing machinery were first identified using the funRNA database (Choi et al., 2014). This is a "comparative genomics platform for the genes encoding Argonaute, Dicer and RNA-dependent RNA Polymerase." The database works by predicting the number of RNAi genes in a genome, using reference sequences obtained from UniProtKB/SwissProt (see Figure 2.9). Amino acid sequences of the identified genes were then used as query sequences in the JGI MycoCosm database (https://mycocosm.jgi.doe.gov/Dotse1/Dotse1.home.html) (Grigoriev et al., 2011) to perform BLASTp analyses (compares a protein query to a protein database) using BLAST (Basic Local Alignment Search Tool), in order to identify any other RNAi genes from *D. septosporum* and from other fungi, including *Fulvia fulva* (previously called *Cladosporium fulvum*), *Fusarium graminearum, Mycosphaerella graminicola* (now *Zymoseptoria tritici*) *and Sclerotinia sclerotiorum.* In addition, reciprocal BLAST analyses were performed to identify orthologues and any potential off-target sites, to determine if the sequences were specific to their target in *D. septosporum.* The sequences provided in the funRNA database and published SIGS target sequences from different fungal genomes (*S. sclerotiorum, F. graminearum, Botrytis cinerea, Aspergillus nidulans* and *A. parasiticus*), were also used as query sequences (Table 2.11) to identify other orthologous genes in the *D. septosporum* genome (de Wit et al. 2012). Multiple ClustalW protein alignments were assembled in Geneious v9.1.8 (https://www.geneious.com/) (Kearse et al., 2012) to analyse the sequences from known fungal genomes in comparison to the *D. septosporum* sequence. Percentage of amino acid identity matrices and neighbour-joining phylogenetic trees from protein alignments of the RNAi machinery proteins were also performed in Geneious. Gene searches resulted in identification of *DsAflR* (*Ds75566*) and *eGFP* as the top candidate genes. The sequences for these genes were obtained from JGI and Clontech (https://www.addgene.org/browse/sequence_vdb/2485/), respectively. Also, the *DsAflR* nt sequences from 18 isolates of *D. septosporum*

from a total of 15 different countries around the world were aligned and compared against the NZE10 reference genome to check for sequence variability (Bradshaw et al., 2019).

To help determine the best regions for siRNA design, various computational tools were used (Jain & Wadhwa, 2018). These included Eurofins MWG Operon's free online siMAXTM Design Tool (https://www.eurofinsgenomics.eu/en/ecom/tools/sirna-design/#), the BLOCK- iTTM RNAi Designer from Invitrogen (https://rnaidesigner.thermofisher.com/rnaiexpress/), the siDESIGN Centre by Dharmacon https://horizondiscovery.com/en/products/tools/siDESIGN Center) and S4 Zao bioinformatics (https://www.zhaolab.org/pssRNAit/). All of these siRNA tools enabled siRNA off-targets to be analysed and to determine efficient siRNAs. Default parameters were used for all computer tools.

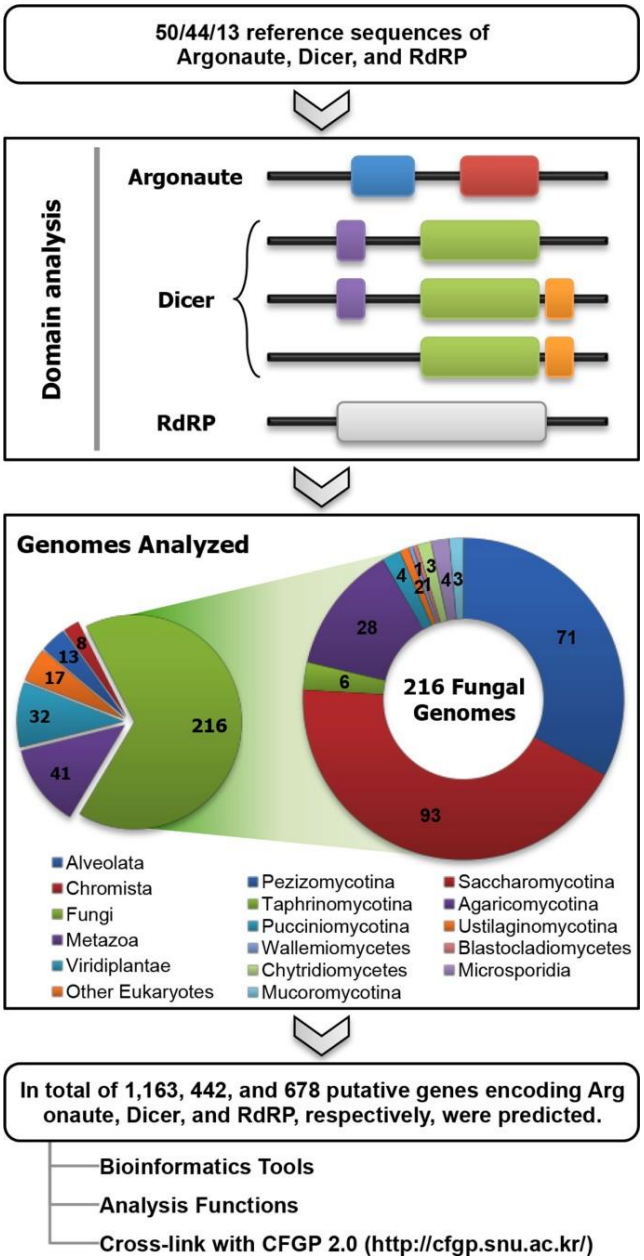

Figure 2.9. Identification pipeline for funRNA. "The identification pipeline for funRNA consists of two steps: i) defining domain profiles from protein sequences encoded by the reference sequences; and ii) scanning 1,440 proteomes with domain profiles for Argonaute, Dicer, and RdRP. In "Domain analysis", coloured boxes indicate essential domains: blue, IPR003100 (Argonaute/Dicer protein, PAZ); red, IPR003165 (Stem cell self-renewal protein Piwi); purple, IPR005034 (Dicer double-stranded RNA-binding fold); green, IPR000999 (Ribonuclease III); orange, IPR001159 (Double-stranded RNA-binding); and grey, IPR007855 (RNA-dependent RNA polymerase, eukaryotic type)." (Choi et al., 2014).

Table 2.11. List of query sequences from published studies used to identify orthologous genes in the *Dothistroma septosporum* genome.

Species	Gene	Name	Accession number (NCBI)	Reference
Aspergillus nidulans	*AflR*	Aflatoxin regulator	AAC49195.1	Chettri et al. (2013)
A. parasiticus	*AflR*	Aflatoxin regulator	AAS66018.1	Chettri et al. (2013)
Botrytis cinerea	*Bctrr1*	Thioredoxin reductase	XP_001560033.1	McLoughlin et al. (2018)
B. cinerea	*TIM44* (BC1G_04775)	Mitochondrial import inner membrane translocase subunit	XP_001556757.1	McLoughlin et al. (2018)
Fusarium graminearum	*DCL1* (FGSG_09025)	Dicer-like protein-1	XP_011328775.1	Werner et al. (2020)
F. graminearum	*DCL2* (FGSG_04408)	Dicer-like protein 2	XP_011321198.1	Werner et al. (2020)
F. graminearum	*CYP51A* (FGSG_04092)	Cytochrome P450 demethylase	XP_011321548.1	Koch et al. (2016)
F. graminearum	*CYP51B* (FGSG_01000)	Cytochrome P450 demethylase	XP_011316750.1	Koch et al. (2016)
F. graminearum	*CYP51C* (FGSG_11024)	Cytochrome P450 demethylase	XP_011325340.1	Koch et al. (2016)
Sclerotinia sclerotiorum	*TIM44* (SS1G_06487)	Mitochondrial import inner membrane translocase subunit	XP_001592247.1	McLoughlin et al. (2018)
S. sclerotiorum	(SS1G_05899)	Thioredoxin reductase	XP_001592977.1	McLoughlin et al. (2018)
S. sclerotiorum	(SS1G_01703)	Aminoacyl tRNA ligase	XP_001597509.1	McLoughlin et al. (2018)

Chapter 3: Identification and Characterisation of Target Gene Candidates for Spray-induced Gene Silencing (SIGS)

3.1 RNA interference (RNAi) silencing machinery genes in fungi

In eukaryotic organisms, such as plants and fungi, gene silencing by RNA is a conserved process. In the fungal kingdom, for example, it occurs in Ascomycetes, Basidiomycetes and Zygomycetes (Cogoni & Macino, 1999; Wang et al., 2010). RNA silencing plays two important roles: to protect cells from viruses and transposons, as well as to regulate the expression of endogenous genes (Borges & Martienssen, 2015; Swarts et al., 2014). There are three key components of the RNAi silencing machinery, which facilitate the recognition and processing of sequence-specific dsRNAs into siRNAs. These are the AGO-PIWI protein family, DCL and RdRP proteins (Casas-Mollano et al., 2016; Shabalina & Koonin, 2008). To regulate the expression of genes and initiate silencing, small non-coding RNAs (sRNAs) interact with protein components of the RNAi machinery (Carthew & Sontheimer, 2009; Guo et al., 2016).

The AGO-PIWI superfamily of proteins generally includes two types of polypeptides, represented by ARGONAUTE1 (AGO1) from *Arabidopsis thaliana* and PIWI from *Drosophila melanogaster* (fruit fly). Importantly, AGO-PIWI proteins are essential components, which can even function in gene silencing independently from Dicer or RdRPs (Casas-Mollano et al., 2016). For example, in animals, a Dicer-independent pathway can be initiated by PIWI-interacting RNAs (piRNAs), which are bound by PIWI proteins in the PIWI pathway (Malone & Hannon, 2009). These are a class of sRNAs that associate with PIWI proteins in animals (Iwasaki et al., 2015). Other RNAi pathways can also function without Dicer, whereby siRNAs can be made by RdRP proteins that make these short transcripts, then bind to AGO proteins to initiate the silencing cascade. This Dicer-independent RNAi pathway has also been found in the nematode *C. elegans* (Aoki et al., 2007; Pak & Fire, 2007; Sijen et al., 2007).

The conserved tertiary structure of AGO-PIWI proteins in eukaryotes includes multiple domains, which play different roles in the RNAi pathway. The N-terminal domain is involved in cleaving target RNA and separating the passenger strand (sense) from the antisense strand (guide) for initiating gene silencing. A second domain, the PIWI-

Argonaute-Zwille (PAZ) domain, binds the 3' end of the guide (antisense) strand. A third domain, named MID (middle), binds the 5' end of the antisense strand, and a fourth domain, called PIWI (RNaseH-like fold domain), cleaves target RNA with complementarity to the antisense strand. Between the N-terminal and PAZ domains is a linker motif, L1; a second linker motif, L2, is between the PAZ and MID domains (see Figure 3.1A). Although AGO-PIWI proteins are prevalent in eukaryotic organisms, these types of proteins are also found in some prokaryotes. It has been suggested that AGO-PIWI proteins originated from a subgroup of PIWIs from Archaea, as eukaryotic AGO-PIWI sequences cluster with those of prokaryotic long PIWIs (Class II type proteins) in phylogenetic analyses (Swarts et al., 2014). AGO-like protein genes are present in genomes characteristic of fungi, green algae and land plants, as well as oomycetes, such as *Phytophthora infestans* (Casas-Mollano et al., 2016).

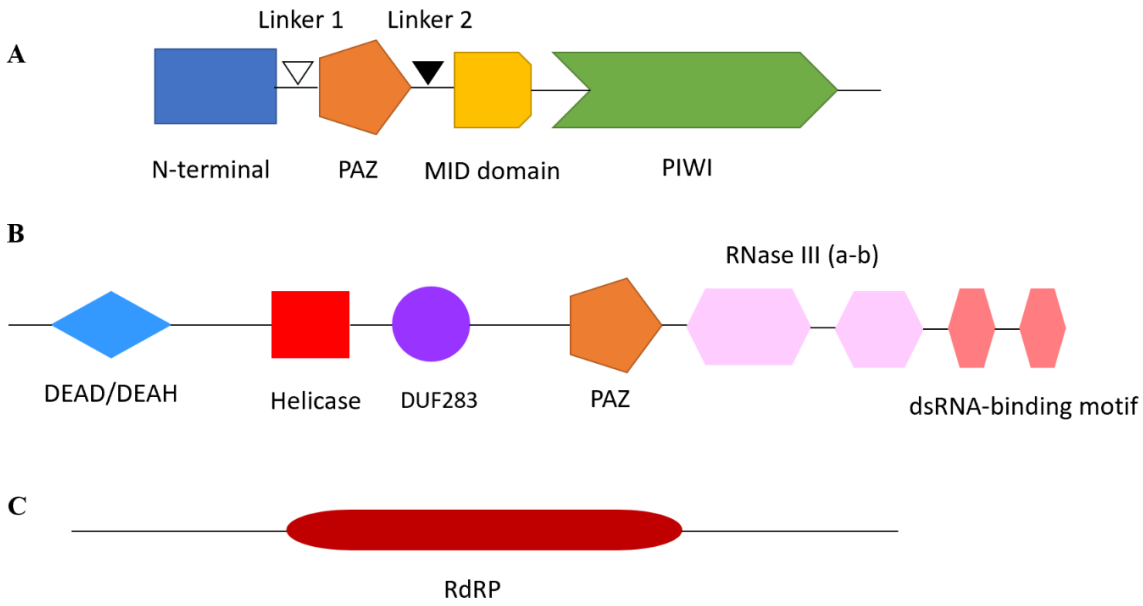

Figure 3.1. Conserved domain structures of Argonaute (AGO)-P-element induced wimpy testis (PIWI), Dicer (or Dicer-like proteins, DCL) and RNA dependent RNA Polymerase (RdRP) proteins in eukaryotes. (A) AGO-PIWI proteins consist of the following domains: N-terminal, PIWI-Argonaute-Zwille (PAZ), Middle (MID) and PIWI. (B) Dicer or DCL proteins have the following domains: DEAD/DEAH, helicase, domain of unknown function 283 (DUF283), PAZ, RNase III (a-b) and a dsRNA binding motif. (C) RdRP proteins have a RdRP domain. The domains and their roles are described in the text. Black bars in all proteins indicate the full protein sequence. Reproduced from Casas-Mollano et al. (2016).

A second component of the RNAi machinery is an RNase III-like enzyme (endonuclease) called Dicer, which functions to process the dsRNAs into 21–24 nt siRNAs (as discussed previously in Chapter 1, section 1.2.2). There is no clear evidence on how Dicer or DCL

proteins evolved, but it has been suggested that the Dicer family became prevalent early in the evolution of eukaryotes and became widespread in eukaryotic organisms like animals, plants, fungi and ciliates (protists) (Cerutti & Casas-Mollano, 2006). The general structure of Dicer or DCL proteins is represented in Figure 3.2B, where it has various domains, including a DEAD/DEAH-like helicase domain, helicase domain (HELICc superfamily C-terminal domain), DUF283 (domain of unknown function, but found to contain a dsRNA-binding fold in *A. thaliana* (Qin et al., 2010)), PAZ domain, two RNase III catalytic domains (a and b) and a dsRNA-binding motif domain (Casas-Mollano et al., 2016). The DEAD/DEAH-like domain is an RNA helicase domain that unwinds the dsRNA with its helicase activity. In turn, there is also another helicase domain also involved in RNA unwinding (Kini & Walton, 2007). The PAZ domain (also present in AGO) is responsible for binding dsRNA. The processing of dsRNA takes place within the two active sites of the RNase III domains to cleave the sense and antisense RNA strands, producing ssRNA (Carthew & Sontheimer, 2009).

The third component of the RNAi machinery, RdRP, has a single RNA-dependent RNA polymerase domain. This enzyme generates dsRNA from single-stranded transcripts and in some cases can act to produce secondary siRNAs. The process of secondary amplification of siRNAs can occur in both the fungus and the plant, whereby these siRNAs are processed by the RNAi machinery in either cell type. The process of synthesising secondary siRNAs requires an RdRP (Pak & Fire, 2007). A single domain is present in RdRP proteins (Figure 3C, Casas-Mollano et al. (2016)) that is required for generating dsRNA from ssRNA, or to amplify siRNA signals (Cogoni & Macino, 1999).

Whilst there is conservation of RNAi genes, some fungal species are known to possess multiple copies of the RNAi genes. Examples where fungal species belonging to the Dothideomycetes harbour different numbers of RNAi genes are shown in Table 3.1. Why certain fungal species have multiple copies whilst other species do not (Choi et al., 2014) is uncertain, although the RNAi machinery is known to have a broad spectrum of roles in fungi. Studies on mutants of the FHB pathogen, *F. graminearum*, that are deficient in one or more of the components of the RNAi machinery, including Dicer, AGO and RdRP, demonstrated important roles of these proteins in other processes, such as conidiation, sexual development and pathogenicity (Gaffar et al., 2019). This is supported by the

findings of Weiberg et al. (2013), Kusch et al. (2018), Carreras-Villasenor et al. (2013), Segers et al. (2007) and Campo et al. (2016), where other roles of RNAi machinery have been elucidated in fungi. In some species there is functional redundancy, with multiple copies of RNAi pathway components, where only one functioning version of a gene is actually required. The genome of *Colletotrichum higginsianum*, for example, encodes two argonaute genes (*agl-1* and *agl-2*), but only one (*agl-1*) functions in RNAi gene silencing (Campo et al., 2016). This suggests the potential for additional copies of RNAi genes to have other roles.

Although the eukaryotic RNAi machinery is proposed to have been present in even early eukaryotes (Shabalina & Koonin, 2008), some fungal species have lost their RNAi machinery completely (Billmyre et al., 2013). For instance, the yeast *Saccharomyces cerevisiae* has completely lost RNAi, due to lacking the core components of the RNAi machinery, but RNAi can be restored by introducing genes such as Dicer and Argonaute from its close relative *Saccharomyces castelli* (Drinnenberg et al., 2009). There are examples where RNAi genes are missing in filamentous fungi, like in *Ustilago maydis*, where the *Ago*1, *RdRP*1-3, and *Dcr*1 genes are absent (Laurie et al., 2012). Species belonging to the subphyla Ustilaginomycotina and Wallemiomycetes, within the phylum Basidiomycota, and some members of the phylum Microsporidia have also lost their RNAi genes (Choi et al., 2014).

Table 3.1. Examples of Dothideomycete fungi that possess multiple copies of genes encoding RNAi machinery components.

Fungal species	Dicer genes	Argonaute genes	RdRP genes
Acidomyces richmondensis	1	2	3
Alternaria brassicicola	2	4	3
*Fulvia fulva***	2	4	3
Cochliobolus heterostrophus	2	3	5
Leptosphaeria maculans	2	3	3
*Mycosphaerella graminicola****	1	4	2
Pyrenophora tritici-repentis	2	4	3

* The numbers of RNAi genes listed are from Choi et al. (2014) (funRNA database, http://funrna.riceblast.snu.ac.kr/index.php?a=view).
** *Fulvia fulva* (syn. *Cladosporium fulvum*).
***Mycosphaerella graminicola* is now known as *Zymoseptoria tritici*.

By targeting components of the RNAi machinery there have been successful RNAi studies that have protected plants from fungal diseases like FHB (Werner et al., 2020) and citrus blue mould (Yin et al., 2020). Manually and computationally designed dsRNA constructs targeting dicer and argonaute in *F. graminearum* were effective in reducing disease symptoms in barley, compared to plants which had not been sprayed with gene-specific dsRNAs (Werner et al., 2020). In contrast, silencing of *DCL-1* and *DCL-2* in *Penicillium italicum* reduced the virulence of the fungal pathogen, especially the *DCL-2* RNAi transformant which severely impaired virulence (Yin et al., 2020). The same authors also applied dsRNAs targeting *DCL-2* to wounds on the surface of oranges inoculated with *P. italicum* and found reduced expression of *DCL-2* as well as reduced virulence (Yin et al., 2020).

Considering that most fungal species have RNAi genes, and consistent with findings that these are important genes required for RNAi-mediated pathways in pathogens, it was expected that *D. septosporum* would have RNAi genes. However these genes had not been studied in *D. septosporum* prior to this work.

3.2 Identification of candidate *Dothistroma septosporum* genes as targets for RNA silencing

In order to identify suitable target genes for RNA silencing in *D. septosporum*, genes associated with virulence and genes that have been targeted successfully in published SIGS studies were assessed. A successful SIGS study conducted by McLoughlin et al. (2018) recommended characteristics of genes which would be good candidates for SIGS and those that should be avoided (Table 3.2). Target genes should not be very lowly or highly expressed, to ensure that any differences in endogenous gene expression due to SIGS treatment can be detected. Essential genes common to closely related species should also be avoided to prevent OTEs in other species (McLoughlin et al., 2018) and transcripts should be no less than 200 nt in length. It has been shown that dsRNA longer than 200 nt results in a wider variety of siRNAs (Andrade & Hunter, 2016).

The first results section of this chapter (Section 3.3) addresses whether *D. septosporum* possesses genes encoding RNAi machinery and whether these genes are expressed. The following parts focus on identifying potential target genes for SIGS trials with *D. septosporum*. An in-depth analysis of the candidate genes was completed to ensure

that the genes used in this study would be specific to *D. septosporum* and would potentially reduce its virulence if they were silenced.

Table 3.2. Criteria for selecting candidate target genes for RNA silencing in phytopathogenic fungi.

Criteria	Choose	Avoid
RNA-seq dataset	Genes upregulated in common host infection conditions	Genes down regulated during host infection
Essential genes	Essential genes. Genes can be found in the Database of Essential Genes[a]	Essential genes highly conserved in closely related species
Biological processes	Genes involved in Reactive Oxygen Species (ROS) response, protein modification, pathogenicity factors, splicing, protein modification, translation, cell wall modification	Genes involved in general growth, transport, electron carriers, signal transduction, pigment synthesis, carbohydrate metabolism
Expression levels	FPKM[b] values between 1 and 500 during host infection	Lowly (FPKM<1) or highly (FPKM>500) expressed during host infection
Transcript length	Above 200 nucleotides	Below 200 nucleotides
Gene location	Nuclear-encoded	Organelle-encoded
Redundancy	Single function or without homologues	Genes with multiple homologues and functionally similar roles

[a]www.essentialgene.org.
[b]Fragments Per Kilobase of transcript per Million mapped reads (FPKM).
Table is adapted from McLoughlin et al. (2018).

3.3 Results

3.3.1 RNAi machinery in *Dothistroma septosporum*

A search for orthologous genes that are components of the RNA silencing machinery was made in the *D. septosporum* genome, using characterised RNAi genes from Dothideomycetes and other fungi that are itemised in the funRNA database (Choi et al., 2014) (Chapter 2, section 2.13). An overview of the *D. septosporum DCL*, *AGO* and *RdRP* genes, and their orthologues in close relatives *F. fulva* and *Z. tritici* is shown in Table 3.3; each of these types of genes are discussed in turn below.

Table 3.3. RNA interference (RNAi) genes in *Dothistroma septosporum* and their similarity to *Fulvia fulva* and *Zymoseptoria tritici* genes.

Gene Information		*Fulvia fulva*			*Zymoseptoria tritici*		
Gene	**Protein ID[a]**	**E-value Ff[c]**	**% ID Ff[d]**	**Accession Ff[e]**	**E-value Zt[f]**	**% ID Zt[g]**	**Accession Zt[h]**
DCL	Ds56023	3.15E-048	85.5	Cf187182	0	63.0	Mg47983
			18.4	Cf186490			
*AGO**	Ds71322	0	87.4	Cf185632	0	59.9	Mg38035
	Ds92165	0	42.2	Cf194206	0	18.2	Mg90232**
	Ds74936	0	89.7	Cf195424	0	73.3	Mg10621
RdRP	Ds69242	3.39E-125	38.1	Cf196780	-	-	-
	Ds138071	0	92.2	Cf197136	0	64.6	Mg49833
	Ds110589	0	80.7	Cf194468	0	56.0	Mg51407

[a]Protein identification (accession; PID) numbers refer to those in the JGI MycoCosm database (http://genome.jgi.doe.gov/Dotse1/Dotse1.home.html) for *Dothistroma septosporum*.
[b]Expression levels of genes in Reads Per Kilobase of transcript per million (RPMK) *in vitro* and the early, mid and late stages of infection *in planta*. Data retrieved from Bradshaw et al. (2016).
[c]The E-value is the probability that the query sequence from *D. septosporum* matches the target gene in *Fulvia fulva* by chance.
[d]Percentage amino acid sequence identity of the *F. fulva* protein sequence to *D. septosporum* ortholog(s).
[e]Number of copies of each gene component of the RNA interference (RNAi) machinery in *F. fulva* and its accession number.
[f]The E-value is the probability that the query sequence from *D. septosporum* matches the target gene in *Zymoseptoria tritici* by chance.
[g]Percentage amino acid sequence identity of the *Z. tritici* protein sequence to *D. septosporum* ortholog(s).
[h]Number of copies of RNAi genes in *Z. tritici* and its accession number (*Mycosphaerella graminicola* (Mg)).
**F. fulva* and *Z. tritici* also have an extra *AGO* gene in their genome (see Appendix Table A7.2) (Cf191892 and Mycgr_fgenesh1_pg.C_chr_1001447 (locus name)).
**Note that Mg90232 is not a reciprocal hit to Ds92165.

From funRNA, it was predicted that the *D. septosporum* genome contains a single copy of the *DCL-1* gene (*Ds56023*) (Table 3.3), which encodes a protein that is 1,549 amino acids (aa) in length. To analyse whether each of the RNAi genes in *D. septosporum* were orthologous to the core genes in the Dothideomycetes, *F. fulva* and *Z. tritici*, a matrix of identity was performed from alignments of the protein sequences (as in Chapter 2, section 2.14). The matrix shows a pairwise comparison of similarity to the genes in each species. Ds56023 and Cf187182 share 85.5% identity, which is higher to that of CfDCL-2 (Cf186490; 18.4%), while Ds56023 and Mg47983 share 63% identity (Appendix Chapter 3, Table A7.1). The expression of the *D. septosporum DCL-1* gene, *Ds56023*, is very low in culture and *in planta*, with not much variation in gene expression in the conditions

tested. The maximum expression of *DCL-1* is only 8 FPKM (Bradshaw et al., 2016). Similarly low levels of expression are also seen in the two *F. fulva DCL* genes (Appendix Chapter 3, Table A7.4) (Mesarich et al., 2014).

DCL protein sequences were compared by performing sequence alignments along with homologues from fungi in other taxonomic classes to determine if there was similarity to *D. septosporum* DCL-1 (Appendix Chapter 3, Figure A7.1C). Phylogenetic trees were constructed using the DCL protein sequences from the alignments. The DCL phylogenetic tree showed that the proteins form two main groups/clusters, which are characteristic of DCL-1 and DCL-2 proteins (Figure 3.2).

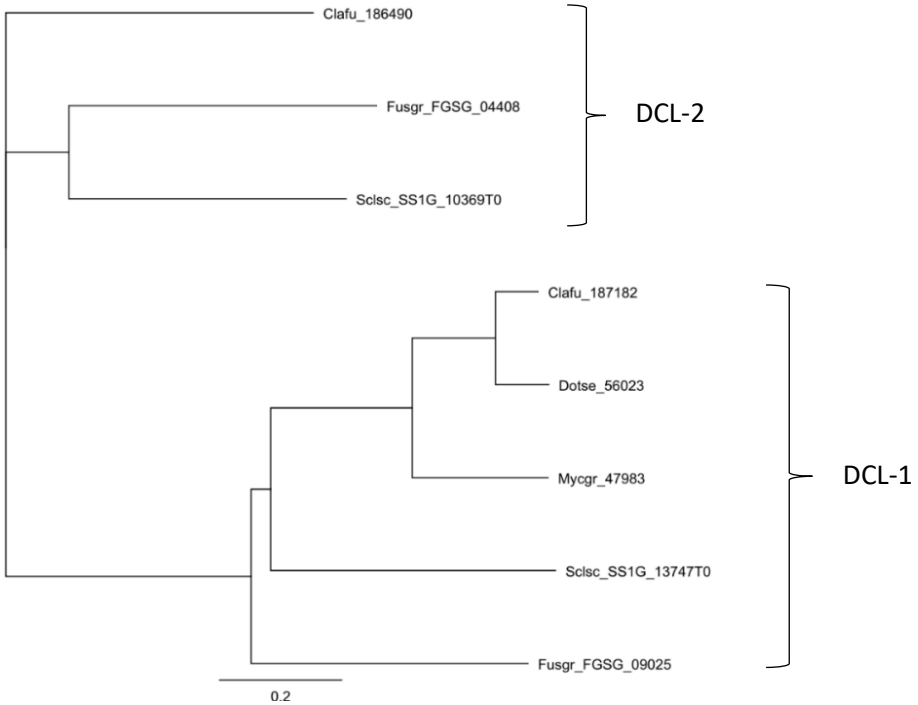

Figure 3.2. Phylogenetic tree of Dicer-like proteins (DCLs) in Dothideomycetes and other fungi. Neighbour-joining tree of DCL homologues from various fungal species including: *Fulvia fulva* (Clafu), *Dothistroma septosporum* (Dotse), *Mycosphaerella graminicola* (*Zymoseptoria tritici*) (Mycgr), *Fusarium graminearum* (Fusgr) and *Sclerotinia sclerotiorum* (Sclsc). The number after the species name is the JGI protein ID number. The bottom group is DCL-1 in all species and the top group DCL-2. The scale bar indicates 0.2 substitutions per site.

Of the five fungal species studied here, only *F. fulva*, *F. graminearum* and *S. sclerotiorum* have two DCL proteins (Figure 3.2). Conservation of amino acids seen in DCL proteins of *D. septosporum*, *F. fulva*, *Z. tritici*, *S. sclerotiorum* and *F. graminearum* correlate with the protein domains, indicating conservation of functional domains across these fungal species (Figure 3.3). In *D. septosporum* DCL-1 there are four domains: DEAD-like

helicase domain, a helicase domain, a dicer dsRNA-binding fold domain and a ribonuclease III domain. All of these are also present in *F. fulva* and *Z. tritici* DCL proteins, but these other species have an additional domain (dsRNA-binding) that does not appear to be present in DsDCL-1. A PAZ domain is absent in all *DCL* genes in these fungal species (Figure 3.3), which is different to the conserved structure of eukaryotic *DCL* genes (Figure 3.1). Another difference among all these aligned DCL proteins is that DCL-1 of *S. sclerotiorum* (SS1G_1347T0) lacks an N-terminal region DEAD domain, however it may be an incorrect gene model or a pseudogene, as the N-terminal region of the protein differs to the other proteins. It also lacks the C-terminal dsRNA-binding domain, which is also absent in DCL-1 of *D. septosporum* (Figure 3.3). However, these domains may be redundant, as most of the fungal DCL proteins shown in Figure 3.3 have two dsRNA-binding domains: the dsRNA-binding domain at the C-terminus and a dsRNA-binding fold and heterodimerisation domain located towards the N-terminus.

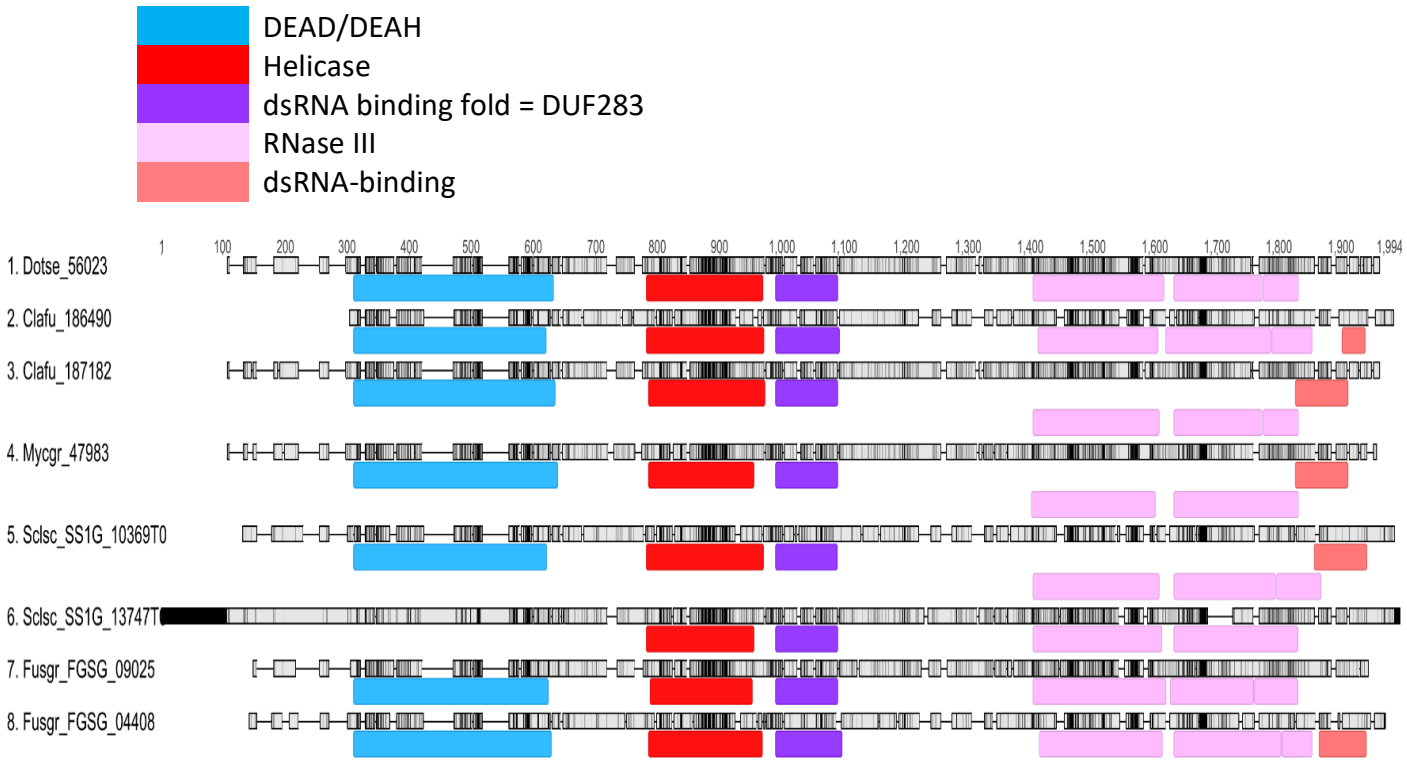

Figure 3.3. Schematic representation of the domains in Dicer-like (DCL) proteins in Dothideomycetes and other fungi. Sequences were obtained from JGI (https://mycocosm.jgi.doe.gov/mycocosm/home) or the funRNA database (http://funrna.riceblast.snu.ac.kr/index.php?a=view) and domains as predicted by Choi et al. (2014) are colour-coded with reference to the same colours used in Figure 3.1 for the general structure of eukaryotic DCL proteins. (1) *Dothistroma septosporum* DCL-1 (Dotse_56023). (2) *Fulvia fulva* DCL-2 (Clafu_186490). (3) *F. fulva* DCL-1 (Clafu_187182). (4) *Zymoseptoria tritici* DCL-1 (Mycgr_47983). (5) *Sclerotinia sclerotiorum* (Sclsc) DCL-2 (SS1G_10369T0) (pseudogene or incorrect gene model). (6)

S. sclerotiorum (Sclsc) DCL-1 (SS1G_13747T0). (7) *Fusarium graminearum* (Fusgr) DCL-1 (FGSG_09025). (8) *F. graminearum* (Fusgr) DCL-2 (FGSG_04408).

Three *AGO* genes were found in the *D. septosporum* genome (*DsAGO*), including *Ds713221*, *Ds92165* and *Ds74936*. These genes encode 1,016 aa, 1,043 aa and 533 aa proteins respectively, as predicted from funRNA. They each appear to be orthologous to one of the three *F. fulva* and *Z. tritici AGO* genes, as shown by the amino identity matrix (Appendix Chapter 3, Table A7.2), except Mg90232 (is not a reciprocal best hit to Ds92165). For example, *Ds74936* (*AGO*) and *Cf195424* (*AGO*) share the highest level of identity with each other (89.7%), indicating these are orthologous. These two AGO proteins also share the highest identity of all of the orthologous *AGO* gene pairs. The relationships between these *AGO* genes are supported by the phylogenetic analysis, showing that they are grouped into three clusters (Figure 3.4). A fourth *AGO* gene exists within the genomes of *F. fulva* (*Cf191892*) and *Z. tritici* (locus name: fgenesh1_pg.C_chr_1001447), forming a fourth group in the phylogeny (Figure 3.4). The most highly expressed of the *AGO* genes in *D. septosporum* (*Ds71332*; Bradshaw et al., 2016) and that of its *F. fulva* orthologue (*Cf185632*; (de Wit et al., 2012; Mesarich et al., 2014)) (Appendix Chapter 3, Table A7.4) were also top matches to each other with 87.4% identity (Table A7.2). All of the other gene copies have low expression in the conditions tested.

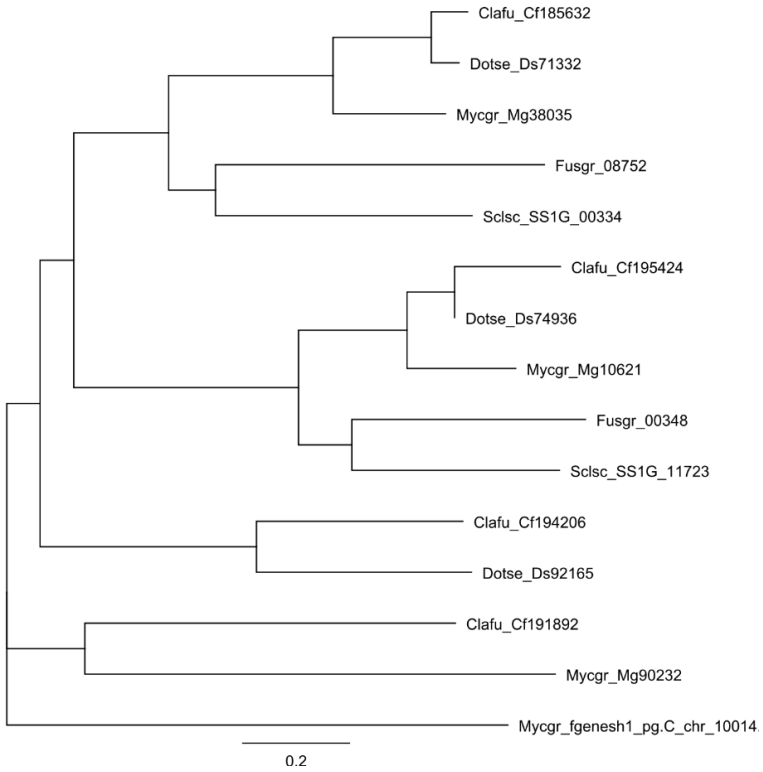

Figure 3.4. Phylogenetic tree of Argonaute (AGO) proteins in Dothideomycetes and other fungi. Phylogenetic tree constructed using the Neighbour-joining method. *Fulvia fulva* (Clafu), *Dothistroma septosporum* (Dotse), *Zymoseptoria tritici* (Mycgr), *Fusarium graminearum* (Fusgr) and *Sclerotinia sclerotiorum* (Sclsc). The scale bar indicates 0.2 substitutions per site. The number after the species name is the JGI protein ID number.

Sequence alignments show conservation of amino acids as seen with the DCL proteins (Figure A7.1B). All three AGO proteins in *D. septosporum* are predicted to have three domains consisting of a ribonuclease H-like domain, a PAZ domain and a DUF1785 domain, with the exception of Ds74936 only having two domains (DUF1785 is absent), as the predicted protein lacks the N-terminal region (Figure 3.5). Of all the conserved domains in eukaryotes shown in Figure 3.1, only a PAZ domain is present in AGO proteins of *D. septosporum*, *F. fulva* and *Z. tritici*. The N-terminal, MID and PIWI domains shown in Figure 3.1 are predicted to be absent in all these fungi (Figure 3.5).

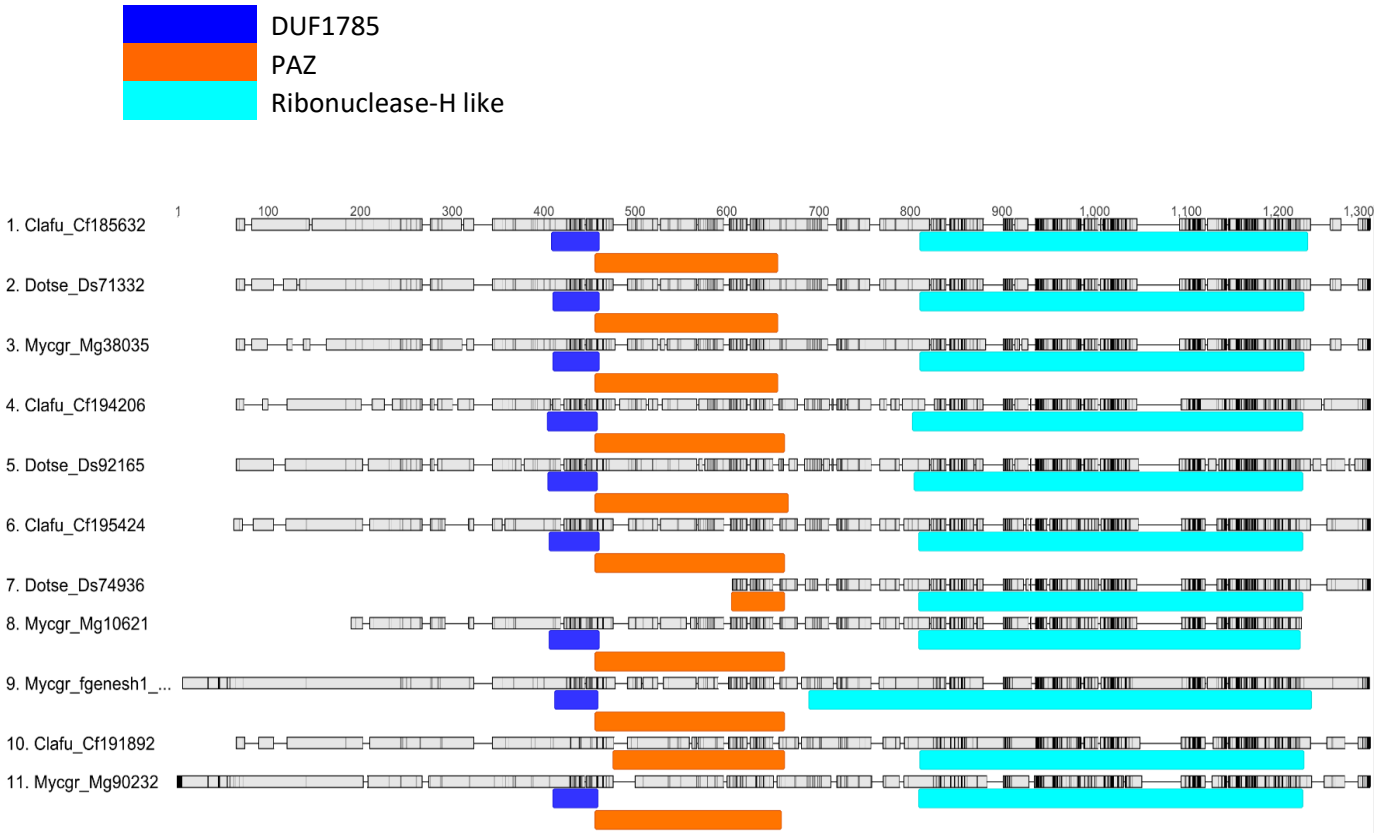

Figure 3.5. Schematic representation of Argonaute (AGO) proteins in Dothideomycete fungi. Sequences were obtained from JGI (https://mycocosm.jgi.doe.gov/mycocosm/home) or the funRNA database (http://funrna.riceblast.snu.ac.kr/index.php?a=view). Domains as predicted by Choi et al. (2014) are shown below each sequence and colour coded with reference to the same colours used in Figure 3.1 for the general structure of eukaryotic AGO proteins. (1) *Fulvia fulva* AGO (Clafu_185632). (2) *Dothistroma septosporum* AGO (Dotse_71332). (3) *Zymoseptoria tritici* AGO (Mycgr_38035). (4) *F. fulva* AGO (Clafu_194206). (5) *D. septosporum* AGO (Dotse_92165). (6) *F. fulva* AGO (Clafu_195424). (7) *D. septosporum* (Dotse_74936) (Pseudogene or incorrect gene model). (8) *Z. tritici* AGO (Mycgr_10621). (9) *Z. tritici* AGO (Mycgr_fgenesh1_pg.C_chr_1001447). (10) *F. fulva* AGO (Clafu_191892). (11) *Z. tritici* AGO (Mycgr_90232).

D. septosporum also harbours three copies of *RdRP* genes (*DsRdRP*) (Table 3.3). These are *Ds69242* (816 aa protein), *Ds138071* (947 aa protein) and *Ds110589* (1,155 aa protein). Table 3.3 shows that Ds138071 has the highest amino acid identity (92.2%) to Cf197136 and 64.6% identity to Mg49833. The matrix shows that all three RdRP proteins in *D. septosporum* are orthologous to the *RdRPs* in *F. fulva* and *Z. tritici* (Appendix Chapter 3, Table A7.3). This is supported by the grouping of these genes into three main clusters in the phylogenetic tree, corresponding to the three sets of orthologous genes (Figure 3.6). The expression levels of *RdRPs* in *D. septosporum* are low (Bradshaw et al., 2016), consistent with low expression of the *RdRPs* in *F. fulva* (Mesarich et al., 2014).

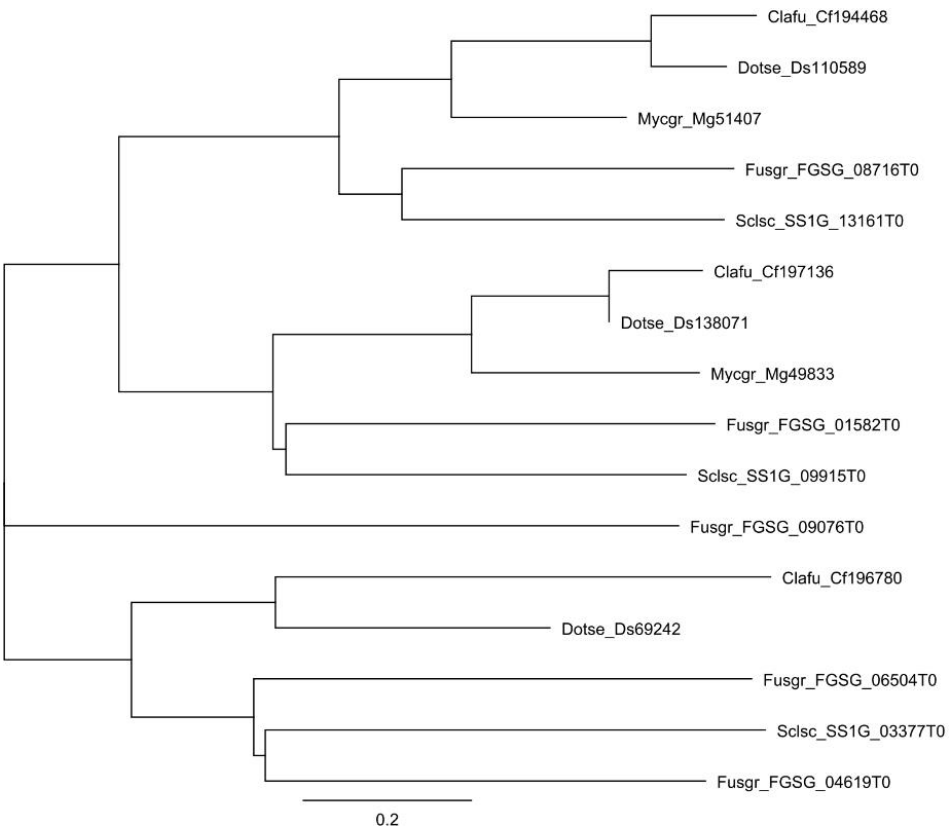

Figure 3.6. Phylogenetic tree of RNA-dependent RNA Polymerase (RdRP) proteins in Dothideomycetes and other fungi. Neighbour-joining tree of RdRP homologues of Dothideomycete fungi and unrelated fungi. *Fulvia fulva* (Clafu), *Dothistroma septosporum* (Dotse), *Zymoseptoria tritici* (Mycgr), *Fusarium graminearum* (Fusgr) and *Sclerotinia sclerotiorum* (Sclsc). The scale bar indicates 0.2 substitutions per site. The number after the species name is the JGI protein ID number.

Amino acid conservation is observed with the RdRP proteins, as with the other gene families (Appendix Chapter 3, Figure A7.1C). All of the *D. septosporum*, *F. fulva* and *Z. tritici* RdRP proteins have a typical eukaryotic-type RdRP domain (Figure 3.7), as predicted by funRNA (Choi et al., 2014), which correlates with the single domain present in most eukaryotic RdRP proteins (Figure 3.1).

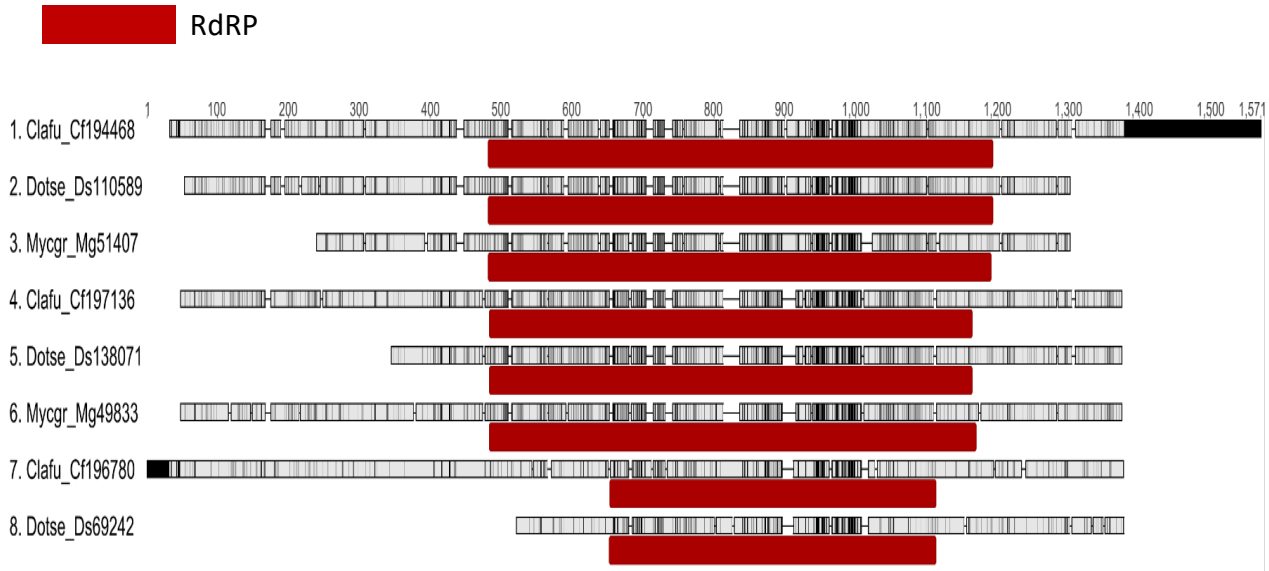

Figure 3.7. Schematic representation of RNA-dependent RNA Polymerase (RdRP) proteins in Dothideomycete fungi. Sequences were obtained from JGI (https://mycocosm.jgi.doe.gov/mycocosm/home) or the funRNA (http://funrna.riceblast.snu.ac.kr/index.php?a=view) database and domains as predicted by Choi et al. (2014) are colour coded with reference to the same colours used in Figure 3.1 for the general structure of eukaryotic RdRP proteins. (1) *Fulvia fulva* RdRP (Clafu_194468). (2) *Dothistroma septosporum* RdRP (Dotse_110589). (3) *Zymoseptoria tritici* RdRP (Mycgr_51407). (4) *F. fulva* RdRP (Clafu_197136). (5) *D. septosporum* RdRP (Dotse_138071). (6) *Z. tritici* RdRP (Mycgr_49833). (7) *F. fulva* RdRP (Clafu_196780). (8) *D. septosporum* RdRP (Dotse_69242).

3.3.2 Determining the best *Dothistroma septosporum* gene targets for spray-induced gene silencing (SIGS)

DCL and AGO

In previous RNA silencing studies in other fungi, *DCL* and *AGO* were effectively silenced, despite the fact that they are part of the fungal silencing machinery and could therefore affect the efficiency of RNA silencing. Werner et al. (2020) showed that SIGS was effective in combating the fungal pathogen *F. graminearum* when *AGO*1, *AGO*2, *DCL*1, and *DCL*2 were individually silenced, leading to effective protection of its host plant barley. These authors used manual- and computational tool-designed dsRNA constructs of various lengths but found greater silencing efficiency using the manually designed dsRNAs. Moreover, the dsRNAs targeting *DCL* had enhanced silencing compared to the dsRNAs targeting *AGO*. In another study, Wang et al. (2016) expressed sRNAs that targeted both *DCL1* and *DCL2* in the grey mould pathogen *Botrytis cinerea*, reducing its virulence to *Arabidopsis* and tomato, as well as to other fruits (strawberry,

grape), vegetables (lettuce, onion) and rose. Their research suggested that "fungal *DCLs* are ideal target genes to knock down in order to control pathogens that use sRNA effectors." (Wang et al., 2016). A single *DCL* gene orthologue (*Ds56023*) was found in the *D. septosporum* genome, using the *F. graminearum DCL-1* genes (Werner et al., 2020) as query sequences (previous results section, 3.3.1). However, because *Ds56023* is only expressed at a low level *in vitro* and *in planta*, it is not a good target for RNA silencing (see Table 3.4). It is important that the gene targets are expressed *in culture* and the early stages *in planta* at sufficient levels to be detectable by qRT-PCR and also to be suppressed by RNA silencing.

PksA, AflR, Ver1 and VbsA

Dothistromin and aflatoxin are toxins produced by some species of fungi. The mycotoxin dothistromin has structural homology to the aflatoxin precursor Versicolorin B (Chapter 1, section 1.1.4) and is known to be a virulence factor in *D. septosporum* (Kabir et al., 2015a). Biosynthetic genes involved in the pathway to produce dothistromin are expressed during the early and mid-stages of infection in *P. radiata* (Bradshaw & Zhang, 2006). Of these biosynthetic genes, polyketide synthase A (*pksA*) is a key gene involved in one of the first steps of dothistromin biosynthesis and is orthologous to the polyketide synthase gene *aflC* in *Aspergillus parasiticus* and *Aspergillus nidulans* (Chettri et al., 2013). *D. septosporum PksA* (*Ds48345*) is a good candidate for SIGS, as it is essential for the production of dothistromin (Bradshaw et al., 2006). However, because of its low expression level *in planta* (Table 3.4), the mRNA may not be detected easily to determine if expression has been reduced.

AflR is an excellent candidate gene to explore the effects of RNAi-mediated knockdown. In *D. septosporum*, this is a dothistromin pathway regulatory gene involved in the production of dothistromin (Chettri et al., 2013). A study showed that inverted repeat transgenes (IRTs) that targeted *AflR* when transformed into *A. parasiticus* or *A. flavus*, or similarly the regulatory gene *Tri6* in *F. graminearum*, could suppress the production of their respective mycotoxins aflatoxin and deoxynivalenol (DON; produced by *F. graminearum*), since there was reduced expression of toxin pathway genes (McDonald et al., 2005).

Table 3.4. List of possible candidate target genes and their relative expression levels *in vitro* and *in planta*.

JGI protein ID	Gene	FM_RPMK (in culture)[1]	E_RPMK (early)[1]	M_RPMK (mid)[1]	L_RPMK (late)[1]
Ds56023	*DCL*	2.22	7.97	2.47	3.08
Ds192192*	*PksA*	26.51	10.02	94.49	63.04
Ds75566	*AflR*	230.30	46.05	89.23	156.68
Ds192193**	*Ver1*	184.76	115.74	1018.31	918.99
Ds75656	*VbsA*	147.19	25.08	488.63	307.50
Ds75009	*Hdp1*	9234.40	455.07	6493.99	4861.60
Ds75130	*C-type lectin*	1338.11	6349.07	860.42	646.51
Ds68376	*Pf2*	33.32	17.81	41.91	26.06
Ds71189	*Nps3*	12.61	46.31	15.38	19.72
Ds56624	*CYP51*	146.88	40.71	33.80	46.93
Ds70643	*Alpha amylase*	7.86	40.47	18.60	533.98
Ds75147	*Alpha amylase*	14.20	153.08	42.62	679.79
Ds75239	*Alpha amylase*	4.03	15.63	1.53	172.35
Ds90760	*Alpha amylase*	5.37	2.21	34.47	58.69
Ds69025	*TIM44*	153.27	100.02	56.87	38.42
Ds92325	*Thioredoxin reductase*	166.64	356.74	379.21	165.13
Ds75609	*Aminoacyl tRNA ligase*	9.29	35.57	24.41	140.92

*An alternative JGI protein ID number is Ds48345.
**Alternative JGI protein ID is Ds75411.
[1]Expression levels of genes from different infection stages of the fungus *in planta* (*P. radiata*; early, mid and late) in Reads Per Kilobase of transcript per million (RPMK). Sourced from a transcriptome study (Bradshaw et al., 2016).

The versicolorin reductase (*Ver1*/*dotA*; Ds75411) and versicolorin B synthase precursor (*VbsA*; Ds75656) dothistromin pathway genes are also possible SIGS targets. These *D. septosporum* genes were identified as orthologues of *aflM* from *A. parasiticus* (*Ver1*), and *AtcN* and *aflK* genes from *A. nidulans* and *A. parasiticus*, respectively (*VbsA*). Both *Ver1* and *VbsA* genes of *D. septosporum* have higher expression levels during the mid and late stages of infection *in planta* compared to growth *in vitro* (Table 3.4). These genes

could be suitable candidates for SIGS in *D. septosporum*, as they are essential for dothistromin production (Bradshaw et al., 2002; Zhang et al., 2007).

Hydrophobin and C-type lectin

Other genes assessed as possible SIGS targets included those involved in fungal growth, and also appear to be highly expressed, or could affect pathogen virulence. These genes included hydrophobin (*Hdp1*) and C-type lectin genes. Dagenais et al. (2010) and Lacroix et al. (2008) showed that hydrophobins in some fungi are responsible for lowering host defences by preventing recognition of fungal spores by the host immune system, suggesting a role in virulence. Hydrophobin proteins also have a role in adhesion. In *D. septosporum*, however, deletion of the highly expressed hydrophobin gene, *Hdp1* (*Ds75009*), did not result in decreased virulence (Bradshaw et al., 2016). Three other hydrophobin genes were found in the *D. septosporum* genome that might have complemented the loss of Hdp1 function, but their expression levels were very low (Table 3.4; Bradshaw et al., 2016). The problem with highly expressed genes, such as *Ds75009*, is that dsRNA targeting these genes may not be as effective since they are already expressed at very high levels. For example, if 90% of silencing is achieved, because the gene is expressed so highly, 10% expression could still be sufficient for the gene to fully carry out its biological function. As noted by McLoughlin et al. (2018), the chances of observing a reduction in target gene expression that has an effect on pathogen virulence will be increased by using genes that are expressed at levels less than 500 FPMK (Table 3.2).

C-type lectins are proteins that harbour a carbohydrate-binding domain (Bradshaw et al., 2016). There are 42 predicted C-type lectin genes in *D. septosporum*, making them unsuitable target gene candidates, due to the potential for a high level of functional redundancy. There is also variable expression among the genes, but one gene, *Ds75130*, is highly expressed *in vitro* and *in planta*, with the highest levels during the early stages of growth in pine (Table 3.4).

Pf2, Nps3

Other possible candidates that are expressed only *in planta* and are possible virulence factor genes include *Pf2* and *Nps3*. Pf2 was identified in the fungus *Parastagonospora*

nodorum as a transcription factor (TF) that positively regulates necrotrophic effector gene expression and is required for virulence on wheat (Jones et al., 2019). A study conducted by McLoughlin et al. (2018) showed that targeting another probable transcription factor with dsRNA, the *SS1G_06305* gene of *Sclerotinia sclerotiorum*, increased, rather than decreased disease symptoms on *Brassica napus* (canola). Instead, the desired outcome should typically be reduced symptoms of disease, or ideally disease-free plants if RNA silencing has worked. The *Pf2* gene in *D. septosporum* is only expressed at low levels (Table 3.4), therefore was excluded as a potential target gene.

Nps3 encodes a non-ribosomal peptide synthase in *D. septosporum.* The Nps3 secondary metabolite is a putative virulence factor in DNB based on studies with *Nps3* mutants (Ozturk et al., 2019) and the expression of *Nps3* in the early stages of infection (Bradshaw et al., 2016). However, since *Nps3* is not a very highly expressed gene, it would not be an ideal gene target for SIGS, as it would be difficult to monitor reductions in gene expression, both *in vitro* and *in planta*.

Cytochrome P450 lanosterol C-14-α-demethylase and alpha amylases

Cytochrome P450 lanosterol C-14-α-demethylase (*CYP51*) and alpha amylase genes are also potentially suitable SIGS targets. CYP51 is an essential enzyme which functions in the synthesis of sterols such as ergosterol, a major component of the cell membrane of fungi (Henneberry & Sturley, 2005), making it a common target for azole fungicides (Koch et al., 2013). SIGS with a *CYP*3-dsRNA targeting three *CYP51* genes (*CYP51A*, *CYP51B* and *CYP51C*) was effective in combating the pathogen *F. graminearum* that causes FHB in its host barley (Koch et al., 2016). A BLAST search of the *D. septosporum* genome using the query sequences from Koch's study (2016) (Chapter 2, Table 2.11) revealed a top hit (*Ds56624*) that is homologous to all three *FgCYP51* genes. *Ds56624* is not very highly expressed either *in vitro* or *in planta*, with quite low expression in pine, therefore is not a suitable candidate.

Other possible target genes that were considered from the literature were *alpha amylases*. Gilbert et al. (2018) tested RNA silencing in the fungal pathogen *A. flavus* to protect maize crops, which was successful in reducing alpha amylase (*amy1*) gene expression within the fungal pathogen and also had a significant effect on reducing the production

of aflatoxins by the fungus. Alpha amylase genes are highly expressed in *D. septosporum* inside pine needles and are thought to be responsible for breaking down the starch stored in green islands around lesions, supposedly for providing a nutrition source for the pathogen (Bradshaw et al., 2016; Kabir et al., 2015a). Four alpha amylase genes were found in the *D. septosporum* genome: *Ds70643*, *Ds75147*, *Ds75239* and *Ds90760*. The expression levels for each of these genes vary, with high expression of *Ds70643* and *Ds75147* (>500RPMK) in the late stages of infection *in planta* and the other two genes (*Ds75239* and *Ds90760*) showing low expression overall *in vitro* and *in planta* (Bradshaw et al., 2016). Although alpha amylases appear to be possible candidate genes, they were not pursued in this current study due to the presence of four gene copies, therefore all genes would need to be targeted.

TIM44, thioredoxin reductase and aminoacyl tRNA ligase

Silencing of genes encoding mitochondrial import inner membrane translocase subunit 44 (*TIM44*), thioredoxin reductase and aminoacyl tRNA ligase, with gene-specific *B. cinerea* and *S. sclerotiorum* dsRNAs, have been shown to reduce oilseed rape infection symptoms (McLoughlin et al., 2018). TIM44 is an inner membrane protein that is a subunit of the PAM complex, which functions in the transfer of substrates into the mitochondrial matrix (Dolezal et al., 2006), whilst thioredoxin reductase is a key enzyme that functions in defence against oxidative stress (Arnér & Holmgren, 2000; Mustacich & Powis, 2000). Aminoacyl tRNA ligases are enzymes involved in attaching specific amino acids to corresponding tRNAs for translation of RNA to proteins (Francklyn et al., 2002). Orthologues of these genes are present in the *D. septosporum* genome: *Ds69025* (*TIM44*), *Ds92325* (thioredoxin reductase) and *Ds75609* (aminoacyl tRNA ligase). All three genes are moderately expressed *in vitro* and *in planta*, but within the range suggested by McLoughlin et al. (2018) (>1 FPMK but <500 FPMK) (Bradshaw et al., 2016), and could be suitable potential targets to explore the RNAi effect, downregulating expression of genes.

GFP

Silencing of *GFP* (green fluorescent protein) in *GFP*-expressing fungal strains has been shown to be successful in RNAi studies and has the advantage of providing visual evidence of a decrease in GFP fluorescence and suppression of *GFP* mRNA transcript

levels (Fitzgerald et al., 2004; Koch et al., 2016; Wytinck, Sullivan, et al., 2020). This makes *GFP* a suitable candidate for silencing trials with *D. septosporum* and therefore was used in this study. An *eGFP*-expressing strain of *D. septosporum* (FJT175) was made via protoplast-based transformation to introduce the *eGFP* gene into its genome as in Appendix section 7.6.1.

3.4 Discussion

3.4.1 The *Dothistroma septosporum* NZE10 genome contains orthologs of genes that are characterised as part of the RNA interference (RNAi) silencing machinery

Identification of RNAi genes is key to determining if *D. septosporum* has a functional RNAi pathway and is able to process dsRNA. Orthologs of core genes involved in RNAi were found in *D. septosporum*. These were one *DCL*, three *AGO* and three *RdRP* genes (Table 3.3). Each of the predicted proteins from these *DCL*, *AGO* and *RdRP* genes in *D. septosporum* share similar features to other fungal RNAi proteins and contain conserved domains characteristic of eukaryotes (Figure 3.2). The DCL protein in *D. septosporum* has DEAD-like, helicase, dsRNA-binding fold (DUF283) and RNase III domains similar to other fungal DCL proteins but appears to lack a second dsRNA-binding domain (Figure 3.5). According to Hu et al. (2013), some Ascomycete fungi have two dsRNA-binding domains but some have only one. The dsRNA-binding fold and heterodimerisation domain present in *D. septosporum*, predicted by the funRNA database, is likely to be the DUF283 domain. In *A. thaliana*, a DUF283 domain was shown to have a fold that is structurally similar to a dsRNA-binding domain, but showed only weak binding to dsRNA, instead selectively binding to other proteins, such as HYL1, which is involved in involved in dsRNA binding in *A. thaliana* (Qin et al., 2010). The PAZ domain, essential for RNA recognition, is also absent in *D. septosporum* and other fungal DCL proteins (Figure 3.2), similar to *Saccharomyces pombe*, which also lacks the PAZ domain (Paturi & Deshmukh, 2021). Choi et al. (2014) found that the PAZ domain is not widely distributed throughout fungi, as it was only shown to be found in 9 of 232 fungal proteomes, indicating that the PAZ domain is rare. This domain is more common in plants and metazoans.

The three AGO proteins in *D. septosporum*, as well as the AGO proteins studied here have different domains from the typical eukaryotic structure of AGO proteins. In comparison to the fungus *Verticillium nonalfalfae* which has an N-terminal domain, as well as DUF, PAZ and PIWI domains, *D. septosporum* does not have an N-terminal domain or PIWI domains in its AGO proteins; instead it has DUF1785, PAZ and ribonucleaseH-like domains. However, the PIWI domain is known to be an RNase-H domain that functions in cleaving mRNA in the RISC complex (Song et al., 2004), suggesting that the alternative domain (RNase-H like) present in *D. septosporum* and other fungi has the same function as PIWI. In Ds74936, which encodes a smaller protein, the DUF domain also appears to be absent, but this could be due to a truncated gene or incorrect gene model.

The three RdRPs in *D. septosporum* contain the eukaryotic RdRP domain, which is consistent with other fungal species such as *F. fulva*, *Z. tritici*, *S. sclerotiorum F. graminearum* and *V. nonalfalfae* that also have this domain (Figure 3.5; Jesenicnik et al. (2019)) and is conserved across eukaryotes (Casas-Mollano et al., 2016).

3.4.2 Variation in gene expression and the number of copies of RNA interference (RNAi) genes in *Dothistroma septosporum* and other fungi

Despite conservation of core genes that form part of the RNA silencing machinery, fungal species show variation in the number of *DCL*, *AGO* and *RdRP* genes within their genomes. A difference in gene copy numbers was seen between *D. septosporum* and its close relative *F. fulva*. One copy of *DCL* was identified in *D. septosporum* and two copies in *F. fulva* (Table 3.3). Most fungi have one or more Dicer and/or *DCL* genes, suggesting that one copy is sufficient for functioning. Other fungi that have one gene copy include *Z. tritici* and *Acidomyces richmondensis*, while other fungi like species of *Aspergillus* (*A. niger*, *A. oryzae*, *A. flavus*, *A. tubingensis* and *A. carbonarius*), can have up to three Dicer genes (Choi et al., 2014). *Neurospora crassa* has two genes encoding DCL proteins (*DCL-1* and *DCL-2*); mutant strains defective in *DCL-1* or *DCL-2* were not impaired in RNA silencing (single mutants), however, the double mutant (Δ*DCL-1/2*) was completely impaired. This result suggested that the activity of Dicer is highly important for silencing RNA in *N. crassa* and the Dicer genes are redundant in the silencing pathway, as only one of them is required. This finding could help explain why some fungal species possess

a single Dicer gene, whereas others have two copies, but these additional copies could have roles in other processes, which have only been characterised in a few fungi (Catalanotto et al., 2004; Gaffar et al., 2019).

D. septosporum has three *AGO* genes, whilst *F. fulva* and *Z. tritici* each have four (Table 3.3). This finding supports the fact that duplications of argonaute genes are common among Ascomycetes (Choi et al., 2014). Three RdRP genes were found in both *D. septosporum* and *F. fulva*, whilst *Z. tritici* only had two (Table 3.3). These results demonstrate that the number of genes varies between fungal species. Amino acid alignments showed that there is conservation in sequence across fungal species in all three core proteins (DCL, AGO and RdRP). This finding is consistent with the idea that components of the RNAi silencing machinery are conserved amongst eukaryotes and fungi belonging to different fungal groups, including Ascomycetes (Cogoni and Macino, 1999; Nicolás et al., 2003; Wang et al., 2010; Billmyre et al., 2013).

Whilst there are multiple copies of RNAi genes in the RNAi pathway, not all genes are expressed. Transcriptome expression analysis data showed that all seven *D. septosporum* core genes have low expression in the conditions tested (Bradshaw et al., 2016) and expression of the *F. fulva* orthologues is also low (Mesarich et al., 2014). The one exception is the *AGO* orthologues *Ds71322* and *Cf185632* (CFU840258) being the most highly expressed genes out of all the core genes in each species (Appendix Table A7.4). More research is required to identify whether any of these RNAi genes in *D. septosporum* are upregulated under different conditions, or in response to treatment with dsRNA, but the fact that *D. septosporum* has RNAi silencing machinery suggests it is possible that the pathogen could be controlled by RNAi to protect pine from DNB.

Loss of RNA interference in some fungal species is due to the lack of core genes required for dsRNA processing and silencing of target genes. Some fungal species, such as *S. cerevisiae* and *U. maydis*, appear to have lost their complete set of RNAi genes and therefore the RNA silencing machinery (Drinnenberg et al., 2011; Billmyre et al., 2013). In some fungi, lack of RNAi is associated with the presence of a dsRNA killer virus in the population; the killer virus encodes a toxin but also confers toxin resistance on its host cells (Drinnenberg et al., 2011). The RNAi pathway would normally be activated to

inhibit the virus. However, as shown in *S. cerevisiae*, there is a selective advantage to losing RNAi, but maintaining the killer virus, because the virus confers resistance to toxins made by other cells that still retain the virus (Drinnenberg et al., 2011; Welsh & Leibowitz, 1982). It is well established that RNAi controls transposons (Billmyre et al., 2013; Mosa & Youssef, 2021; Yamanaka et al., 2013). In cases where there is a need to rapidly adapt to a new environment, there is a selective advantage to losing RNAi because this leads to more frequent transposon movement, and consequently a hypermutator phenotype (Oliver et al., 2000). It is possible that an ancestor of *D. septosporum* did have a second dicer gene that was lost (as hypothesised previously), maybe as there was no selection pressure to keep this second dicer gene.

3.4.3 Identification of *DsAflR* as a virulence gene in *Dothistroma septosporum* to target for spray-induced gene silencing

The *DsAflR* gene in *D. septosporum* is the regulatory gene for the biosynthetic pathway genes involved in producing the virulence factor dothistromin (Chettri et al., 2013; Kabir et al., 2015a). By targeting the *DsAflR* gene there is potential for the fungus to be less virulent if there is a reduction in dothistromin levels, as a result of lower expression of the pathway genes. *DsAflR* is not too highly or lowly expressed and there is only one copy of this gene in the genome, which fits the McLoughlin et al. (2018) criteria. Orthologues of this gene are only present in few fungi, most notably species of *Aspergillus* (Bradshaw et al., 2013).

Silencing of *AflR* and *pksA* in *Aspergillus species* has been successful in reducing aflatoxin levels. Aflatoxins are potent secondary metabolite compounds or toxins produced by species of *Aspergillus*, such as *A. flavus* and *A. parasiticus* (Wu et al., 2009). Thakare et al. (2017) showed that HIGS is successful in eliminating aflatoxins by use of transgenic maize plants containing RNAi constructs targeting *A. flavus, AflC*, a polyketide synthase (*PksA*), which is a key enzyme in the aflatoxin biosynthetic pathway. HIGS was also explored in another study by Masanga et al. (2015), to reduce the production of aflatoxins by targeting the transcription factor *AflR* in *A. flavus*. In both HIGS studies the outcomes were similar in terms of a significant reduction in the accumulation of aflatoxins. These toxins were not detected in transgenic maize lines infected with *A. flavus* (Thakare et al., 2017) and low levels of aflatoxins were observed compared to WT maize

plants (Masanga et al., 2015). These studies highlight the potential for suppression of aflatoxin levels in fungal contaminants of crops.

RNA silencing has been performed by targeting genes involved in production of another fungal toxin, cercosporin. Cercosporin absorbs light energy to generate reactive oxygen species (ROS), such as singlet oxygen (Daub & Hangarter, 1983) and is an important virulence factor in *Cercospora species* including *Cercospora nicotianae*, the causal agent of cercospora leaf blight (CLB). RNA silencing studies involving cercosporin genes as targets led to a reduction in the production of this toxic compound during disease development, therefore having a significant effect on reducing disease symptoms (Thomas et al., 2020; Zivanovic & Chen, 2021). HIGS to produce transgenic strains of tobacco with constructs targeting *CTB1* (cercosporin toxin biosynthesis 1), a polyketide synthase, and *CTB8*, a pathway regulator of the cercosporin biosynthetic pathway, were effective in HIGS to control *C. nicotianae*. However, silencing of these genes showed high levels of resistance to *C. nicotianae* in some lines and variable resistance in other lines, and also silencing of *CTB1* was more effective than that of *CTB8* (Thomas et al., 2020). Suppression of cercosporin production via HIGS has also been characterised in *Cercospora* cf. *flagellaris* (*C. kikuchiivia*) (Zivanovic & Chen, 2021). Genes that played vital roles in cercosporin production and are also important for virulence were candidate target genes. Of these, dsRNAs were produced targeting either *CTB1*, *CTB8*, *HNR* (hydroxynaphthalene reductase) and *AHCY* (adenosylhomocysteinase). *In vitro* cultures treated with dsRNAs showed that the most significant effect on silencing cercosporin production was seen for *CTB8* (Zivanovic & Chen, 2021). This result differed to Thomas et al. (2020), where silencing was most efficient for *CTB1*, but silencing was achieved in a different *Cercospora* species, suggesting that the choice of target genes needs to be tailored to the pathogen of interest. However, silencing of genes that contribute to pathogen virulence is successful in decreasing levels of cercosporin produced by *Cercospora species*.

3.4.4 *GFP* as a marker gene for spray-induced gene silencing

The *GFP* gene provides a visual marker for RNA silencing. In this way, GFP can serve as a control to determine if *GFP* is silenced within a target fungal pathogen by inhibitory *GFP*-dsRNAs, making it advantageous since a visual reduction in GFP fluorescence will be seen. A study where *GFP*-dsRNA has been used as a control was in a GFP strain of *F. graminearum* (Koch et al., 2016). GFP was also silenced in another study (Fitzgerald et al., 2004) in a different fungal pathogen, *Venturia inaequalis*, the causal agent of apple scab. In that species, another marker gene trihydroxynaphthalene reductase (*THN*) was also silenced and a chimeric inverted repeat hairpin construct targeting both *GFP* and *THN* was created to initiate multiple gene silencing. There was found to be a 71% efficiency of gene silencing for *GFP* and 61% for *THN*. There was also a 51% frequency of silencing for both genes (*GFP* and *THN*) from the inverted repeat hairpin construct (Fitzgerald et al., 2004). GFP has also been used as a marker for RNAi in the fungal rice blast pathogen *Magnaporthe oryzae* by introducing sense, antisense and hairpin RNA constructs targeting *eGFP* in an *eGFP*-expressing transformant strain. A greater efficiency of silencing was observed using hairpin RNA rather than sense or antisense RNA, as confirmed by a reduction in *eGFP* fluorescence in *eGFP* (Kadotani et al., 2003). The fact that there have been many successes in silencing the marker gene *GFP* highlights its potential as a suitable target gene, so *D. septosporum* transformants constitutively expressing an *eGFP* gene were produced for the purposes of this study (Appendix 7.6.1).

3.4.5 Summary of gene candidates for spray-induced gene silencing (SIGS) in *Dothistroma septosporum*

An extensive evaluation of candidate genes was necessary to determine the best targets for gene silencing, alongside *eGFP* as a target gene control. Among these, *DsAflR* (*Ds75566*) was the most promising and was therefore selected as the top candidate to pursue for this study and to potentially reduce the virulence of *D. septosporum. DsAflR* is a known virulence factor and is a single-copy gene that is only found in a restricted range of fungi (Chettri et al., 2013; Bradshaw et al., 2013), therefore is less likely to have off target effects on other fungi, than if targeting genes that are widespread throughout many fungi, such as housekeeping genes. Two other top candidates are *Ver1* (*Ds75411*) (Bradshaw et al., 2002) and *VbsA* (*Ds75656*) (Zhang et al., 2007). These genes are expressed at a sufficient level in culture and *in planta*, and gene knockouts have shown that these genes have a role in dothistromin production. These genes were not included

in RNA silencing trials in this study but could be used as targets for future research on RNAi in *D. septosporum.*

Chapter 4: Design, Production and Efficacy of Uptake of dsRNA

4.1 Importance of dsRNA design and uptake

The choice of target genes for gene silencing studies remains vital to achieving suppression of pathogen genes involved in the disease process. Similarly, the location of the target region within a gene, and the length of the dsRNA target, are also important. Höfle et al. (2020) compared efficiencies of gene silencing by dsRNA with varying lengths of dsRNAs that targeted either the full sequence or partial sequences of a gene. When silencing *CYP51* genes in *F. graminearum* that are involved in virulence, they found that the size of the dsRNA influenced the efficiency of SIGS, but with HIGS there was no correlation with the length of dsRNAs used. Furthermore, by spraying barley leaves with 400 nt *CYP51*-dsRNA constructs, they found lower levels of infection by *F. graminearum*, when compared to spraying with dsRNAs targeting the full-length gene. The number of off-target sequences were also investigated using *CYP51* dsRNA and found to increase with increasing dsRNA length (Höfle et al., 2020).

Successful uptake of dsRNA is also highly important for silencing fungal genes by SIGS. If there is low efficiency of dsRNA uptake, silencing is unlikely to be effective and therefore SIGS targeted to virulence genes will not inhibit infection by the target pathogen. Qiao et al. (2021) acknowledged that the efficacy of uptake is dependent on the pathogen itself and demonstrated differences in uptake efficiency among a range of plant-pathogenic fungi. Their study determined whether the selected pathogens (*S. sclerotiorum, A. niger, Rhizoctonia solani, Verticillium dahliae, Colletotrichum gloeosporioides*) were able to take up RNA from the environment. Further, they investigated whether a non-pathogenic fungus called *Trichoderma virens*, and an oomycete pathogen *Phytophthora infestans*, were also able to take up environmental RNA. The pathogens able to take up RNA with a high efficiency included *S. sclerotiorum, A. niger, R. solani* and *V. dahliae.* No RNA uptake was seen in *C. gloeosporioides*, there was moderate uptake in *T. virens*, and limited uptake in *P. infestans.* Consistent with these findings was suppression of disease that occurred as a result of the pathogens having high uptake efficiency; conversely those that had a much lower uptake efficiency did not show a reduction in symptoms of infection (Qiao et al., 2021). In another study *Z. tritici* was

shown not to take up dsRNA (Kettles et al., 2019). The aim of this chapter is to address the importance of dsRNA design and delivery strategies, based on current recommendations in the literature, and apply these to the design and synthesis of dsRNAs specific to *D. septosporum.* It also aims to address whether the dsRNAs used in this study are able to be taken up directly by *D. septosporum.*

4.2 Results

4.2.1 Construction of *DsAflR* and *eGFP* templates for dsRNA synthesis

In the previous section (Chapter 3), the choice of gene targets was discussed. Two successful gene candidates that were pursued as targets for RNA silencing in this study were an *eGFP* control and *DsAflR*. The target regions for each of these genes were amplified using template DNA as described previously (Chapter 2, section 2.9.2); the positions of the two target regions within *DsAflR* are shown in Appendix Figure A7.24. Sense and antisense plasmids, used for dsRNA synthesis to produce the dsRNA, were distinguished by the presence of a single T7 promoter on opposing primers (5'-end). A 509 bp fragment of *DsAflR* was amplified (Figure 4.1A, lanes 1 and 2) for *DsAflR* 1 and 408 bp for *DsAflR* 2 (Figure 4.1A, lanes 3 and 4) using phosphorylated primers shown in Table 2.3 (Chapter 2, section 2.4). A 737 bp fragment of *eGFP* was also amplified (Figure 4.1B, lanes 1 and 2).

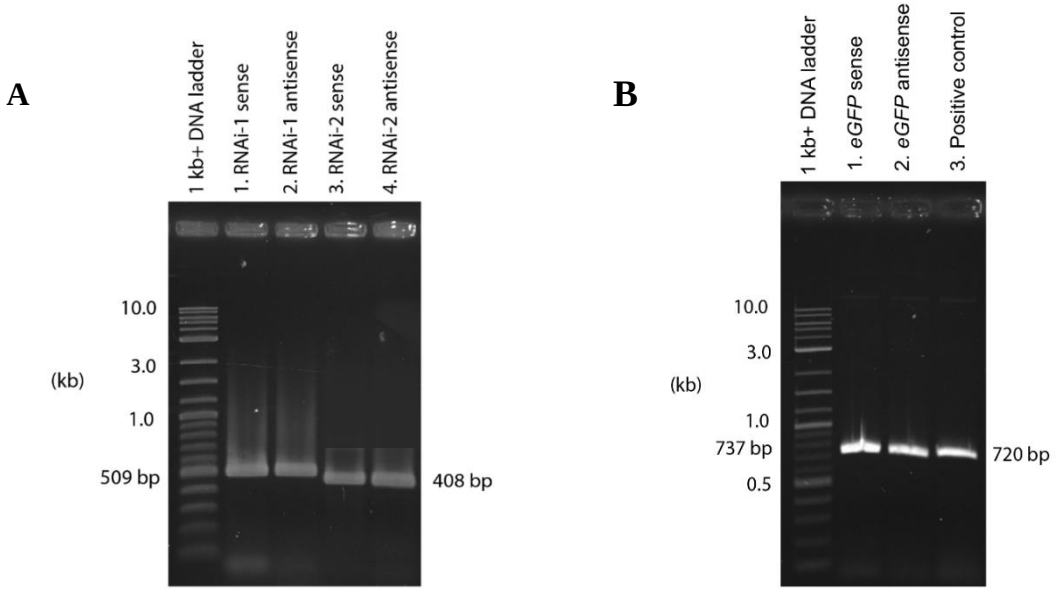

Figure 4.1. Polymerase Chain Reaction (PCR)-mediated amplification of nucleotide sequences from genes encoding the dothistromin pathway regulatory protein (*DsAflR*) and enhanced green fluorescent protein (*eGFP*). (A) Amplification of *DsAflR* sense and antisense templates for *DsAflR* 1 (509 bp) and *DsAflR* 2 (408 bp) from WT *D. septosporum* genomic DNA (gDNA). (B) Amplification of *eGFP* templates for sense and antisense from the plasmid pPN82 (pR239). As a positive control, a 720 bp product of *eGFP* was amplified from pR239 plasmid DNA. A 1 kb+ DNA ladder is shown for size reference.

The *eGFP* and *DsAflR* PCR products were then cloned into the pICH41021 plasmid, using a series of steps as shown in Figure 4.2 and described in Chapter 2 (Section 2.9), to create sense and antisense dsRNA constructs for *eGFP*, *DsAflR* 1 and *DsAflR* 2. To linearise the pICH41021 plasmid for ligating the sense and antisense PCR products, the enzyme *Sma*I was used to produce a blunt end. PCR products were ligated into the plasmid vector (dephosphorylated), transformed into *E. coli* and selected plasmids extracted, screened by PCR (Figure 4.3), and sequenced to confirm the correct sequence (Appendix Chapter 4).

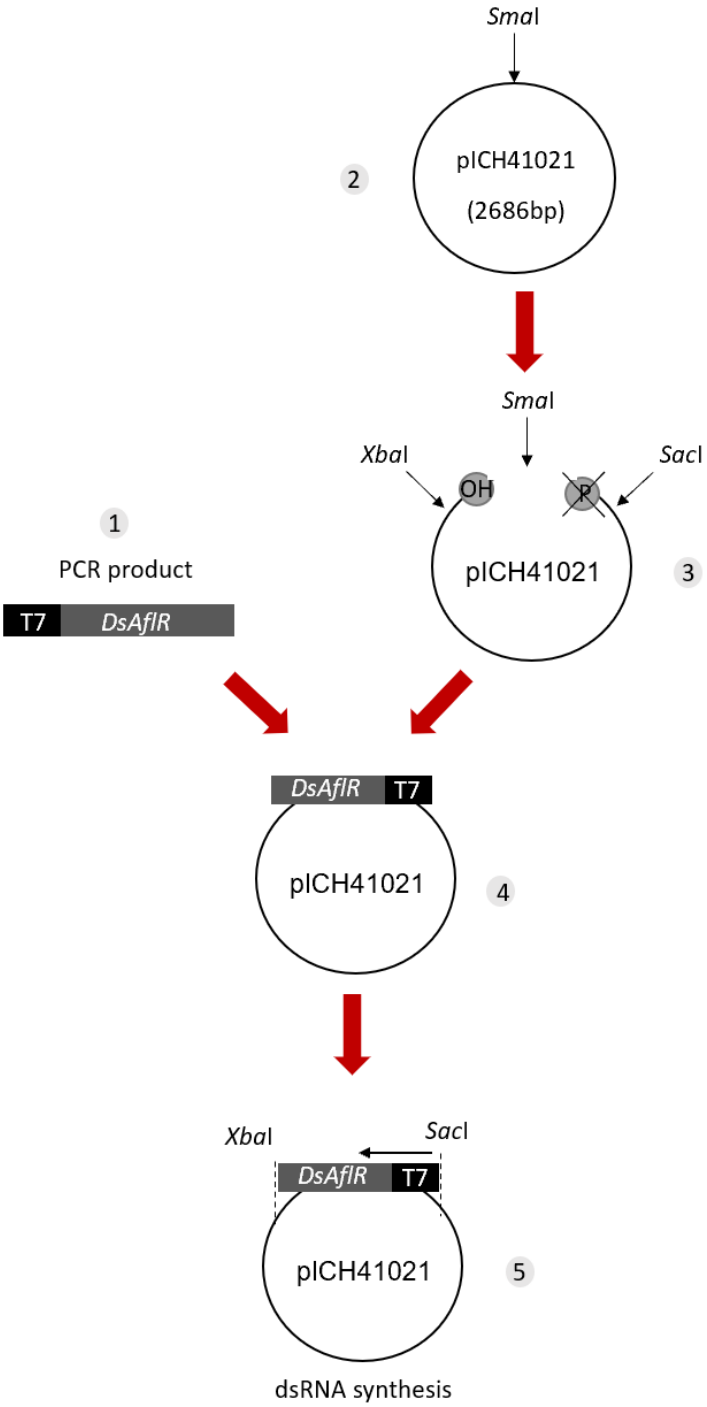

Figure 4.2. Example of the experimental design for cloning *DsAflR* 1 sense sequence *in vitro*. (1) Amplification of *DsAflR* 1 sense sequence by Polymerase Chain Reaction (PCR). (2) Digestion of plasmid with *Sma*I to make a single cut to open up the plasmid for insertion of the PCR product. (3) Dephosphorylation of plasmid. (4) Ligation of PCR product into the plasmid. (5) Orientation of the fragment in the plasmid with respect to the enzyme downstream of the insert. Here it shows that *Xba*I is downstream of the insert.

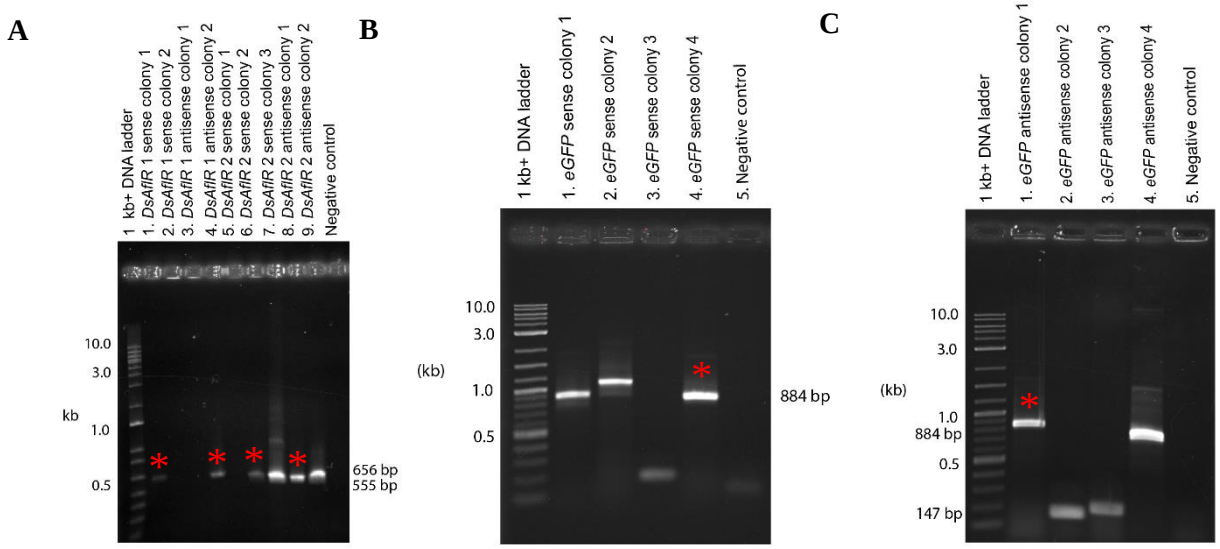

Figure 4.3. Confirmation of positive bacterial clones that have taken up the plasmid containing the insert via Polymerase Chain Reaction (PCR). A blue colony from the control ligation plate (*Sma*I-cut pICH41021) was used as a negative control in all PCRs. Primers M13 LacZ fwd and M13 LacZ rev were used in all cases (Chapter 2, Table 2.3). (A) Verification of *DsAflR* 1 in the dsRNA sense and antisense plasmid constructs using plasmid primers to amplify a 656 bp fragment (509 bp (insert) + 147 bp (flanking plasmid sequence)). Verification of *DsAflR* 2 in the dsRNA sense and antisense plasmid constructs to amplify a 555 bp product (408 bp (insert) + 147 bp (flanking plasmid sequence)). (B, C) Verification of an 884 bp fragment of *eGFP* in the dsRNA sense (B) and antisense (C) plasmid constructs. See Appendix Chapter 4 section 7.5.3 for the plasmid maps and sequence text files. A 1 kb+ DNA ladder is shown. Bacterial clones that were carried forward for extracting plasmid DNA are indicated by an asterisk.

4.2.2 Optimisation of the transcription reaction

Various DNA templates and different incubation times were used in the transcription reaction to optimise conditions for dsRNA synthesis. These conditions and the efficiencies of each dsRNA synthesis reaction are summarised in Table 4.1. DNA templates included (1) gel-purified linearised plasmids, (2) sodium acetate and ethanol-precipitated linearised plasmids and (3) commercially synthesised fragments. To test that the RNAi kit was working properly, the positive control template provided in the kit was also used to synthesise dsRNA (Chapter 2, section 2.10.1). Gel-purified linearised plasmids (1) were sense and antisense plasmid constructs that were linearised with respect to the enzyme in the plasmid backbone downstream from the T7 promoter (*Xba*I or *Sac*I) and the linear bands extracted from an agarose gel. In contrast, ethanol-precipitated plasmids (2) were plasmids that had been linearised and then precipitated using sodium

acetate and ethanol. Synthesised fragments (3) were linear fragments made commercially by Twist BioScience (Decode Science). An example calculation for determining the amount of synthesised *eGFP* fragments (sense and antisense) to use for *in vitro* transcription is provided in Appendix section 7.5.4.1. Mixed DNA templates refer to two templates used in the same transcription reaction, including the positive control template and the test DNA template, to determine if there is inhibition of RNA Polymerase, since the control template should always amplify. Synthesised fragments were also used to determine if higher yields of dsRNA were obtained using these templates, compared to using PCR-amplified and manually-constructed plasmids. A series of steps were perfomed to synthesise dsRNA including: transcription, annealing of the two RNA strands (sense and antisense), nuclease digestion to remove ssRNA, and purification of the dsRNA by column purification using ethanol (Chapter 2, section 2.10.4). At each step, an aliquot (0.5 µL) was resolved on an agarose gel.

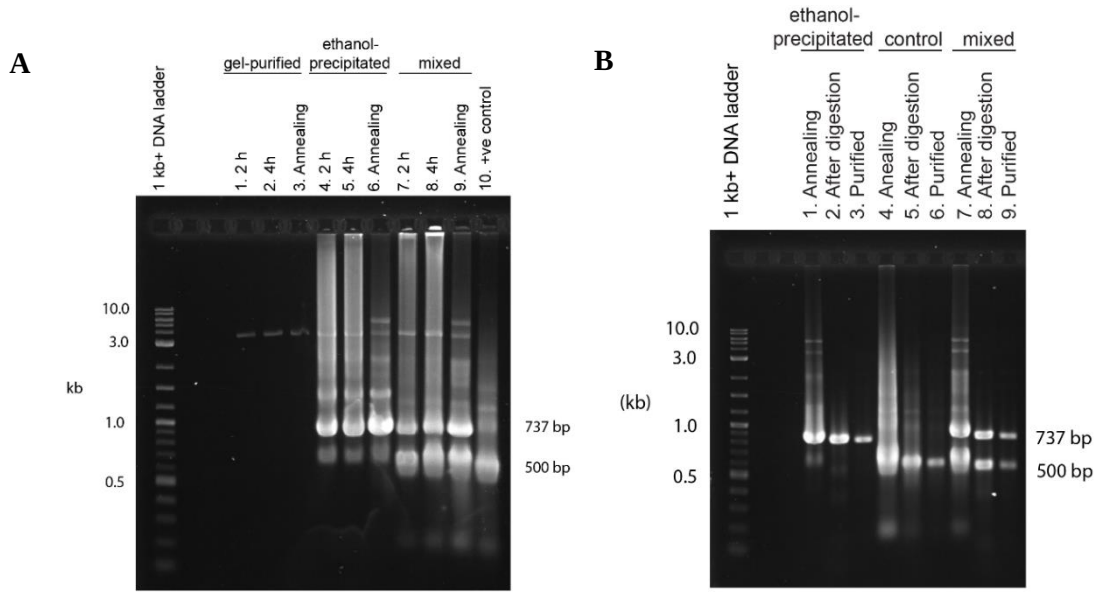

Figure 4.4. Enhanced green fluorescent protein gene (*eGFP*)-dsRNA production using different DNA templates and purification of the dsRNA. (A) Various DNA templates and different incubation times were used in the transcription reaction to optimise conditions for *eGFP*-dsRNA synthesis as described in Section 2.10. Sample lanes 1–3 show *eGFP*-dsRNA production after 2 h and 4 h incubations, and after annealing of the sense and antisense strands, by heating the reaction to 75˚C and cooling to room temperature for 1 h (to maximise duplex yield). The initial plasmids used for transcription were gel-purified. Lanes 4–6 indicate the production of a 737 bp *eGFP*-dsRNA after 2 h and 4 h from DNA template that was linearised first and then purified using ethanol-precipitation. Lanes 7–9 show the production of a 737 bp *eGFP*-dsRNA (ethanol-precipitated plasmid) and 500 bp positive (+ve) control dsRNA (from MEGAScript RNAi kit) from a mixed DNA template (*eGFP* and positive control) after 2 h and 4 h, and after the annealing step. Lane 10 shows positive control dsRNA at an expected size of 500 bp. (B) Nuclease digestion and purification of dsRNA to yield a

single band. Lanes 1–3 are *eGFP*-dsRNA (single purified plasmid template) after the annealing, nuclease digestion and purification steps. Lanes 4–6 are the positive control dsRNA and lanes 7–9 dsRNA from a mixed template (*eGFP* and control) at the same indicated steps. A 1 kb+ DNA size ladder was used in both gels (A, B).

When comparing the sizes of the *eGFP*- and *DsAflR*-1/2-dsRNAs (Figures 4.4–4.7), they both seemed to be bigger than expected based on the 1 kb+ DNA ladder sizes, which may suggest that RNA runs faster than DNA, or there may have been the formation of secondary structures, which altered their mobility on the gel (Livshits et al., 1990).

Figures 4.4A-B show production of a 737 bp *eGFP*-dsRNA using either gel-purified, ethanol-precipitated or mixed (ethanol-precipitated and control) linearised DNA templates. No 737 bp product was seen in lanes 1–3, indicating that detectable amounts of dsRNA were not synthesised from the gel-purified linearised templates (Table 4.1). The slower migrating band is likely to be the size of the entire plasmid (3.4 kb). A 2–4 h incubation time (Figure 4.4A, lane 5) was sufficient to produce *eGFP*-dsRNA from sense and antisense linearised plasmid DNA that was ethanol-precipitated (Table 4.1) as shown by a bright band. After the annealing step, a smear with multiple faint bands was still seen (Figure 4.4A, lane 6; Figure 4.4B, lane 1). However, after nuclease digestion (Figure 4.4B, lane 2) and purification, only a single band of expected size was seen for the final dsRNA product (Figure 4.4B, lane 3). Production of *eGFP*-dsRNA was also successful using mixed DNA templates, consisting of the *eGFP* sense and antisense linearised plasmids (ethanol-precipitated, as above) and the positive control linear fragment (Table 4.1). Two dsRNA products are visible, a 737 bp *eGFP* and a 500 bp control dsRNA (Figure 4.4B, lane 9), showing that transcription of the control template was not inhibited in the presence of the *eGFP* template.

Commercially synthesised DNA fragments were also used as templates for transcription to produce *eGFP*-dsRNA and compared to ethanol-precipitated DNA templates over a longer incubation period (Figure 4.5). A 2–6 h incubation was sufficient to produce dsRNA, and similar band intensities were seen for *eGFP* using commercially synthesised fragments and ethanol-precipitated plasmids (Figure 4.5A-B) along with similar yields of dsRNAs (Table 4.1). Quantification of the dsRNA yield was done at the conclusion of each of the experiments shown in Figures 4.4 and 4.5. A higher dsRNA yield was seen

using ethanol-precipitated plasmid that was transcribed over 6 h, compared to 4 h (Table 4.1) in the previous experiment, although similar band intensities were seen on the gel.

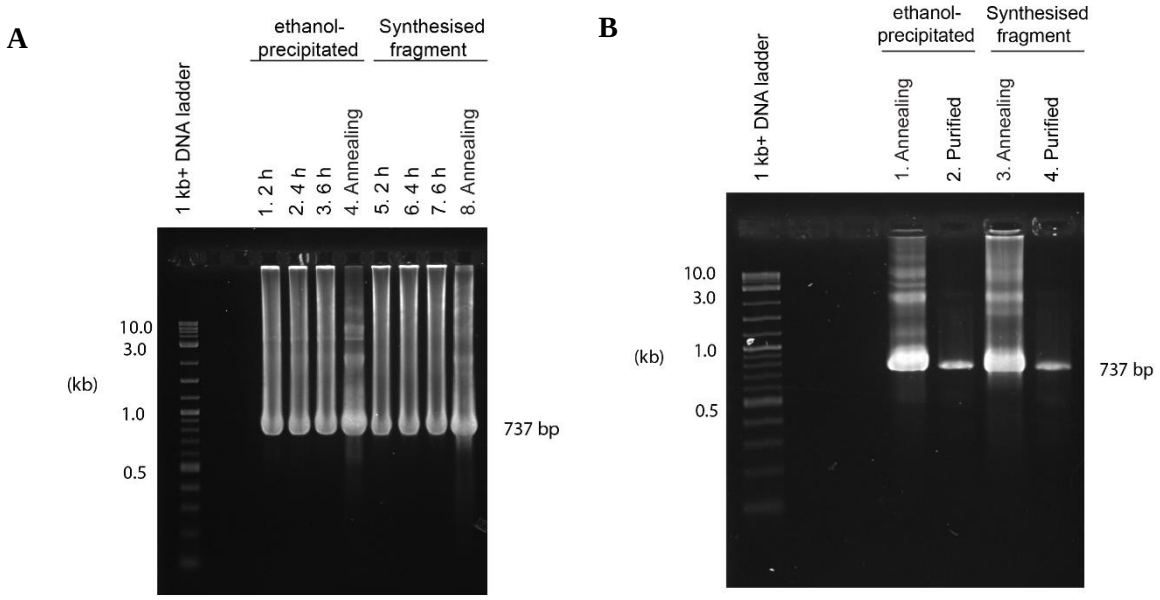

Figure 4.5. Agarose gel electrophoresis showing production of dsRNAs targeting an enhanced green fluorescent protein-encoding gene (*eGFP*) as a control. (A) Transcription reaction incubation times (2, 4 and 6 h) for production of dsRNA. Sample lanes 1–4 indicate the production and annealing of a 737 bp *eGFP*-dsRNA using ethanol-precipitated plasmids as template. Lanes 5–8 indicate a 737 bp *eGFP*-dsRNA derived from a commercially synthesised fragment (Twist BioScience). (B) Annealing and purification of dsRNA using the 6 h samples as shown in (A) (lanes 1–2, dsRNA derived from ethanol-precipitated plasmids and lanes 3–4, synthesized fragments). A 1 kb+ DNA ladder was used.

Table 4.1. Efficiency and yield of dsRNA from *in vitro* transcription using different DNA templates.

Target gene	Template DNA used[a]	Incubation time (h)	Figure number	Successful production of dsRNA	Size of dsRNA	Amount of dsRNA (µg)[b]
eGFP	EtOH ppt plasmid[c]	4	4.4	Yes	737	39.0
eGFP	Gel purified plasmid	4	4.4	No	737	-
eGFP	EtOH ppt plasmid[c]	6	4.5	Yes	737	51.5
eGFP	Synthesised fragment	6	4.5	Yes	737	48.0
Positive control[d]	Linear fragment	2	4.4	Yes	500	56.7
Mixed template (positive control[d] and *eGFP*)	Linear fragment and EtOH ppt plasmid[c]	4	4.4	Yes	500 737	45.6
DsAflR 1	EtOH ppt plasmid[c]	16	4.6	See footnote[e]	509	-
DsAflR 1	Synthesised fragment	16	4.6	Yes	509	27.4
DsAflR 1	Synthesised fragment	6	4.7	Yes	509	78.7
DsAflR 2	EtOH ppt plasmid[c]	16	4.6	See footnote[e]	408	-
DsAflR 2	Synthesised fragment	16	4.6	Yes	408	42.5
DsAflR 2	Synthesised fragment	6	4.7	Yes	408	39.8

[a]Sense and antisense plasmids were linearised with the appropriate enzyme to aid in correct termination of transcription. The positive control dsRNA provided with the MEGAScript RNAi kit was already linearised.
[b]Total amount in 100 µL as made for each dsRNA.
[c]Ethanol-precipitated linearised plasmids (see Chapter 2, methods section 2.10.1).
[d]The positive control dsRNA provided in the MEGAScript RNAi kit was used to ensure the kit was working properly (Methods section 2.10.2). This control template was a linear fragment with opposing T7 promoters and was transcribed over 2 h (Figure 4.4) as per the manufacturers instructions.
[e]A faint band was seen indicating a very low yield of RNA.

Two *DsAflR*-dsRNAs were made in this study targeting two different regions of the *AflR* gene in *D. septosporum*. Production of a 509 bp *DsAflR* 1-dsRNA and a 408 bp *DsAflR* 2-dsRNA is shown in Figure 4.6 after 16 h of transcription, and the amounts of dsRNA made in Table 4.1. Different templates were used to produce dsRNA as used for the *eGFP*-dsRNA; these included commercially synthesised fragments and ethanol-

precipitated linearised plasmids. Since the product size of both *DsAflR*-dsRNAs was smaller compared to the *eGFP*-dsRNA, different incubations were trialled to compare dsRNA yields. A shorter incubation time of 6 h was found to increase the amount of dsRNA synthesised for *DsAflR* 1-dsRNA compared to 16 h (Table 4.1), but not for *DsAflR* 2-dsRNA (Table 4.1) (Figures 4.7A–B). A longer incubation of 16 h was trialled for the *DsAflR*-dsRNAs to determine if it increased the yield compared to a 6 h incubation.

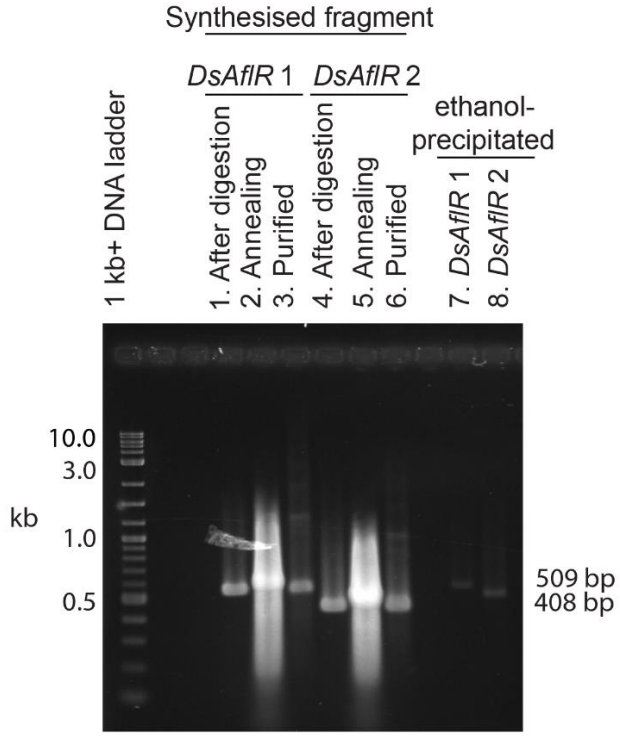

Figure 4.6. Dothistromin pathway regulatory gene (*DsAflR*)-dsRNA production using different DNA templates and purification (16 h transcription). Ethanol-precipitated linearised plasmids and commercially synthesised fragments (Twist BioScience) were used as templates for *in vitro* transcription. Transcription of all dsRNAs was over 16 h. Lanes 1–3 and 4–6 show *DsAflR* 1-dsRNA (509 bp) and *DsAflR* 2-dsRNA (408 bp) respectively synthesised from linear synthesized fragments, after annealing, single-stranded nuclease digestion and purification as for *eGFP* in Figure 4.4. Lanes 7 and 8 are dsRNA transcribed from ethanol-precipitated linearised *DsAflR* 1 and *DsAflR* 2 plasmids. This dsRNA was not used for subsequent steps (annealing, nuclease digestion and purification), due to the lower amounts of dsRNA synthesised. A 1 kb+ DNA ladder was used.

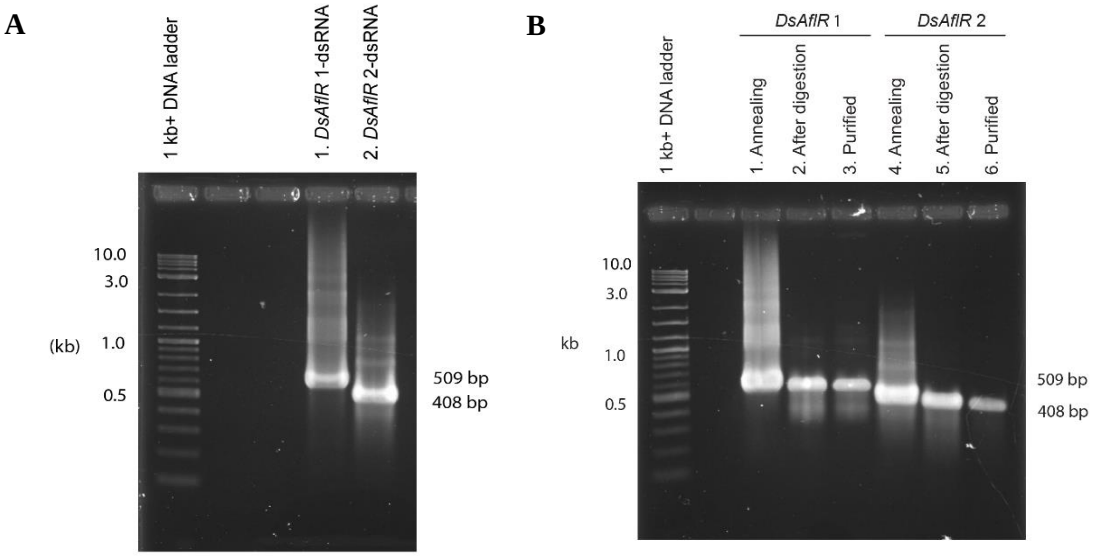

Figure 4.7. Gel electrophoresis showing dsRNAs synthesised from commercial templates targeting either region 1 or region 2 of the dothistromin pathway regulatory gene (*DsAflR*) of *Dothistroma septosporum* (6 h transcription). (A) dsRNA products after a 6 h transcription reaction using commerially synthesised linear templates (Twist BioScience). The sizes of dsRNA products are as follows: 509 bp for *DsAflR* 1 (lane 1) and 408 bp for *DsAflR* 2 (lane 2). (B) Lanes 1–3 represent *DsAflR* 1-dsRNA after annealing of the sense and antisense templates, nuclease digestion and purification. Lanes 4–6 contain *DsAflR* 2-dsRNA, as shown by a band after each step. A 1 kb+ DNA ladder was used.

4.2.3 dsRNA uptake into fungal mycelium can be monitored successfully

To detect if dsRNA can be directly taken up by WT or *eGFP*-expressing *D. septosporum* hyphae (Appendix Chapter 4, section 7.6), it was labelled with a fluorescent dye (Cy3). An example calculation to determine how much dsRNA was required for a fluorescent labelling reaction is provided in Appendix section 7.5.4.2. Fluorescently labelled dsRNA was resolved on an agarose gel to determine if the labelling reaction was successful (Section 2.10.5). Figures 4.7A-D show successful labelling of the positive control, *eGFP*-, *DsAflR* 1- and *DsAflR* 2-dsRNAs, as detected by a slight increase in size in comparison to the unlabelled dsRNAs, as expected. The fluorescently labelled dsRNA was then applied to *in vitro* liquid cultures of *D. septosporum* and incubated for 72 h (Chapter 2, section 2.11). Confocal imaging was carried out to examine dsRNA uptake at 24 h intervals. WT *D. septosporum* mycelium treated with either *DsAflR* 1- or *DsAflR* 2-dsRNA was stained with an aniline blue and trypan blue solution (AB:TB) to visualise hyphal structures as utilised by Hoffmeister et al. (2020).

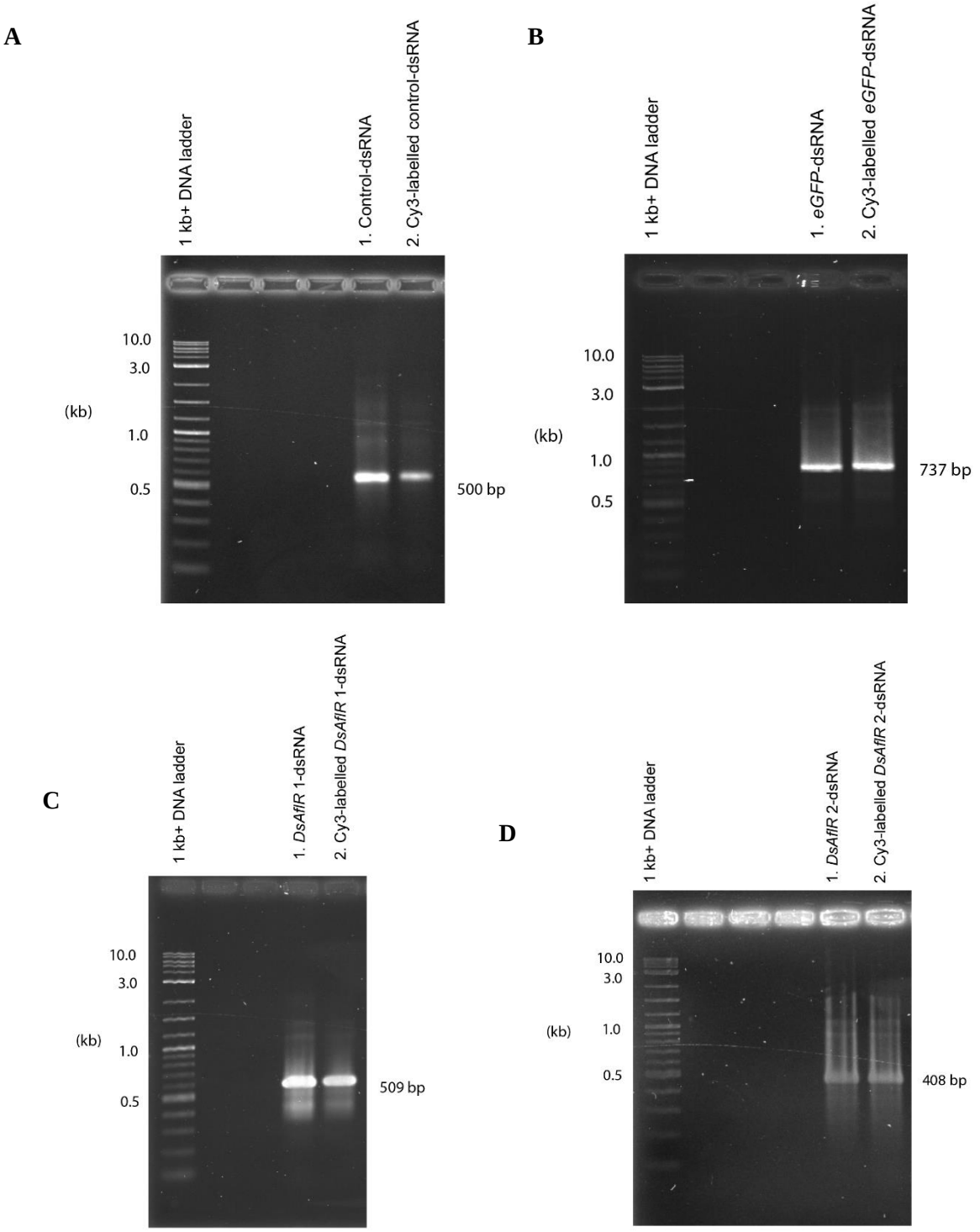

Figure 4.8. Verification of fluorescent labelling of dsRNAs. (A) Labelling of the positive control dsRNA provided in the MEGAScript RNAi kit with Cy3 (lane 2), as indicted by a slight shift in size and unlabelled control dsRNA (lane 1). (B-D) Unlabelled dsRNA (lane 1) and Cy3-labelled dsRNA (lane 2) of *eGFP* (B), *DsAflR* 1 (C) and *DsAflR* 2 (D). DsRNAs were successfully labelled, as indicated by a slower migrating band with a higher molecular weight. A 1 kb+ DNA ladder was used as a size marker.

Uptake of Cy3-labelled *eGFP*-dsRNA was detected 24 h after inoculation with 2000 ng of dsRNA, but little uptake was seen with 1000 ng or 500 ng of dsRNA (Appendix Figure A7.21). However by 48 h, uptake of *eGFP*-dsRNA was seen at all three dsRNA concentrations used (Figure 4.9). GFP fluorescence was not uniform throughout the hyphae (0 ng). There was also non-uniform uptake of the dsRNA, and both Cy3 and GFP appeared mutually exclusive, suggesting that some target (*eGFP*) gene silencing may have occurred. Uptake was not examined after 72 h, as this was a preliminary experiment trialling different amounts of dsRNA and time points, and there was not enough time to repeat it.

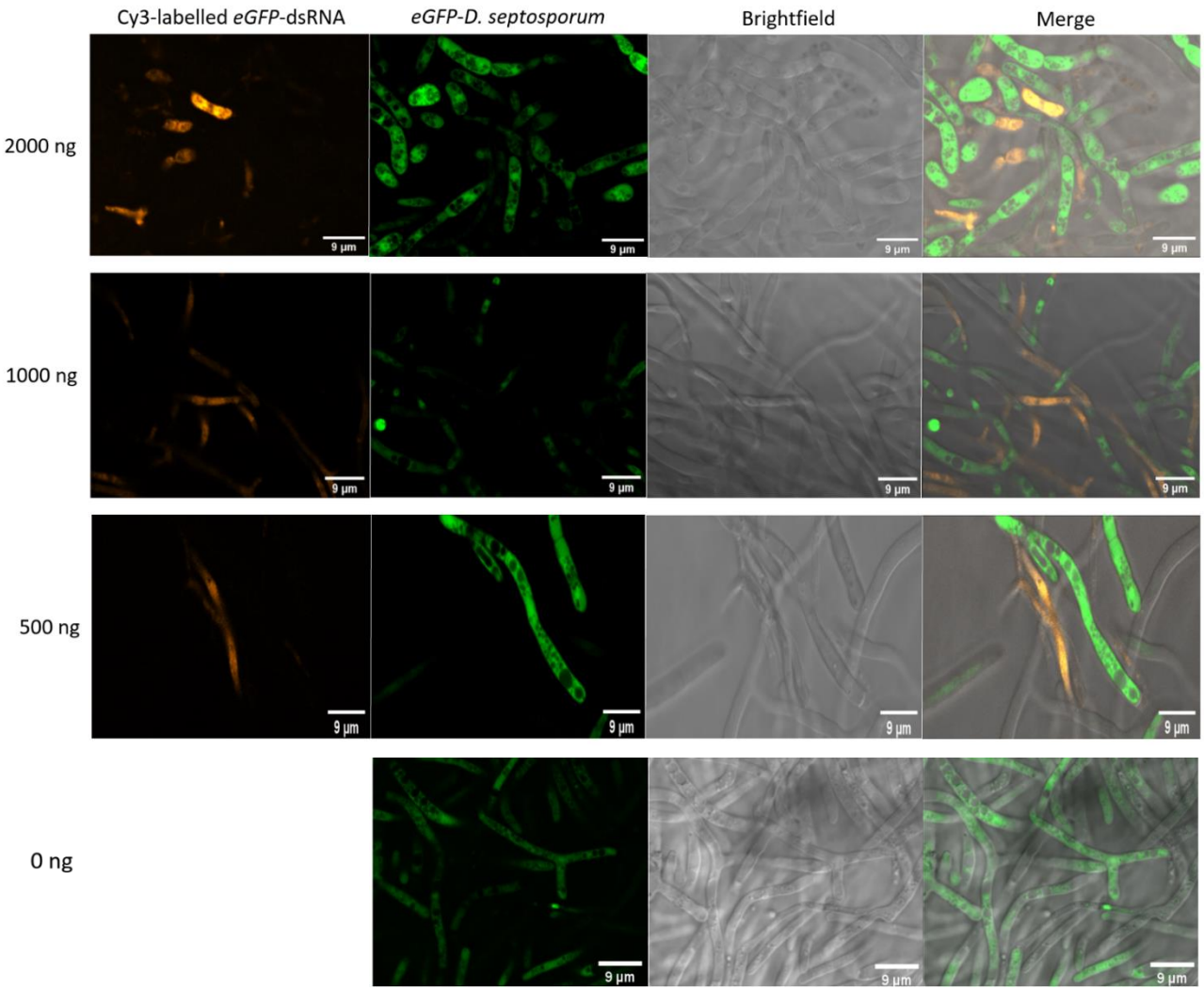

Figure 4.9. Uptake of fluorescently labelled enhanced green fluorescent protein gene (*eGFP*)-dsRNA in *Dothistroma septosporum* 48 hours post-inoculation with the dsRNA. Hyphae were grown on water agar (WA) with microscope slides (Figure 2.5) and inoculated into liquid cultures as outlined in Section 2.11. Different amounts of *eGFP*-dsRNA were applied: 2000 ng (top panel), 100 ng, 500 ng and 0 ng (no dsRNA, bottom panel). From confocal microscopy imaging, orange fluorescence indicates Cy3-labelled dsRNA, green fluorescence shows *eGFP*-expression, grey image brightfield view of hyphae and a merged image of all three channels. Scale bars are 9 µm.

The addition of SILWET L-77 to the liquid *D. septosporum* mycelial cultures with *DsAflR* 1-dsRNA appeared to improve dsRNA uptake compared to that of *eGFP*-dsRNA, which was done in the absence of SILWET L-77 (not available at the time). SILWET L-77 is a non-ionic surfactant that helps to reduce surface tension and was utilised in a SIGS study by McLoughlin et al. (2018) to enhance dsRNA uptake into *Brassica napus* leaves. Cy3-labelled *DsAflR* 1-dsRNA accumulated in compartments within fungal hyphae (Figure 4.10). Amongst the assays done, uptake appeared to be optimal 24 h post-inoculation with 500 ng of dsRNA, and less Cy3 fluorescence was seen with increasing amounts of dsRNA (2000 ng) across 24–72 h, although there was not always consistency between replicates.

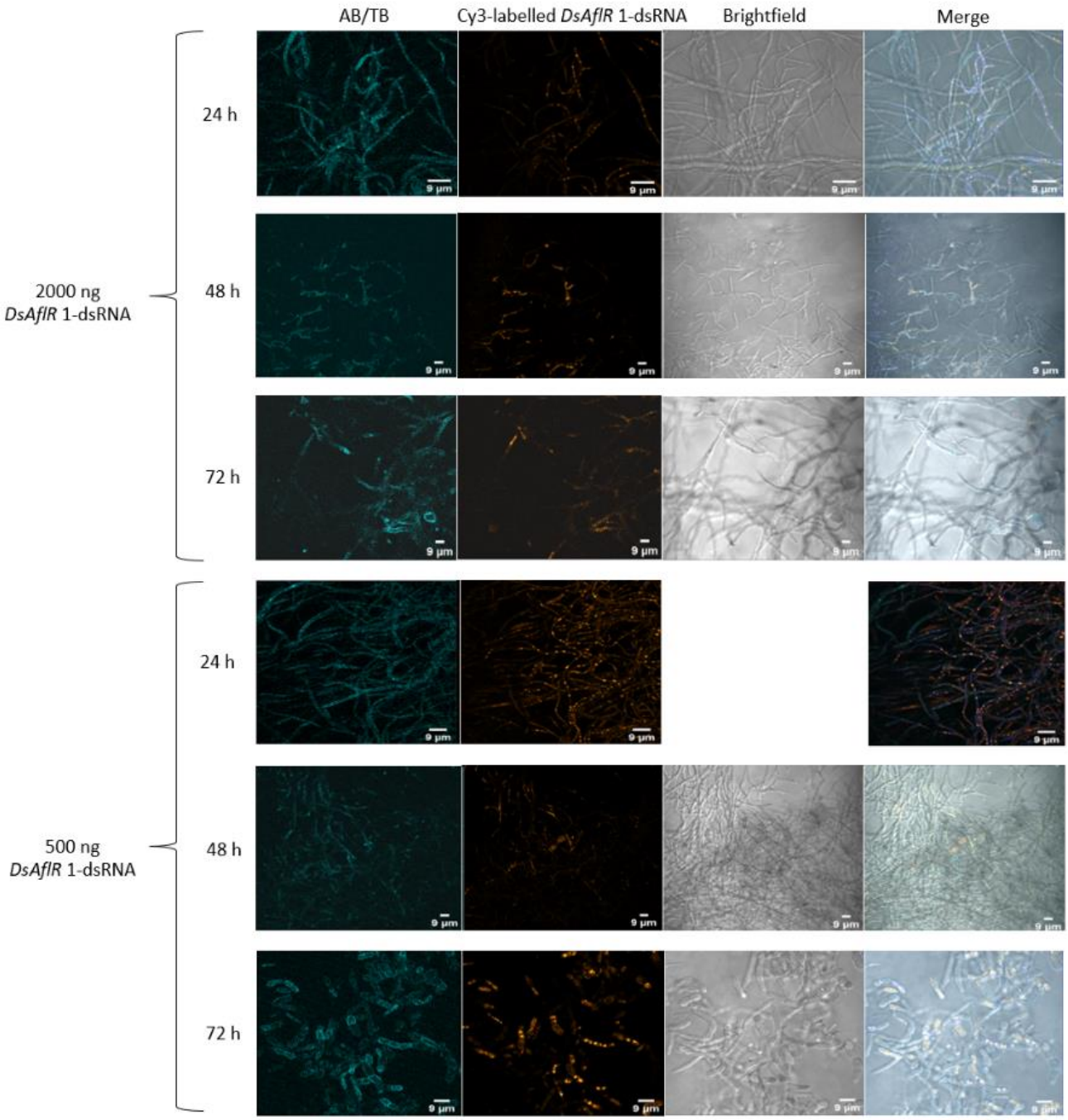

Figure 4.10. Uptake of fluorescently labelled dothistromin pathway regulatory gene (*DsAflR*) 1-dsRNA in *Dothistroma septosporum* 24, 48 and 72 hours (h) post-inoculation with the dsRNA. Hyphae were grown on water agar (WA) with microscope slides (Figure 2.5) and inoculated into liquid cultures, as outlined in Section 2.11. Different amounts of *DsAflR* 1-dsRNA were applied as indicated: 2000 ng and 500 ng, in the presence of 0.03% SILWET L-77, and imaged using confocal microscopy. As a control sample no dsRNA (0 ng) was added to mycelium cultures (not shown). The different colours represent different fluorescence channels, from left to right: cyan fluorescence is representative of Aniline Blue (AB) and Trypan Blue (TB), and orange is Cy3 fluorescence. Grey image is brightfield and the merged image is of all channels. Brightfield images for 500 ng of *DsAflR* 1-dsRNA were not captured due to technical difficulties with the microscope. Scale bars are 9 µm.

D. septosporum was also capable of taking up a 408 bp *DsAflR* 2-dsRNA (Figure 4.11 and Appendix Figure A7.22). Optimal uptake was detected 48 h after addition of 500 ng of synthesised dsRNA to mycelium cultures. Less dsRNA uptake was seen when viewed after 72 h. Incubation of *D. septosporum* cultures with 1000 ng dsRNA did not appear to improve dsRNA uptake above that seen with 500 ng. DsRNA appeared to be localised within vacuoles or vesicles within fungal cells.

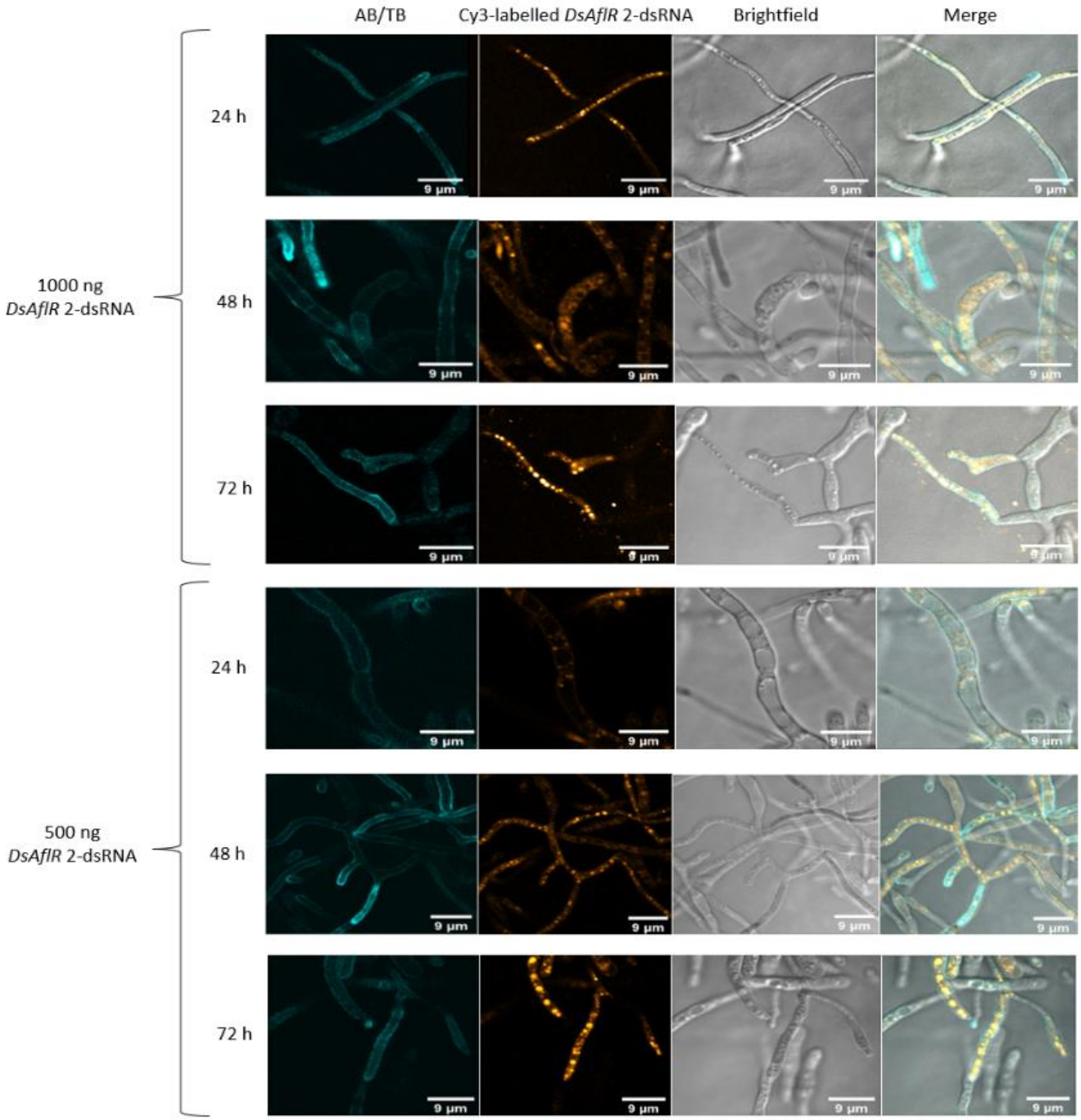

Figure 4.11. Uptake of fluorescently labelled dothistromin pathway regulatory gene (*DsAflR*) 2-dsRNA in *Dothistroma septosporum* 24, 48 and 72 hours (h) post-inoculation with the dsRNA. Hyphae were grown on water agar (WA) with microscope slides (Figure 2.5) and inoculated into liquid cultures as outlined in Section 2.11. Different amounts of *DsAflR* 2-dsRNA were applied as indicated: 2000 ng and 500 ng, in the presence of 0.03% SILWET L-77, and imaged using confocal microscopy. As a control sample no dsRNA (0 ng) was added to mycelium cultures (not shown). The different colours represent different fluorescence channels, from left to right: cyan fluorescence is representative of Aniline Blue (AB) and Trypan Blue (TB), and orange is Cy3 fluorescence. Grey image is brightfield and the merged image is of all channels. Scale bars are 9 µm.

4.3 Discussion

4.3.1 Factors impacting dsRNA yield

The quality of DNA template is important for synthesising high yields of dsRNA. To assess which templates resulted in higher dsRNA yields, different DNA templates were used, contributing to variable success. Gel-purified linearised plasmids were found to be insufficient for producing dsRNA in this study, as shown in Figure 4.4A. A major limitation of using gel-purified linearised plasmids was also the need to run multiple gels and extract the linearised DNA bands to get enough template (1 µg of each sense and antisense template) to use in the transcription reaction. In contrast, ethanol-precipitated linearised plasmids were sufficient for dsRNA production for *eGFP*, but not *DsAflR* (Figures 4.5 and 4.6). However, commercially synthesised fragments produced higher yields of dsRNA. Overall, the DNA templates synthesised by Twist BioScience were found to be highly efficient for synthesising *eGFP*- and *DsAflR*-dsRNA (Table 4.1). Published work has used manually constructed plasmid templates for RNA synthesis, rather than commercially synthesised DNA templates (McLoughlin et al., 2018; Wang et al., 2016; Koch et al., 2016 and others).

The DNA template and transcription incubation time contribute to variations in dsRNA yields. Different sizes of dsRNA can also produce different yields. There was variation seen in the yields of *eGFP*-, *DsAflR* 1- and *DsAflR* 2-dsRNAs (Table 4.1), which suggests that the transcriptional efficiency may depend on the size of the dsRNA and the template. For example, a slightly higher yield of the 737 bp *eGFP*-dsRNA (515 µg) was obtained, compared to that of the 408 bp *DsAflR* 2-dsRNA (425 µg) from the same amount of starting template. To determine if this is a consistent pattern, additional replicates would be needed, with standardised incubation times. Optimisation of the reaction incubation time is also required for maximal yield, which was why different time points were trialled. A longer incubation (16 h) resulted in almost a 3-fold decrease in dsRNA yield for *DsAflR* 1 compared to a 6 h reaction, but this was not observed for *DsAflR* 2-dsRNA, where a slightly higher dsRNA yield was obtained after 16 h. The target sequence for *DsAflR* 2-dsRNA was smaller compared to the other dsRNAs (101 bp difference from *DsAflR* 1), although any effect of the size of dsRNA target sequences on the optimal incubation time would need to be investigated with further replicated experiments. A 2–4 h incubation

was recommended for the first time synthesising dsRNA, for any template, according to the MEGAScript RNAi kit manual.

4.3.2 MEGAScript RNAi kit for small scale production of dsRNA

Commercially available kits are widely used for synthesising dsRNA. The MEGAScript RNAi kit was used in this study to synthesise each of the dsRNAs specific to *D. septosporum*. This kit has the capacity to synthesise 50 µg or more dsRNA per reaction, depending on the size and sequence of the dsRNA (https://www.thermofisher.com/order/catalog/product/AM1626#/AM1626). SIGS studies where dsRNA has been produced using the MEGAScript RNAi kit, to silence fungal genes, include those of *A. niger* (Qiao et al., 2021), *Fusarium asiaticum* (Gu et al., 2019; Song & Thomma, 2018), *Fusarium oxysporum* and *Mycosphaerella fijiensis* (Mumbanza et al., 2013), as well as others involving a range of pathogenic fungal species (McLoughlin et al., 2018; Wang et al., 2016; Werner et al., 2020) (Chapter 1, Table 1.3). Using the MEGAScript RNAi kit, concentrations of dsRNAs are highlighted in Table 4.2 generated by Koch et al. (2016), Werner et al. (2020), McLoughlin et al. (2018) and Wang et al. (2016). However, a limitation of using a kit to synthesise dsRNA *in vitro* is obtaining only small amounts of dsRNA. This makes it expensive when large amounts of synthesised dsRNA are needed and the MEGAScript RNAi kit is not able to synthesise dsRNAs on a large enough scale required for commercial application. Alternative methods, such as cell-free synthesis, are discussed in the next section.

Table 4.2. DsRNA size and concentrations used in spray-induced gene silencing (SIGS) studies controlling fungi.

Target gene	dsRNA size (bp)	*In vitro*/*In planta*	Conc[a] (ng/µL)	Volume (µL)[b]	Amount[c] (µg)	Reference
Range of genes	200–450	*In vitro*	0.1	3000	0.3	McLoughlin et al. (2018)
			0.2	3000	0.6	
			0.5	3000	1.5	
			1	3000	3	
		In planta	20	-	-	
			-	Followed by 25 µL	0.2	
			-	12	0.5	
			-	10	0.2	
CYP51	791	*In vitro*	810	200	162	Koch et al. (2013)
		In planta	20	500	10 µg per plate	Koch et al. (2016)
AGO1, *AGO2*, *DCL1* and *DCL2*	1500-1800	*In vitro*	-	-	-	Werner et al. (2020)
		In planta	20	500	10	
DCL1 and *DCL2*	490	*In vitro*	20	20	0.4	Wang et al. (2016)
		In planta	20	400	8	

[a]Conc refers to the concentration of dsRNA.
[b]Volume refers to the volume of dsRNA used.
[c]Amount refers to the amount of dsRNA.
Table is adapted from Gebremichael et al. (2021).

4.3.3 Scaling up dsRNA synthesis

The development of large-scale production of dsRNAs is required for field applications. Companies like Monsanto, GreenLight BioSciences (https://www.greenlightbiosciences.com/how- to- scale- rna- production/), RNAgri and AgroRNA (Genolution) (http://genolution.co.kr/agrorna/service-overview/) are producing, or are in the process of developing methods to produce, mass quantities of dsRNA at a relatively low cost (Taning et al., 2020). Three common methods used are chemical synthesis, cell-factory synthesis (fermentation) and *in vitro* transcription. Costs to produce dsRNA via chemical synthesis are $100,000 per gram (/g), $1/g for fermentation and $1000/g for *in vitro* transcription of dsRNA (http://www.globalengage.co.uk/pgc/docs/PosterMaxwell.pdf). Chemical synthesis of dsRNA is achieved by a process called solid-phase chemical

synthesis and is capable of synthesising RNA that is up to 80 nt in length (Dominguez et al., 2011), but the cost is prohibitive.

Fermentation platforms to synthesise dsRNA *in vivo* use genetically modified bacteria, such as *E. coli*, *Pseudomonas syringae* or the yeast, *Yarrowia lipolytica*. A disadvantage of this method is that it is labour-intensive. However, this has been attempted by Nerva et al. (2020), whereby dsRNA was made to target the *CYP51*, *Chs1* and *EF2* genes of *B. cinerea* using dsRNA heterologously produced by *E. coli* HT115 (DE3), which is the most commonly used bacterial strain for dsRNA synthesis (Tenllado et al., 2003; Yin et al., 2009). Crude extracts of dsRNA from *E. coli* HT115 have been successfully applied to plants to silence genes, such as for example in the fungal pathogen *B. cinerea* (Nerva et al., 2020) and the insect pest *Chilo suppressalis* (Zhu et al., 2016).

An alternative to heterologous production of dsRNA is to scale up and reduce the cost of *in vitro* synthesis methods, compared to that of the widely used MEGAScript RNAi kit. GreenLight BioSciences are producing dsRNA using a cell-free *in vitro* transcription system, costing as little as $0.50/g (http://www.globalengage.co.uk/pgc/docs/PosterMaxwell.pdf). The company uses a 1,250-litre (L) reactor to scale up large volumes of dsRNA for production and uses their own components. *E. coli* cells make the starting materials for the cell-free reaction, such as enzymes, which synthesise and assemble dsRNA molecules. Just as with the MEGAScript RNAi kit used here, templates need to be made, but the dsRNA synthesis reaction is performed in a large reactor provided with nucleotide precursors. This method is advantageous over the MEGAScript RNAi kit, due to the lower cost and high scale production of dsRNA.

4.3.4 dsRNA can be labelled to detect its delivery into fungal hyphae

The labelling of dsRNA molecules is advantageous for detecting their uptake by fungi. It is an essential step in studies with exogenous applications of dsRNAs, since it provides a visual assessment of whether sufficient dsRNA uptake into fungal cells is achieved. Confocal microscopy demonstrated that all three dsRNAs (*eGFP*, *DsAflR* 1 and *DsAflR* 2) were successfully taken up into *D. septosporum*, but were not evenly dispersed throughout hyphae, suggesting that there is compartmentalisation of the dsRNA (Figures 4.9–4.11 and Appendix Figures A7.21–A7.22). Interestingly, uptake of *DsAflR* 1- and *DsAflR* 2-dsRNAs were observed in what appeared to be vacuoles or vesicles within

fungal cells, whereas *eGFP*-dsRNA uptake appeared to be either cytoplasmic or in large vacuoles. Further study is required to confirm these results.

A previous study in which dsRNA uptake was assessed in *B. cinerea* indicated the absence of dsRNA in vacuoles (Wang et al., 2016). A possible reason for this could be the presence of nucleases in the vacuole that could degrade dsRNA (Klionsky et al., 1990). Kalyandurg et al. (2021) found that the oomycete *P. infestans* was able to take up Cy3-labelled *GFP*-dsRNA into sporangia. Uptake was not evident in all sporangia, but those that did take up the dsRNA had reduced GFP fluorescence compared to those treated with control dsRNA provided by the MEGAScript RNAi kit. They also examined the accumulation of dsRNA sprayed onto potato leaves, demonstrating the distribution of fluorescence of the *GFP*-dsRNA and Cy3-labelled *GFP*-dsRNA. Uptake of fluorescent *GFP*-dsRNA was also observed by Wytinck, Sullivan, et al. (2020). In their study, GFP fluorescence accumulated at the tips of *S. sclerotiorum* hyphae, suggesting that this was the site for dsRNA delivery or accumulation.

In summary, this chapter addressed the design, production and labelling of dsRNAs targeting *eGFP* and *DsAflR*. Various templates were trialled to improve the yield of dsRNAs. Greatest success was seen with synthesised DNA templates and the use of the MEGAScript RNAi kit to transcribe the DNA. All three dsRNAs were taken up by fungal hyphae. The next chapter describes *in vitro* and *in planta* trials with these dsRNAs to determine their effects on target gene expression and virulence of *D. septosporum*.

Chapter 5: Effect of *DsAflR* and *eGFP* knockdown using *in vitro* and *in planta* assays

5.1 Application of dsRNA

DsAflR and *eGFP* dsRNA constructs were produced and shown to be directly taken up into *D. septosporum* hyphae as in the previous chapter (Chapter 4). Whether these dsRNAs knock down the expression of their respective target genes is addressed within this chapter. It focusses on the administration of dsRNA to *in vitro* cultures, as well as direct spray application on pine shoots inoculated with *D. septosporum*. This chapter also explores the use of different amounts/concentrations of the dsRNA and different timings of dsRNA application, in an attempt to optimise gene silencing.

A landmark study, which was used as a guide for this study, targeted specific genes of the fungal pathogens *S. sclerotiorum* and *B. cinerea* affecting *Brassica napus* (canola) (McLoughlin et al., 2018). Although McLoughlin et al. (2018) successfully tested dsRNA in *B. napus*-infected plants, the ability for dsRNAs to silence specific target genes was firstly tested in a simpler *in vitro* system. In their study, *in vitro S. sclerotiorum* cultures were incubated with different doses/concentrations of dsRNA (100 ng/mL–1000 ng/mL) and transcript levels were measured at different times post-inoculation with the dsRNA (24–72 h). DsRNA was also exogenously sprayed onto infected *B. napus* leaves to determine if there was any reduction in lesion progression. The current study aimed to test different concentrations of dsRNA on *in vitro D. septosporum* cultures according to the SIGS study by McLoughlin et al. (2018) and also by spraying pine shoots with a single dose of dsRNA.

In planta infection assays with *D. septosporum* are challenging, even under controlled glasshouse conditions. The life cycle of the pathogen is long (6–12 weeks), not all needles exhibit DNB disease symptoms (Kabir et al., 2013, 2015b), and it is difficult to achieve synchronous infection in which needles on replicate pines have similar stages of infection (Bradshaw et al., 2016). Methods have been developed to improve success rates for infecting pine seedlings (Kabir et al., 2013). Due to the need to use small plants in an enclosed space, it was decided that clonal pine microshoots in sealed glass jars (Hargreaves & Reeves, 2014) would be used in this study. Clonal pine shoots have been

used to assay the effects of infiltrating small amounts of purified effector proteins (Hunziker et al., 2021; Tarallo et al., 2022), but had only been trialled once in a pathogenicity assay by inoculating the shoots with spores of *D. septosporum* (McCarthy, unpublished). In the current study, pine microshoots were used for *D. septosporum* infection assays to determine if spraying with gene-specific dsRNA would have an effect on the outcome of disease, protecting pines from DNB. The advantages of using these shoots for RNA silencing trials were that the shoots are clonal (so less genetic variation), and only a small amount of dsRNA was needed to spray entire pine shoots. GFP-fluorescing isolates of *D. septosporum* were used for *in planta* infection assays, as it was easier to depict if lesions present on needles were due to *D. septosporum*, since they fluoresce green under UV light. Therefore, the microshoots were infected with an eGFP-fluorescing strain of *D. septosporum*.

5.2 Results

5.2.1 dsRNA treatment affects the expression of targeted genes

To determine if the specific dsRNAs could lower the expression of their target genes, *D. septosporum* mycelium cultures were treated with Cy3-fluorescently labelled dsRNA and incubated for 72 h. Different concentrations of the dsRNA were applied and changes in transcript levels of the target genes determined, relative to the reference gene, *DsTEF1α*. Different media were used to trial different ways to grow *D. septosporum* as in Chapter 2, section 2.11; mycelium was grown on either DM or 1/2 x PDA. Two different methods were exploited for *in vitro* silencing trials. The 12-well plate method involved transferring a mycelium plug (3 mm^2) from agar medium (DM or 1/2 x PDA) into a multi-well plate with PDB, and dsRNA mixed with SILWET-L77 was then added to the liquid cultures (Chapter 2, Figure 2.11). In contrast, the agar plate method involved transferring three 3 mm^2 mycelium plugs from a *D. septosporum* culture plate (DM or 1/2 x PDA) to a fresh agar plate of the same medium, containing three holes premade in the agar with a cork borer (Chapter 2, Figure 2.11), prior to adding dsRNA. A water (no-dsRNA) control was run alongside the dsRNA treatments. Table 5.1 summarises the gene expression data obtained by qRT-PCR from the different methods used in this study.

Table 5.1. Quantitative reverse transcription Polymerase Chain Reaction (qRT-PCR) results for gene expression analyses with *in vitro* dsRNA-treated *Dothistroma septosporum* cultures.

Treatment	Sample type[a]	dsRNA (ng)[b]	Incubation (h)	Medium[c]	Rep[d]	Ct Tar[e]	Ct Ref[f]	2^-ΔΔCt[g]	T Test[h]
eGFP-dsRNA	12-well plate	500	72	DM	1	14.43	16.75	0.73	0.49
					3	13.68	15.65		
Water	12-well plate	-	72	DM	1	13.72	15.77	1	
					3	16.78	20.25		
eGFP-dsRNA	12-well plate	500	72	½ x PDA	2	17.93	20.58	0.51	0.14
					3	16.94	19.21	0.39	
Water	12-well plate	-	72	½ x PDA	2	17.46	20.63	1	
					3	18.03	22.09		
eGFP-dsRNA	Agar plate	500	72	DM	1	18.64	24.85	1.19	0.07
					2	20.35	26.57	1.19	
Water	Agar plate	-	72	DM	1	19.18	25.21	1	
					3	17.23	23.15		
DsAflR 1-dsRNA	12-well plate	500	72	DM	1	23.11	14.09	0.71	0.63
					2	21.74	12.48	0.60	
Water	12-well plate	-	72	DM	2	20.12	10.53	1	
					3	21.94	14.47		
DsAflR 1-dsRNA	agar plate	500	72	DM	1	23.26	15.24	0.14	0.02
					2	21.94	13.72	0.12	
Water	agar plate	-	72	DM	1	25.37	20.63	1	
					2	26.71	21.06		
DsAflR 2-dsRNA	12-well plate	500	24	DM	1	22.11	12.48	0.49	0.57
					2	22.76	13.42	0.59	
DsAflR 2-dsRNA	12-well plate	1000	24	DM	1	20.15	11.01	0.69	0.88
					2	20.12	11.57	1.04	
DsAflR 2-dsRNA	12-well plate	500	48	DM	1	22.22	12.73	0.54	0.67
					2	19.60	10.57	0.75	
DsAflR 2-dsRNA	12-well plate	1000	48	DM	1	19.28	10.83	1.11	0.90
					2	22.24	13.83	1.15	
DsAflR 2-dsRNA	12-well plate	500	72	DM	1	22.71	13.16	0.52	0.61
					2	20.25	11.01	0.64	
DsAflR 2-dsRNA	12-well plate	1000	72	DM	1	20.79	12.84	1.59	0.83
					2	20.70	12.08	0.99	
Water[i]	12-well plate	-	24	DM	1	21.40	11.49	1	
			72	DM	2	19.90	12.59		

[a]Sample type refers to the application method used for adding dsRNA. This was either in 12-well plates containing 1–3 mycelium plugs (3 mm^2) in each well or dsRNA directly added to the surface of mycelium plugs on agar plates (Chapter 2, section 2.11).

[b]Amount of dsRNA used in either 2 mL of Potato Dextrose Broth (PDB) in 12-well plates, or 5 µL aliquots (mixed with 0.03% SILWET L-77) onto mycelium on agar plates, either DM or half-strength Potato Dextrose Agar (1/2 x PDA).

[c]Medium for growing *Dothistroma septosporum* mycelium was either Dothistroma Medium (DM) or 1/2 x PDA. Mycelium plugs were transferred to either 12-well plates containing PDB, or to agar plates of the same medium used to grow mycelia. Results were not obtained for mycelium on 1/2 x PDA agar plates, as the amount of RNA extracted was too low for cDNA synthesis.

[d]Three biological replicates were carried out for each treatment, but only two replicates were subjected to qRT-PCR due to lack of time.

[e]Cycle threshold (Ct) for amplification of the target gene (either enhanced green fluorescent protein (*eGFP*) or the dothistromin pathway regulatory gene (*DsAflR*)), shown as the average of two technical replicates.

[f]Ct for amplification of the reference gene translation elongation factor 1 alpha (*DsTEF1α*), shown as the average of two technical replicates.

[g]2^-ΔΔCt is the formula used to calculate the fold gene expression of target genes relative to reference gene *DsTEF1α*.

[h]T-test in Excel comparing the differences in fold gene expression between dsRNA-treated and untreated samples. This was calculated from the ΔCt (target – ref) values.

[i]Both the 24 and 72 h water controls were included in statistical analyses, as sufficient RNA could not be extracted from other control samples.

Using the 12-well plate method, expression of *eGFP* was reduced by addition of 500 ng (final concentration of 250 ng/mL in 2 mL of PDB) of *eGFP*-dsRNA, compared to the water control. Mycelium plugs initially grown on DM or 1/2 x PDA showed around a 34% or 55% decrease in expression respectively (Figure 5.1), although these differences were not statistically significant compared to the untreated water controls (Table 4.1) and there was high variability between some of the replicates. Using the agar plate method instead, with mycelium grown on DM agar and dsRNA applied directly to the inoculation point, resulted in a small but not statistically significant increase in expression of *eGFP* following dsRNA treatment (Table 5.1, Figure 5.1). Data are not shown for expression of *eGFP* in *D. septosporum* grown on 1/2 x PDA agar plates, as the concentrations of RNA extracted were too low for cDNA synthesis and qRT-PCR.

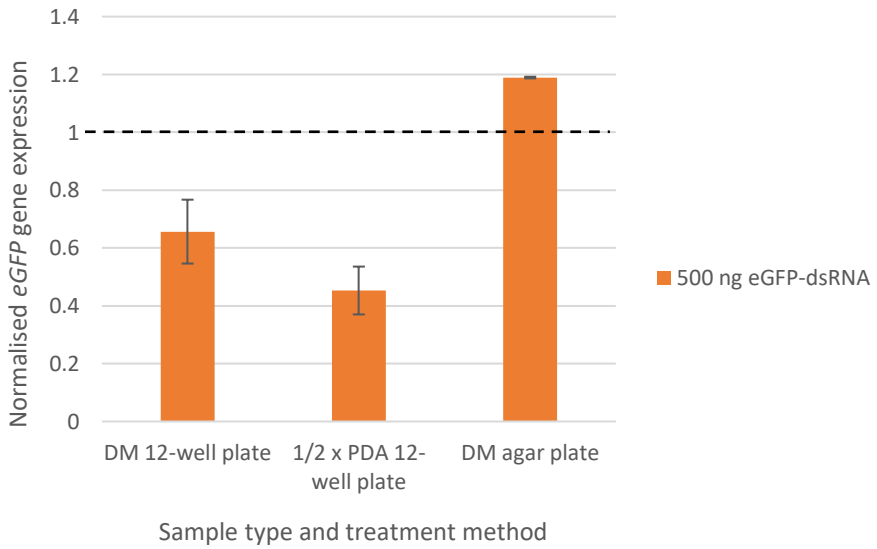

Figure 5.1. Relative expression of enhanced green fluorescent protein (*eGFP*) gene in *Dothistroma septosporum* in response to dsRNA treatment. Mycelium was grown on either Dothistroma Medium (DM) or half-strength Potato Dextrose Agar (1/2 x PDA) as in Chapter 2, section 2.11. A total of 500 ng of dsRNA (+SILWET L-77) was applied to liquid cultures in 12-well plates (2 mL liquid media) or directly applied to agar plugs (5 µL) in agar medium (agar plate). Relative expression of the target gene was calculated using the ΔΔCt method, compared to the reference gene, translation elongation factor 1 alpha (*DsTEF1α*), then normalised to untreated control samples which were given an expression value of 1, indicated by the dotted line. Transcript levels were measured at 72 h post-treatment with dsRNA. Data represent the mean and standard deviation for two biological replicates. T-tests were performed to compare means of ΔCt values of dsRNA treatments to water controls; none of these sample treatments showed a significant difference.

For *DsAflR*, a reduction in gene expression was seen using both the 12-well plate and agar plate methods after treatment with 500 ng of *DsAflR* 1-dsRNA targeting region 1 of *DsAflR* (Figure 5.2). The greatest reduction (87% decrease) was observed by exogenously applying dsRNA to point inoculations on agar medium for 72 h and was shown to be significant (P = 0.02) (Table 5.1) in comparison to the mean ΔCt values of the water control. Around a 34% decrease in *DsAflR* gene expression was also seen after 72 h, by exogenously applying dsRNA to 12-well plates with mycelium plugs but was not statistically significant. The experiment was repeated in 12-well plates only and using different amounts of dsRNA (500 ng and 2000 ng), but qRT-PCR expression analyses were not conducted due to the concentration of RNA extracted from the mycelium plugs being too low (data not shown).

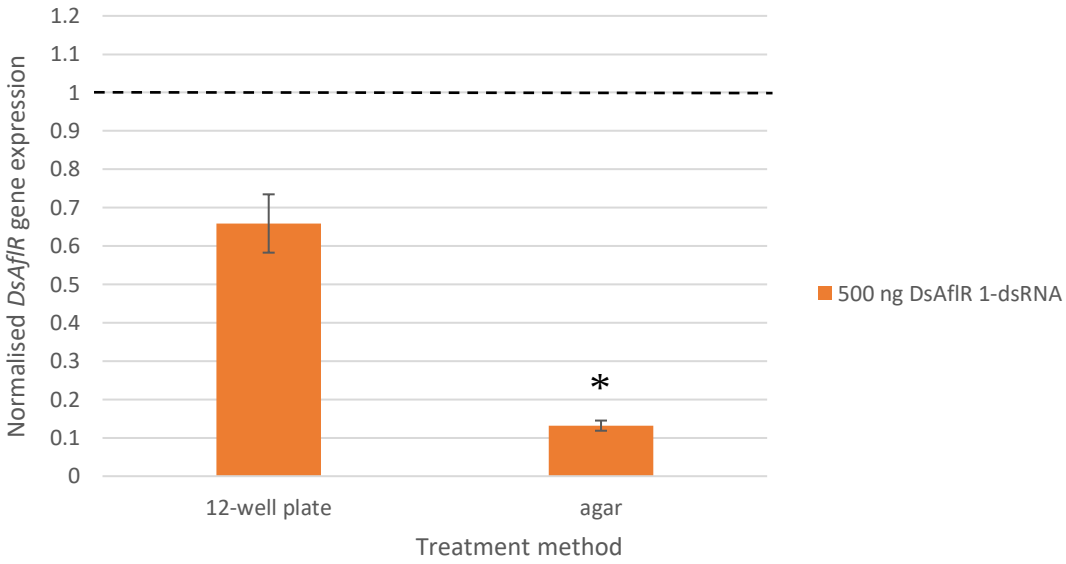

Figure 5.2. Relative expression of the dothistromin pathway regulatory gene (*DsAflR*) in *Dothistroma septosporum* in response to dsRNA treatment. Mycelium was grown on Dothistroma Medium (DM) and 500 ng of dsRNA was applied targeting region 1 of *DsAflR*. Relative expression of each target gene was calculated using the ΔΔCt method as in Figure 5.1 and normalised in the same way. Transcript levels were measured at 72 h post-treatment with dsRNA. Data represent two biological replicates. Error bars represent standard deviation. T-tests confirmed a significant difference ($p \leq 0.05$) between mean ΔCt values of the target and reference genes (shown by asterisk).

Based on variable success with the *eGFP*- and *DsAflR* 1-dsRNA trials, it was decided that, for *DsAflR* 2, the dsRNA would be added to mycelium plugs of DM medium in 12-well plates and different amounts of the dsRNA would be tested. A time course experiment was conducted over 72 h to determine changes in *DsAflR* gene expression, using either 500 ng or 1000 ng (250 ng/mL and 500 ng/mL respectively) of *DsAflR* 2-dsRNA. There was variation in *DsAflR* transcript levels after 24, 48 and 72 h (Figure 5.3). Addition of 500 ng of dsRNA showed a decrease in *DsAflR* gene expression at all three time points, although none of these were statistically significant when compared to the water controls (Table 5.1). A higher amount of dsRNA (1000 ng) did not appear to result in any silencing effect, with mean expression levels higher than the controls after 48 and 72 h post-inoculation (Figure 5.3), suggesting that silencing was ineffective, even after 24 h. A common trend between the trials with different amounts of dsRNA was that the greatest decrease in transcript levels was after 24 h of incubation. In this experiment there was large variability in gene expression in the water control samples, which may have contributed to the lack of significant differences observed between the untreated and dsRNA-treated samples in the 500 ng samples.

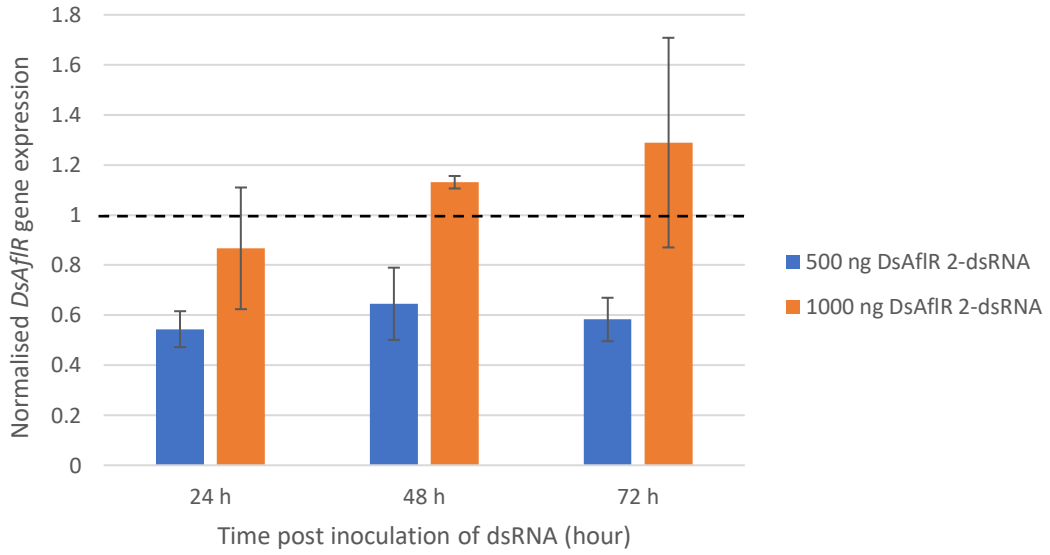

Figure 5.3. Effect of changes in dothistromin pathway regulatory gene (*DsAflR*) expression in response to treatment with different concentrations of dsRNA targeting region 2 of *DsAflR* in *Dothistroma septosporum*. Transcript levels were measured at 24, 48 and 72 h post-treatment with 500 ng and 1000 ng of *DsAlfR* 2-dsRNA. Mycelium was grown on Dothistroma Medium (DM) and dsRNA was applied to liquid cultures in 12-well plates as in Chapter 2, section 2.11. Data represent two biological replicates. Error bars represent standard deviation. Target gene expression was normalised to the reference gene, as in Figures 5.1 and 5.2. No statistically significant differences between dsRNA-treated and untreated samples were found.

Taken together, the results for *in vitro* assays with dsRNA targeting *eGFP* or *DsAflR*, demonstrated promising results. There were few statistically significant differences in gene expression between dsRNA-treated (500 ng of dsRNA applied) and untreated samples, but high variability between replicate water controls. Differences might have been statistically significant for *eGFP*-, *DsAflR* 1- and *DsAflR* 2-dsRNA treatments, using the 12-well plate method, if the water controls had been more consistent. The next part of this results section addresses *in planta* assays with the dsRNA to access the overall health of pines and to determine if they are protected from infection by *D. septosporum*.

5.2.2 RNA silencing trials with pine microshoots

To evaluate the efficacy of SIGS against *D. septosporum in planta*, assays were undertaken using pine microshoots in sealed jars (Chapter 2, section 2.12). The pine shoots were sprayed with dsRNA (1 mL mixed with 0.03% SILWET L-77), then sprayed with spores from an *eGFP*-expressing *D. septosporum* strain (Chapter 2, section 2.8), and either air-dried before sealing the jars (one set of jars) or sealed immediately after spraying with the spore suspension (a separate set of jars). Pine shoots were sampled to analyse fluorescent eGFP lesions on needles after 4.5 and 5.5 weeks. Needle samples were taken from one set of jars at each of these time points. Figure 5.4 shows pine shoots in sealed glass jars 4.5 weeks after treatment with *D. septosporum* and dsRNA. An overall disease assessment of the pine shoots was completed to ascertain if there was some level of protection by exogenous spray applications with the gene-specific dsRNAs. Within each jar, some shoots had more needle death compared to others, indicating variability between replicate shoots (Figure 5.4).

Pine shoots sampled at 4.5 weeks that were sealed immediately (not air-dried) after spraying with *D. septosporum* spores, as explained in methods section 2.12, appeared to have less needle death overall compared to the air-dried shoots (Figure 5.4). However, there were no visible trends across these two sets of jars with respect to results from spraying with *DsAflR*-dsRNAs, compared to the *eGFP*-dsRNA and water controls. The use of two different methods, air drying and sealing immediately after spray inoculation with dsRNA and fungal spores, may have contributed to variability in shoots between the two sets of jars (Figure 5.4). After the conclusion of the experiment at 5.5 weeks, the remaining jars of shoots were photographed with the lids removed (Figure 5.5). Although fewer dead needles were observed on microshoots sprayed with *DsAflR* 2-dsRNA

compared to shoots sprayed with *eGFP*-dsRNA as a control in this figure, there was variability between replicate shoots. After treatment with the *eGFP*-dsRNA control, more needle death was seen after 5.5 weeks compared to 4.5 weeks.

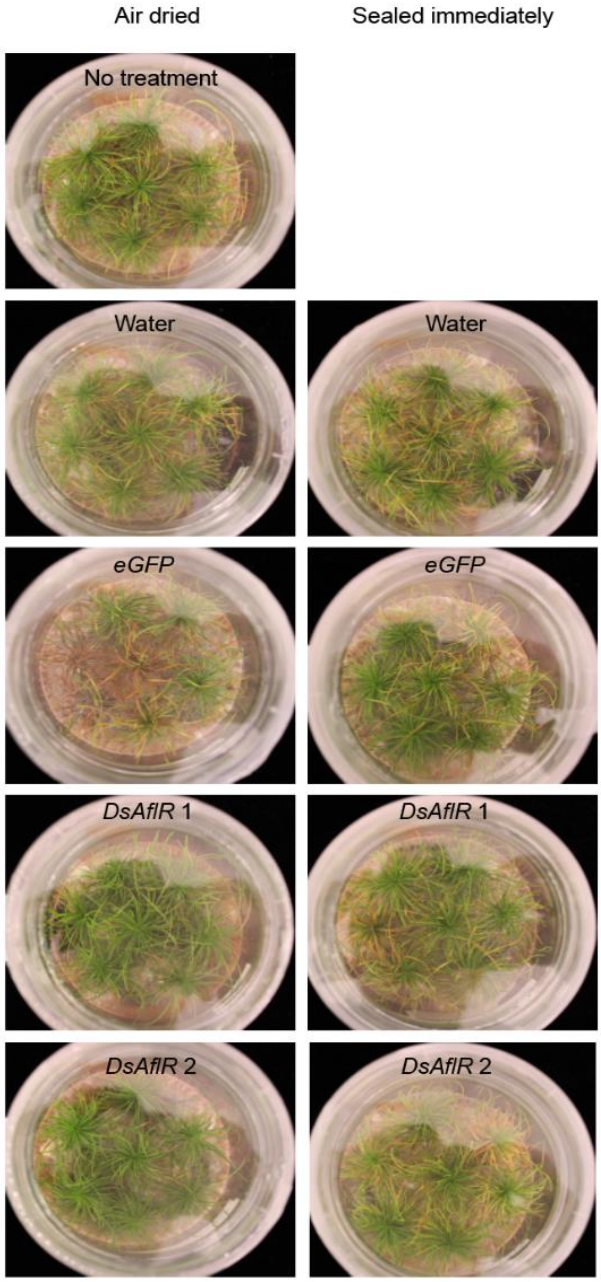

Figure 5.4. Spray-induced gene silencing in *Dothistroma septosporum* in *Pinus radiata* clonal shoots in sealed glass jars. Pine shoots were sprayed with 1 mL of dsRNA (*eGFP*, *DsAflR* 1 or *DsAflR* 2) diluted with DEPC-treated water (+ 0.03% SILWET-L77), as in section 2.12.1, followed by spray inoculation with *D. septosporum* spores and air-dried (left panel) or sealed immediately (right panel). As a control, water was sprayed instead of dsRNA. An extra jar was provided, which was used as a no-dsRNA treatment control. Pine shoots within this jar were infected with *D. septosporum* but were not treated with dsRNA. Photographs were taken with petri dish lids on after 4.5 weeks of incubation to avoid contamination.

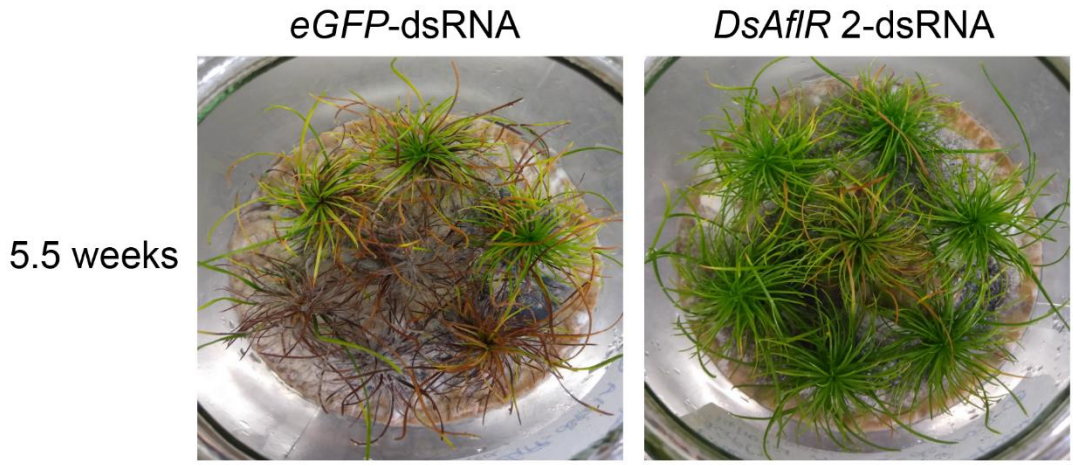

Figure 5.5. *Pinus radiata* shoots showing Dothistroma needle blight (DNB) disease on needles. *DsAflR* 2-dsRNA (500 ng/mL) (+ 0.03% SILWET-L77) was sprayed onto pine shoots on LPch media in glass jars. Once dsRNA dried to the surface of needles (air-dried), needles were sprayed with *D. septosporum* spores (Chapter 2, methods section 2.12.1). Pine shoots sprayed with *eGFP*-dsRNA targeting an enhanced green fluorescent protein gene are shown as a control. Jars sprayed with *DsAflR* 1-dsRNA and water (control) were not photographed at this stage.

After opening the jars, *D. septosporum* and other fungi were found to be growing on the pine shoots and on the medium, suggesting there was contamination (Appendix Figure A7.31). Saprophytic growth was observed on some needles, as shown in Appendix Figure A7.32. Orange/brown colonies were also found to be growing on the agar, which was evidence of *D. septosporum* secreting dothistromin into the medium, but also fluffy white and grey mycelium, which was most likely not *D. septosporum* (Appendix Figure A7.31). This assay could not be repeated to eliminate contamination, due to lack of time, but suggested that there may be other causes of death to needles besides infection with *D. septosporum*, such as toxicity due to the production of dothistromin in the agar.

To analyse whether the death of needles, or damage to needles, was due to infection by *D. septosporum*, individual needles were checked for eGFP-fluorescing lesions. Figures 5.6–5.7 show fluorescence images of GFP lesions on needles with visible lesions after 4.5 and 5.5 weeks, respectively. No overall differences in types of eGFP lesions were observed, but rather results were consistent across both sampling timepoints for all treatments. Additional images capturing growth of eGFP-labelled *D. septosporum* are shown in Appendix Figure A7.32.

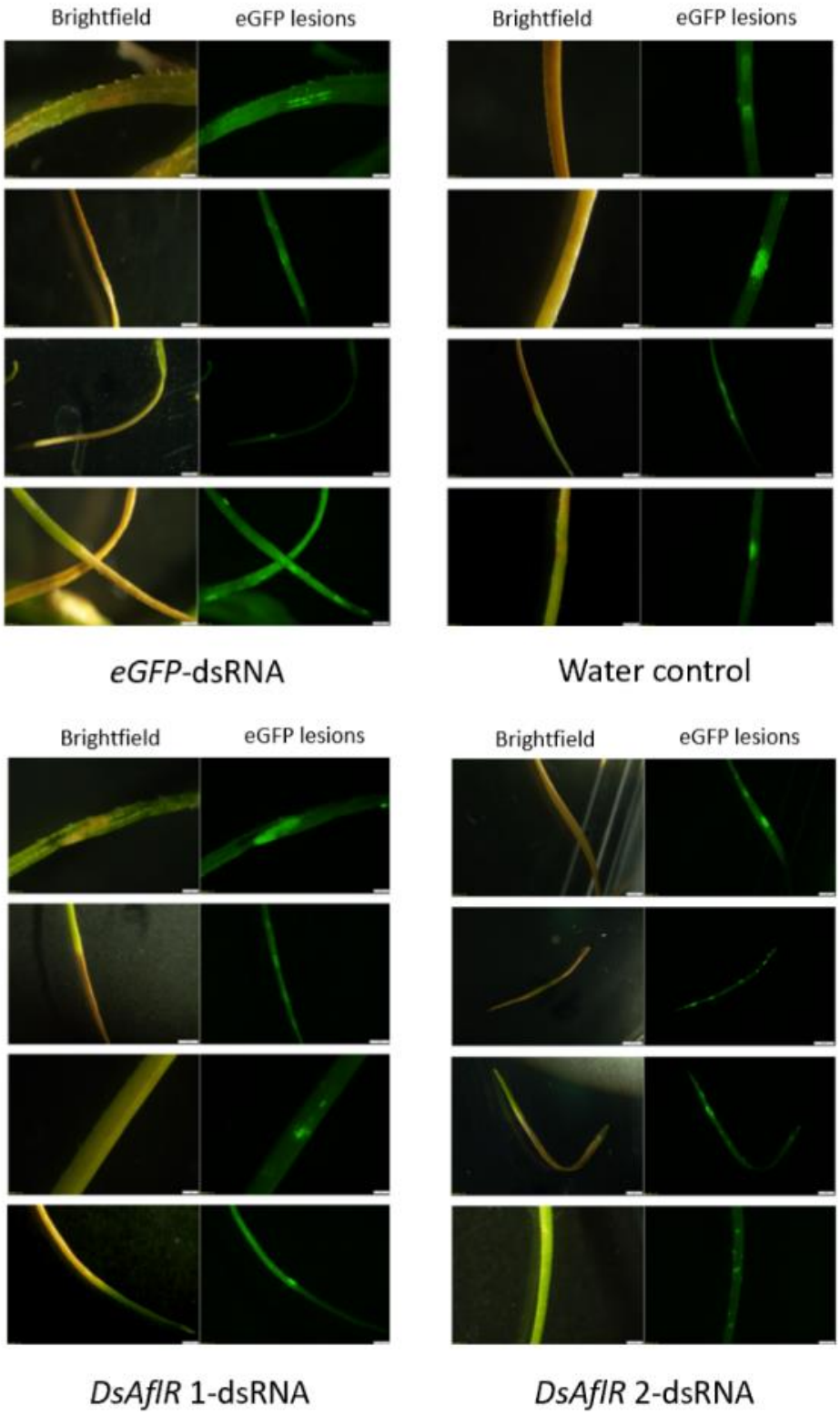

Figure 5.6. *Pinus radiata* needles sprayed with dsRNA showing fluorescent eGFP lesions at 4.5 weeks. Images were captured post-inoculation with dsRNA (+ SILWET-L77) as shown and *Dothistroma septosporum* (eGFP) spores. Individual needles were sampled from pine microshoots in glass jars and examined for the presence of fluorescent eGFP lesions, indicative of infection. Scale bar is 100 µM.

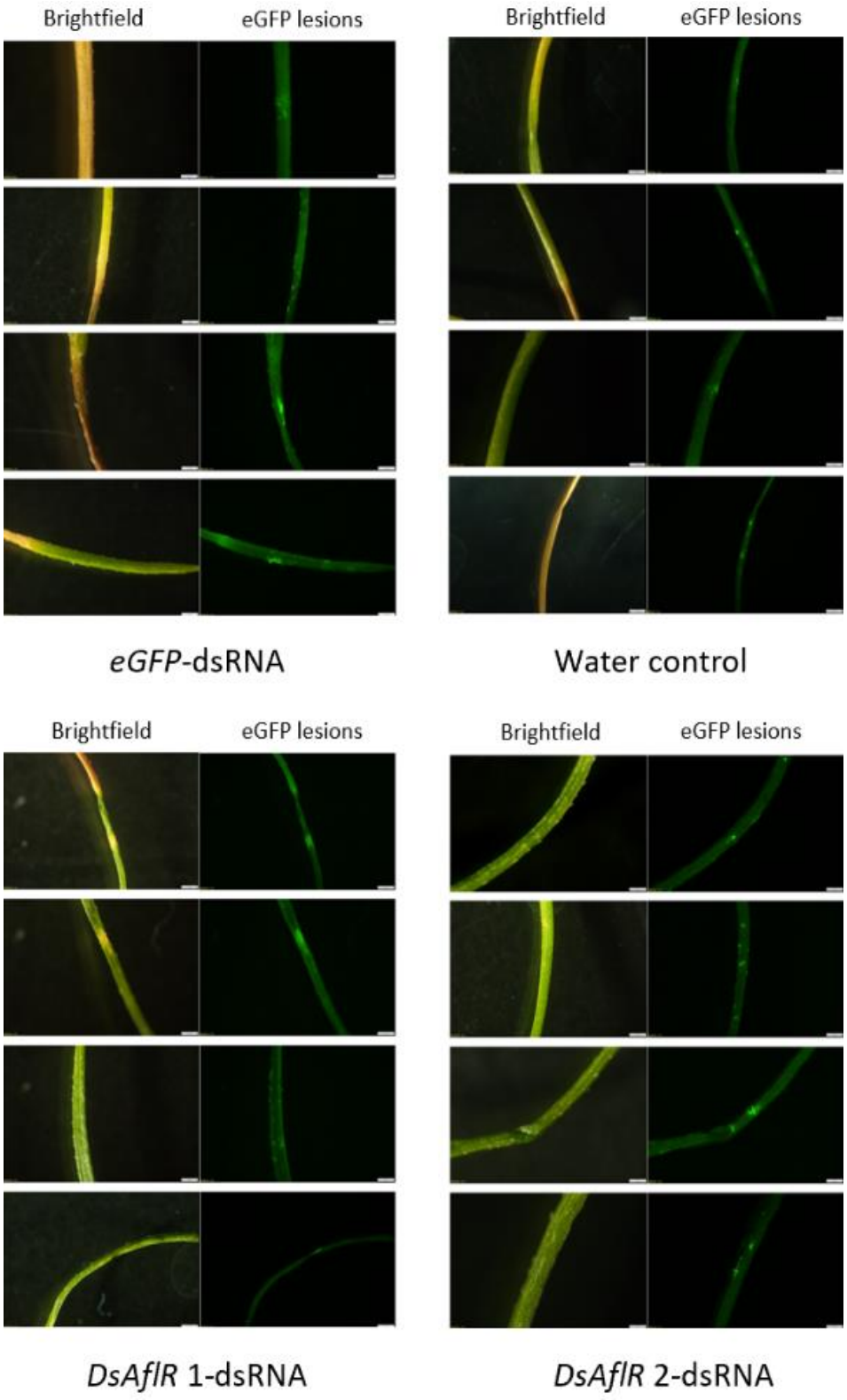

Figure 5.7. *Pinus radiata* needles sprayed with dsRNA showing fluorescent eGFP lesions at 5.5 weeks. Images were captured post-inoculation with dsRNA (+ SILWET-L77) and *Dothistroma septosporum* (eGFP) spores. Individual needles were sampled from pine microshoots in glass jars and examined for the presence of fluorescent eGFP lesions, indicative of infection. Scale bar is 100 µM.

Needles were categorised into groups based on whether they were healthy (green), dead or dying (brown), had fluorescent lesions indicative of eGFP *D. septosporum*, or lesions that were not fluorescent (Appendix Chapter 5, Table A7.6). The percentages of needles with eGFP lesions are shown in Table 5.2 and highlight no statistically significant differences between needles sprayed with dsRNA or water ($p \geq 0.05$) and high variability between replicates. Needles treated with *DsAflR* 1 and 2-dsRNAs exhibited a higher mean percentage of needles with eGFP lesions 4.5 weeks after spray inoculation, but a lower mean percentage in the 5.5 weeks (air dried) samples (Table 5.2, Figure 5.8). There were also no significant differences in the percentage of needles with eGFP lesions between needles sprayed with *DsAflR* 1- and *DsAflR* 2-dsRNAs, compared to the those sprayed with the *eGFP* control dsRNA at 4.5 weeks. However, a chi-squared test based on actual numbers of needles (rather than percentages) suggested significantly fewer lesions in needles treated with either *DsAflR* 1- or *DsAflR* 2-dsRNA compared to *eGFP*-dsRNA at 5.5 weeks (air-dried jars) ($P = \leq 0.05$) (Table 5.2, Figure 5.8).

Table 5.2. Summary of *Pinus radiata* needles showing fluorescent lesions in response to treatment with dsRNA and infection by *Dothistroma septosporum*.

	4.5 weeks incubation[a]				**5.5 weeks incubation[a]**			
# needles	**Water**	***eGFP*-dsRNA**	***DsAflR* 1-dsRNA**	***DsAflR* 2-dsRNA**	**Water**	***eGFP*-dsRNA**	***DsAflR* 1-dsRNA**	***DsAflR* 2-dsRNA**
With eGFP lesions (fluorescent)	39 ± 7.0	35 ± 8.9	34 ± 7.5	48 ± 6.4	29 ± 21.1	37 ± 21.8	19 ± 7.8	30 ± 7.9
Total needles[b]	144 ± 5.5	184 ± 34.4	157 ± 39.5	203 ± 17.4	159 ± 40.4	147 ± 19.7	160 ± 34.6	191 ± 27.0
% needles with eGFP lesions	27 ± 5.3	19 ± 1.2	22 ± 1.7	24 ± 4.2	17 ± 8.4	24 ± 12.3	12 ± 3.6	16 ± 3.0
T-test (water)[c]	-	0.06	0.17	0.49	-	0.42	0.42	0.85
χ^2 (water)[d]	-	0.08 (3.00)	0.27 (1.20)	0.48 (0.49)	-	0.14 (2.17)	0.11 (2.53)	0.53 (0.40)
T-test (eGFP)[e]	-	-	0.08	0.12	-	-	0.17	0.3
χ^2 (eGFP)[f]	-	-	0.55 (0.36)	0.26 (1.28)	-	-	0.002 (9.08)	0.03 (4.68)

[a]Microshoots in glass jars containing LPch agar were sprayed with dsRNA (either enhanced green fluorescent protein (*eGFP*), dothistromin pathway regulatory protein (*DsAflR*) 1 or *DsAflR* 2), or water (control) and infected with *D. septosporum* spores, as outlined in Section 2.12.1. Pine shoots were sampled at 4.5 and 5.5 weeks. Jars at 4.5 weeks had been sealed immediately and jars at 5.5 weeks air-dried after inoculation. The mean ± standard deviation of three biological replicates (shoots) are shown.

[b]Excludes dead and dried needles with no eGFP fluorescence but includes needles with lesions that did not appear to fluoresce (needles with non-eGFP lesions).

[c]A type 2 equal variance t-test was conducted on the percentage of needles with eGFP lesions. A p-value of 0.05 or lower indicates a significant difference between dsRNA-treated and untreated (water control) samples.
[d]Chi square value (χ^2) in backets and probability for comparison of numbers of needles with eGFP lesions sprayed with dsRNA or water.
[e]T-test comparing treatment with *DsAflR*-dsRNAs to treatment with the *eGFP*-dsRNA control.
[f]Chi square value (χ^2) in brackets and probability for comparison of numbers of needles with eGFP lesions sprayed with *DsAflR*-dsRNAs or the *eGFP*-dsRNA control.

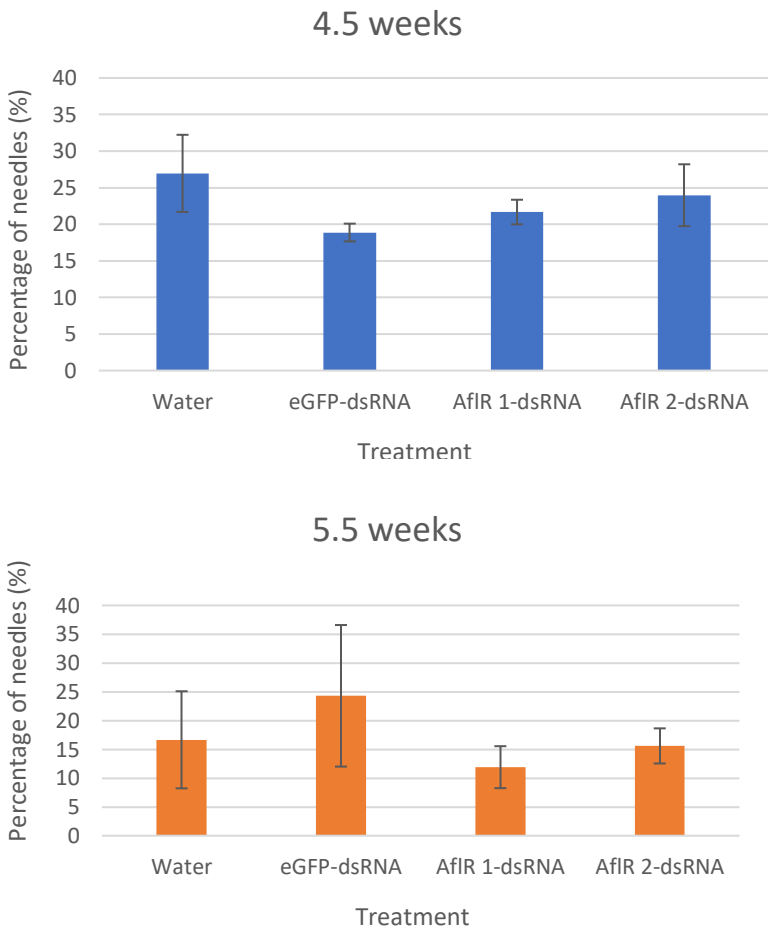

Figure 5.8. Percentages of needles with enhanced green fluorescent protein (eGFP) fluorescing lesions 4.5 and 5.5 weeks after spray application with dsRNA targeting their respective genes. *Pinus radiata* clonal shoots in glass jars were sprayed with dsRNA targeting *eGFP* or *DsAflR* regions 1 or 2, or water (+0.03% SILWET-L77), followed by spray-inoculation with *Dothistroma septosporum* spores as in Chapter 2, section 2.12.1. Data represent the mean and standard deviation of three biological replicates (shoots). T-tests showed no significant differences in the percentage of eGFP lesions between dsRNA-treated and water-treated samples as in Table 5.2 ($p \geq 0.05$), but a significant difference was seen using the Chi square method for 5.5 week (air-dried) samples treated with *DsAflR*-dsRNAs compared to the *eGFP*-dsRNA control.

To determine if there was reduced pathogen growth on *P. radiata*, qPCR was performed to estimate *D. septosporum* biomass in needles with eGFP lesions at 4.5 weeks post-inoculation. Due to the time required to examine each needle for individual eGFP lesions prior to gDNA extraction, gDNA was also extracted from some whole shoots (with a mix of needles with and without lesions) to determine if this would be a suitable alternative sampling method for biomass estimation. The proportion of fungal biomass was estimated by comparing the gene concentration, as the ratio of two genes, the fungal gene *DsPksA*, and the pine gene *CAD* (Chapter 2, section 2.12). For each of these methods (needles with verified lesions or whole shoots), three biological replicates were carried out for each treatment, which were three different shoots within one set of jars (air-dried or sealed immediately).

There was no successful PCR amplification of the *CAD* and/or *DsPksA* genes in at least half of the gDNA samples from both the needles with lesions and the whole shoots (Appendix Tables A7.12-A7.13, Test 1). In case there were inhibitors present in the sample that prevented amplification, such as a high content of polysaccharides, the gDNA samples were purified with an additional chloroform isoamyl alcohol extraction and ethanol precipitation step. However, all but one of the non-amplifying samples still did not amplify in the qPCR, despite the extra clean-up step (Appendix Tables A7.12-A7.13, Test 2), and increased Ct values for the amplifying samples from needles with lesions indicated possible loss of gDNA during the clean-up (Appendix Tables A7.12).

For the subset of qPCR biomass estimations that were successful, Table 5.3 shows the results using needle samples and Table 5.4 for shoot samples (taken from the full results shown in Appendix Tables A7.12 and A7.13). For both, there was high variability in results between replicate samples, particularly for the water controls. The analysis undertaken with samples of needles with confirmed eGFP lesions (Table 5.3) showed no significant differences in fungal biomass in needles treated with dsRNA and those treated with water, even when comparing to the *eGFP*-dsRNA control (Table 5.3 and Figure 5.9).

Table 5.3. Quantitative Polymerase Chain Reaction (qPCR) results for biomass estimation in pine needles with eGFP lesions 4.5 weeks post-inoculation.

Treatment	Shoot #[a]	Rep[b]	Ct target (*PksA*)[c]	Ct ref (*CAD*)[d]	Target/Ref[e]	T Test[f]	T-test (eGFP)[g]
eGFP-dsRNA	7	1	23.94	21.69	0.013	0.39	-
		2	24.07	21.99	0.014		
DsAflR 1-dsRNA	5	1	24.33	22.80	0.021	0.68	0.06
		2	24.62	22.90	0.018		
DsAflR 2-dsRNA	1	1	23.76	21.78	0.015	0.49	0.12
		2	23.73	21.83	0.016		
Water	2	1	22.01	21.46	0.043	-	-
		2	22.17	21.18	0.031		
Water	7	1	24.68	22.13	0.010	-	-
		2	24.61	22.48	0.014		

[a]Shoot refers to the number of the pine shoot from which the needles with lesions were taken for each independent treatment (dsRNA targeting *eGFP* or *DsAflR* regions 1 or 2, or water). Raw data are provided in Appendix Table A7.12. Data shown here are a subset of those results, since only some samples were successfully amplified.
[b]Rep refers to technical replicates used for qPCR.
[c]Cycle threshold (Ct) for amplification of polyketide synthase A (*DsPksA*). Regression line equation:
Y = -3.267x + 23.73
[d]Ct for amplification of cinnamyl alcohol dehydrogenase (*CAD*). Regression line equation:
Y = -3.365x + 27.84
[e]Target/Ref refers to the ratio of *DsPksA* (target gene) to *CAD* (reference gene), calculated from the regression equation.
[f]T-tests using the ratio of target to reference values, calculated from the regression equation, to compare treated samples to the four water samples shown (untreated controls).
[g]T-test as done above, except comparing the ratio of target to reference values between *DsAflR*-dsRNA-treated samples to the *eGFP*-dsRNA control.

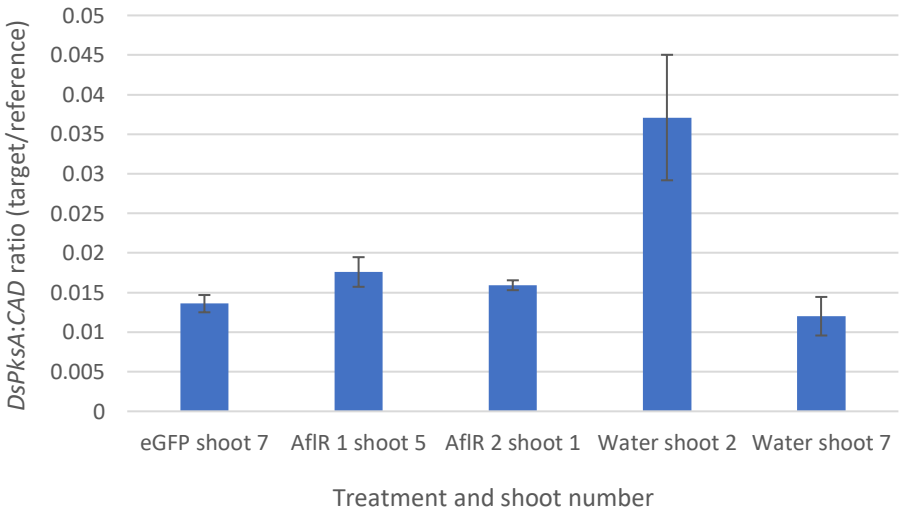

Figure 5.9. Estimation of fungal biomass after 4.5 weeks in disease lesions on *Pinus radiata* needles after treatment with dsRNA. A graphical representation of the results shown in Table 5.3. Pine shoots were sprayed with dsRNA targeting either the *eGFP* or *DsAflR* genes. The ratio of fungal polyketide synthase A (*DsPksA*) to pine cinnamyl alcohol dehydrogenase (*CAD*) (target/reference) is shown. X axis shows treatment with the dsRNA or water. Y axis shows the ratio between the two genes. Data represent one biological replicate for each dsRNA treatment and two biological replicates for the water controls; two technical replicates are shown for all treatments. Error bars represent standard deviation.

Estimation of *D. septosporum* biomass from whole pine shoots was only successful for some of the samples treated with dsRNA targeting *DsAflR*-2, and some water controls, but from each of the tests 1 and 2 (i.e. before and after re-purification of the gDNA templates) (Table 5.4). In this case, there was a signficant difference in fungal biomass between *DsAflR* 2-dsRNA-treated and untreated whole pine shoots (Table 5.4 and Figure 5.10). Estimates for *D. septosporum* biomass were consistent across both tests, showing similar ratios of the two genes. In both tests, there was a higher proportion of fungal biomass in shoot 1 sprayed with *DsAlfR* 2-dsRNA than in shoot 6 treated with the same dsRNA. High variability was also seen for the three water controls, highlighting immense variability in *D. septosporum* biomass estimations between clonal shoots (Figure 5.10).

Table 5.4. Quantitative Polymerase Chain Reaction (qPCR) results for biomass estimation in whole pine shoots 4.5 weeks post-inoculation.

Test #[a]	Treatment	Shoot #[b]	Rep[c]	Ct target (*PksA*)[d]	Ct ref (*CAD*)[e]	Target/Ref[f]	T Test[g]
1	*DsAflR* 2-dsRNA	1	1	21.35	22.13	0.108	0.008
			2	21.06	21.97	0.118	
2	*DsAflR* 2-dsRNA	1	1	23.6	24.89	0.146	0.054
			2	23.9	24.83	0.113	
1	*DsAflR* 2-dsRNA	6	1	-	-	-	0.147
			2	26.45	24.48	0.015	
2	*DsAflR* 2-dsRNA	6	1	28.01	26.35	0.018	0.308
			2	27.82	26.03	0.016	
1	Water	1	1	23.2	21.85	0.024	-
			2	23.22	22.01	0.027	
2	Water	1	1	24.92	24.17	0.035	-
			2	25.62	24.46	0.026	
1	Water	3	1	23.61	22.08	0.021	-
			2	23.74	22.17	0.021	
2	Water	3	1	26.90	25.22	0.018	-
			2	26.27	24.87	0.022	
1	Water	6	1	20.88	21.09	0.074	-
			2	20.93	21.07	0.070	
2	Water	6	1	24.18	24.89	0.097	-
			2	23.96	24.91	0.114	

[a]Test refers to the experimental number. In test 1, the assay was done with genomic DNA (gDNA) extracted from whole pine shoots and test 2 was a repeat of test 1 with gDNA further purified as in Chapter 2, section 2.12.

[b]Shoot refers to the number of the pine shoot from which the needles with lesions were taken for each treatment (dsRNA targeting *eGFP* or *DsAflR* regions 1 or 2, or water). Raw data are provided in Appendix Table A7.13.

[c]Rep refers to technical replicates used for qPCR.

[d]Cycle threshold (Ct) for amplification of polyketide synthase A (*DsPksA*). Regression line equation: $Y = -3.267x + 23.73$

[e]Ct for amplification of cinnamyl alcohol dehydrogenase (*CAD*). Regression line equation: $Y = -3.365x + 27.84$

[f]Target/Ref refers to the ratio of *DsPksA* (target gene) to *CAD* (reference gene).

[g]T-tests using the ratio of target to reference values, calculated from the regression equation, to compare individual treated samples to the combined replicate water samples from three shoots (untreated controls).

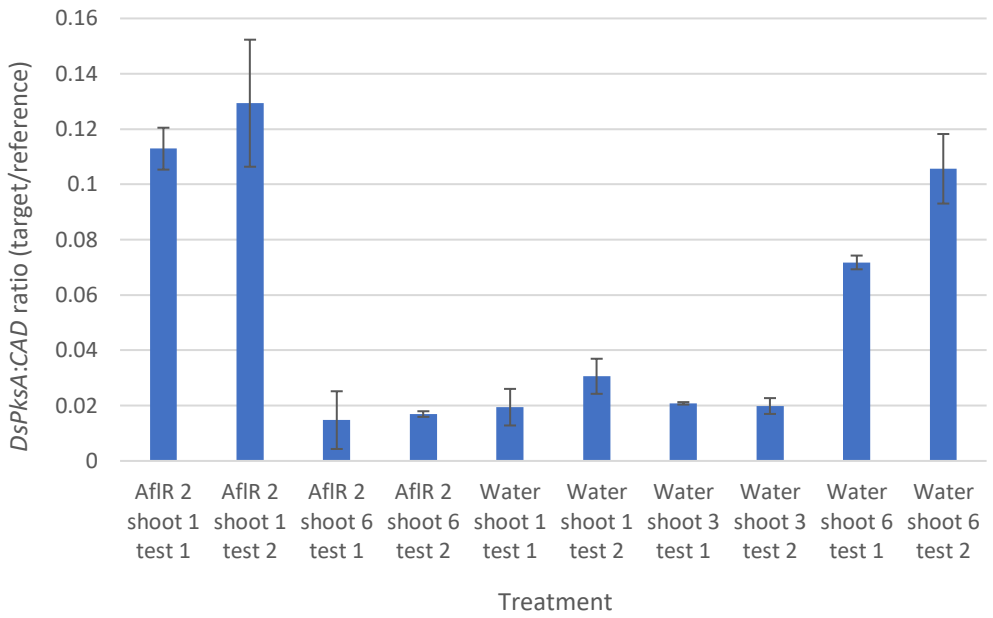

Figure 5.10. Estimation of fungal biomass after 4.5 weeks in *Pinus radiata* shoots after treatment with dsRNA. A graphical representation of the results shown in Table 5.4. Pine shoots were sprayed with dsRNA targeting either the enhanced green fluorescent protein-encoding gene (*eGFP*) or dothistromin pathway regulatory gene (*DsAflR*). The ratio of polyketide synthase A (*DsPksA*) to cinnamyl alcohol dehydrogenase (*CAD*) (target/reference) is shown. In test 1 the assay was first done with gDNA and in test 2 the assay was repeated with gDNA purified with an additional chloroform and ethanol precipitation step. X axis shows treatment with the dsRNA or water. Y axis shows the ratio between the two genes, *DsPksA* and *CAD*. Data represent two biological replicates for treatment with *DsAflR* 2-dsRNA and three replicates for water. Error bars represent standard deviation. Shoot and test numbers are allocated under the treatment type on the X axis.

Overall, the results for exogenous spray applications of dsRNA *in vitro* demonstrate variability in terms of the efficiency of silencing achieved, or lack of silencing in *D. septosporum* (Figures 5.1–5.3). The *in planta* artificial system using pine microshoots in glass jars also demonstrated considerable variability between shoots, but significantly fewer needles with confirmed lesions were noted for needles from three replicate shoots sprayed with either *DsAflR* 1- or *DsAflR* 2-dsRNA, compared to those sprayed with *eGFP*-dsRNA (Table 5.2, Figure 5.8). In future, more replicates should be included to minimise variability. Nevertheless, there are many challenges associated with silencing trials *in planta*, which are discussed further below.

5.3 Discussion

5.3.1 Suppression of genes by RNA interference (RNAi) depends on a number of factors

There are many contributing factors that affect uptake of dsRNA and gene silencing. One of these factors is the length of the target gene. Some differences in gene silencing between the two *DsAflR*-dsRNAs were observed. *In vitro* assays suggested reductions in gene expression following dsRNA treatment but this was not statistically significant (Figures 5.1–5.3), apart from treatment with *DsAflR* 1-dsRNA applied to the surface of mycelium on agar plates (Figure 5.2). Further trials need to be conducted with more replicates to take account of the high level of variability between replicates. However, the trend for decreased expression of *DsAflR* in these results suggest that the dsRNA may be successfully processed by the RNAi machinery in *D. septosporum* to elucidate changes in pathogen gene expression. These findings differ to McLoughlin et al. (2018), where dsRNA targeting the *thioredoxin reductase* gene in *S. sclerotiorum* showed a 79–85% reduction in transcript levels *in vitro*. They also observed a 45–60% reduction by treating *S. sclerotiorum* mycelium plugs with dsRNA targeting the *TIM44* gene. Other dsRNAs (59 tested) showed variable reductions in lesion sizes, with 20 different dsRNAs showing reductions in lesion sizes during *in planta* trials (26–85% reductions). Koch et al. (2016) found transcripts of the *CYP51* genes, *CYP51A*, *CYP51B* and *CYP51C*, in *F. graminearum* showed 58%, 50% and 48% reductions respectively compared to their *GFP*-dsRNA control, as a result of spraying barley leaves. In another study, Werner et al. (2020) found up to 50% inhibition of fungal infection for all constructs used.

The size and length of dsRNA molecules influence the uptake of dsRNAs by the fungus and the efficiency of gene silencing. Both *DsAflR* dsRNAs were of different lengths, targeted to different locations within the *DsAflR* gene and appeared to be associated with different silencing efficiencies (Figures 5.2–5.3). Hofle et al. (2020) found that the silencing efficiency for SIGS in *F. graminearum* was correlated with the length of the dsRNA sprayed, and further by spraying longer dsRNAs a higher silencing efficiency was achieved, possibly due to a greater number of siRNAs which are processed out of the dsRNA precursor. In another study, it was noted that dsRNAs designed to target sequences of RNAi machinery genes, such as *DCL* and *AGO* within *F. graminearum*, that were less than 200 bp in length (computationally designed dsRNA constructs) (173 bp

for *FgAGO1*, 192 bp for *FgAGO2*, 182 bp for *FgDCL1* and 193 bp for *FgDCL2*), had lower silencing efficiencies compared to dsRNAs longer than 650 bp (manually designed dsRNA constructs) (658 bp for *FgAGO1*, 871 bp for *FgAGO2*, 912 bp for *FgDCL1* and 870 bp for *FgDCL2*) (Werner et al., 2020). Although differences in lengths of the *DsAflR*-dsRNAs in this study were small compared to those compared in other studies described above (Höfle et al., 2020; Werner et al., 2020), this highlights differences in gene silencing efficiencies between different dsRNAs.

The concentration or amount of dsRNA used has the potential to affect the silencing efficiency of target genes in an organism. In the current study, an experiment was conducted to determine if greater silencing was achieved using more dsRNA. A lower amount (500 ng) of *DsAflR* 2-dsRNA was sufficient to silence *DsAflR* and achieved more silencing than 1000 ng of dsRNA (Figure 5.3). Differences in silencing efficiencies with dsRNAs applied at varying concentrations could be explained by the amount of RNA molecules present at the site for processing by the RNAi machinery. For example, with higher doses of the potent dsRNA it may be that the silencing machinery is not able to keep up with the high demand of RNA molecules. Therefore, the effects of silencing could be less than that of dsRNAs of lower concentrations where the RNA molecules can all be processed at once (McLoughlin et al., 2018). McLoughlin et al. (2018) also found that once maximal knockdown was achieved with a certain dsRNA concentration, stronger silencing responses were not seen with higher concentrations beyond this. RNAi studies in insects and mice have also shown that oversaturation of the RNAi machinery can occur due to an abundance of dsRNAs or siRNAs at the site for processing, resulting in competition between molecules (Grimm et al., 2006; Miller et al., 2012).

Successful silencing also depends on whether the fungal pathogen possesses components of the RNAi silencing machinery and their regulation. An attempt was made to investigate expression of the core RNAi gene, *DCL*, to determine if there was upregulation in response to treatment with dsRNA in *D. septosporum* (Appendix Figure A7.30 and Table A7.10). However, due to the presence of multiple peaks from the melt curve analysis using test samples, the *DCL* primers were deemed non-specific. Future work in designing a new set of primers with a higher primer specificity is required to investigate gene expression levels. Despite trends that indicated reductions in gene expression in response to treatment with dsRNA *in vitro* (section 5.3.1), it could be that *DCL* is very lowly

expressed or is not expressed at all (as shown by late amplification in some samples, Appendix Table A7.10), which could be a contributing factor for the lack of significant differences between dsRNA-treated and untreated samples. Further investigation of dicer expression is needed to determine whether this gene, or any of the other core genes (*AGO* and *RdRP*), are upregulated in response to addition of dsRNA. If *DCL* is not expressed in *D. septosporum*, SIGS could still be achieved via the plant processing route, where the dsRNA firstly gets taken up into plant cells, then processed into 21-bp siRNA, prior to transfer into the fungus where targeted gene silencing occurs. Song and Thomma (2018) found that the two dicer genes (*FaDicer1* and *FaDicer2*) in *F. graminearum* showed differential expression. A significant reduction was observed in *FaDicer2* expression 1 h and 5 h after removal of the *Myo5*-8-dsRNA targeting the *myosin 5* gene (myo5 segment 8) compared to time 0 h; there was also a decrease in *AGO1* expression after 5 h in the same experiment. This suggests that expression of fungal dicer genes may be regulated by the presence or absence of dsRNA.

5.3.2 Factors impacting exogenous applications of dsRNA *in planta*

The stability of RNA molecules represents another important factor impacting gene silencing. It is possible that the dsRNA used for experiments in this study for *in vitro* and *in planta* assays may have degraded, reducing the effectiveness of the dsRNA. Various strategies can be used to increase the stability of dsRNA molecules, such that they are not degraded by RNases. Although this was not tested in this study, future work in using formulations and carriers should be undertaken. This may improve dsRNA uptake and delivery, preventing the dsRNA molecules from degradation and providing different silencing outcomes. UV light, oxygen and temperature are all environmental factors, which influence the stability of dsRNA molecules. The use of edible coatings and nanoencapsulation of dsRNA for controlling diseases of post-harvest crops appears promising to improve stability of the dsRNA in the environment (de Oliveira Filho et al., 2021). Without formulations and carriers, naked dsRNAs can be degraded within two days of soil application (Dubelman et al., 2014), emphasising that this is a major limitation to applications of this technology. Mitter et al. (2017) and Jain et al. (2022) have used nanoparticles as carriers for delivery of dsRNA, such as layered double hydroxide (LDH) clay nanosheets. These carriers also help to stabilise dsRNA and have been shown to improve the longevity of dsRNAs for up to 30 days on leaves (Mitter et

al., 2017). Nanoparticles work by binding to the dsRNA, forming a dsRNA-LDH complex called BioClay and the dsRNA is released from the nanoparticle, due to the production of carbonic acid from the nanoparticle reacting with carbon dioxide and water in the environment. Over time the LDH nanosheets are degraded (Mitter et al., 2017; Niehl et al., 2018).

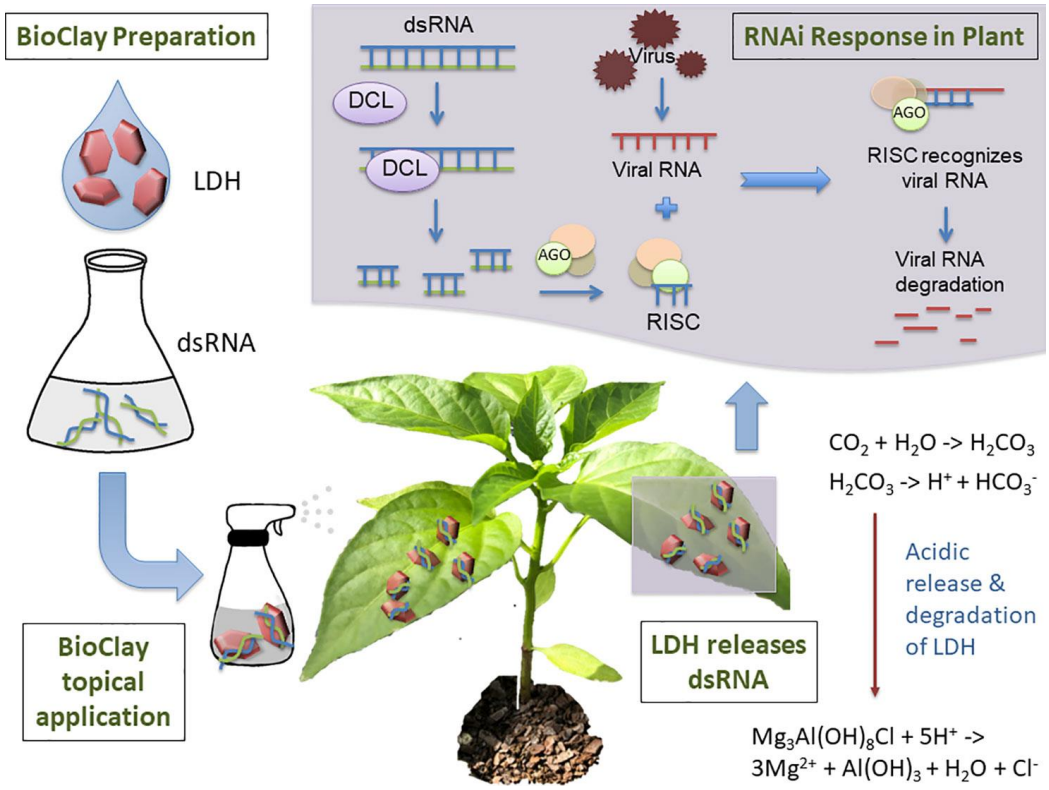

Figure 5.11. Topical applications of BioClay enhance RNAi protection window from plant viruses. dsRNA and layered double hydroxide (LDH) form a complex referred to as BioClay, which can be utilised as a RNAi spray for crop protection. Acidic release and degradation of LDH causes gradual release of the dsRNA, as a result of chemical interactions with carbonic acid from the nanoparticle and carbon dioxide from the environment. dsRNA is able to be taken up by the plant and confers protection (in this case from a virus), such that the dsRNA spray can remain effective for days or even weeks (Fletcher et al., 2020; Mitter et al., 2017).

The timing of external applications of fungicides is an important factor to consider for the prevention and management of fungal diseases. Each pathogen has a specific lifestyle, and by spraying at a particular time during development of infection, there is the best possible outcome for prevention of disease. Another important consideration with SIGS is whether leaves or uninfected tissue not sprayed by the dsRNA are protected from fungal infection, implying the importance of spray coverage (Šečić & Kogel, 2021). This should be considered for future experiments to determine if the pines would be protected if the

entire plant is not adequately sprayed on all needles. In addition to spraying for disease control, factors such as growing fungal pathogens under suboptimal conditions, like temperature and nutrient availability, can increase the sensitivity of the fungus to dsRNA. A silencing study where treatment with dsRNA at multiple time points under variable environmental conditions was explored for controlling *Macrophomina phaseolina in vitro* with application of a siRNA targeting a chitin synthase gene. Their results suggested that silencing can be successful under variable climate conditions, proposing that, for *in planta* RNAi assays, the efficacy of RNAi-based silencing technologies could potentially be advanced by adding dsRNA molecules at the time of planting, coordinated with periods where there are variable soil temperatures where *M. phaseolina* does not grow as well. This could, in turn, inhibit fungal growth and offer additional protection to the host plant (Forster & Shuai, 2020). As with timing of spray application and conditions affecting dsRNA uptake by fungi, it is likely that multiple sprays of the dsRNA solution should be applied to the host plant for effective treatment for future studies with *D. septosporum* and other pathogens, to inhibit the pathogen from sporulating and completing its life cycle.

Whilst developing an RNA bio-fungicide spray for disease control there are other considerations that need to be addressed. Firstly, this includes the need for quality dsRNA that is of a high yield for spraying crops. Production of large volumes of dsRNA can be achieved using platforms such as fermentation (Nerva et al., 2020; Zhu et al., 2016), which was discussed in the previous chapter (section 4.3.3). Secondly, the dsRNA must be sufficiently stable for commercialisation purposes. To improve the shelf life of RNA bio-fungicide sprays the dsRNA could be mixed with a formulation of nanoparticles or encapsulated in a coating (de Oliveira Filho et al., 2021). Thirdly, the efficacy of the dsRNA should be tested in the greenhouse, and further in field trials. However, methods to enhance dsRNA stability are promising for future disease control.

5.3.3 Limitations and challenges of pine infection assays

A limitation of the infection assay with *D. septosporum* was not being able to get similar levels of infection within replicate microshoots. Not all needles showed symptoms and it was hard to determine if there were lesions, as many needles were already dying (dark brown) and some had saprophytic fungal growth. An eGFP-labelled strain of

D. septosporum was used in this study to determine if DNB lesions were present, as the lesions fluoresced green under UV light. Some replicate shoots within each jar displayed more disease lesions than others and there was variability in *D. septosporum* biomass, despite them being clonal shoots (Tables 5.3–5.4 and Figures 5.9–5.10). More replicates are needed for further analysis of whether there is a reduction in disease symptoms, and further a reduction in fungal biomass due to dsRNA targeting *DsAflR*.

Numerous species of endophytes inhabit needle foliage of pines. Within the natural environment, endophytes would be present within pine foliage. The lack of endophytes in the sterile clonal pine shoots, grown on LPch agar medium in glass jars in this study, reinforces that this is an artificial system. In order to overcome this limitation field trials would be needed, in which dsRNA would be sprayed onto pine seedlings or young trees. In addition to endophytes, other fungi can be contaminants. Although the pine microshoots used in this study were derived from embryo cotyledon tissue under sterile conditions, there was some contamination of the pine shoots, probably introduced during the treatment or infection procedures (Appendix A7.31).

Chapter 6: Conclusions and Future Outlook

6.1 General conclusions and limitations of the study

This study explores the potential for external RNA in the management of a fungal disease, DNB. In the long term, this technology could potentially replace fungicides with RNAi bio-fungicides. The work described here provides a framework for future gene silencing studies with the forest pathogen *D. septosporum.* SIGS has not been attempted so far to control this fungal pathogen. The present work was undertaken to determine if the *DsAflR* gene of *D. septosporum*, and the *eGFP* control gene in transgenic *D. septosporum*, can serve as potential targets for achieving reduced DNB disease using SIGS.

DsAflR is a dothistromin pathway regulatory gene, deemed as the master regulator for the biosynthetic pathway involved in making the toxic virulence factor dothistromin. This gene was identified from a comprehensive literature study as a successful target for RNA silencing (Chapter 3) and most likely to have an effect on suppressing the virulence of *D. septosporum*. Two types of *DsAflR*-dsRNA, targeting different regions (1 and 2) of the *DsAflR* gene, were synthesised using an *in vitro* MEGAScript RNAi kit. Both *DsAflR*-dsRNAs were successfully taken up directly into *D. septosporum* (Chapter 4) and effectively silenced *DsAflR in vitro* (Chapter 5); however, not all reductions in *DsAflR* gene expression were statistically significant. *In planta* silencing trials revealed significantly fewer needles with disease lesions on shoots sprayed with *DsAflR* 1- and *DsAflR* 2-dsRNA respectively (12% and 16% of needles) compared to 24% of needles treated with *eGFP*-dsRNA in the 5.5 week samples (Table 5.2). However, fungal biomass in either pine needles or whole shoots sprayed with *DsAflR*-dsRNA was not significantly reduced compared to untreated controls, although due to lack of time these assays were only done with the 4.5 week samples. However, estimations of fungal biomass revealed significantly higher *D. septosporum* biomass in one of the 4.5 week whole shoot samples in *DsAflR* 2-dsRNA-treated pines compared to pines sprayed with water ($P = 0.008$ for test 1 and 0.054 for test 2; Table 5.4), opposite to what was predicted.

The *eGFP* gene was used as a control in this study to provide proof of concept of whether RNA silencing occurs in *D. septosporum* (Chapter 3). The use of commercially synthesised and manually constructed templates facilitated synthesis of *eGFP*-dsRNA (Chapter 4). Confocal microscopy showed that *eGFP*-dsRNA was capable of being taken

up directly into *D. septosporum* hyphae (Chapter 4) and *in vitro* silencing showed a reduction in *eGFP* gene expression in eGFP-labelled *D. septosporum*. Further, reductions in *D. septosporum* biomass *in planta* were not significant when compared to water controls (Chapter 5), as expected.

Due to a high level of variability between replicates, additional experiments need to be carried out with more replicates to determine if there are significant differences between dsRNA-treated and untreated samples. However, this study provides suggestions for protocols to follow, such as the choice of target gene(s) and the best way to generate dsRNA, fungal growth conditions, how best to apply dsRNA to *in vitro D. septosporum* cultures and suggestions for *in planta* silencing trials.

The experimental approach to testing dsRNA represents many challenges associated with uptake and RNAi-mediated gene silencing in fungi. Factors affecting *eGFP*-dsRNA and *DsAflR*-dsRNA uptake and silencing are represented in Figure 6.1. The design of dsRNAs is important to ensure target specificity and complementarity (blue box, left). Off-target sequences were investigated in this study through bioinformatic analyses (blue box, right). Factors such as the length of the dsRNA molecules, secreted nucleases, and CME (yellow box) impact on uptake and silencing. Other factors affecting uptake of dsRNAs in *D. septosporum* are whether the pathogen has the required RNAi machinery to carry out processing of the dsRNA and its expression (orange box) (Šečić & Kogel, 2021). All three components of the RNAi machinery, DCL, AGO and RdRPs, were identified and characterised in *D. septosporum* (Chapter 3). The stability of dsRNA is also important, but was not tested in this study; however, this would be important for future testing with the synthesised dsRNAs (discussed further in section 6.2).

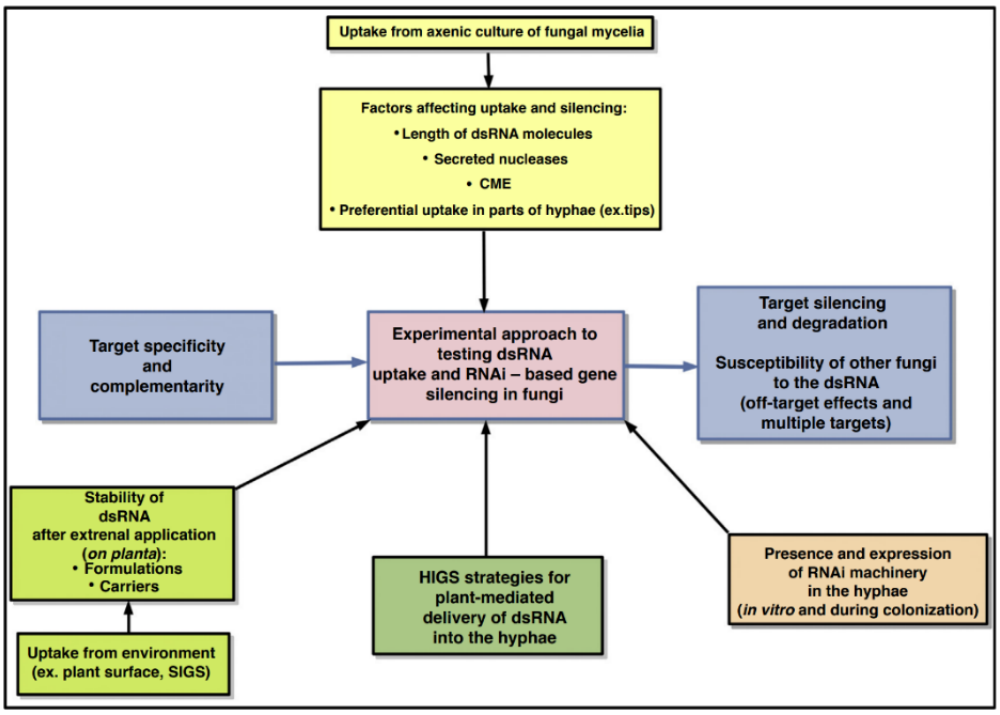

Figure 6.1. Factors impacting the uptake of dsRNA into fungal cells for gene silencing. Factors affecting uptake and silencing are target specificity and complementarity, off-target effects, length of dsRNA molecules, secreted nucleases, and clathrin-mediated endocytosis (CME). Also, the presence of RNAi machinery in the hyphae. (Image retrieved from Šečić & Kogel, 2021).

Optimal enzymatic synthesis of dsRNA *in vitro* requires changing certain variables to maximise yields. For this study, more trials with more replicates are needed in future to determine the optimal amount of dsRNA that can be synthesised. For example, a range of different incubation times for synthesising *eGFP*-dsRNA could be tested to determine if an increased production yield would be obtained within the same experiment. This would allow for the T7 RNA Polymerase to engage in a greater number of transcription initiation events. However, since there was a limited number of reactions with the MEGAScript RNAi kit, there were not enough reagents to explore a range of incubation times to synthesise all dsRNAs to determine optimal conditions for dsRNA synthesis in this study.

In vitro RNAi assays provide key information on whether gene silencing can be achieved prior to *in planta* assays. From the *in vitro* assays done there was variability in the water controls, therefore affecting the results obtained. A significant difference in gene expression was only noted for treatment with *DsAflR* 1-dsRNA to *D. septosporum* cultures using the agar plate method. More replicates are required to minimise variability

between samples and varying dsRNA concentrations should be analysed for treatment with *eGFP*-dsRNA and *DsAflR* 1-dsRNA, similar to what was done with the time course with the *DsAflR* 2-dsRNA.

Quantification of GFP fluorescence is useful for determining a reduction in fluorescence in response to dsRNA treatment. Further experiments could be aimed at quantifying GFP fluorescence to better determine if there is a reduction in treated samples, as this was not seen in the qualitative confocal imaging done. This could be done by culturing *D. septosporum* spores and quantifying how many spores are inoculated into each well of a 12-well plate as part of the experimental set-up. Fluorescence can be measured indicating within each well how many germinating spores are fluorescing. Even better, a plate reader that has the capabilities to quantify GFP fluorescence and Cy3 accumulation would contribute to findings of whether silencing of *eGFP* has occurred. Unfortunately, there were no plate readers with this function in the facility where this research was being carried out, and even in untreated samples the fluorescence of eGFP in transgenic *D. septosporum* was variable.

Pathogenicity assays can provide important information about whether disease symptoms on *P. radiata* can be reduced by exogenous spray applications of dsRNA. Preliminary results were obtained using clonal pine shoots in glass jars as an artificial system. Since this assay has only been trialled once by spraying pine shoots with spores (McCarthy, unpublished), the system is still in development. Adjustments were made in an attempt to improve the assay, such as air-drying the shoots in one set of jars after inoculation before sealing them closed. To determine if there are significant differences in fungal biomass between pines sprayed with dsRNA and those treated with water or *eGFP*-dsRNA controls, the assays should be repeated. There was some contamination from what appeared to be saprophytic fungi. It was difficult to prevent contamination whilst opening lids on the jars for sampling, even though precautions were taken to minimise this. The infection assay should also be repeated with more replicates, such as 5–6 replicate jars (each with multiple shoots) for each treatment and by sampling from a larger number of needles, although the very high cost of the clonal shoots is prohibitive. The use of more replicates could help account for variability between shoots developing DNB lesions. Not all needles sprayed with *D. septosporum* spores developed lesions and those that showed

disease progression indicated that disease lesions develop at different rates on various needles, as reported previously for *D. septosporum* (Bradshaw et al., 2016).

Biomass measurements by qPCR are useful for determining the growth of *D. septosporum* in *P. radiata*. The biomass results for needles differed considerably compared to the results for whole pine shoots. Needle samples were more reliable than the whole shoots, as needles were only chosen that had fluorescent lesions. Lesions were not able to be cut out of individual needles to minimise variation, as a considerable amount of pine tissue was required for extracting gDNA, and since the numbers of eGFP-fluorescing lesions differed in the different treatments, this could not be done. Given that all biomass estimates were taken at 4.5 weeks for qPCR, gDNA could be extracted from needles and whole shoots sampled at a later timepoint (e.g. at 5.5 weeks) to determine differences in fungal biomass between the two timepoints in future. However, in this work there was an extra variable, in that the two sets of jars were treated differently - air drying or sealing jars immediately after inoculation - as it was not certain which would best support *D. septosporum* infection of the pine shoots. In future work, only one of these conditions should be used for all jars. Pine shoots would be sealed immediately after spray inoculation with the fungus, as in general there were higher numbers of DNB lesions under these conditions (4.5 week samples in Table 5.2) compared to air-dried samples. This would maintain a higher level of needle wetness and also minimise opportunities for introduction of other contaminants.

To determine if SIGS could be successful for nursery applications, an assay could be performed by infecting pine seedlings or saplings. Differences in the effects of dsRNA treatments on targeted gene silencing and disease levels could also be compared on young seedlings and mature pines to provide an insight into efficacy of the treatment on pines in different seasons of the year and on different ages of pine trees. Optimal conditions for spraying *Pinus radiata* will help prevent infection by *D. septosporum*. Determining the best time of year to spray will also aid in most effective disease control. Wang et al. (2016) showed that by spraying with dsRNA two days before inoculation with *B. cinerea*, *Arabidopsis* plants were protected against disease.

To study the function of genes it is useful to make mutant strains lacking each gene of interest and determining the effect of the loss of gene function. In future, *D. septosporum* mutants could be made knocking out or mutating RNAi genes, such as *DCL* for example. Disruption of the *DCL* gene could be achieved using clustered regularly interspaced short palindromic repeats and CRISPR-associated protein 9 (CRISPR/Cas9) technology, which has been a successful method for generating disruption mutations in the *AflR* gene of *D. septosporum* (McCarthy et al., 2022). However, firstly, it would be important to identify if *DCL* is expressed and if the dsRNA is processed into siRNAs. Also, the functions of other potential target genes, could be explored to elucidate their function by disrupting or knocking out genes completely using CRISPR/Cas9 technology. This could determine if they play a role in reducing the production of dothistromin and affect the virulence of the fungal pathogen.

6.2 Future outlook

Future applications of RNA bio-fungicides could be aimed at spraying plants in nurseries, or existing forest management strategies could be adapted to spray forests with dsRNA. RNA silencing technologies could also be applicable to other pathogens of interest and if the pathogen became resistant due to mutation of the target gene, new sequences could be deployed in the dsRNA formulations, or new gene targets could be used. This section addresses potential applications of SIGS in the forest to control *D. septosporum*. These include developing an RNAi bio-fungicide that is capable of targeting multiple genes, is specific in that it does not target other organisms and has increased longevity.

Transcriptome analysis and literature searches enabled identification of *D. septosporum* SIGS gene candidates. Careful considerations were taken into account for choosing target genes and the location of the target region within a gene for which dsRNA could be synthesised. In future RNAi studies, other target genes could be explored, or multiple genes could be targeted at once, rather than creating an RNAi fungicide targeting a single gene. For example, multiple genes in the biosynthetic pathway for making dothistromin could be targeted. Studies have shown effective disease management through targeting multiple genes at once. A key study showed that transgenic *A. thaliana* plants expressing hairpin dsRNAs targeting two *DCL* genes (*DCL 1* and *DCL 2*) of both *B. cinerea* and

V. dahliae simultaneously were effective in suppressing disease, increasing resistance to both pathogens (Wang et al., 2016).

The specificity of target genes is highly important to avoid silencing unintended genes in other organisms. Endophytes and other organisms within the environment could be affected, potentially disturbing the balance between beneficial organisms in the plant community. Future work should determine if there are off-target effects on unwanted organisms prior to production of dsRNA at a commercial level. Before conducting field trials in the forest, it would be important to determine which organisms (e.g. endophytic fungi) are present in the forest environment. Genomes of these organisms could be sequenced to look for matches to the dsRNA sequence and also to matches of the 21-base siRNAs created once the dsRNA is processed. In this study, the *DsAflR* gene was chosen as a candidate gene, as it is not known to be found in other forest fungi, but a broader search would be needed for field trials.

The ability of dsRNA to degrade in the environment represents an important factor to consider for future *in planta* RNAi experiments, especially for field trials. The viability of dsRNAs should be tested to determine how long the dsRNA persists within pine seedlings. Further experiments exploring the use of nanoclay carriers to improve the longevity of the dsRNA within the plant, or on the surface of the plant, and/or in the environment should be investigated. This will help to ensure the dsRNA is successfully delivered and can withstand degradation by RNases (Landry & Mitter, 2019). dsRNA in combination with nanoclay particles can also be applied to plants in different ways, not just by spraying leaves in laboratory settings (Mosa & Youssef, 2021). For example, in the case of targeting root pathogens, the dsRNA can be directly applied to roots by dipping them in a dsRNA solution. For leaf pathogens the dsRNA solution mixed with a formulation could be applied to pine shoots by dipping the whole shoot in solution for *in vitro* tests with the dsRNA or via leaf petiole adsorption *in vitro*; however, these are not practical in forest settings. Seed coatings - encasing seeds with dsRNA - could also be applicable for applying dsRNA for protection against pathogens. SILWET L-77 was used within this study to help improve dsRNA uptake, as used by McLoughlin et al. (2018), but this does not protect dsRNA from degradation.

The ability to silence pathogen genes in various isolates of a fungal pathogen could enable broader protection against disease. Although NZ has a clonal population of *D. septosporum*, future work could be aimed at determining if other *D. septosporum* isolates found overseas (Barnes et al., 2014) are able to be controlled effectively using dsRNAs targeted to the *DsAflR* gene and/or other target genes. The genomes of 18 *D. septosporum* isolates are available (Supplementary Figure S4 in Bradshaw et al., 2019), and although the relative virulence levels of these isolates are not known, they all produce dothistromin and have *DsAflR* genes. The diversity in sequences between the different isolates should be considered when designing dsRNA constructs, if required for overseas applications where there are other isolates.

In conclusion, due to the global distribution of DNB disease and increased epidemics, new tools to manage DNB disease, caused by *D. septosporum*, are needed. This study lays down the groundwork for further research to be conducted to optimise SIGS specific to this forest pathogen and serves as a blueprint for managing other forest tree diseases worldwide. SIGS is a feasible option for the future, as it eliminates the need for generating GMOs and it can be designed to specifically target pathogens of interest. RNAi-based technologies could be the way of the future to control pathogens and can even be effective against viruses, insects, and bacteria (Zotti et al., 2018). There are many benefits for deploying RNA molecules in the form of an RNAi spray for disease management and prevention, such as "low toxicity relative to many existing pesticides, species-specificity, and a nominal environmental impact with appropriate dsRNA design." (Fletcher et al., 2020). As with any crop protection measure, the risks need to be identified, as illustrated in Figure 6.2. These risks include OTEs to non-target organisms in the environment and effects on human health, such as inhalation and ingestion of aerosols of dsRNA molecules. However, since dsRNA is able to degrade rapidly in the environment, this limits its impact to non-target organisms (Fletcher et al., 2020). Careful design of dsRNA sequences can minimise OTEs, and precautions for application can mitigate risks and aid in providing a ground-breaking plant protection strategy that can be utilised safely.

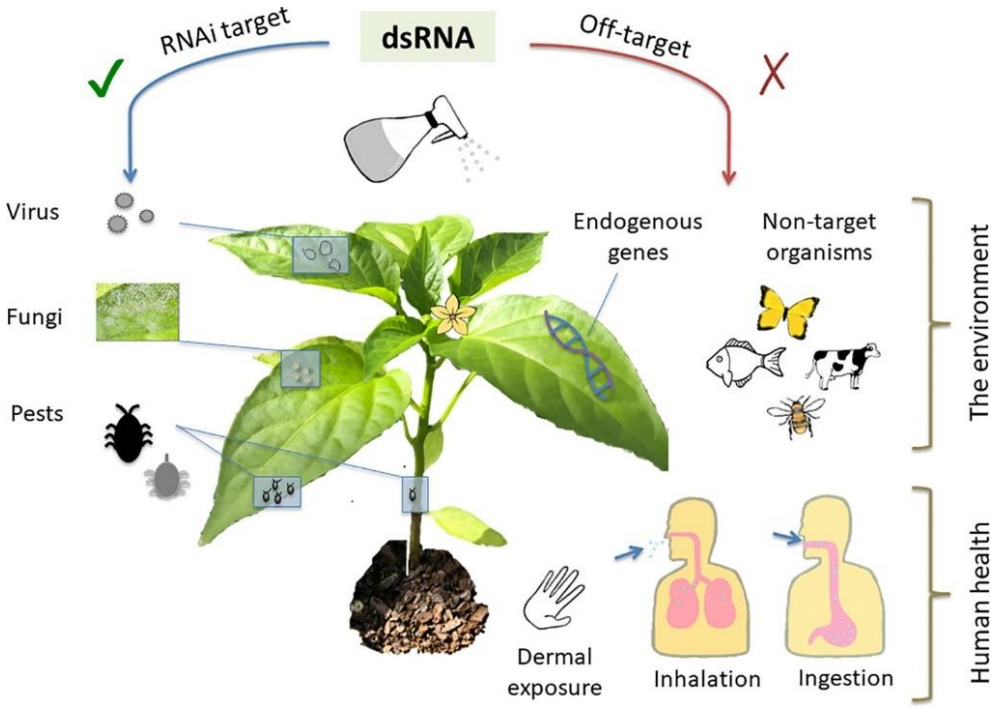

Figure 6.2. Potential risks for topical applications of dsRNAs. DsRNA molecules can be sprayed on plants to protect against various pathogens as shown here. To mitigate risks associated with spraying, the dsRNA should be specific to the pathogen, so that it does not target other organisms. Exposure to dsRNA could create potential risks for human health (Fletcher et al., 2020).

References

Alenezi, F. N., Fraser, S., Bełka, M., Doğmuş, T. H., Heckova, Z., Oskay, F., Belbahri, L., & Woodward, S. (2016). Biological control of Dothistroma needle blight on pine with *Aneurinibacillus migulanus*. *Forest Pathology, 46*(5), 555-558. https://doi.org/10.1111/efp.12237

Allen, C. D., Breshears, D. D., & McDowell, N. G. (2015). On underestimation of global vulnerability to tree mortality and forest die-off from hotter drought in the Anthropocene. *Ecosphere, 6*(8), 1-55. https://doi.org/10.1890/es15-00203.1

Andrade, C. M., Tinoco, M. L. P., Rieth, A. F., Maia, F. C. O., & Aragão, F. J. L. (2016). Host-induced gene silencing in the necrotrophic fungal pathogen *Sclerotinia sclerotiorum*. *Plant Pathology, 65*(4), 626-632. https://doi.org/10.1111/ppa.12447

Andrade, E. C., & Hunter, W. B. (2016). RNA interference–natural gene-based technology for highly specific pest control (HiSPeC). *RNA interference, 1*, 391-409. https://doi.org/10.5772/61612

Aoki, K., Moriguchi, H., Yoshioka, T., Okawa, K., & Tabara, H. (2007). *In vitro* analyses of the production and activity of secondary small interfering RNAs in *C. elegans*. *The EMBO Journal, 26*(24), 5007-5019. https://doi.org/10.1038/sj.emboj.7601910

Arif, M., Azhar, U., Arshad, M., Zafar, Y., Mansoor, S., & Asad, S. (2012). Engineering broad-spectrum resistance against RNA viruses in potato. *Transgenic Research, 21*(2), 303-311. https://doi.org/10.1007/s11248-011-9533-7

Arnér, E. S. J., & Holmgren, A. (2000). Physiological functions of thioredoxin and thioredoxin reductase. *Euorpean Journal of Biochemistry, 267*(20), 6102-6109. https://doi.org/10.1046/j.1432-1327.2000.01701.x

Barnes, I., Crous, P. W., Wingfield, B. D., & Wingfield, M. J. (2004). Multigene phylogenies reveal that red band needle blight of *Pinus* is caused by two distinct species of *Dothistroma, D. septosporum* and *D. pini*. *Studies in Mycology, 50*(2), 551–565. https://library.wur.nl/WebQuery/wurpubs/fulltext/24026

Barnes, I., Wingfield, M. J., Carbone, I., Kirisits, T., & Wingfield, B. D. (2014). Population structure and diversity of an invasive pine needle pathogen reflects anthropogenic activity. *Ecology and Evolution, 4*(18), 3642-3661. https://doi.org/10.1002/ece3.1200

Bassett, C., & Buchanan, M. (1970). A toxic difuroanthraquinone from *Dothistroma pini*. *Chemistry and Industry,* (52), 1659-1660.

Bauhus, J., Meer, P. V. D., & Kanninen, M. (2010). *Ecosystem Goods and Services from Plantation Forests* (1 ed.). Earthscan. https://doi-org.ezproxy.massey.ac.nz/10.4324/9781849776417

Baulcombe, D. (2004). RNA silencing in plants. *Nature, 431*(7006), 356-363. https://doi.org/10.1038/nature02874

Baum, J. A., Bogaert, T., Clinton, W., Heck, G. R., Feldmann, P., Ilagan, O., Johnson, S., Plaetinck, G., Munyikwa, T., Pleau, M., Vaughn, T., & Roberts, J. (2007). Control of coleopteran insect pests through RNA interference. *Nature Biotechnology, 25*(11), 1322-1326. https://doi.org/10.1038/nbt1359

Bednářová, M., Palovčíková, D., & Jankovský, L. (2006). The host spectrum of Dothistroma needle blight *Mycospharella pini* E. Rostrup - new hosts of Dothistroma needle blight observed in the Czech Republic. *Journal of Forest Science, 52*(1), 30-36. https://doi.org/10.17221/4484-jfs

Bennett, M., Deikman, J., Hendrix, B., & Iandolino, A. (2020). Barriers to efficient foliar uptake of dsRNA and molecular barriers to dsRNA activity in plant cells. *Frontiers in Plant Science, 11*, 1-7. https://doi.org/10.3389/fpls.2020.00816

Bilir, O., Telli, O., Norman, C., Budak, H., Hong, Y., & Tor, M. (2019). Small RNA inhibits infection by downy mildew pathogen *Hyaloperonospora arabidopsidis*. *Molecular Plant Pathology, 20*(11), 1523-1534. https://doi.org/10.1111/mpp.12863

Billmyre, R. B., Calo, S., Feretzaki, M., Wang, X., & Heitman, J. (2013). RNAi function, diversity, and loss in the fungal kingdom. *Chromosome Research, 21*(6-7), 561-572. https://doi.org/10.1007/s10577-013-9388-2

Boateng, K., & Lewis, K. J. (2015). Spore dispersal by *Dothistroma septosporum* in Northwest British Columbia. *Phytopathology, 105*(1), 69-79. https://doi.org/10.1094/PHYTO-06-13-0175-R

Borges, F., & Martienssen, R. A. (2015). The expanding world of small RNAs in plants. *Nature Reviews Molecular Cell Biology, 16*(12), 727-741. https://doi.org/10.1038/nrm4085

Boureau, T., ElMaarouf-Bouteau, H., Garnier, A., Brisset, M.-N., Perino, C., Pucheu, I., & Barny, M.-A. (2006). DspA/E, a type III effector essential for *Erwinia amylovora* pathogenicity and growth *in planta*, induces cell death in host apple and nonhost tobacco plants. *Molecular Plant-Microbe Interactions, 19*(1), 16-24. https://doi.org/10.1094/MPMI-19-0016

Bradshaw, R. E. (2004). Dothistroma (red-band) needle blight of pines and the dothistromin toxin: a review. *Forest Pathology, 34*(3), 163-185. https://doi.org/10.1111/j.1439-0329.2004.00356.x

Bradshaw, R. E., Bhatnagar, D., Ganley, R. J., Gillman, C. J., Monahan, B. J., & Seconi, J. M. (2002). *Dothistroma pini*, a forest pathogen, contains homologs of aflatoxin biosynthetic pathway genes. *Applied Environmental Microbiology, 68*(6), 2885-2892. https://doi.org/10.1128/aem.68.6.2885-2892.2002

Bradshaw, R. E., Bidlake, A., Forester, N., & Scott, D. B. (1997). Transformation of the fungal forest pathogen *Dothistroma pini* to hygromycin resistance. *Mycological Research, 101*(10), 1247-1250. https://doi.org/10.1017/s0953756297003870

Bradshaw, R. E., Guo, Y., Sim, A. D., Kabir, M. S., Chettri, P., Ozturk, I. K., Hunziker, L., Ganley, R. J., & Cox, M. P. (2016). Genome-wide gene expression dynamics of the fungal pathogen *Dothistroma septosporum* throughout its infection cycle of the gymnosperm host *Pinus radiata*. *Molecular Plant Pathology, 17*(2), 210-224. https://doi.org/10.1111/mpp.12273

Bradshaw, R. E., Jin, H., Morgan, B. S., Schwelm, A., Teddy, O. R., Young, C. A., & Zhang, S. (2006). A polyketide synthase gene required for biosynthesis of the aflatoxin-like toxin, dothistromin. *Mycopathologia, 161*(5), 283-294. https://doi.org/10.1007/s11046-006-0240-5

Bradshaw, R. E., Sim, A. D., Chettri, P., Dupont, P. Y., Guo, Y., Hunziker, L., McDougal, R. L., Van der Nest, A., Fourie, A., Wheeler, D., Cox, M. P., & Barnes, I. (2019). Global population genomics of the forest pathogen *Dothistroma septosporum* reveal chromosome duplications in high dothistromin-producing strains. *Molecular Plant Pathology, 20*(6), 784-799. https://doi.org/10.1111/mpp.12791

Bradshaw, R. E., Slot, J. C., Moore, G. G., Chettri, P., de Wit, P. J., Ehrlich, K. C., Ganley, A. R., Olson, M. A., Rokas, A., Carbone, I., & Cox, M. P. (2013). Fragmentation of an aflatoxin-like gene cluster in a forest pathogen. *New Phytologist, 198*(2), 525-535. https://doi.org/10.1111/nph.12161

Bradshaw, R. E., & Zhang, S. (2006). Biosynthesis of dothistromin. *Mycopathologia, 162*(3), 201-213. https://doi.org/10.1007/s11046-006-0054-5

Brakhage, A. A. (2013). Regulation of fungal secondary metabolism. *Nature Reviews Microbiology, 11*(1), 21-32. https://doi.org/10.1038/nrmicro2916

Brockerhoff, E. G., Jactel, H., Parrotta, J. A., & Ferraz, S. F. B. (2013). Role of eucalypt and other planted forests in biodiversity conservation and the provision of biodiversity-related ecosystem services. *Forest Ecology and Management, 301*, 43-50. https://doi.org/10.1016/j.foreco.2012.09.018

Brown, A., & Webber, J. (2008). Red band needle blight of conifers in Britain. *Forestry Commission*, (2). http://www.forestry.gov.uk/publications

Bulman, L., Ganley, R. J., & Dick, M. (2008). Needle diseases of radiata pine in New Zealand. *Scion Client Report, 13010*, 1-81. http://www.nzfoa.org.nz/images/stories/pdfs/content/fhrc_reports/2008-13010x.pdf

Bulman, L. S. (1993). Cyclaneusma needle-cast and Dothistroma needle blight in NZ pine plantations. *New Zealand Forestry, 38*(2), 21-24. https://www.researchgate.net/profile/L-Bulman/publication/265264385_Cyclaneusma_needle-cast_and_Dothistroma_needle_blight_in_NZ_pine_plantations/links/55d1b34208aee55

04f68ebfe/Cyclaneusma-needle-cast-and-Dothistroma-needle-blight-in-NZ-pine-plantations.pdf

Bulman, L. S., Bradshaw, R. E., Fraser, S., Martín-García, J., Barnes, I., Musolin, D. L., La Porta, N., Woods, A. J., Diez, J. J., Koltay, A., Drenkhan, R., Ahumada, R., Poljakovic-Pajnik, L., Queloz, V., Piškur, B., Doğmuş-Lehtijärvi, H. T., Chira, D., Tomešová-Haataja, V., Georgieva, M., Jankovský, L., Anselmi, N., Markovskaja, S., Papazova-Anakieva, I., Sotirovski, K., Lazarević, J., Adamčíková, K., Boroń, P., Bragança, H., Vettraino, A. M., Selikhovkin, A. V., Bulgakov, T. S., Tubby, K., & Cleary, M. (2016). A worldwide perspective on the management and control of Dothistroma needle blight. *Forest Pathology, 46*(5), 472-488. https://doi.org/10.1111/efp.12305

Bulman, L. S., Dick, M. A., Ganley, R. J., McDougal, R. L., Schwelm, A., & Bradshaw, R. E. (2013). Dothistroma Needle Blight. *Infectious Forest Diseases*, 436-457. https://www.researchgate.net/profile/Margaret_Dick/publication/249012109_Dothistroma_needle_blight/links/55f60a2208ae63926cf4f7da.pdf

Bulman, L. S., Gadgil, P. D., Kershaw, D. J., & Ray, J. W. (2004). Assessment and control of Dothistroma needle-blight. *Forest Research Bulletin No. 229*, 1-50. http://www.nzfoa.org.nz/images/stories/pdfs/content/fhrc_reports/2002-01.pdf

Burroughs, A. M., Ando, Y., & Aravind, L. (2014). New perspectives on the diversification of the RNA interference system: insights from comparative genomics and small RNA sequencing. *Wiley Interdisciplinary Reviews: RNA, 5*(2), 141-181. https://wires.onlinelibrary.wiley.com/doi/pdf/10.1002/wrna.1210?casa_token=J2REpEWpH-QAAAAA%3A1M89gi64R0PWGz8as9E93vDhjmv3cpZQKitxClw-5DhLkD5AzQvvJd0K7W7j6kCcOpn5jInt4I8nZV7-

Cai, W., Borlace, S., Lengaigne, M., van Rensch, P., Collins, M., Vecchi, G., Timmermann, A., Santoso, A., McPhaden, M. J., Wu, L., England, M. H., Wang, G., Guilyardi, E., & Jin, F. (2014). Increasing frequency of extreme El Niño events due to greenhouse warming. *Nature Climate Change, 4*(2), 111-116. https://doi.org/10.1038/nclimate2100

Campo, S., Gilbert, K. B., & Carrington, J. C. (2016). Small RNA-based antiviral defense in the phytopathogenic fungus *Colletotrichum higginsianum*. *PLoS Pathogens, 12*(6), 1-36. https://doi.org/10.1371/journal.ppat.1005640

Carreras-Villasenor, N., Esquivel-Naranjo, E. U., Villalobos-Escobedo, J. M., Abreu-Goodger, C., & Herrera-Estrella, A. (2013). The RNAi machinery regulates growth and development in the filamentous fungus *Trichoderma atroviride*. *Molecular Microbiology, 89*(1), 96-112. https://doi.org/10.1111/mmi.12261

Carthew, R. W., & Sontheimer, E. J. (2009). Origins and mechanisms of miRNAs and siRNAs. *Cell, 136*(4), 642-655. https://doi.org/10.1016/j.cell.2009.01.035

Casas-Mollano, J. A., Zacarias, E., Ma, X., Kim, E.-J., & Cerutti, H. (2016). mRNA-mediated silencing in eukaryotes: evolution of protein components and biological roles. In G. Hernández & R. Jagus (Eds.), *Evolution of the protein synthesis machinery and its*

regulation (pp. 513-529). Springer International Publishing. https://doi.org/10.1007/978-3-319-39468-8_20

Catalanotto, C., Pallotta, M., ReFalo, P., Sachs, M. S., Vayssie, L., Macino, G., & Cogoni, C. (2004). Redundancy of the two dicer genes in transgene-induced posttranscriptional gene silencing in *Neurospora crassa*. *Molecular and Cellular Biology, 24*(6), 2536-2545. https://doi.org/10.1128/MCB.24.6.2536-2545.2004

Cerutti, H., & Casas-Mollano, J. A. (2006). On the origin and functions of RNA-mediated silencing: from protists to man. *Current Genetics, 50*(2), 81-99. https://doi.org/10.1007/s00294-006-0078-x

Chen, W., Kastner, C., Nowara, D., Oliveira-Garcia, E., Rutten, T., Zhao, Y., Deising, H. B., Kumlehn, J., & Schweizer, P. (2016). Host-induced silencing of *Fusarium culmorum* genes protects wheat from infection. *Journal of Experimental Botany, 67*(17), 4979-4991. https://doi.org/10.1093/jxb/erw263

Cheng, W., Song, X. S., Li, H. P., Cao, L. H., Sun, K., Qiu, X. L., Xu, Y. B., Yang, P., Huang, T., Zhang, J. B., Qu, B., & Liao, Y. C. (2015). Host-induced gene silencing of an essential *chitin synthase* gene confers durable resistance to Fusarium head blight and seedling blight in wheat. *Plant Biotechnology Journal, 13*(9), 1335-1345. https://doi.org/10.1111/pbi.12352

Chettri, P. (2014). *Regulation of dothistromin toxin biosynthesis by the pine needle pathogen Dothistroma septosporum* [Doctoral Thesis, Massey University]. http://hdl.handle.net/10179/5950

Chettri, P., Calvo, A. M., Cary, J. W., Dhingra, S., Guo, Y., McDougal, R. L., & Bradshaw, R. E. (2012). The *veA* gene of the pine needle pathogen *Dothistroma septosporum* regulates sporulation and secondary metabolism. *Fungal Genetics and Biology, 49*(2), 141-151. https://doi.org/10.1371/journal.pgen.1003088

Chettri, P., Dupont, P. Y., & Bradshaw, R. E. (2018). Chromatin-level regulation of the fragmented dothistromin gene cluster in the forest pathogen *Dothistroma septosporum*. *Molecular Microbiology, 107*(4), 508-522. https://doi.org/10.1111/mmi.13898

Chettri, P., Ehrlich, K. C., Cary, J. W., Collemare, J., Cox, M. P., Griffiths, S. A., Olson, M. A., de Wit, P. J., & Bradshaw, R. E. (2013). Dothistromin genes at multiple separate loci are regulated by *AflR*. *Fungal Genetics Biology, 51*, 12-20. https://doi.org/10.1016/j.fgb.2012.11.006

Choi, J., Kim, K. T., Jeon, J., Wu, J., Song, H., Asiegbu, F. O., & Lee, Y. H. (2014). FunRNA: a fungi-centered genomics platform for genes encoding key components of RNAi. *BMC Genomics, 15*, 1-10. https://doi.org/10.1186/1471-2164-15-S9-S14

Chomczynski, P., & Sacchi, N. (1987). Single step method of RNA isolation by acid guanidinium thiocyanate-phenol-chloroform extraction. *Analytical Biochemistry, 162*(1), 156-159. https://doi.org/10.1016/0003-2697(87)90021-2

Cogoni, C., & Macino, G. (1999). Gene silencing in *Neurospora crassa* requires a protein homologous to RNA-dependent RNA polymerase. *Nature, 399*(6732), 166-169. https://doi.org/10.1038/20215

Cogoni, C., & Macino, G. (2000). Post-transcriptional gene silencing across kingdoms. *Current Opinion in Genetics and Development, 10*(6), 638-643. https://doi.org/10.1016/S0959-437X(00)00134-9

Dagenais, T. R., Giles, S. S., Aimanianda, V., Latge, J. P., Hull, C. M., & Keller, N. P. (2010). *Aspergillus fumigatus* LaeA-mediated phagocytosis is associated with a decreased hydrophobin layer. *Infection and Immunity, 78*(2), 823-829. https://doi.org/10.1128/IAI.00980-09

Daub, M. E., & Hangarter, R. P. (1983). Light-induced production of singlet oxygen and superoxide by the fungal toxin, cercosporin 1. *Plant Physiology, 73*(3), 855-857. https://doi.org/10.1104/pp.73.3.855

de Oliveira Filho, J. G., Silva, G. D. C., Cipriano, L., Gomes, M., & Egea, M. B. (2021). Control of postharvest fungal diseases in fruits using external application of RNAi. *Journal of Food Science, 86*(8), 3341-3348. https://doi.org/10.1111/1750-3841.15816

de Wit, P. J., van der Burgt, A., Okmen, B., Stergiopoulos, I., Abd-Elsalam, K. A., Aerts, A. L., Bahkali, A. H., Beenen, H. G., Chettri, P., Cox, M. P., Datema, E., de Vries, R. P., Dhillon, B., Ganley, A. R., Griffiths, S. A., Guo, Y., Hamelin, R. C., Henrissat, B., Kabir, M. S., Jashni, M. K., Kema, G., Klaubauf, S., Lapidus, A., Levasseur, A., Lindquist, E., Mehrabi, R., Ohm, R. A., Owen, T. J., Salamov, A., Schwelm, A., Schijlen, E., Sun, H., van den Burg, H. A., van Ham, R. C., Zhang, S., Goodwin, S. B., Grigoriev, I. V., Collemare, J., & Bradshaw, R. E. (2012). The genomes of the fungal plant pathogens *Cladosporium fulvum* and *Dothistroma septosporum* reveal adaptation to different hosts and lifestyles but also signatures of common ancestry. *PLoS Genetics, 8*(11), 1-22. https://doi.org/10.1371/journal.pgen.1003088

Dolezal, P., Likic, V., Tachezy, J., & Lithgow, T. (2006). Evolution of the molecular machines for protein import into mitochondria. *Science, 313*(5785), 314-318. https://doi.org/10.1126/science.1127895

Dominguez, C., Schubert, M., Duss, O., Ravindranathan, S., & Allain, F. H.-T. (2011). Structure determination and dynamics of protein–RNA complexes by NMR spectroscopy. *Progress in Nuclear Magnetic Resonance Spectroscopy, 58*(1-2), 1-61. https://doi.org/10.1016/j.pnmrs.2010.10.001

Doroguine, G. (1911). Une maladie cryptogamique du Pin. *Bulletin Trimestriel de la Société Mycologique de France, 27*(1), 105-106.

Dou, T., Shao, X., Hu, C., Liu, S., Sheng, O., Bi, F., Deng, G., Ding, L., Li, C., Dong, T., Gao, H., He, W., Peng, X., Zhang, S., Huo, H., Yang, Q., & Yi, G. (2020). Host-induced gene silencing of *Foc TR4 ERG6/11* genes exhibits superior resistance to Fusarium wilt

of banana. *Plant Biotechnology Journal, 18*(1), 11-13. https://doi.org/10.1111/pbi.13204

Dower, W. J., Miller, J. F., & Ragsdale, C. W. (1988). High efficiency transformation of *E. coli* by high voltage electroporation. *Nucleic Acids Research, 16*(13), 6127–6145. https://doi-org.ezproxy.massey.ac.nz/10.1093/nar/16.13.6127

Doyle, J. J., & Doyle, J. L. (1987). A rapid DNA isolation procedure for small quantities of fresh leaf tissue. *Phytochemical Bulletin, 19*(1), 11-15.

Draper, B. W., Mello, C. C., Bowerman, B., Hardin, J., & Priess, J. R. (1996). MEX-3 is a KH domain protein that regulates blastomere identity in early *C. elegans* embryos. *Cell, 87*(2), 205-216. https://doi.org/10.1016/S0092-8674(00)81339-2

Drenkhan, R., Tomešová-Haataja, V., Fraser, S., Bradshaw, R. E., Vahalík, P., Mullett, M. S., Martín-García, J., Bulman, L. S., Wingfield, M. J., Kirisits, T., Cech, T. L., Schmitz, S., Baden, R., Tubby, K., Brown, A., Georgieva, M., Woods, A., Ahumada, R., Jankovský, L., Thomsen, I. M., Adamson, K., Marçais, B., Vuorinen, M., Tsopelas, P., Koltay, A., Halasz, A., La Porta, N., Anselmi, N., Kiesnere, R., Markovskaja, S., Kačergius, A., Papazova-Anakieva, I., Risteski, M., Sotirovski, K., Lazarević, J., Solheim, H., Boroń, P., Bragança, H., Chira, D., Musolin, D. L., Selikhovkin, A. V., Bulgakov, T. S., Keča, N., Karadžić, D., Galovic, V., Pap, P., Markovic, M., Poljakovic Pajnik, L., Vasic, V., Ondrušková, E., Piškur, B., Sadiković, D., Diez, J. J., Solla, A., Millberg, H., Stenlid, J., Angst, A., Queloz, V., Lehtijärvi, A., Doğmuş-Lehtijärvi, H. T., Oskay, F., Davydenko, K., Meshkova, V., Craig, D., Woodward, S., Barnes, I., & Cleary, M. (2016). Global geographic distribution and host range of *Dothistroma* species: a comprehensive review. *Forest Pathology, 46*(5), 408-442. https://doi.org/10.1111/efp.12290

Drinnenberg, I. A., Fink, G. R., & Bartel, D. P. (2011). Compatibility with killer explains the rise of RNAi-deficient fungi. *Science, 333*(6049), 1592-1592. https://doi.org/10.1126/science.1209575

Drinnenberg, I. A., Weinberg, D. E., Xie, K. T., Mower, J. P., Wolfe, K. H., Fink, G. R., & Bartel, D. P. (2009). RNAi in budding yeast. *Science, 326*(5952), 544-550. https://doi.org/10.1126/science.1176945

Dubelman, S., Fischer, J., Zapata, F., Huizinga, K., Jiang, C., Uffman, J., Levine, S., & Carson, D. (2014). Environmental fate of double-stranded RNA in agricultural soils. *PLoS One, 9*(3), 1-7. https://doi.org/10.1371/journal.pone.0093155

Edwards, D. W., & Walker, J. (1978). Dothistroma needle blight in Australia. *Australian Forest Research, 8*(2), 125-137.

Fire, A., Xu, S., Montgomery, M. K., Kostas, S. A., Driver, S. E., & Mello, C. C. (1998). Potent and specific genetic interference by double-stranded RNA in *Caenorhabditis elegans*. *Nature, 391*(6669), 806-811. http://citeseerx.ist.psu.edu/viewdoc/download?doi=10.1.1.458.2627&rep=rep1&type=pdf

Fitzgerald, A., Van Kan, J. A., & Plummer, K. M. (2004). Simultaneous silencing of multiple genes in the apple scab fungus, *Venturia inaequalis*, by expression of RNA with chimeric inverted repeats. *Fungal Genetics and Biology, 41*(10), 963-971. https://doi.org/10.1016/j.fgb.2004.06.006

Fletcher, S. J., Reeves, P. T., Hoang, B. T., & Mitter, N. (2020). A perspective on RNAi-based biopesticides. *Frontiers in Plant Science, 11*, 1-10. https://doi.org/10.3389/fpls.2020.00051

Forster, H., & Shuai, B. (2020). Exogenous siRNAs against chitin synthase gene suppress the growth of the pathogenic fungus *Macrophomina phaseolina*. *Mycologia, 112*(4), 699-710. https://doi.org/10.1080/00275514.2020.1753467

Francklyn, C., Perona, J. J., Puetz, J., & Hou, Y. M. (2002). Aminoacyl-tRNA synthetases: versatile players in the changing theater of translation. *RNA, 8*(11), 1363–1372. https://doi.org/https://doi-org.ezproxy.massey.ac.nz/10.1017/s1355838202021180

Franich, R. A. (1988). Chemistry of weathering and solubilisation of copper fungicide and the effect of copper on germination, growth, metabolism, and reproduction of *Dothistroma pini*. *New Zealand Journal of Forestry Science, 18*, 318-328. http://citeseerx.ist.psu.edu/viewdoc/download?doi=10.1.1.703.9003&rep=rep1&type=pdf

Gadgil, P. D. (1977). Duration of leaf wetness periods and infection of *Pinus radiata* by *Dothistroma pini*. *New Zealand Journal of Forestry Science, 7*(1), 83-90. https://www.scionresearch.com/__data/assets/pdf_file/0009/58977/NZJFS711977GADGIL83-90.pdf

Gaffar, F. Y., Imani, J., Karlovsky, P., Koch, A., & Kogel, K.-H. (2019). Various components of the RNAi pathway are required for conidiation, ascosporogenesis, virulence, DON production and SIGS-mediated fungal inhibition by exogenous dsRNA in the head blight pathogen *Fusarium graminearum*. *Frontiers in Microbiology, 10*, 1-13. https://doi.org/10.3389/fmicb.2019.01662

Gebremichael, D. E., Haile, Z. M., Negrini, F., Sabbadini, S., Capriotti, L., Mezzetti, B., & Baraldi, E. (2021). RNA interference strategies for future management of plant pathogenic fungi: prospects and challenges. *Plants, 10*(4), 1-21. https://doi.org/10.3390/plants10040650

Gibson, I. A. S. (1974). Impact and control of dothistroma blight of pines. *European Journal of Forest Pathology, 4*(2), 89-100.

Gilbert, M. K., Majumdar, R., Rajasekaran, K., Chen, Z. Y., Wei, Q., Sickler, C. M., Lebar, M. D., Cary, J. W., Frame, B. R., & Wang, K. (2018). RNA interference-based silencing of the alpha-amylase (*amy1*) gene in *Aspergillus flavus* decreases fungal growth and aflatoxin production in maize kernels. *Planta, 247*(6), 1465-1473. https://doi.org/10.1007/s00425-018-2875-0

Gilmour, J. W. (1967). Distribution and significance of the needle blight of pines caused by *Dothistroma pini* in New Zealand. *Plant Disease Report, 51*(9), 727-730.

Goulding, C. (2016). New Zealand's export of wood products. *NZ Journal of Forestry, 61*(1), 1-3. https://nzjf.org.nz/free_issues/NZJF61_1_2016/7E574050-45F4-404f-9C98-7BDFAB94BD6A.pdf

Grigoriev, I. V., Nordberg, H., Shabalov, I., Aerts, A., Cantor, M., Goodstein, D., Kuo, A., Minovitsky, S., Nikitin, R., & Ohm, R. A. (2012). The genome portal of the Department of Energy Joint Genome Institute. *Nucleic Acids Research, 40*(1), 26-32. https://doi.org/10.1093/nar/gkr947

Grimm, D., Streetz, K. L., Jopling, C. L., Storm, T. A., Pandey, K., Davis, C. R., Marion, P., Salazar, F., & Kay, M. A. (2006). Fatality in mice due to oversaturation of cellular microRNA/short hairpin RNA pathways. *Nature, 441*(7092), 537-541. https://doi.org/10.1038/nature04791

Groenewald, M., Barnes, I., Bradshaw, R. E., Brown, A. V., Dale, A., Groenewald, J. Z., Lewis, K. J., Wingfield, B. D., Wingfield, M. J., & Crous, P. W. (2007). Characterization and distribution of mating type genes in the Dothistroma needle blight pathogens. *Phytopathology, 97*(7), 825-834. https://apsjournals.apsnet.org/doi/pdf/10.1094/PHYTO-97-7-0825

Gu, K. X., Song, X. S., Xiao, X. M., Duan, X. X., Wang, J. X., Duan, Y. B., Hou, Y. P., & Zhou, M. G. (2019). A *β_2-tubulin* dsRNA derived from *Fusarium asiaticum* confers plant resistance to multiple phytopathogens and reduces fungicide resistance. *Pesticide Biochemistry and Physiology, 153*, 36-46. https://doi.org/10.1016/j.pestbp.2018.10.005

Guo, Q., Liu, Q., Smith, N. A., Liang, G., & Wang, M. B. (2016). RNA silencing in plants: mechanisms, technologies and applications in horticultural crops. *Current Genomics, 17*(6), 476-489. https://doi.org/10.2174/1389202917666616052010

Guo, X. Y., Li, Y., Fan, J., Xiong, H., Xu, F. X., Shi, J., Shi, Y., Zhao, J. Q., Wang, Y. F., Cao, X. L., & Wang, W. M. (2019). Host-induced gene silencing of *MoAP1* confers broad-spectrum resistance to *Magnaporthe oryzae*. *Frontiers in Plant Science, 10*, 1-12. https://doi.org/10.3389/fpls.2019.00433

Guo, Y., Hunziker, L., Mesarich, C. H., Chettri, P., Dupont, P. Y., Ganley, R. J., McDougal, R. L., Barnes, I., & Bradshaw, R. E. (2020). *DsEcp2-1* is a polymorphic effector that restricts growth of *Dothistroma septosporum* in pine. *Fungal Genetics and Biology, 135*, 2-10. https://doi.org/10.1016/j.fgb.2019.103300

Hammond, S., Caudy, A., & Hannon, G. (2001). Post-transcriptional gene silencing by double-stranded RNA. *Nature Review Genetics, 2*, 110-119. https://doi.org/10.1038/35052556

Hargreaves, C. L., & Reeves, C. B. (2014). Progress towards initiation of somatic embryogenesis from differentiated tissues of radiata pine (*Pinus radiata* D. Don) using cotyledonary embryos. *In Vitro Cellular & Developmental Biology-Plant, 50*(2), 190-198. https://doi.org/10.1007/s11627-013-9581-1

Heath, M. C. (2000). Hypersensitive response-related death. *Plant Molecular Biology*, *44*, 321–334. https://doi-org.ezproxy.massey.ac.nz/10.1023/A:1026592509060

Henneberry, A. L., & Sturley, S. L. (2005). Sterol homeostasis in the budding yeast, *Saccharomyces cerevisiae*. *Seminars in Cell and Developmental Biology*, *16*(2), 155-161. https://doi.org/10.1016/j.semcdb.2005.01.006

Hennon, P. E., Frankel, S. J., Woods, A. J., Worrall, J. J., Norlander, D., Zambino, P. J., Warwell, M. V., Shaw, C. G., & Woodward, S. (2020). A framework to evaluate climate effects on forest tree diseases. *Forest Pathology*, *50*(6), 1-10. https://doi.org/10.1111/efp.12649

Hoffmeister, M., Maier, W., Thines, M., & Becker, Y. (2020). Tracking host infection and reproduction of *Peronospora salviae-officinalis* using an improved method for confocal laser scanning microscopy. *Plant Pathology*, *69*(5), 922-931. https://doi.org/10.1111/ppa.13173

Höfle, L., Biedenkopf, D., Werner, B. T., Shrestha, A., Jelonek, L., & Koch, A. (2020). Study on the efficiency of dsRNAs with increasing length in RNA-based silencing of the *Fusarium CYP51* genes. *RNA biology*, *17*(4), 463-473. https://doi.org/10.1080/15476286.2019.1700033

Hu, Y., Stenlid, J., Elfstrand, M., & Olson, A. (2013). Evolution of RNA interference proteins dicer and argonaute in Basidiomycota. *Mycologia*, *105*(6), 1489-1498. https://doi.org/10.3852/13-171

Huang, C. Y., Wang, H., Hu, P., Hamby, R., & Jin, H. (2019). Small RNAs - big players in plant-microbe interactions. *Cell Host Microbe*, *26*(2), 173-182. https://doi.org/10.1016/j.chom.2019.07.021

Hunziker, L., Tarallo, M., Gough, K., Guo, M., Hargreaves, C., Loo, T. S., McDougal, R. L., Mesarich, C. H., & Bradshaw, R. E. (2021). Apoplastic effector candidates of a foliar forest pathogen trigger cell death in host and non-host plants. *Science Reports*, *11*(1), 1-12. https://doi.org/10.1038/s41598-021-99415-5

Iwasaki, Y. W., Siomi, M. C., & Siomi, H. (2015). PIWI-interacting RNA: Its biogenesis and functions. *Annual Review in Biochemistry*, *84*, 405-433. https://doi.org/10.1146/annurev-biochem-060614-034258

Jahan, S. N., Asman, A. K., Corcoran, P., Fogelqvist, J., Vetukuri, R. R., & Dixelius, C. (2015). Plant-mediated gene silencing restricts growth of the potato late blight pathogen *Phytophthora infestans*. *Journal of Experimental Botany*, *66*(9), 2785-2794. https://doi.org/10.1093/jxb/erv094

Jain, C. K., & Wadhwa, G. (2018). Computational tools: RNA interference in fungal therapeutics. In *Current trends in Bioinformatics: An Insight* (pp. 207-225). Springer. https://doi.org/10.1007/978-981-10-7483-7_12

Jain, R. G., Fletcher, S. J., Manzie, N., Robinson, K. E., Li, P., Lu, E., Brosnan, C. A., Xu, Z. P., & Mitter, N. (2022). Foliar application of clay-delivered RNA interference for whitefly control. *Nature Plants, 8*(5), 535-548. https://doi.org/10.1038/s41477-022-01152-8

Jayawickrama, K. J. S., & Carson, M. J. (2000). A breeding strategy for the New Zealand Radiata Pine Breeding Cooperative. *Silvae Genetica, 49*(2), 82-89. https://www.thuenen.de/media/institute/fg/PDF/Silvae_Genetica/2000/Vol._49_Heft_2/49_2_82.pdf

Jesenicnik, T., Stajner, N., Radisek, S., & Jakse, J. (2019). RNA interference core components identified and characterised in *Verticillium nonalfalfae*, a vascular wilt pathogenic plant fungi of hops. *Science Reports, 9*(1), 8651. https://doi.org/10.1038/s41598-019-44494-8

Jones, D. A. B., John, E., Rybak, K., Phan, H. T. T., Singh, K. B., Lin, S. Y., Solomon, P. S., Oliver, R. P., & Tan, K. C. (2019). A specific fungal transcription factor controls effector gene expression and orchestrates the establishment of the necrotrophic pathogen lifestyle on wheat. *Science Reports, 9*(1), 1-13. https://doi.org/10.1038/s41598-019-52444-7

Kabir, M. S., Ganley, R. J., & Bradshaw, R. E. (2013). An improved artificial pathogenicity assay for Dothistroma needle blight on *Pinus radiata*. *Australasian Plant Pathology, 42*(4), 503-510. https://doi.org/10.1007/s13313-013-0217-z

Kabir, M. S., Ganley, R. J., & Bradshaw, R. E. (2015a). Dothistromin toxin is a virulence factor in dothistroma needle blight of pines. *Plant Pathology, 64*(1), 225-234. https://doi.org/10.1111/ppa.12229

Kabir, M. S., Ganley, R. J., & Bradshaw, R. E. (2015b). The hemibiotrophic lifestyle of the fungal pine pathogen *Dothistroma septosporum*. *Forest Pathology, 45*(3), 190-202. https://doi.org/10.1111/efp.12153

Kadotani, N., Nakayashiki, H., Tosa, Y., & Mayama, S. (2003). RNA silencing in the phytopathogenic fungus *Magnaporthe oryzae*. *Molecular Plant-Microbe Interactions, 16*(9), 769-776. https://doi.org/10.1094/MPMI.2003.16.9.769

Kalyandurg, P. B., Sundararajan, P., Dubey, M., Ghadamgahi, F., Zahid, M. A., Whisson, S., & Vetukuri, R. R. (2021). Spray-induced gene silencing as a potential tool to control potato late blight disease. *Phytopathology, 111*(12), 2168-2175. https://doi.org/10.1094/PHYTO-02-21-0054-SC

Kearse, M., Moir, R., Wilson, A., Stones-Havas, S., Cheung, M., Sturrock, S., Buxton, S., Cooper, A., Markowitz, S., & Duran, C. (2012). Geneious Basic: an integrated and extendable desktop software platform for the organization and analysis of sequence data. *Bioinformatics, 28*(12), 1647-1649. https://doi.org/10.1093/bioinformatics/bts199

Keenan, R. J., Reams, G. A., Achard, F., de Freitas, J. V., Grainger, A., & Lindquist, E. (2015). Dynamics of global forest area: Results from the FAO Global Forest Resources

Assessment 2015. *Forest Ecology and Management, 352*, 9-20. https://doi.org/10.1016/j.foreco.2015.06.014

Keller, N. P. (2019). Fungal secondary metabolism: regulation, function and drug discovery. *Nature Reviews Microbiology, 17*(3), 167-180. https://doi.org/10.1038/s41579-018-0121-1

Kennedy, J. J., Kendon, M., Killick, R. E., Dunn, R. J., Allan, R. J., Rayner, N. A., & McCarthy, M. (2020). Global and regional climate in 2019. *Weather, 75*(9), 264-271. https://doi.org/10.1002/wea.3822

Kettles, G. J., Hofinger, B. J., Hu, P., Bayon, C., Rudd, J. J., Balmer, D., Courbot, M., Hammond-Kosack, K. E., Scalliet, G., & Kanyuka, K. (2019). sRNA profiling combined with gene function analysis reveals a lack of evidence for cross-kingdom RNAi in the wheat - *Zymoseptoria tritici* pathosystem. *Frontiers in Plant Science, 10*, 1-16. https://doi.org/10.3389/fpls.2019.00892

Kini, H. K., & Walton, S. P. (2007). *In vitro* binding of single-stranded RNA by human dicer. *FEBS Letters, 581*(29), 5611-5616. https://doi.org/10.1016/j.febslet.2007.11.010

Klionsky, D. J., Herman, P. K., & Emr, S. D. (1990). The fungal vacuole: composition, function, and biogenesis. *Microbiological Reviews, 54*(3), 266-292. https://doi.org/10.1128/mr.54.3.266-292.1990

Koch, A., Biedenkopf, D., Furch, A., Weber, L., Rossbach, O., Abdellatef, E., Linicus, L., Johannsmeier, J., Jelonek, L., Goesmann, A., Cardoza, V., McMillan, J., Mentzel, T., & Kogel, K. H. (2016). An RNAi-based control of *Fusarium graminearum* infections through spraying of long dsRNAs involves a plant passage and is controlled by the fungal silencing machinery. *PLoS Pathogens, 12*(10), 1-22. https://doi.org/10.1371/journal.ppat.1005901

Koch, A., & Kogel, K. H. (2014). New wind in the sails: improving the agronomic value of crop plants through RNAi-mediated gene silencing. *Plant Biotechnology Journal, 12*(7), 821-831. https://doi.org/10.1111/pbi.12226

Koch, A., Kumar, N., Weber, L., Keller, H., Imani, J., & Kogel, K. H. (2013). Host-induced gene silencing of cytochrome P450 lanosterol C14 alpha-demethylase-encoding genes confers strong resistance to *Fusarium* species. *Proceedings of the National Academy of Sciences of the United States of America, 110*(48), 19324-19329. https://doi.org/10.1073/pnas.1306373110

Koch, A., Stein, E., & Kogel, K.-H. (2018). RNA-based disease control as a complementary measure to fight *Fusarium* fungi through silencing of the azole target Cytochrome P450 Lanosterol C-14 α-Demethylase. *European Journal of Plant Pathology, 152*(4), 1003-1010. https://doi.org/10.1007/s10658-018-1518-4

Konakalla, N. C., Kaldis, A., Berbati, M., Masarapu, H., & Voloudakis, A. E. (2016). Exogenous application of double-stranded RNA molecules from TMV *p126* and *CP*

genes confers resistance against TMV in tobacco. *Planta, 244*(4), 961-969. https://doi.org/10.1007/s00425-016-2567-6

Krstić, M. (1958). Unrecorded phytopathological records in nurseries and forests of Serbia. *Zaštita bilja, 45*, 75-79.

Kusch, S., Frantzeskakis, L., Thieron, H., & Panstruga, R. (2018). Small RNAs from cereal powdery mildew pathogens may target host plant genes. *Fungal Biology, 122*(11), 1050-1063. https://doi.org/10.1016/j.funbio.2018.08.008

Lacroix, H., Whiteford, J. R., & Spanu, P. D. (2008). Localization of *Cladosporium fulvum* hydrophobins reveals a role for HCf-6 in adhesion. *FEMS Microbiology Letters, 286*(1), 136-144. https://doi.org/10.1111/j.1574-6968.2008.01227.x

Landry, M. P., & Mitter, N. (2019). How nanocarriers delivering cargos in plants can change the GMO landscape. *Nature Nanotechnology, 14*(6), 512-514. https://doi.org/10.1038/s41565-019-0463-5

Laurie, J. D., Ali, S., Linning, R., Mannhaupt, G., Wong, P., Guldener, U., Munsterkotter, M., Moore, R., Kahmann, R., Bakkeren, G., & Schirawski, J. (2012). Genome comparison of barley and maize smut fungi reveals targeted loss of RNA silencing components and species-specific presence of transposable elements. *Plant Cell, 24*(5), 1733-1745. https://doi.org/10.1105/tpc.112.097261

Lee, H. C., Li, L., Gu, W., Xue, Z., Crosthwaite, S. K., Pertsemlidis, A., Lewis, Z. A., Freitag, M., Selker, E. U., Mello, C. C., & Liu, Y. (2010). Diverse pathways generate microRNA-like RNAs and Dicer-independent small interfering RNAs in fungi. *Molecular Cell, 38*(6), 803-814. https://doi.org/10.1016/j.molcel.2010.04.005

Livshits, M. A., Amosova, O. A., & Lyubchenko Yu, L. (1990). Flexibility difference between double-stranded RNA and DNA as revealed by gel electrophoresis. *Journal of Biomolecular Structure and Dynamic, 7*(6), 1237-1249. https://doi.org/10.1080/07391102.1990.10508562

Lo Presti, L., Lanver, D., Schweizer, G., Tanaka, S., Liang, L., Tollot, M., Zuccaro, A., Reissmann, S., & Kahmann, R. (2015). Fungal effectors and plant susceptibility. *Annual Review of Plant Biology, 66*, 513-545. https://doi.org/10.1146/annurev-arplant-043014-114623

Lu, M., Feau, N., Vidakovic, D. O., Ukrainetz, N., Wong, B., Aitken, S. N., Hamelin, R. C., & Yeaman, S. (2021). Comparative gene expression analysis reveals mechanism of *Pinus contorta* response to the fungal pathogen *Dothistroma septosporum*. *Molecular Plant Microbe Interactions, 34*(4), 397-409. https://doi.org/10.1094/MPMI-10-20-0282-R

Machado, A. K., Brown, N. A., Urban, M., Kanyuka, K., & Hammond-Kosack, K. E. (2018). RNAi as an emerging approach to control Fusarium head blight disease and mycotoxin contamination in cereals. *Pest Management Science, 74*(4), 790-799. https://doi.org/10.1002/ps.4748

Majumdar, R., Rajasekaran, K., & Cary, J. W. (2017). RNA Interference (RNAi) as a potential tool for control of mycotoxin contamination in crop plants: concepts and considerations. *Frontiers in Plant Science, 8*, 1-14. https://doi.org/10.3389/fpls.2017.00200

Malone, C. D., & Hannon, G. J. (2009). Small RNAs as guardians of the genome. *Cell, 136*(4), 656-668. https://doi.org/10.1016/j.cell.2009.01.045

Masanga, J. O., Matheka, J. M., Omer, R. A., Ommeh, S. C., Monda, E. O., & Alakonya, A. E. (2015). Downregulation of transcription factor *aflR* in *Aspergillus flavus* confers reduction to aflatoxin accumulation in transgenic maize with alteration of host plant architecture. *Plant Cell Reports, 34*(8), 1379-1387. https://doi.org/10.1007/s00299-015-1794-9

McCarthy, H. M., Tarallo, M., Mesarich, C. H., McDougal, R. L., & Bradshaw, R. E. (2022). Targeted gene mutations in the forest pathogen *Dothistroma septosporum* using CRISPR/Cas9. *Plants, 11*(8), 1-16. https://doi.org/10.3390/plants11081016

McDonald, T., Brown, D., Keller, N. P., & Hammond, T. M. (2005). RNA silencing of mycotoxin production in *Aspergillus* and *Fusarium* species. *Molecular Plant-Microbe Interactions, 18*(6), 539-545. https://doi.org/10.1094/MPMI-18-0539

McDougal, R., Yang, S., Schwelm, A., Stewart, A., & Bradshaw, R. (2011). A novel GFP-based approach for screening biocontrol microorganisms *in vitro* against *Dothistroma septosporum*. *Journal of Microbiology Methods, 87*(1), 32-37. https://doi.org/10.1016/j.mimet.2011.07.004

McLoughlin, A. G., Wytinck, N., Walker, P. L., Girard, I. J., Rashid, K. Y., de Kievit, T., Fernando, W. G. D., Whyard, S., & Belmonte, M. F. (2018). Identification and application of exogenous dsRNA confers plant protection against *Sclerotinia sclerotiorum* and *Botrytis cinerea*. *Scientific Reports, 8*(1), 1-14. https://doi.org/10.1038/s41598-018-25434-4

Mesarich, C. H., Griffiths, S. A., van der Burgt, A., Okmen, B., Beenen, H. G., Etalo, D. W., Joosten, M. H., & de Wit, P. J. (2014). Transcriptome sequencing uncovers the *Avr5* avirulence gene of the tomato leaf mold pathogen *Cladosporium fulvum*. *Molecular Plant Microbe Interactions, 27*(8), 846-857. https://doi.org/10.1094/MPMI-02-14-0050-R

Miller, S. C., Miyata, K., Brown, S. J., & Tomoyasu, Y. (2012). Dissecting systemic RNA interference in the red flour beetle *Tribolium castaneum*: parameters affecting the efficiency of RNAi. *PLoS One, 7*(10), 1-14. https://doi.org/10.1371/journal.pone.0047431

Mitter, N., Worrall, E. A., Robinson, K. E., Li, P., Jain, R. G., Taochy, C., Fletcher, S. J., Carroll, B. J., Lu, G. Q., & Xu, Z. P. (2017). Clay nanosheets for topical delivery of RNAi for sustained protection against plant viruses. *Nature Plants, 3*, 1-10. https://doi.org/10.1038/nplants.2016.207

Morris, K. V., & Mattick, J. S. (2014). The rise of regulatory RNA. *Nature Reviews Genetics, 15*(6), 423-437. https://doi.org/10.1038/nrg3722

Mosa, M. A., & Youssef, K. (2021). Topical delivery of host induced RNAi silencing by layered double hydroxide nanosheets: an efficient tool to decipher pathogenicity gene function of Fusarium crown and root rot in tomato. *Physiological and Molecular Plant Pathology, 115*, 1-16. https://doi.org/10.1016/j.pmpp.2021.101684

Muir, J. A., & Cobb, J. F. W. (2005). Infection of radiata and bishop pine by *Mycosphaerella pini* in California. *Canadian Journal of Forest Research, 35*(11), 2529-2538. https://doi.org/10.1139/x05-165

Mullett, M. S., Drenkhan, R., Adamson, K., Boron, P., Lenart-Boron, A., Barnes, I., Tomsovsky, M., Janosikova, Z., Adamcikova, K., Ondruskova, E., Queloz, V., Piskur, B., Musolin, D. L., Davydenko, K., Georgieva, M., Schmitz, S., Kacergius, A., Ghelardini, L., Kranjec Orlovic, J., Muller, M., Oskay, F., Hauptman, T., Halasz, A., Markovskaja, S., Solheim, H., Vuorinen, M., Heinzelmann, R., Hamelin, R. C., & Konecny, A. (2021). Worldwide genetic structure elucidates the eurasian origin and invasion pathways of *Dothistroma septosporum*, causal agent of dothistroma needle blight. *Journal of Fungi, 7*(2), 1-28. https://doi.org/10.3390/jof7020111

Mumbanza, F. M., Kiggundu, A., Tusiime, G., Tushemereirwe, W. K., Niblett, C., & Bailey, A. (2013). *In vitro* antifungal activity of synthetic dsRNA molecules against two pathogens of banana, *Fusarium oxysporum* f. sp. *cubense* and *Mycosphaerella fijiensis*. *Pest Management Science, 69*(10), 1155-1162. https://doi.org/10.1002/ps.3480

Murray, J. S., & Batko, S. (1962). *Dothistroma pini* Hulbary: A new disease on pine in Britain. *Forestry: An International Journal of Forest Research, 33*(1), 57-65. https://doi.org/10.1093/forestry/33.1.57

Mustacich, D., & Powis, G. (2000). Thioredoxin reductase. *Biochemical Journal, 346*(1), 1-8. https://doi.org/10.1042/bj3460001

Napoli, C., Lemieux, C., & Jorgensen, R. (1990). Introduction of a chimeric *chalcone synthase* gene into petunia results in reversible co-suppression of homologous genes in trans. *The Plant Cell, 2*(4), 279-289. http://www.plantcell.org/content/plantcell/2/4/279.full.pdf

Navarro, L., Jay, F., Nomura, K., He, S. Y., & Voinnet, O. (2008). Suppression of the microRNA pathway by bacterial effector proteins. *Science, 321*(5891), 964-967. https://science.sciencemag.org/content/sci/321/5891/964.full.pdf?casa_token=6p8k1udvIDcAAAAA:oPvH4aX_MsEeU2603Ynn1UraNo_QrHweGpGNy7LL5nPDqEq04ZwzvEWceVSJoeLo3FvztQjfcfUt9g

Nerva, L., Sandrini, M., Gambino, G., & Chitarra, W. (2020). Double-stranded RNAs (dsRNAs) as a sustainable tool against gray mold (*Botrytis cinerea*) in grapevine: effectiveness of different application methods in an open-air environment. *Biomolecules, 10*(2), 1-14. https://doi.org/10.3390/biom10020200

Newmark, P. A., Reddien, P. W., Cebria, F., & Alvarado, A. S. (2003). Ingestion of bacterially expressed double-stranded RNA inhibits gene expression in planarians. *Proceedings of the National Academy of Sciences, 100*(1), 11861-11865. https://www.pnas.org/content/100/suppl_1/11861.long

Niehl, A., Soininen, M., Poranen, M. M., & Heinlein, M. (2018). Synthetic biology approach for plant protection using dsRNA. *Plant Biotechnology Journal, 16*(9), 1679-1687. https://doi.org/10.1111/pbi.12904

Nowara, D., Gay, A., Lacomme, C., Shaw, J., Ridout, C., Douchkov, D., Hensel, G., Kumlehn, J., & Schweizer, P. (2010). HIGS: host-induced gene silencing in the obligate biotrophic fungal pathogen *Blumeria graminis*. *Plant Cell, 22*(9), 3130-3141. https://doi.org/10.1105/tpc.110.077040

Oliver, A., Cantón, R., Campo, P., Baquero, F., & Blázquez, J. (2000). High frequency of hypermutable *Pseudomonas aeruginosa* in cystic fibrosis lung infection. *Science, 288*(5469), 1251-1254. https://doi.org/10.1126/science.288.5469.1251

Ozturk, I. K., Dupont, P. Y., Chettri, P., McDougal, R., Bohl, O. J., Cox, R. J., & Bradshaw, R. E. (2019). Evolutionary relics dominate the small number of secondary metabolism genes in the hemibiotrophic fungus *Dothistroma septosporum*. *Fungal Biology, 123*(5), 397-407. https://doi.org/10.1016/j.funbio.2019.02.006

Pak, J., & Fire, A. (2007). Distinct populations of primary and secondary effectors during RNAi in *C. elegans*. *Science, 315*(5809), 241-244. https://doi.org/10.1126/science.1132839

Panwar, V., McCallum, B., & Bakkeren, G. (2013). Host-induced gene silencing of wheat leaf rust fungus *Puccinia triticina* pathogenicity genes mediated by the Barley stripe mosaic virus. *Plant Molecular Biology, 81*(6), 595-608. https://doi.org/10.1007/s11103-013-0022-7

Panwar, V., McCallum, B., Jordan, M., Loewen, M., Fobert, P., McCartney, C., & Bakkeren, G. (2016). RNA silencing approaches for identifying pathogenicity and virulence elements towards engineering crop resistance to plant pathogenic fungi. *CAB Reviews, 11*, 1-13. https://www3.botany.ubc.ca/bakkeren/Panwar_CABIreview_2016.pdf

Paturi, S., & Deshmukh, M. V. (2021). A glimpse of "dicer biology" through the structural and functional perspective. *Frontiers in Molecular Biosciences, 8*, 1-18. https://doi.org/10.3389/fmolb.2021.643657

Petrick, J. S., Brower-Toland, B., Jackson, A. L., & Kier, L. D. (2013). Safety assessment of food and feed from biotechnology-derived crops employing RNA-mediated gene regulation to achieve desired traits: a scientific review. *Regulatory Toxicology and Pharmacology, 66*(2), 167-176. https://doi.org/10.1016/j.yrtph.2013.03.008

Pliego, C., Nowara, D., Bonciani, G., Gheorghe, D. M., Xu, R., Surana, P., Whigham, E., Nettleton, D., Bogdanove, A. J., Wise, R. P., Schweizer, P., Bindschedler, L. V., & Spanu, P. D. (2013). Host-induced gene silencing in barley powdery mildew reveals a

class of ribonuclease-like effectors. *Molecular Plant Microbe Interactions, 26*(6), 633-642. https://doi.org/10.1094/MPMI-01-13-0005-R

Qi, T., Zhu, X., Tan, C., Liu, P., Guo, J., Kang, Z., & Guo, J. (2018). Host-induced gene silencing of an important pathogenicity factor *PsCPK1* in *Puccinia striiformis* f. sp. *tritici* enhances resistance of wheat to stripe rust. *Plant Biotechnology Journal, 16*(3), 797-807. https://doi.org/10.1111/pbi.12829

Qiao, L., Lan, C., Capriotti, L., Ah-Fong, A., Nino Sanchez, J., Hamby, R., Heller, J., Zhao, H., Glass, N. L., Judelson, H. S., Mezzetti, B., Niu, D., & Jin, H. (2021). Spray-induced gene silencing for disease control is dependent on the efficiency of pathogen RNA uptake. *Plant Biotechnology Journal, 19*(9), 1756-1768. https://doi.org/10.1111/pbi.13589

Qiao, Y., Liu, L., Xiong, Q., Flores, C., Wong, J., Shi, J., Wang, X., Liu, X., Xiang, Q., Jiang, S., Zhang, F., Wang, Y., Judelson, H. S., Chen, X., & Ma, W. (2013). Oomycete pathogens encode RNA silencing suppressors. *Nature Genetics, 45*(3), 1-17. https://doi.org/10.1038/ng.2525

Qin, H., Chen, F., Huan, X., Machida, S., Song, J., & Yuan, Y. A. (2010). Structure of the *Arabidopsis thaliana* DCL4 DUF283 domain reveals a noncanonical double-stranded RNA-binding fold for protein-protein interaction. *RNA, 16*(3), 474-481. https://doi.org/10.1261/rna.1965310

Rasmann, S., De Vos, M., Casteel, C. L., Tian, D., Halitschke, R., Sun, J. Y., Agrawal, A. A., Felton, G. W., & Jander, G. (2012). Herbivory in the previous generation primes plants for enhanced insect resistance. *Plant Physiology, 158*(2), 854-863. https://doi.org/10.1104/pp.111.187831

Ray, J. W., & Vanner, A. L. (1988). Improvements in the technology of Dothistroma control. *What's New in Forest Research No. 169*.

Ridout, M., & Newcombe, G. (2015). The frequency of modification of Dothistroma pine needle blight severity by fungi within the native range. *Forest Ecology and Management, 337*, 153-160. https://doi.org/10.1016/j.foreco.2014.11.010

Riquelme, M., Aguirre, J., Bartnicki-Garcia, S., Braus, G. H., Feldbrugge, M., Fleig, U., Hansberg, W., Herrera-Estrella, A., Kamper, J., Kuck, U., Mourino-Perez, R. R., Takeshita, N., & Fischer, R. (2018). Fungal morphogenesis, from the polarized growth of hyphae to complex reproduction and infection structures. *Microbiology and Molecular Biology Reviews, 82*(2), 1-47. https://doi.org/10.1128/MMBR.00068-17

Roberts, A. F., Devos, Y., Lemgo, G. N., & Zhou, X. (2015). Biosafety research for non-target organism risk assessment of RNAi-based GE plants. *Frontiers in Plant Science, 6*, 1-9. https://doi.org/10.3389/fpls.2015.00958

Rocafort, M., Fudal, I., & Mesarich, C. H. (2020). Apoplastic effector proteins of plant-associated fungi and oomycetes. *Current Opinion in Plant Biology, 56*, 9-19. https://doi.org/10.1016/j.pbi.2020.02.004

Rodas, C. A., Wingfield, M. J., Granados, G. M., & Barnes, I. (2016). Dothistroma needle blight: an emerging epidemic caused by *Dothistroma septosporum* in Colombia. *Plant Pathology, 65*(1), 53-63. https://doi.org/10.1111/ppa.12389

Rodriguez-Hernandez, A. M., Gosalvez, B., Sempere, R. N., Burgos, L., Aranda, M. A., & Truniger, V. (2012). Melon RNA interference (RNAi) lines silenced for *Cm-eIF4E* show broad virus resistance. *Molecular Plant Pathology, 13*(7), 755-763. https://doi.org/10.1111/j.1364-3703.2012.00785.x

Rokas, A., Wisecaver, J. H., & Lind, A. L. (2018). The birth, evolution and death of metabolic gene clusters in fungi. *Nature Reviews Microbiology, 16*(12), 731-744. https://doi.org/10.1038/s41579-018-0075-3

Rolando, C., Baillie, B., Withers, T., Bulman, L., & Garrett, L. (2016). Pesticide use in planted forests in New Zealand. *New Zealand Journal of Forestry, 61*(2), 3-10. http://nzjf.org.nz/free_issues/NZJF61_2_2016/BE450C21-9BB0-4280-A26D-FD61EFFF0D82.pdf

Romano, N., & Macino, G. (1992). Quelling: transient inactivation of gene expression in *Neurospora crassa* by transformation with homologous sequences. *Molecular Microbiology, 6*(22), 3343-3353. https://doi.org/10.1111/j.1365-2958.1992.tb02202.x

Rueden, C. T., Schindelin, J., Hiner, M. C., DeZonia, B. E., Walter, A. E., Arena, E. T., & Eliceiri, K. W. (2017). ImageJ2: ImageJ for the next generation of scientific image data. *BMC Bioinformatics, 18*(1), 1-26. https://doi.org/10.1186/s12859-017-1934-z

San Miguel, K., & Scott, J. G. (2016). The next generation of insecticides: dsRNA is stable as a foliar-applied insecticide. *Pest Management Science, 72*(4), 801-809. https://doi.org/10.1002/ps.4056

Sang, H., & Kim, J. (2020). Advanced strategies to control plant pathogenic fungi by host-induced gene silencing (HIGS) and spray-induced gene silencing (SIGS). *Plant Biotechnology Reports, 14*(1), 1-8. https://doi.org/10.1007/s11816-019-00588-3

Schreiber, L. (2005). Polar paths of diffusion across plant cuticles: new evidence for an old hypothesis. *Annals of Botany, 95*(7), 1069-1073. https://doi.org/10.1093/aob/mci122

Schwelm, A. (2007). *Investigations of dothistromin gene expression in Dothistroma septosporum and the putative role of dothistromin toxin* [Doctoral Thesis, Massey University]. http://hdl.handle.net/10179/1187

Šečić, E., & Kogel, K.-H. (2021). Requirements for fungal uptake of dsRNA and gene silencing in RNAi-based crop protection strategies. *Current Opinion in Biotechnology, 70*, 136-142. https://doi.org/10.1016/j.copbio.2021.04.001

Segers, G. C., Zhang, X., Deng, F., Sun, Q., & Nuss, D. L. (2007). Evidence that RNA silencing functions as an antiviral defense mechanism in fungi. *Proceedings of the National Academy of Sciences, 104*(31), 12902-12906. https://doi.org/10.1073/pnas.0702500104

Shabalina, S. A., & Koonin, E. V. (2008). Origins and evolution of eukaryotic RNA interference. *Trends in Ecology and Evolution, 23*(10), 578-587. https://doi.org/10.1016/j.tree.2008.06.005

Shekhawat, U. K. S., Ganapathi, T. R., & Hadapad, A. B. (2012). Transgenic banana plants expressing small interfering RNAs targeted against viral replication initiation gene display high-level resistance to banana bunchy top virus infection. *Journal of General Virology, 93*(8), 1804-1813. https://doi.org/10.1099/vir.0.041871-0

Shimizu, T., Nakazono-Nagaoka, E., Akita, F., Wei, T., Sasaya, T., Omura, T., & Uehara-Ichiki, T. (2012). Hairpin RNA derived from the gene for Pns9, a viroplasm matrix protein of *Rice gall dwarf virus*, confers strong resistance to virus infection in transgenic rice plants. *Journal of Biotechnology, 157*(3), 421-427. https://doi.org/10.1016/j.jbiotec.2011.12.015

Sijen, T., Steiner, F. A., Thijssen, K. L., & Plasterk, R. H. (2007). Secondary siRNAs result from unprimed RNA synthesis and form a distinct class. *Science, 315*(5809), 244-247. https://doi.org/10.1126/science.1136699

Silar, P. (1995). Two new easy to use vectors for transformations. *Fungal Genetics Reports, 42*(73), 1-3. https://doi.org/10.4148/1941-4765.1353

Song, J. J., Smith, S. K., Hannon, G. J., & Joshua-Tor, L. (2004). Crystal structure of argonaute and its implications for RISC slicer activity. *Science, 305*(5689), 1434-1437. https://doi.org/10.1126/science.1102514

Song, Y., & Thomma, B. P. H. J. (2018). Host-induced gene silencing compromises Verticillium wilt in tomato and *Arabidopsis*. *Molecular Plant Pathology, 19*(1), 77-89. https://doi.org/10.1111/mpp.12500

Spoel, S. H., & Dong, X. (2012). How do plants achieve immunity? Defence without specialized immune cells. *Nature Reviews Immunology, 12*(2), 89-100. https://doi.org/10.1038/nri3141

Swarts, D. C., Jore, M. M., Westra, E. R., Zhu, Y., Janssen, J. H., Snijders, A. P., Wang, Y., Patel, D. J., Berenguer, J., & Brouns, S. J. (2014). DNA-guided DNA interference by a prokaryotic Argonaute. *Nature, 507*(7491), 258-261. https://doi.org/10.1038/nature12971

Tanaka, A., Christensen, M. J., Takemoto, D., Park, P., & Scott, B. (2006). Reactive oxygen species play a role in regulating a fungus–perennial ryegrass mutualistic interaction. *The Plant Cell, 18*(4), 1052-1066. https://doi.org/10.1105/tpc.105.039263

Taning, C. N., Arpaia, S., Christiaens, O., Dietz-Pfeilstetter, A., Jones, H., Mezzetti, B., Sabbadini, S., Sorteberg, H. G., Sweet, J., Ventura, V., & Smagghe, G. (2020). RNA-based biocontrol compounds: current status and perspectives to reach the market. *Pest Management Science, 76*(3), 841-845. https://doi.org/10.1002/ps.5686

Tarallo, M., McDougal, R. L., Chen, Z. Y., Wang, Y., Bradshaw, R. E., & Mesarich, C. H. (2022). *Characterization of two conserved cell death elicitor families from the Dothideomycete fungal pathogens Dothistroma septosporum and Fulvia fulva (syn. Cladosporium fulvum)*. https://www.biorxiv.org/content/biorxiv/early/2022/06/09/2022.06.07.495221.full.pdf

Taylor, R. G., Walker, D. C., & Mclnnes, R. R. (1993). *E. coli* host strains significantly affect the quality of small scale plasmid DNA preparations used for sequencing. *Nucleic Acids Research, 21*(7), 1677-1678. https://doi.org/10.1186/1472-6750-3-3

Tenllado, F., Martínez-García, B., Vargas, M., & Díaz-Ruíz, J. R. (2003). Crude extracts of bacterially expressed dsRNA can be used to protect plants against virus infections. *BMC Biotechnology, 3*(1), 1-11. https://doi.org/10.1186/1472-6750-3-3

Thakare, D., Zhang, J. B., Wing, R. A., Cotty, P. J., & Schmidt, M. A. (2017). Aflatoxin-free transgenic maize using host-induced gene silencing. *Science Advances, 3*(3), 1-8. https://advances.sciencemag.org/content/advances/3/3/e1602382.full.pdf

Thomas, E., Herrero, S., Eng, H., Gomaa, N., Gillikin, J., Noar, R., Beseli, A., & Daub, M. E. (2020). Engineering Cercospora disease resistance via expression of *Cercospora nicotianae* cercosporin-resistance genes and silencing of cercosporin production in tobacco. *PLoS One, 15*(3), 1-19. https://doi.org/10.1371/journal.pone.0230362

Untergasser, A., Cutcutache, I., Koressaar, T., Ye, J., Faircloth, B. C., Remm, M., & Rozen, S. G. (2012). Primer3—new capabilities and interfaces. *Nucleic Acids Research, 40*(15), 1-12. https://doi.org/10.1093/nar/gks596

van Lierop, P., Lindquist, E., Sathyapala, S., & Franceschini, G. (2015). Global forest area disturbance from fire, insect pests, diseases and severe weather events. *Forest Ecology and Management, 352*, 78-88. https://doi.org/10.1016/j.foreco.2015.06.010

Villebonne, D., & Maugard, F. (1999). Rapid development of Dothistroma needle blight (*Scirrhia pini*) on Corsican pine (*Pinus nigra* subsp. *laricio*) in France. *Annual Report 1998*, 30-32.

Wagner, A., Ralph, J., Akiyama, T., Flint, H., Phillips, L., Torr, K., Nanayakkara, B., & Te Kiri, L. (2007). Exploring lignification in conifers by silencing hydroxycinnamoyl-CoA shikimate hydroxycinnamoyltransferase in *Pinus radiata*. *Proceedings of the National Academy of Sciences of the USA, 104*(28), 11856-11861. https://doi.org/10.1073/pnas.0701428104

Wang, M., & Jin, H. (2017). Spray-induced gene silencing: a powerful innovative strategy for crop protection. *Trends in Microbiology, 25*(1), 4-6. https://doi.org/10.1016/j.tim.2016.11.011

Wang, M., Weiberg, A., Lin, F. M., Thomma, B. P., Huang, H. D., & Jin, H. (2016). Bidirectional cross-kingdom RNAi and fungal uptake of external RNAs confer plant protection. *Nature Plants, 2*, 1-10. https://doi.org/10.1038/nplants.2016.151

Wang, X., Hsueh, Y.-P., Li, W., Floyd, A., Skalsky, R., & Heitman, J. (2010). Sex-induced silencing defends the genome of *Cryptococcus neoformans* via RNAi. *Genes & development, 24*(22), 2566-2582. https://doi.org/10.1101/gad.1970910

Watt, M. S., Kriticos, D. J., Alcaraz, S., Brown, A. V., & Leriche, A. (2009). The hosts and potential geographic range of Dothistroma needle blight. *Forest Ecology and Management, 257*(6), 1505-1519. https://doi.org/10.1016/j.foreco.2008.12.026

Weiberg, A., Wang, M., Lin, F. M., Zhao, H., Zhang, Z., Kaloshian, I., Huang, H. D., & Jin, H. (2013). Fungal small RNAs suppress plant immunity by hijacking host RNA interference pathways. *Science, 342*(6154), 118-123. https://doi.org/10.1126/science.1239705

Welsh, C., Lewis, K., & Woods, A. (2009). The outbreak history of Dothistroma needle blight: an emerging forest disease in northwestern British Columbia, Canada. *Canadian Journal of Forest Research, 39*(12), 2505-2519. https://doi.org/10.1139/x09-159

Welsh, J. D., & Leibowitz, M. J. (1982). Localization of genes for the double-stranded RNA killer virus of yeast. *Proceedings of the National Academy of Sciences of the USA, 79*(3), 786-789. https://doi.org/10.1073/pnas.79.3.786

Wen, S., Wen, N., Pang, J., Langen, G., Brew-Appiah, R. A., Mejias, J. H., Osorio, C., Yang, M., Gemini, R., Moehs, C. P., Zemetra, R. S., Kogel, K. H., Liu, B., Wang, X., von Wettstein, D., & Rustgi, S. (2012). Structural genes of wheat and barley 5-methylcytosine DNA glycosylases and their potential applications for human health. *Proceeding of the National Academy of Sciences of the USA, 109*(50), 20543-20548. https://doi.org/10.1073/pnas.1217927109

Werner, B., Gaffar, F. Y., Schuemann, J., Biedenkopf, D., & Koch, A. (2020). RNA-spray-mediated silencing of *Fusarium graminearum AGO* and *DCL* genes improve barley disease resistance. *Frontiers in Plant Science, 11*, 1-11. https://doi.org/10.3389/fpls.2020.00476

Wingfield, M. J., Brockerhoff, E. G., Wingfield, B. D., & Slippers, B. (2015). Planted forest health: The need for a global strategy. *Science, 349*(6250), 832-836. https://doi.org/10.1126/science.aac6674

Woods, A., Coates, K. D., & Hamann, A. (2005). Is an unprecedented Dothistroma needle blight epidemic related to climate change. *BioScience, 55*(9), 761-769. https://doi.org/10.1641/0006-3568(2005)055[0761:IAUDNB]2.0.CO;2

Woods, A. J., Martín-García, J., Bulman, L., Vasconcelos, M. W., Boberg, J., La Porta, N., Peredo, H., Vergara, G., Ahumada, R., Brown, A., Diez, J. J., & Stenlid, J. (2016).

Dothistroma needle blight, weather and possible climatic triggers for the disease's recent emergence. *Forest Pathology, 46*(5), 443-452. https://doi.org/10.1111/efp.12248

Wu, Q., Jezkova, A., Yuan, Z., Pavlikova, L., Dohnal, V., & Kuca, K. (2009). Biological degradation of aflatoxins. *Drug Metabolism Reviews, 41*(1), 1-7. https://doi.org/10.1080/03602530802563850

Wytinck, N., Manchur, C. L., Li, V. H., Whyard, S., & Belmonte, M. F. (2020). dsRNA uptake in plant pests and pathogens: insights into RNAi-based insect and fungal control technology. *Plants 9*(12), 1-17. https://doi.org/10.3390/plants9121780

Wytinck, N., Sullivan, D. S., Biggar, K. T., Crisostomo, L., Pelka, P., Belmonte, M. F., & Whyard, S. (2020). Clathrin mediated endocytosis is involved in the uptake of exogenous double-stranded RNA in the white mold phytopathogen *Sclerotinia sclerotiorum*. *Scientific Reports, 10*(1), 12773. https://doi.org/10.1038/s41598-020-69771-9

Yamanaka, S., Mehta, S., Reyes-Turcu, F. E., Zhuang, F., Fuchs, R. T., Rong, Y., Robb, G. B., & Grewal, S. I. S. (2013). RNAi triggered by specialized machinery silences developmental genes and retrotransposons. *Nature, 493*(7433), 557-560. https://doi.org/10.1038/nature11716

Yang, J., Sun, X.-Q., Zhu-Salzman, K., Qin, Q.-M., Feng, H.-Q., Kong, X.-D., Zhou, X.-G., & Cai, Q.-N. (2020). Host-induced gene silencing of brown planthopper glutathione S-transferase gene enhances rice resistance to sap-sucking insect pests. *Journal of Pest Science, 94*(3), 769-781. https://doi.org/10.1007/s10340-020-01296-6

Yelton, M. M., Hamer, J. E., & Timberlake, W. E. (1984). Transformation of *Aspergillus nidulans* by using a *trpC* plasmid. *Proceedings of the National Academy of Science USA, 81*(5), 1470-1474. https://doi.org/10.1073/pnas.81.5.1470

Yin, C., Zhu, H., Jiang, Y., Shan, Y., & Gong, L. (2020). Silencing dicer-like genes reduces virulence and sRNA generation in *Penicillium italicum*, the cause of citrus blue mold. *Cells, 9*(2), 1-16. https://doi.org/10.3390/cells9020363

Yin, G., Sun, Z., Liu, N., Zhang, L., Song, Y., Zhu, C., & Wen, F. (2009). Production of double-stranded RNA for interference with TMV infection utilizing a bacterial prokaryotic expression system. *Applied Microbiology and Biotechnology, 84*(2), 323-333. https://doi.org/10.1007/s00253-009-1967-y

Zebiak, S. E., Orlove, B., Muñoz, Á. G., Vaughan, C., Hansen, J., Troy, T., Thomson, M. C., Lustig, A., & Garvin, S. (2014). Investigating El Niño-Southern Oscillation and society relationships. *WIREs Climate Change, 6*(1), 17-34. https://doi.org/10.1002/wcc.294

Zhang, S., Schwelm, A., Jin, H., Collins, L. J., & Bradshaw, R. E. (2007). A fragmented aflatoxin-like gene cluster in the forest pathogen *Dothistroma septosporum*. *Fungal Genetics Biology, 44*(12), 1342-1354. https://doi.org/10.1016/j.fgb.2007.06.005

Zhu, J., Dong, Y. C., Li, P., & Niu, C. Y. (2016). The effect of silencing 20E biosynthesis relative genes by feeding bacterially expressed dsRNA on the larval development of *Chilo suppressalis*. *Science Reports, 6*, 1-12. https://doi.org/10.1038/srep28697

Zhu, L., Zhu, J., Liu, Z., Wang, Z., Zhou, C., & Wang, H. (2017). Host-induced gene silencing of rice blast fungus *Magnaporthe oryzae* pathogenicity genes mediated by the brome mosaic virus. *Genes, 8*(10), 1-14. https://doi.org/10.3390/genes8100241

Zhu, X., Qi, T., Yang, Q., He, F., Tan, C., Ma, W., Voegele, R. T., Kang, Z., & Guo, J. (2017). Host-induced gene silencing of the MAPKK gene *PsFUZ7* confers stable resistance to wheat stripe rust. *Plant Physiology, 175*(4), 1853-1863. https://doi.org/10.1104/pp.17.01223

Zivanovic, M., & Chen, Z.-Y. (2021). *In vitro* screening of various bacterially produced double-stranded RNAs for silencing *Cercospora* cf. *flagellaris* target genes and suppressing cercosporin production. *Phytopathology, 111*(7), 1228-1237. https://doi.org/10.1094/PHYTO-09-20-0409-R

Zotti, M., Dos Santos, E. A., Cagliari, D., Christiaens, O., Taning, C. N. T., & Smagghe, G. (2018). RNA interference technology in crop protection against arthropod pests, pathogens and nematodes. *Pest Management Science, 74*(6), 1239-1250. https://doi.org/10.1002/ps.4813

Chapter 7: Appendices

7.1 Media

Media were adjusted to the final volume with MQ water and autoclaved at 121˚C for 15 min. Molten agar was left in a 50˚C water bath before adding antibiotics for selection.

7.1.1 Media for culturing *Dothistroma septosporum*

Dothistroma Medium (DM)

Bacteriological agar (Oxoid) 15 g/L, malt extract (Oxoid) 50 g/L, nutrient broth (Oxoid) 23 g/L.

Dothistroma Broth (DB)

Malt extract (Oxoid) 50 g/L, nutrient broth (Oxoid) 23 g/L.

Dothistroma Sporulating Medium (DSM)

Malt extract (Oxoid) 20 g/L, yeast extract (BD) 5 g/L, bacteriological agar (Oxoid) 15 g/L.

Pine needle Minimal Media with Glucose (PMMG)

Magnesium sulphate heptahydrate (Merk Darmstadt, Germany) 0.2 g/L, di-potassium hydrogen orthophosphate (BDH, Poole, England) 0.9 g/L, potassium chloride (Sigma, Louis, Germany) 0.2 g/L, ammonium nitrate (Sigma Aldrich, Steinheim, Germany) 1 g/L, iron sulphate (APS Chem.Ltd. NSW, Australia) 0.002 g/L, zinc sulphate heptahydrate (BDH, Poole, England) 0.002 g/L, manganese chloride (BDH, Poole, England) 0.002 g/L, asparagine (Sigma Life Science, St.Louis, USA) 2 g/L, glucose (APS Chem.Ltd. NSW, Australia) 2%, bacteriological agar (Neogen Corporation, Michigan, USA) 15 g/L.

10% (w/v) fresh pine needles were soaked in MQ for 24 h and the pH of this medium, with all the ingredients (listed above) except glucose and asparagine, was adjusted to 4.0–6.2 before autoclaving. After maintaining the media at 50˚C, glucose and asparagine (filter sterilized using a 0.22 µm filter) were added just before pouring plates.

7.1.2 Media for *Escherichia coli*

Lysogeny broth (LB) agar

Lenox L broth base (Invitrogen) 20 g/L, bacteriological agar (Oxoid) 15 g/L.

Lysogeny Broth (LB)

Lenox L broth base (Invitrogen) 20 g/L.

Selective media:

Compound	Stock concentration	Final concentration
Ampicillin	100 mg/mL	100 µg/mL
X-gal	20 mg/mL	20 µg/mL
IPTG	100 mM	100 µM

7.1.3 Media for *Dothistroma septosporum* transformation

Regeneration Media (RG)

Malt extract (Oxoid) 50 g/L, nutrient broth (Oxoid) 23 g/L, 0.8M sucrose (BDH) 273.8 g/L, 1.5% bacteriological agar (Oxoid) 15 g/L.

Selection media: hygromycin B 50 mg/mL (Roche); used at a final concentration of 70 µg/ml.

0.8% Regeneration Media Overlay

Malt extract (Oxoid) 50 g/L, nutrient broth (Oxoid) 23 g/L, 0.8M sucrose (BDH) 273.8 g/L, 0.8% bacteriological agar (Oxoid) 8 g/L.

Was autoclaved in 50 mL aliquots.

7.1.4 Media for growing mycelia for confocal microscopy

The following media were prepared on microscope slides. A small volume (~15–20 mL) of water agar (WA) medium was poured onto sterile petri dishes and left to set for ~20 min. After this time microscope slides were flamed with ethanol to sterilize, transferred onto the agar plate and a thin layer of the same medium was poured on top to cover the slide (as shown in Chapter 2, Figure 2.5).

Water agar (WA)

1.5% bacteriological agar (Oxoid) 15g/L. A glass microscope slide was covered with a layer of 1.5% water agar on top of a pre-poured agar plate with 3% WA.

Potato Dextrose Agar (PDA)

Potato dextrose agar (Merck) 39 g/L.

1/2 x PDA: potato dextrose agar (Merck) 19.5 g/L.

Potato Dextrose Broth (PDB)

Potato dextrose broth (Merck) 24 g/L.

7.2 Buffers/Solutions

All buffers and solutions were adjusted to the final volume with MQ water and autoclaved at 121˚C for 15 min.

7.2.1 Reagents for *Dothistroma septosporum* transformation

Glucanex

10 mg/mL Glucanex® 200G (Novozymes, Denmark) in OM buffer.

OM buffer

1.4 M $MgSO_4.7H_2O$ (Ajax) 103.6 g, 10 mM Na_2HPO_4 (BDH) 30 mL of a 100 mM stock (1.42 g/100 mL). Add 100 mL of water to dissolve then add $NaH_2PO_4.2H_2O$ (BDH) of a 100 mM stock (1.56 g/100 mL) until it reaches a pH of 5.8 and then top up to a 300 mL volume with MQ water.

ST buffer

0.6 M sorbitol (Sigma) 10.93 g, 100 mM Tris-HCI (Carl Roth) pH 8.0 (10 mL of 1 M stock).

STC buffer

1 M sorbitol (Sigma) 36.4 g, 50 mM Tris-HCI (Carl Roth) pH 8.0 (10 mL of 1 M stock), $CaCl_2.2H_2O$ (Merck) 1.47 g.

40% Polyethylene glycol (PEG)

40% (w/v) PEG 4000 (BDH) 40.0g, 50 mM $CaCl_2$ (Merck) 0.56g, 50 mM Tris-HCI (Carl Roth) pH 8.0 (5.0 mL of 1M stock), 1M sorbitol (Sigma) 18.21g.

7.2.2 Reagents for genomic DNA extraction

2% CTAB buffer

2% (w/v) CTAB; 1% (w/v) PVP40; 1.4 M NaCl; 20 mM EDTA; 0.1 M Tris HCl (pH 8.0).

TE buffer

10 mM Tris (Carl Roth), 1 mM EDTA (Sigma) pH 8.0.

TBE buffer

Tris (Carl Roth) 108.0 g/L, boric acid (Ajax) 55 g/L, EDTA (Sigma) 7.44 g/L, dissolved in 750 mL of MQ water and adjusted to pH 8.2 with the addition of 10 M HCl (BDH). The final volume of 1 L was made up with MQ water.

RNase A

20 mg of RNase A (Sigma) was dissolved in 1 mL of MQ water to make a 20 mg/mL stock solution and vortexed to mix.

7.2.3 Reagents for RNA manipulations

All Schott bottles and spatulas used to prepare reagents were baked in a sterilizing oven at 160˚C for 1 h, while plastic caps were autoclaved at 121˚C for 15 min. Also, diethylpyrocarbonate (DEPC)-treated water was added to the desired volume instead of MQ water, as this was RNase-free and hence prevented the degradation of RNA. To prepare RNase-free water, distilled water was treated with DEPC overnight in a fume hood with the cap loosely screwed on and autoclaved the following day. Before running RNA gels the tank, gel tray and comb were rinsed with DEPC-treated water.

10 M Lithium chloride (RNase-free)

Lithium chloride (Sigma) 424 g/L.

TE buffer (RNase-free)

10 mM Tris (Carl Roth), 1 mM EDTA (Sigma) pH 8.0.

3M Sodium acetate (RNase-free)

Sodium acetate (Sigma) 246.09 g/L. Add 700 mL of MQ to dissolve and adjust pH to 5.2 using acetic acid. Add remaining MQ to top up to 1 L.

0.5 M EDTA

EDTA (Sigma) 186.12 g/L, pH to 8.0 using sodium hydroxide (BDH).

200 mM MOPS (pH 7.5) (RNase-free)

Morpholinepropanesulfonic acid (MOPS) (Sigma) 41.852 g/L.

Aniline blue (AB) and trypan blue (TB) staining solution

A 1% aniline blue stock solution was prepared by dissolving 10 mg aniline blue diammonium salt (Sigma-Aldrich) in 1 mL MQ. A 1% trypan blue stock solution was prepared by dissolving 10 mg trypan blue powder (Merck) in 1 mL MQ. To mix both staining solutions (AB20/TB20) 20 µL of each stain was combined.

7.3 Reagents for running gels

7.3.1 DNA gels

10X TBE

Tris (Invitrogen) 108 g/L, EDTA (Sigma) 9.3 g/L, boric acid (Univar) 55 g/L, dissolved in MQ and adjusted to pH 8.2 using concentrated HCl (BDH). MQ was added to reach the desired final volume.

1X TBE

Dilute 40 mL of 10X TBE with 360 mL of DEPC-treated water to a 1X solution.

6X loading dye

20% (w/v) sucrose (BDH), 5 mM EDTA Na2.H2O (BDH), 1% (w/v) SDS (BDH), 0.2% (w/v) bromophenol blue (J.T. Baker Chemical Co) and 0.2% (w/v) xylene cyanol (Sigma).

Agarose gels

1 g of agarose was dissolved in 100 mL of 1X TBE (1% agarose gel) and heated in the microwave with intermittent swirling until the agarose was fully melted. The agarose gel was left to cool for ~10 min before pouring into the gel mold. The amount of agarose was adjusted for higher or lower percentage gels.

Ethidium bromide gel staining solution

For staining DNA gels, 40 µL of ethidium bromide (BDH; 10 mg/mL) was added to 400 mL of DEPC-treated water (1 µL of BDH per 10 mL of water). Gels were stained for 15 min and visualised on the UV transilluminator.

7.3.2 RNA gels

All Schott bottles and spatulas used to prepare reagents were baked in a sterilizing oven at 160˚C for 1 h as above (section 7.2.3).

10X TBE (RNase-free)

0.9 M Tris base (Carl Roth) 109 g/L, 0.9 M boric acid (Ajax) 55 g/L, 20 mM EDTA (Sigma) (40 mL of 0.5 M stock).

1X TBE (RNase-free)

Dilute 40 mL of 10X TBE with 360 mL of DEPC-treated water to a 1X solution.

6X non-denaturing gel loading buffer (RNase-free)

37% (w/v) glycerol (100%) 3.7 mL, 0.025% bromophenol blue 2.5 mg, 0.025% xylene cyanol 2.5 mg, 20 mM Tris HCL (1M stock, pH 8.0) 200 µL, 5 mM EDTA (Sigma) (500 mM stock) 100 µL, top up to 10 mL with DEPC-treated water.

1% agarose gel (non-denaturing) (RNase-free)

1 g of agarose was dissolved in 100 mL of 1X TBE (RNase-free) and heated in the microwave with intermittent swirling until the agarose was fully melted. The agarose gel was left to cool for ~10 min before pouring into the gel tray.

0.8% agarose, 0.3% SDS denaturing gel (RNase-free)

0.8% of agarose was dissolved in 97 mL of 1X TBE and heated in the microwave with intermittent swirling until the agarose was fully melted and cooled to 50˚C. To this, 3 mL of 10% SDS was added and mixed by swirling and poured into the gel mold.

Ethidium bromide gel staining solution (RNase-free)

For staining RNA gels, 20 µL of ethidium bromide (BDH; 10 mg/mL) was added to 200 mL of DEPC-treated water (1 µL of BDH per 10 mL of water). Gels were stained for 15 min and visualised on the UV transilluminator.

7.4 Appendices for Chapter 3

7.4.1 Protein alignments

A

DCL

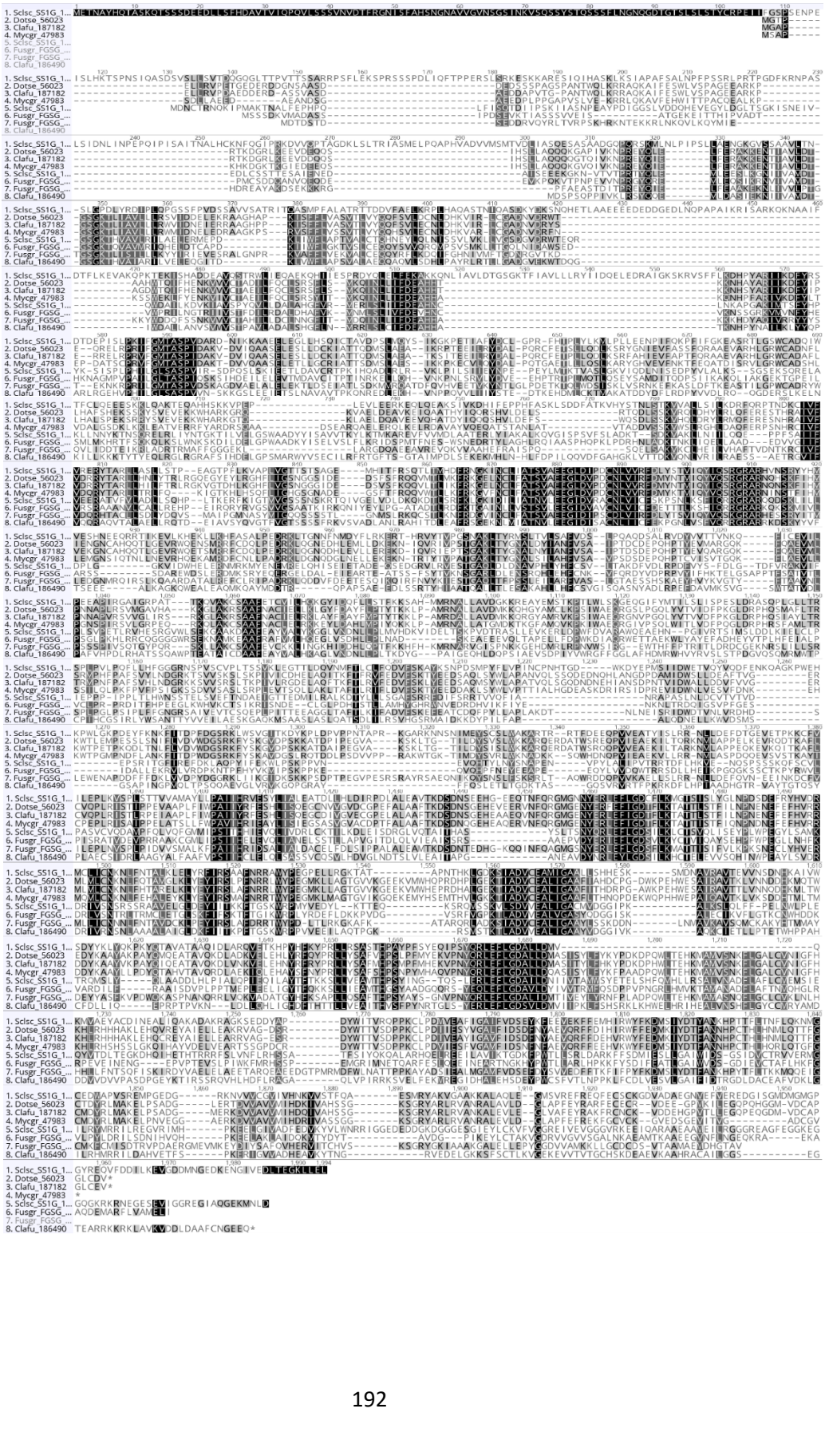

B

AGO

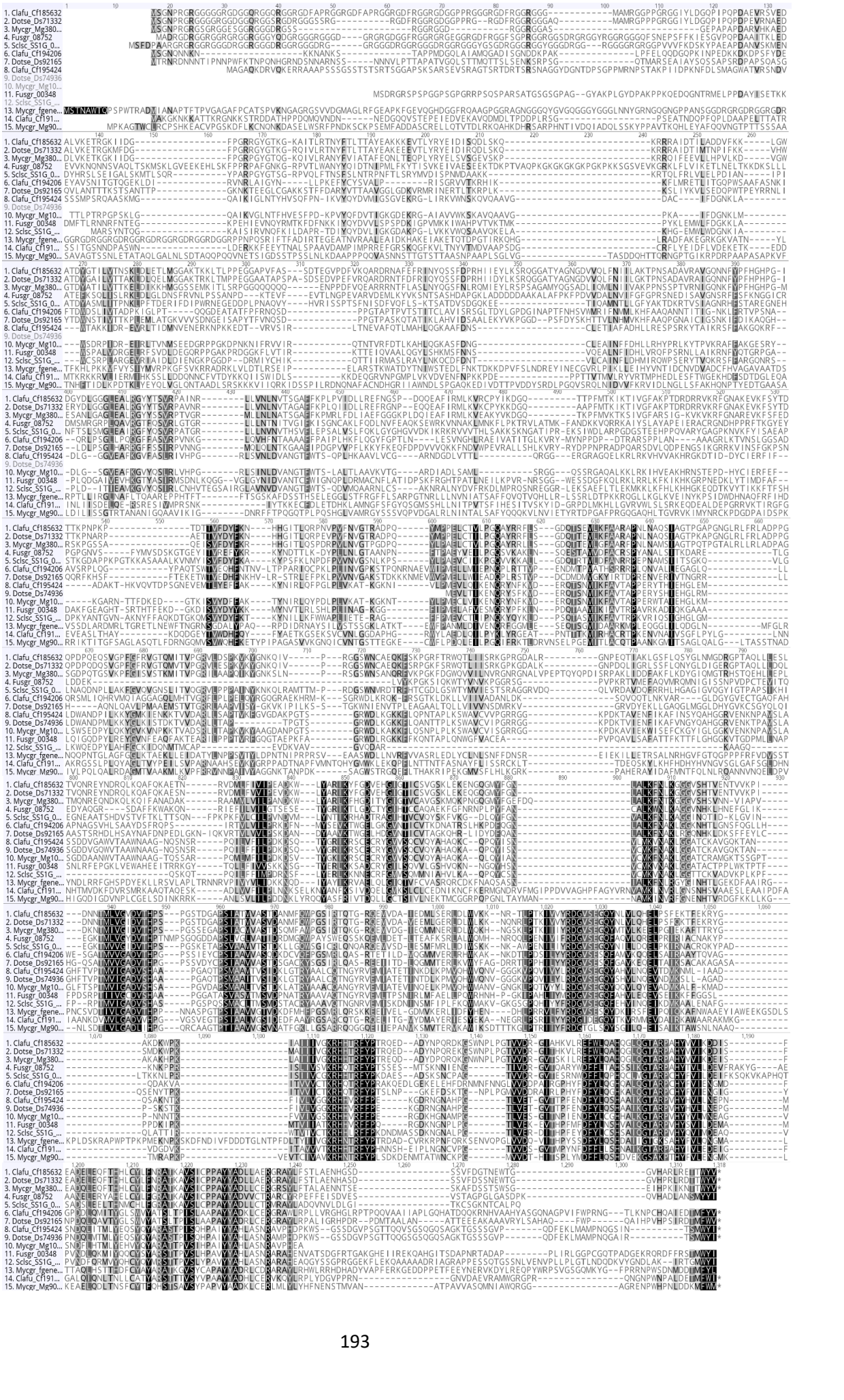

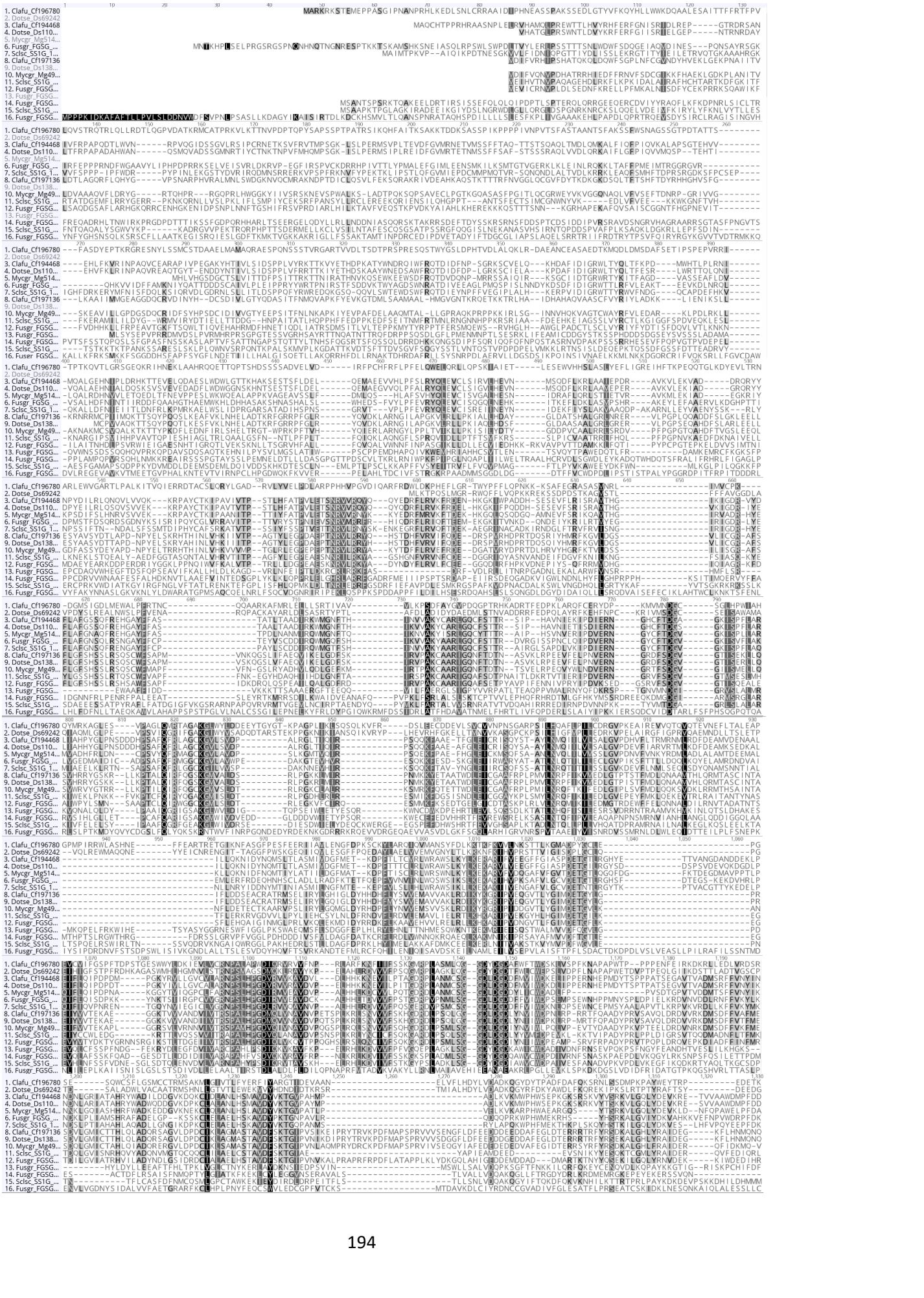

C

RdRP

Figure A7.1. Protein alignments of RNAi proteins from Dothideomycetes and other fungi. (A) Dicer-like (DCL) proteins. (B) Argonaute (AGO). (C) RNA-dependent RNA Polymerase (RdRP). The ClustalW alignment was generated in Geneious v9.1.8 (https://www.geneious.com/) using protein sequences from the JGI MycoCosm (https://mycocosm.jgi.doe.gov/Dotse1/Dotse1.home.htm) and funRNA databases (Choi et al., 2014). DCL, AGO and RdRP amino acid sequences are from *Dothistroma septosporum* (Dotse), *Fulvia fulvum* (syn. *Cladosporium fulvum*) (Clafu), *Zymoseptoria tritici* (*Mycosphaerella graminicola*; Mycgr), *Sclerotinia sclerotiorum* (Sclsc) and *Fusarium graminearum* (Fusgr). Various shading (back to grey) indicates conservation of amino acid residues (black = most conserved residues).

7.4.2 Matrices

Table A7.1. Matrix of percentage amino acid identity of Dicer-like proteins (DCL) in *Dothistroma septosporum*, *Fulvia fulva* and *Zymoseptoria tritici*.

	Dotse_56023
Clafu_187182	85.5
Clafu_186490	18.4
Mycgr_47983	63

Proteins shown are the top three DCL proteins orthologous to *D. septosporum* (Dotse) and either *F. fulva* (*C. fulvum*; Clafu) or *Z. tritici* (*M. graminicola*; Mycgr) as identified by BLAST searches.
Yellow = Reciprocal best hits of *D. septosporum* and *F. fulva* DCL proteins.
Green = Reciprocal best hits of *D. septosporum* and *Z. tritici* DCL proteins.

Table A7.2. Matrix of percentage amino acid identity of Argonaute (AGO) proteins in *Dothistroma septosporum*, *Fulvia fulva* and *Zymoseptoria tritici*.

	Dotse_Ds71332	Dotse_Ds92165	Dotse_Ds74936
Clafu_Cf185632	87.4	21.7	23.8
Clafu_Cf194206	22.3	42.2	24.1
Clafu_Cf195424	18.5	16.9	89.7
Clafu_Cf191892*	18.2	17.5	23.6
Mycgr_Mg38035	59.9	21.4	24.2
Mycgr_Mg90232**	16.6	18.2	18.9
Mycgr_Mg10621	21.4	19.7	73.3
Mycgr_fgenesh1_pg.C_chr_1001447*	19.8	18.2	19.8

Proteins shown are the top three AGO proteins orthologous to *D. septosporum* (Dotse) and either *F. fulva* (*C. fulvum*; Clafu) or *Z. tritici* (*M. graminicola*; Mycgr) as identified in Table 3.3.
Yellow = Reciprocal best hits of *D. septosporum* and *F. fulva* AGO proteins.
Green = Reciprocal best hits of *D. septosporum* and *Z. tritici* AGO proteins.
**F. fulva* and *Z. tritici* also have an extra *AGO* gene in their genome (Cf191892 and Mycgr_fgenesh1_pg.C_chr_1001447 (locus name)).
**Note that Mg90232 is not a reciprocal hit to Ds92165.

Table A7.3. Matrix of percentage amino acid identity of RNA-dependent RNA Polymerase (RdRP) proteins in *Dothistroma septosporum*, *Fulvia fulva* and *Zymoseptoria tritici*.

	Dotse_Ds110589	Dotse_Ds138071	Dotse_Ds69242
Clafu_Cf194468	80.7	22.2	12.6
Clafu_Cf197136	18.8	92.2	12.4
Clafu_Cf196780	11.4	11.4	38.1
Mycgr_Mg51407	56	22.6	13.2
Mycgr_Mg49833	18.7	64.6	12.3

Proteins shown are the top three RdRP proteins orthologous to *D. septosporum* (Dotse) and either *F. fulva* (*C. fulvum*; Clafu) or *Z. tritici* (*M. graminicola*; Mycgr) as identified in Table 3.3.
Yellow = Reciprocal best hits of *D. septosporum* and *F. fulva* RdRP proteins.
Green = Reciprocal best hits of *D. septosporum* and *Z. tritici* RdRP proteins.

Table A7.4. Comparison of the expression of the core RNAi genes in *Dothistroma septosporum* orthologous to *Fulvia fulva* core genes.

Gene information				*D. septosporum*				*F. fulva*			
Gene	**Protein ID[a]**	**Protein ID[b]**	**% ID[c]**	***In vitro*[d]**	**Early[d]**	**Mid[d]**	**Late[d]**	***In vitro*[e]**	**4 dpi[e]**	**8 dpi[e]**	**12 dpi[e]**
DCL	Ds56023	Cf187182	85.5	2.2	8.0	2.5	3.1	6.2	0	0.2	0.4
DCL		Cf186490	18.4					12.3	0	1.2	1.0
AGO	Ds92165	Cf194206	42.2	0.9	0	1.1	2.4	0.9	0	0	0.1
AGO	Ds71332	Cf185632	87.4	67.8	199.8	145.5	77.7	138.9	36.8	17.9	58.0
AGO	Ds74936	Cf195424	89.7	28.4	56.0	5.0	23.2	11.3	0	0.3	2.3
RdRP	Ds110589	Cf194468	80.7	1.7	11.8	2.0	1.4	3.5	0	0.5	0
RdRP	Ds138071	Cf197136	92.2	29.9	24.7	31.1	22.2	7.0	16.9	0	1.6
RdRP	Ds69242	Cf196780	38.1	21.0	19.1	11.7	14.1	7.4	0	0.5	0.2

[a]Protein ID of *D. septosporum* as in the JGI database (https://mycocosm.jgi.doe.gov/Dotse1/Dotse1.home.html).
[b]Protein ID of *F. fulvia* (*C. fulvum*) as in the JGI database (https://mycocosm.jgi.doe.gov/Clafu1/Clafu1.home.hml).
[c]Percentage amino acid identity values from the matrix output in Geneious v9.1.8 software (https://www.geneious.com/) (Kearse et al., 2012).
[d]Expression levels of *D. septosporum* NZE10 genes in Reads Per Kilobase of transcript per million (RPMK) based on a transcriptome study (Bradshaw et al., 2016) during growth *in vitro* and *in planta* during the early, mid and late stages of infection in *Pinus radiata*.
[e]Expression levels of *F. fulva* during growth *in vitro* (Potato Dextrose Broth (PDB)) and during various stages of infection in tomato (dpi = days post inoculation) (Mesarich et al., 2014). Values are expressed as RNA-Seq fragments per kilobase of exon per million fragments mapped (FPKM). The *F. fulva* genes have CFU numbers as in the Mesarich et al. (2014) gene expression study as follows: CFU840832 (Cf187182), CFU840627 (Cf186490), CFU (Cf194206), CFU840258 (Cf185632), CFU832045 (Cf195424), CFU829205 (Cf194468), CFU833764 (Cf197136), CFU829728 (Cf196780).

7.5 Appendices for Chapter 4

7.5.1 Positions of primers for RNA interference (RNAi) target gene design

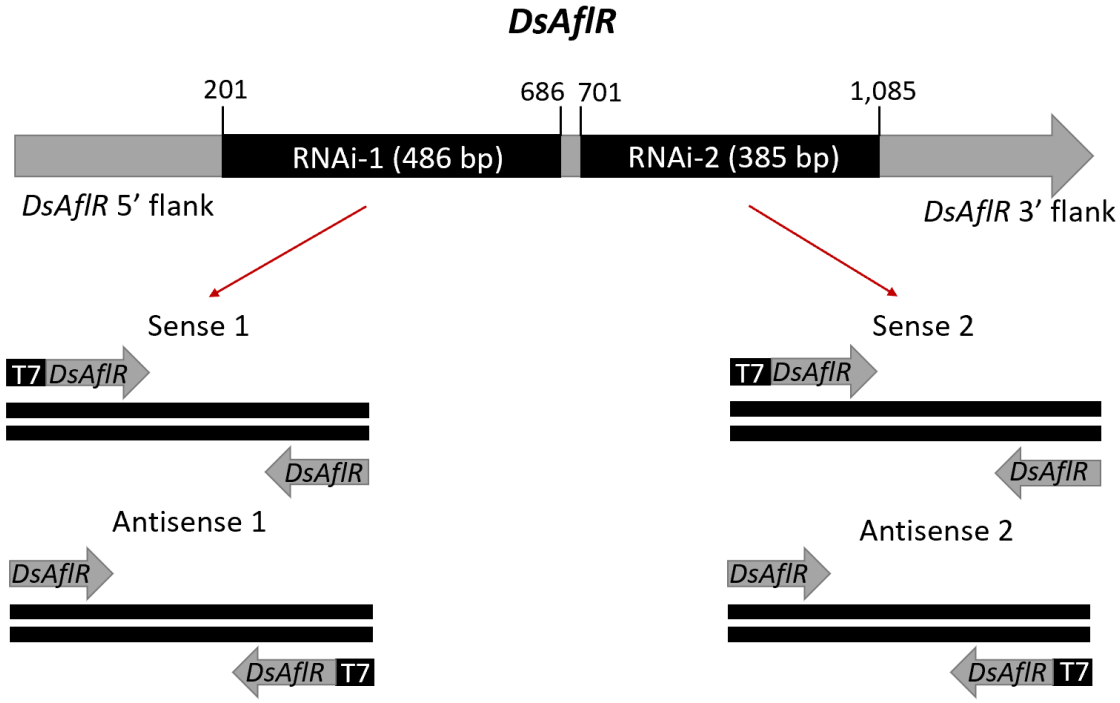

Figure A7.2. Regions for Polymerase Chain Reaction (PCR) amplification of the dothistromin pathway regulatory gene (*DsAflR*) and the positions of primers for each of the sense and antisense strands. Two *DsAflR* sites selected for RNAi are 486 bp (509 bp including T7 promoter) and 385 bp (408 bp including T7 promoter) in length for RNAi-1 (*DsAflR* 1) and RNAi-2 (*DsAflR* 2) respectively. The numbers refer to nucleotide positions.

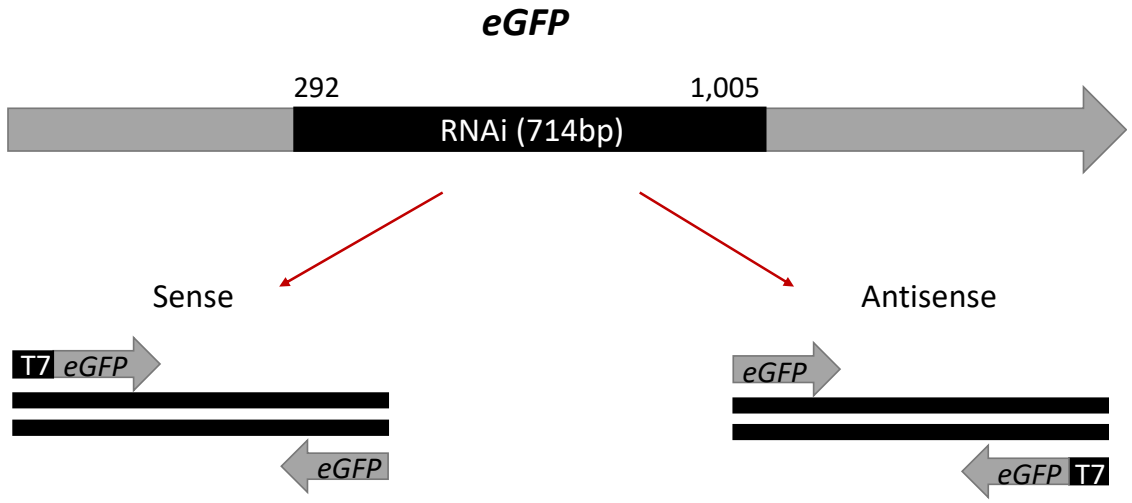

Figure A7.3. Region for Polymerase Chain reaction (PCR) amplification of the target gene enhanced green fluorescent protein (*eGFP*). The 714 bp region of *eGFP* to be amplified is indicated (737 bp including T7 promoter). The numbers refer to nucleotide positions.

7.5.2 Plasmid vectors used for transformation

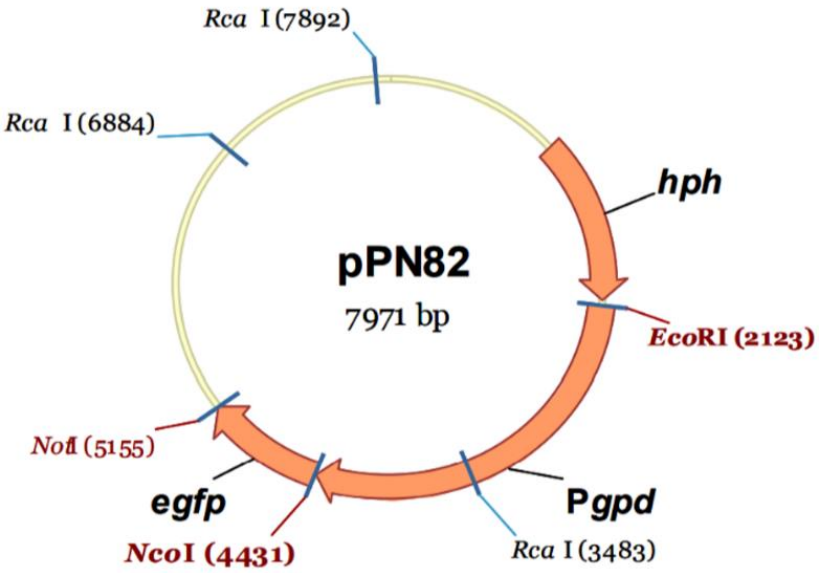

Figure A7.4. Plasmid map of pPN82 (GFP vector). This plasmid (9.7 kb) was prepared by Tanaka et al. (2006) for the constitutive expression of GFP. The construction of this plasmid was described by Tanaka et al. (2006), as involving "sequentially ligating into pBluescriptII KS+ a 0.7-kb BamHI/SalI fragment of *eGFP* from pEGFP (Clontech), a 1.4-kb HindIII fragment of *hph* under the control of the *trpC* promoter from pCB1004 (Carroll et al., 1994), a 2.3-kb EcoRI/NcoI fragment of *gpd* promoter from pAN7-1 (Punt et al., 1987), and a 0.6-kb NotI/SalI fragment of *trpC* terminator from pII99 (Namiki et al., 2001). The *gpd* promoter fragment was prepared by digesting a PCR product amplified with primer set M13-reverse and using pAN7-1 as template. The fragment of the *trpC* terminator was prepared by digesting a PCR product amplified with primer set TnotI and Tsc2 using pII99 as template." (Tanaka et al., 2006) (Plasmid map adapted from Schwelm (2007)).

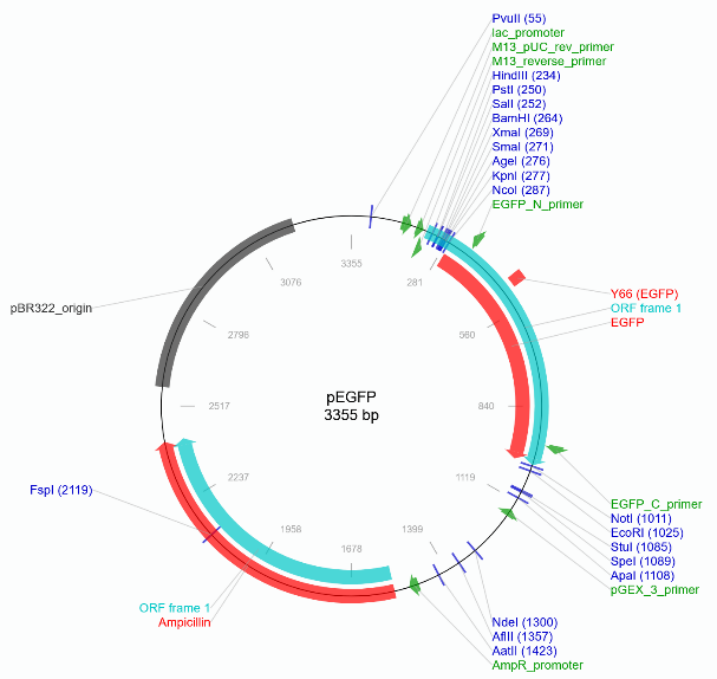

Figure A7.5. Plasmid map of pEGFP from Clontech (https://www.addgene.org/browse/sequence_vdb/2485/).

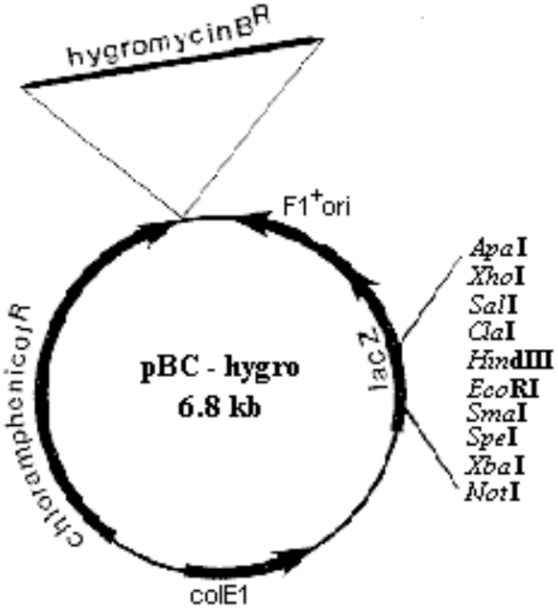

Figure A7.6. Plasmid map of pBC-hygro used for *Dothistroma septosporum* transformation (Silar, 1995).

7.5.3 dsRNA plasmid constructs for RNAi

Inserts were cloned into the plasmid pICH41021, modified by S. Marillonet. This plasmid is pUC19 with the *Bsa*I site removed.

The following key applies to Figures A7.7-A7.12.

Key:
Alpha: LacZ alpha fragment
AP(R): Ampicillin resistance gene
Dark blue: Insert
Green: M13 LacZ primer sites
Light green: RNA interference (RNAi) primer sites
Light pink: T7 promoter
Light brown: P lac prom (lactose inducible promoter)
ORI: Origin of replication

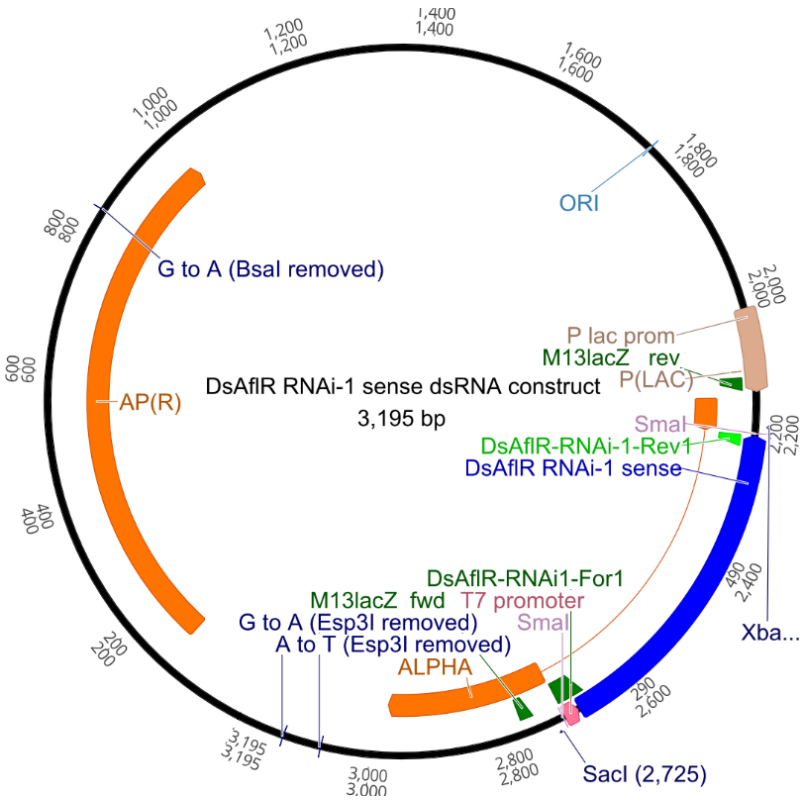

Figure A7.7. DsRNA construct for *DsAflR* RNAi-1 sense.

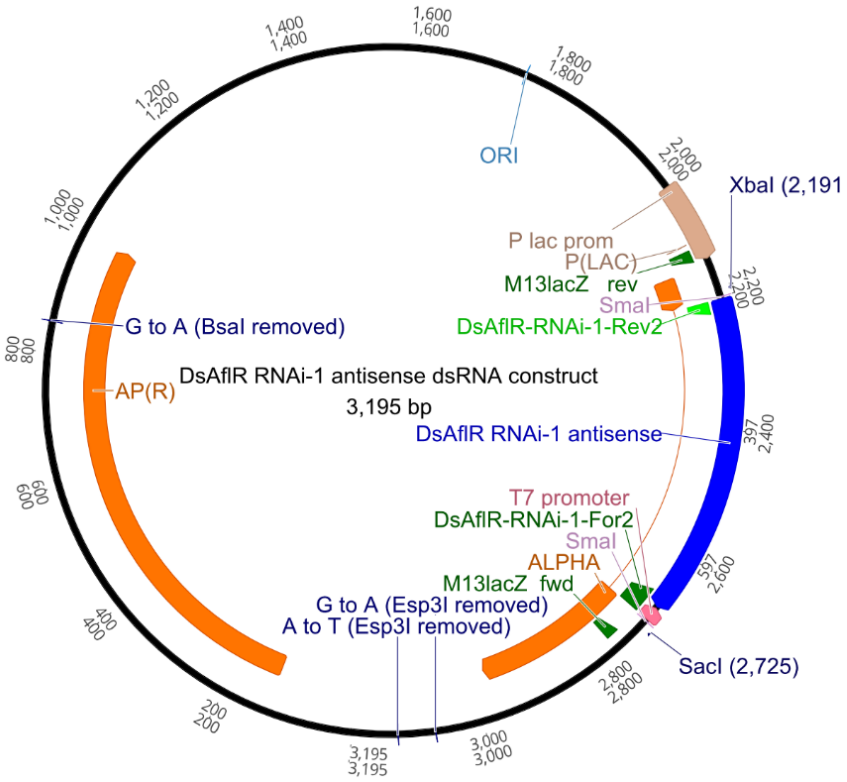

Figure A7.8. DsRNA construct for *DsAflR* RNAi-1 antisense.

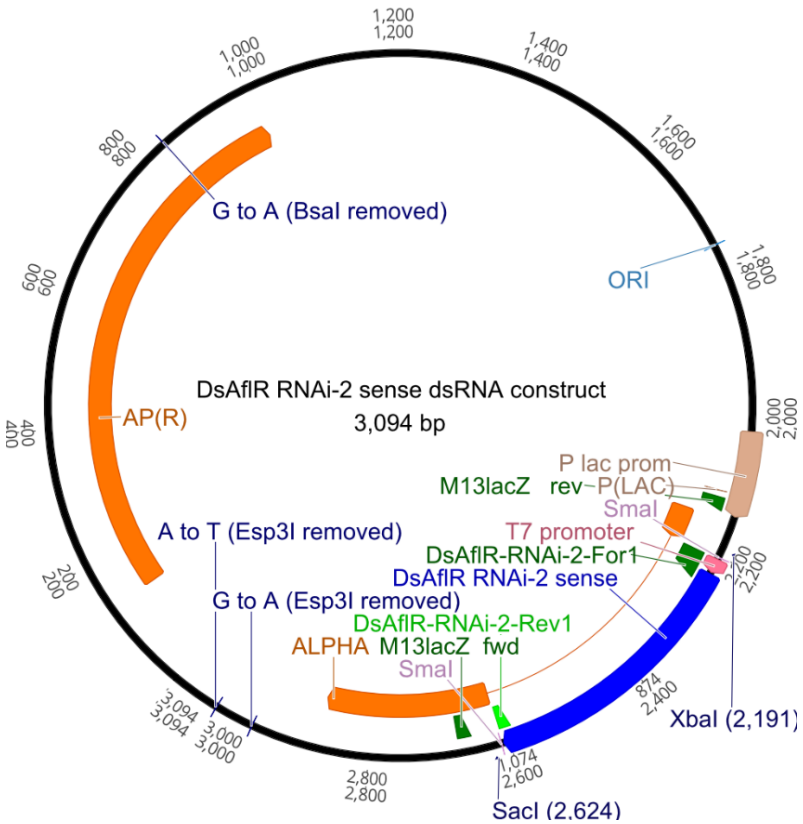

Figure A7.9. DsRNA construct for *DsAflR* RNAi-2 sense.

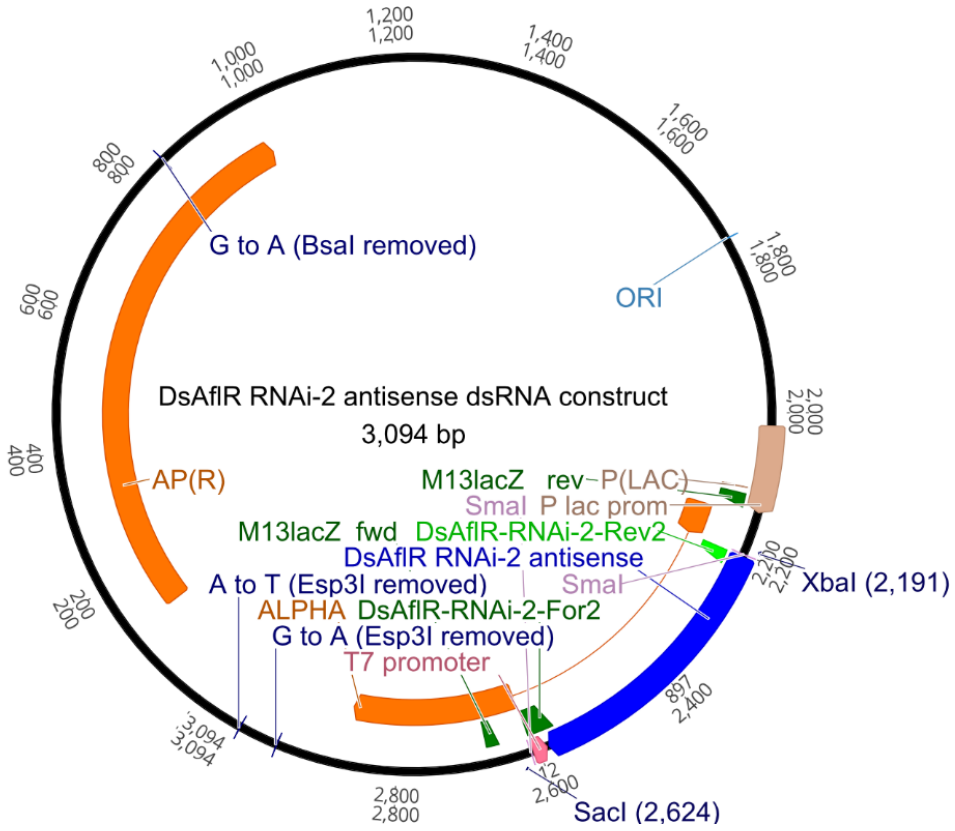

Figure A7.10. DsRNA construct for *DsAflR* RNAi-2 antisense.

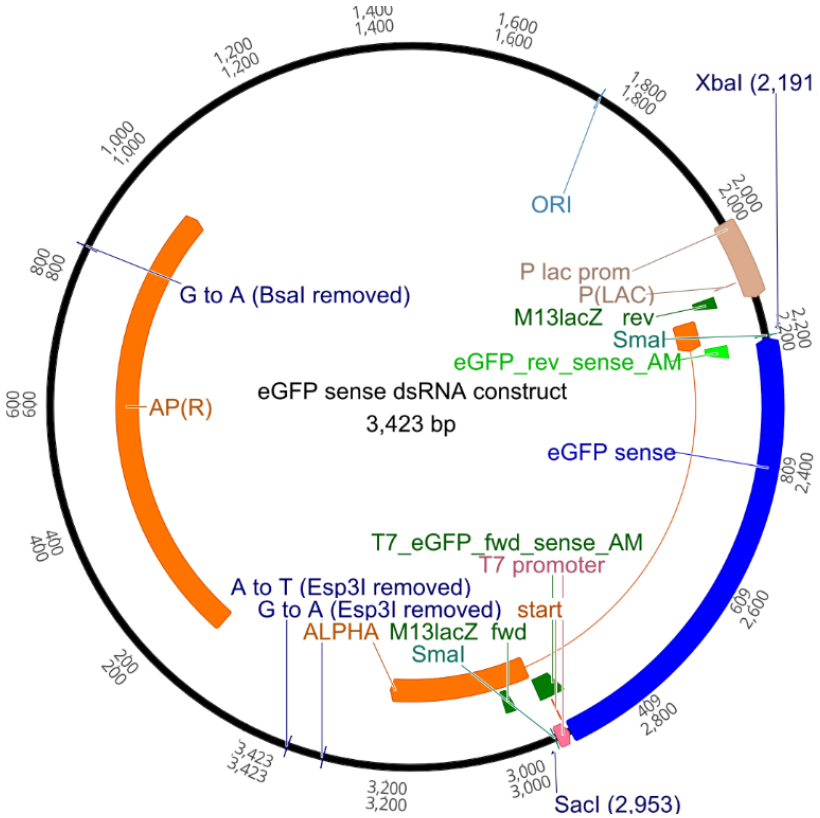

Figure A7.11. DsRNA construct for *eGFP* sense.

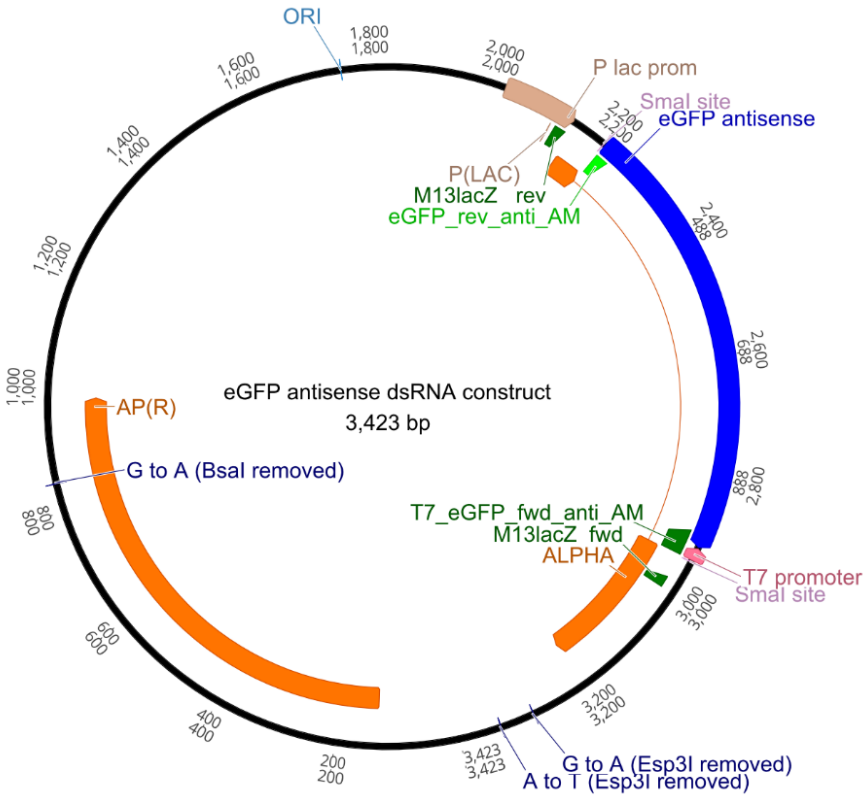

Figure A7.12. DsRNA construct for *eGFP* antisense.

Sequences of dsRNA plasmid inserts

Colour codes are shown below apply to all sequence files (Figures A7.13-A7.18):

Grey: Plasmid backbone
Blue: Insert
Red: LacZ primer sites for sequencing across insert
Black: *Xba*I or *Sac*I recognition sites (enzyme downstream from T7 promoter)
SmaI restriction enzyme cutting site (bisected by the insert)
T7 promoter sequence
→ ← Direction for synthesis of dsRNA by the T7 RNA Polymerase

M13 LacZ rev
GCGGATAACAATTTCACACAGGAAACAGCTATGACCATGATTACGCCAAGCTTGCATGCCTGCAGGTCGA
CGCCTATTGTTAAAGTGTGTCCTTTGTCGATACTGGTACTAATGCGGTTCGAACGTACGGACGTCCAGCT

XbaI *SmaI*
C**TCTAGA**GGATCCCCCCCATGTCGGACACCGAGGTGAGTTGGTCGAATGGGCTTATCGAAGATGAAGTAT
GAGATCTCCTAGGGGGGGTACAGCCTGTGGCTCCACTCAACCAGCTTACCCGAATAGCTTCTACTTCATA

CGGAAAACGTATGTGTATGCTGATTTGACATTGCAGTGTCTGTTGGCTCTCCAAGCATGCTGTAGGATGT
GCCTTTTGCATACACATACGACTAAACTGTAACGTCACAGACAACCGAGAGGTTCGTACGACATCCTACA

GAGGTCGTTGAATAGATGATCAATGTCGTTGCCATTGCCGCCATGGGTCTGCATTGTGTTTGCTGGAGTG
CTCCAGCAACTTATCTACTAGTTACAGCAACGGTAACGGCGGTACCCAGACGTAACACAAACGACCTCAC

TTGTTTGAGCTTGGTTCGTTCGGGGCGAACATGGTCGACCACAGATCTGAATTCCACTGATCCAGGCCAG
AACAAACTCGAACCAAGCAAGCCCCGCTTGTACCAGCTGGTGTCTAGACTTAAGGTGACTAGGTCCGGTC

CTTGTGAGCCGCTGGTGCTGAGATCTGGCATGAGCGTGGGGGAAAGTATCGAAGACTCTTGCAGTGACAT
GAACACTCGGCGACCACGACTCTAGACCGTACTCGCACCCCCTTTCATAGCTTCTGAGAACGTCACTGTA

CGGCGAGATGAACTCATCTACGTCTGGGAGCATATTGGCCACAGGGACTGCGGACTGGCTGACCCTCCTA
GCCGCTCTACTTGAGTAGATGCAGACCCTCGTATAACCGGTGTCCCTGACGCCTGACCGACTGGGAGGAT

TCTGCTGCTTCTTGTTGACTTTGTTGTTGTTGCTGTCGTTGTTGCTGTTGCTTCTGAGCAGTGGCGTGCG
AGACGACGAAGAACAACTGAAACAACAACAACGACAGCAACAACGACAACGAAGACTCGTCACCGCACGC

← T7 promoter *SmaI* ***SacI***
AAGTCCGTCCG**TCTCCCTATAGTGAGTCGTATTA**GGGTACC**GAGCTC**GAATTCACTGGCCGTCGTTTTAC
TTCAGGCAGGCAGAGGGATATCACTCAGCATAATCCCATGGCTCGAGCTTAAGTGACCGGCAGCAAAATG

M13 LacZ fwd
AACGTCGTGACTGGGAAAACCCTGGC
TTGCAGCACTGACCCTTTTGGGACCG

Figure A7.13. Sequence file of *DsAflR* RNAi-1 sense dsRNA construct indicating 656 bp of plasmid DNA sequenced.

M13 LacZ rev

GCGGATAACAATTTCACACAGGAAACAGCTATGACCATGATTACGCCAAGCTTGCATGCCTGCAGGTCGA
CGCCTATTGTTAAAGTGTGTCCTTTGTCGATACTGGTACTAATGCGGTTCGAACGTACGGACGTCCAGCT

XbaI *SmaI*
C**TCTAGA**GGATC**CCC**CGGACGGACTTCGCACGCCACTGCTCAGAAGCAACAGCAACAACGACAGCAACAA
GAGATCTCCTAGGGGGCCTGCCTGAAGCGTGCGGTGACGAGTCTTCGTTGTCGTTGTTGCTGTCGTTGTT

CAACAAAGTCAACAAGAAGCAGCAGATAGGAGGGTCAGCCAGTCCGCAGTCCCTGTGGCCAATATGCTCC
GTTGTTTCAGTTGTTCTTCGTCGTCTATCCTCCCAGTCGGTCAGGCGTCAGGGACACCGGTTATACGAGG

CAGACGTAGATGAGTTCATCTCGCCGATGTCACTGCAAGAGTCTTCGATACTTTCCCCCACGCTCATGCC
GTCTGCATCTACTCAAGTAGAGCGGCTACAGTGACGTTCTCAGAAGCTATGAAAGGGGGTGCGAGTACGG

AGATCTCAGCACCAGCGGCTCACAAGCTGGCCTGGATCAGTGGAATTCAGATCTGTGGTCGACCATGTTC
TCTAGAGTCGTGGTCGCCGAGTGTTCGACCGGACCTAGTCACCTTAAGTCTAGACACCAGCTGGTACAAG

GCCCCGAACGAACCAAGCTCAAACAACACTCCAGCAAACACAATGCAGACCCATGGCGGCAATGGCAACG
CGGGGCTTGCTTGGTTCGAGTTTGTTGTGAGGTCGTTTGTGTTACGTCTGGGTACCGCCGTTACCGTTGC

ACATTGATCATCTATTCAACGACCTCACATCCTACAGCATGCTTGGAGAGCCAACAGACACTGCAATGTC
TGTAACTAGTAGATAAGTTGCTGGAGTGTAGGATGTCGTACGAACCTCTCGGTTGTCTGTGACGTTACAG

AAATCAGCATACACATACGTTTTCCGATACTTCATCTTCGATAAGCCCATTCGACCAACTCACCTCGGTG
TTTAGTCGTATGTGTATGCAAAAGGCTATGAAGTAGAAGCTATTCGGGTAAGCTGGTTGAGTGGAGCCAC

← **T7 promoter** *SmaI* ***SacI***
TCCGACATGGG**TCTCCCTATAGTGAGTCGTATTA**G**GG**TACC**GAGCTC**GAATTCACTGGCCGTCGTTTTAC
AGGCTGTACCCAGAGGGATATCACTCAGCATAATCCCATGGCTCGAGCTTAAGTGACCGGCAGCAAAATG

M13 LacZ fwd
AACGTCGTGACTGGGAAAACCCTGGC
TTGCAGCACTGACCCTTTTGGGACCG

Figure A7.14. Sequence file of *DsAflR* RNAi-1 antisense dsRNA construct indicating 656 bp of plasmid DNA sequenced.

M13 LacZ rev
GCGGATAACAATTTCACACAGGAAACAGCTATGACCATGATTACGCCAAGCTTGCATGCCTGCAGGTCGA
CGCCTATTGTTAAAGTGTGTCCTTTGTCGATACTGGTACTAATGCGGTTCGAACGTACGGACGTCCAGCT

XbaI *SmaI* **T7 promoter** →
C**TCTAGA**GGATC**CCC****TAATACGACTCACTATAGGGAGA**CAAACATCGATTTGTCAATGACCAACTGCACA
GAGATCTCCTAGGGGATTATGCTGAGTGATATCCCTCTGTTTGTAGCTAAACAGTTACTGGTTGACGTGT

CCAGCCATTCAGCAATCAGTCGAGCCAGCGAACTGCTGCTTGACTGTTGCTCTTGGGTTCATGACGCAGC
GGTCGGTAAGTCGTTAGTCAGCTCGGTCGCTTGACGACGAACTGACAACGAGAACCCAAGTACTGCGTCG

TGTGTGCCACAGCATCATCGTCATGTACCATGCCGGGTAGCCACAATGGTAACACTACTCTTCCAACCAT
ACACACGGTGTCGTAGTAGCAGTACATGGTACGGCCCATCGGTGTTACCATTGTGATGAGAAGGTTGGTA

CGACTCTGTTATCACAGAGAACAGGCAGATTGTGGACCAGATCGTCAAGATTCTTGAGTGCCCGTGCTCT
GCTGAGACAATAGTGTCTCTTGTCCGTCTAACACCTGGTCTAGCAGTTCTAAGAACTCACGGGCACGAGA

CATGATGAATATCTGCTCACCATTGTGCATCTTGTCGTCTTCAAAGTAATGGCTTGGTACGCAGCAGCAG
GTACTACTTATAGACGAGTGGTAACACGTAGAACAGCAGAAGTTTCATTACCGAACCATGCGTCGTCGTC

CTCGCGAGAAGCCCTCTCTGGCGGAAGAGATAAACTGGACAGACCAGCAATCCGGTCGACCTCGCAGCCG
GAGCGCTCTTCGGGAGAGACCGCCTTCTCTATTTGACCTGTCTGGTCGTTAGGCCAGCTGGAGCGTCGGC

SmaI ***SacI*** M13 LacZ fwd
CAC**GGG**TACC**GAGCTC**GAATTCACTGGCCGTCGTTTTACAACGTCGTGACTGGGAAAACCCTGGC
GTGCCCATGGCTCGAGCTTAAGTGACCGGCAGCAAAATGTTGCAGCACTGACCCTTTTGGGACCG

Figure A7.15. Sequence file of *DsAflR* RNAi-2 sense dsRNA construct indicating 555 bp of plasmid DNA sequenced.

M13 LacZ rev
GCGGATAACAATTTCACACAGGAAACAGCTATGACCATGATTACGCCAAGCTTGCATGCCTGCAGGTCGA
CGCCTATTGTTAAAGTGTGTCCTTTGTCGATACTGGTACTAATGCGGTTCGAACGTACGGACGTCCAGCT

XbaI *SmaI*
C**TCTAGA**GGATC**CCC**CAAACATCGATTTGTCAATGACCAACTGCACACCAGCCATTCAGCAATCAGTCGA
GAGATCTCCTAGGGGGTTTGTAGCTAAACAGTTACTGGTTGACGTGTGGTCGGTAAGTCGTTAGTCAGCT

GCCAGCGAACTGCTGCTTGACTGTTGCTCTTGGGTTCATGACGCAGCTGTGTGCCACAGCATCATCGTCA
CGGTCGCTTGACGACGAACTGACAACGAGAACCCAAGTACTGCGTCGACACACGGTGTCGTAGTAGCAGT

TGTACCATGCCGGGTAGCCACAATGGTAACACTACTCTTCCAACCATCGACTCTGTTATCACAGAGAACA
ACATGGTACGGCCCATCGGTGTTACCATTGTGATGAGAAGGTTGGTAGCTGAGACAATAGTGTCTCTTGT

GGCAGATTGTGGACCAGATCGTCAAGATTCTTGAGTGCCCGTGCTCTCATGATGAATATCTGCTCACCAT
CCGTCTAACACCTGGTCTAGCAGTTCTAAGAACTCACGGGCACGAGAGTACTACTTATAGACGAGTGGTA

TGTGCATCTTGTCGTCTTCAAAGTAATGGCTTGGTACGCAGCAGCAGCTCGCGAGAAGCCCTCTCTGGCG
ACACGTAGAACAGCAGAAGTTTCATTACCGAACCATGCGTCGTCGTCGAGCGCTCTTCGGGAGAGACCGC

T7 promoter
GAAGAGATAAACTGGACAGACCAGCAATCCGGTCGACCTCGCAGCCGCAC**TCTCCCTATAGTGAGTCGTA**
CTTCTCTATTTGACCTGTCTGGTCGTTAGGCCAGCTGGAGCGTCGGCGTGAGAGGGATATCACTCAGCAT

SmaI *SacI* M13 LacZ fwd
TTACCC**GAGCTC**GAATTCACTGGCCGTCGTTTTACAACG**TCGTGACTGGGAAAACCCTGGC**
AATCCCATGGCTCGAGCTTAAGTGACCGGCAGCAAAATGTTGCAGCACTGACCCTTTTGGGACCG

Figure A7.16. Sequence file of *DsAflR* RNAi-2 antisense dsRNA construct indicating 555 bp of plasmid DNA sequenced.

Figure A7.17. Sequence file of *eGFP* sense dsRNA construct indicating 884 bp of plasmid DNA sequenced.

M13 LacZ rev
GCGGATAACAATTTCACACAGGAAACAGCTATGACCATGATTACGCCAAGCTTGCATGCCTGCAGGTCGA
CGCCTATTGTTAAAGTGTGTCCTTTGTCGATACTGGTACTAATGCGGTTCGAACGTACGGACGTCCAGCT

XbaI *SmaI*
C**TCTAGA**GGATC**CCC**GTGAGCAAGGGCGAGGAGCTGTTCACCGGGGTGGTGCCCATCCTGGTCGAGCTGG
GAGATCTCCTAGGGGCACTCGTTCCCGCTCCTCGACAAGTGGCCCCACCACGGGTAGGACCAGCTCGACC

ACGGCGACGTAAACGGCCACAAGTTCAGCGTGTCCGGCGAGGGCGAGGGCGATGCCACCTACGGCAAGCT
TGCCGCTGCATTTGCCGGTGTTCAAGTCGCACAGGCCGCTCCCGCTCCCGCTACGGTGGATGCCGTTCGA

GACCCTGAAGTTCATCTGCACCACCGGCAAGCTGCCCGTGCCCTGGCCCACCCTCGTGACCACCCTGACC
CTGGGACTTCAAGTAGACGTGGTGGCCGTTCGACGGGCACGGGACCGGGTGGGAGCACTGGTGGGACTGG

TACGGCGTGCAGTGCTTCAGCCGCTACCCCGACCACATGAAGCAGCACGACTTCTTCAAGTCCGCCATGC
ATGCCGCACGTCACGAAGTCGGCGATGGGGCTGGTGTACTTCGTCGTGCTGAAGAAGTTCAGGCGGTACG

CCGAAGGCTACGTCCAGGAGCGCACCATCTTCTTCAAGGACGACGGCAACTACAAGACCCGCGCCGAGGT
GGCTTCCGATGCAGGTCCTCGCGTGGTAGAAGAAGTTCCTGCTGCCGTTGATGTTCTGGGCGCGGCTCCA

GAAGTTCGAGGGCGACACCCTGGTGAACCGCATCGAGCTGAAGGGCATCGACTTCAAGGAGGACGGCAAC
CTTCAAGCTCCCGCTGTGGGACCACTTGGCGTAGCTCGACTTCCCGTAGCTGAAGTTCCTCCTGCCGTTG

ATCCTGGGGCACAAGCTGGAGTACAACTACAACAGCCACAACGTCTATATCATGGCCGACAAGCAGAAGA
TAGGACCCCGTGTTCGACCTCATGTTGATGTTGTCGGTGTTGCAGATATAGTACCGGCTGTTCGTCTTCT

ACGGCATCAAGGTGAACTTCAAGATCCGCCACAACATCGAGGACGGCAGCGTGCAGCTCGCCGACCACTA
TGCCGTAGTTCCACTTGAAGTTCTAGGCGGTGTTGTAGCTCCTGCCGTCGCACGTCGAGCGGCTGGTGAT

CCAGCAGAACACCCCCATCGGCGACGGCCCCGTGCTGCTGCCCGACAACCACTACCTGAGCACCCAGTCC
GGTCGTCTTGTGGGGGTAGCCGCTGCCGGGGCACGACGACGGGCTGTTGGTGATGGACTCGTGGGTCAGG

GCCCTGAGCAAAGACCCCAACGAGAAGCGCGATCACATGGTCCTGCTGGAGTTCGTGACCGCCGCCGGGA
CGGGACTCGTTTCTGGGGTTGCTCTTCGCGCTAGTGTACCAGGACGACCTCAAGCACTGGCGGCGGCCCT

T7 promoter *SmaI* ***SacI***
TCACTCTCGGCATGGACGAGCTGTACAAG**TCTCCCTATAGTGAGTCGTATTA**GGGTACC**GAGCTC**GAATT
AGTGAGAGCCGTACCTGCTCGACATGTTCAGAGGGATATCACTCAGCATAATCCCATGGCTCGAGCTTAA

M13 LacZ fwd
CACTGGCCGTCGTTTTACAACGTCGTGACTGGGAAAACCCTGGC
GTGACCGGCAGCAAAATGTTGCAGCACTGACCCTTTTGGGACCG

Figure A7.18. Sequence file of *eGFP* antisense dsRNA construct indicating 884 bp of plasmid DNA sequenced.

7.5.4 Calculations

7.5.4.1 Example calculation for working out the amount of synthesised enhanced green fluorescent protein (*eGFP*) fragments (sense and antisense) to use for *in vitro* transcription

Linear fragments were synthesised via Twist BioScience to compare the dsRNA production efficiency to those of the manually constructed linearised plasmids. However, less than 1 µg of DNA (sense and antisense – 2 µg in total) was needed since the commercially synthesised fragments (Twist BioScience) did not contain the entire plasmid backbone.

Size of plasmid DNA is 3423 bp.

Size of synthesised fragment for *eGFP* is 737 bp.

For 1 µg of a 737 bp molecule the amount of template DNA was calculated as follows:

1 µg × (737 bp/3423 bp) = 0.215 µg (~0.2 µg)

0.2 µg of a 737 bp molecule was required for the transcription reaction.

7.5.4.2 Example calculation for fluorescent labelling of enhanced green fluorescent protein (*eGFP*)-dsRNA

Average molecular weight of dsRNA is calculated as the number of nt x 640 g/mol (molecular weight (MW) of dsRNA)

***eGFP*-dsRNA (737 bp in length):**

MW = 640 g/mol × 737 bp = 471680 g/mol

$= 4.7168 \times 10^5$ µg/µmol

The kit labels 40-80 pmoles of dsRNA
e.g. **40 pmol** = 4.0×10^5 µmol

Amount of dsRNA required = $(4.7168 \times 10^5$ µg/µmol) × $(4.0 \times 10^5$ µmol)
= 18.867 µg (× 1000 =18867 ng)

Concentration of dsRNA = 51.477 ng/µL (1:10 dilution therefore × 10)
51.477 ng/µL × 10 = 514.77 ng/µL

$\frac{18867 \text{ ng}}{51.477 \text{ ng/µL}}$ = 36.7 µL of dsRNA was required for 40 pmol of dsRNA in the reaction

7.6 *Dothistroma septosporum* transformation

7.6.1 Production of an *eGFP*-expressing *Dothistroma septosporum* strain by transformation

The use of fungal strains that constitutively express a *GFP* gene have been shown to be useful for RNAi studies silencing *GFP* with a control *GFP*-dsRNA (Koch et al., 2016). In an attempt to generate an *eGFP*-expressing strain of *D. septosporum* to serve as a control (by providing a visual reduction in *GFP* fluorescence if SIGS is effective), a protoplast-based transformation was performed (Chapter 2, section 2.8). Screening identified 10 out of 30 transformants that expressed *eGFP*, based on strong fluorescence after each round of purification. Transformants 2 and 7 were selected as *eGFP* strains for further study (see Figure A7.19 below and refer to Figure A7.20 for the PCR products amplified to verify that the transformation was successful).

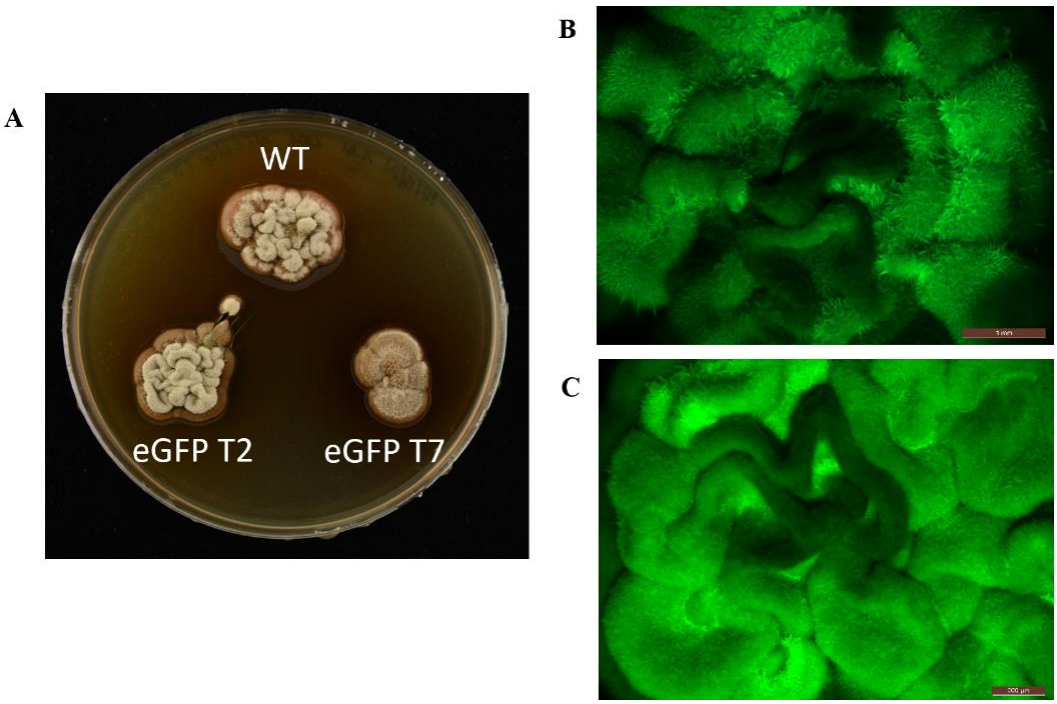

Figure A7.19. Wildtype (WT) and enhanced green fluorescent protein (*eGFP*)-expressing strains of *Dothistroma septosporum*. (A) Growth of colonies on Dothistroma Medium (DM). (B–C) Fluorescence microscopy of colonies of eGFP transformants (B – eGFP transformant 2 (T2) and C – transformant 7 (T7)), indicating the strains are expressing *eGFP*. Scale bars are 1 mm (B) and 0.2 mm (200 µM) (C) respectively.

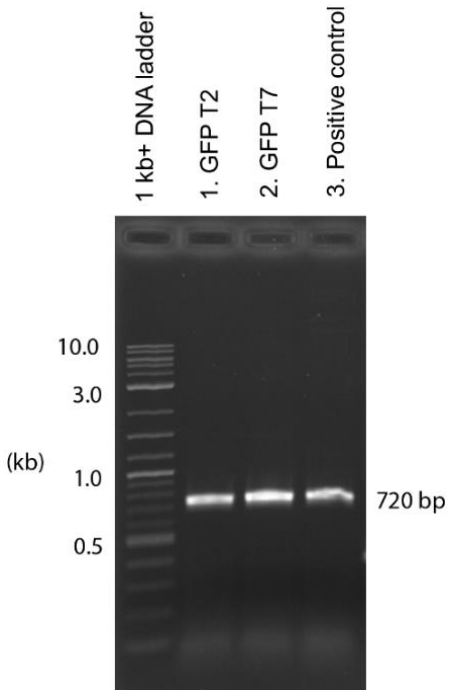

Figure A7.20. Polymerase Chain Reaction (PCR) screening of enhanced green fluorescent protein (eGFP) *Dothistroma septosporum* transformants to verify the presence of *eGFP*. Lanes 1 and 2 show amplification of a 720 bp product of *eGFP* using genomic DNA (gDNA) extracted from GFP transformants 2 (T2) and 7 (T7) (as described in section 2.8.3). As a positive control, *eGFP* was amplified from the pPN82 plasmid (R239; 20 ng) (lane 3).

7.7 Confocal microscopy imaging

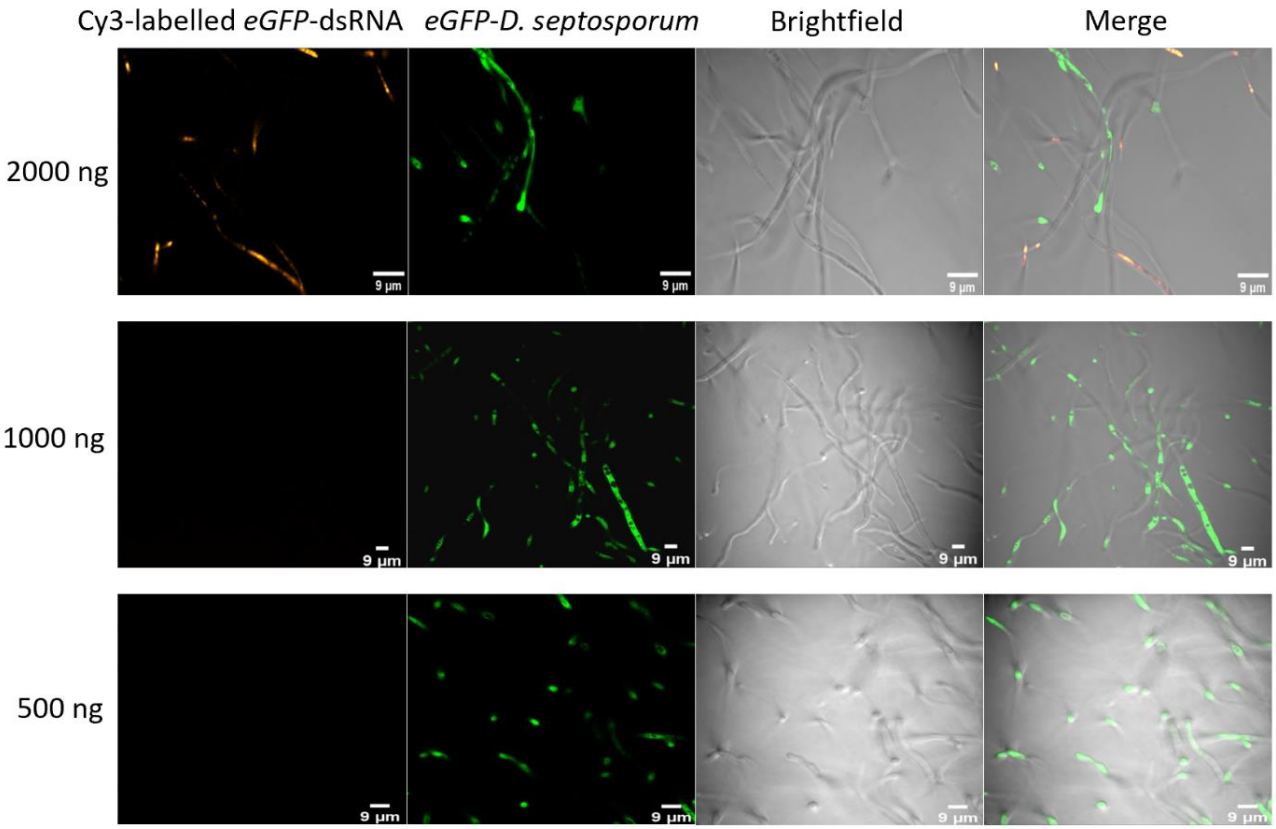

Figure A7.21. Monitoring uptake of fluorescently labelled enhanced GFP (*eGFP*)-dsRNA in *Dothistroma septosporum* 24 h post-inoculation with the dsRNA. Little uptake of Cy3-labelled dsRNA was seen after 24 h. Hyphae were grown on water agar (WA) with microscope slides and inoculated into liquid cultures as outlined in Section 2.11. Different amounts of *eGFP*-dsRNA were applied: 2000 ng (top panel), 1000 ng (middle panel) and 500 ng (bottom panel). From confocal microscopy imaging, orange fluorescence indicates Cy3-labelled dsRNA, green fluorescence shows *eGFP*-expression, grey image brightfield view of hyphae and a merged image of all three channels. Scale bar is 9 µm.

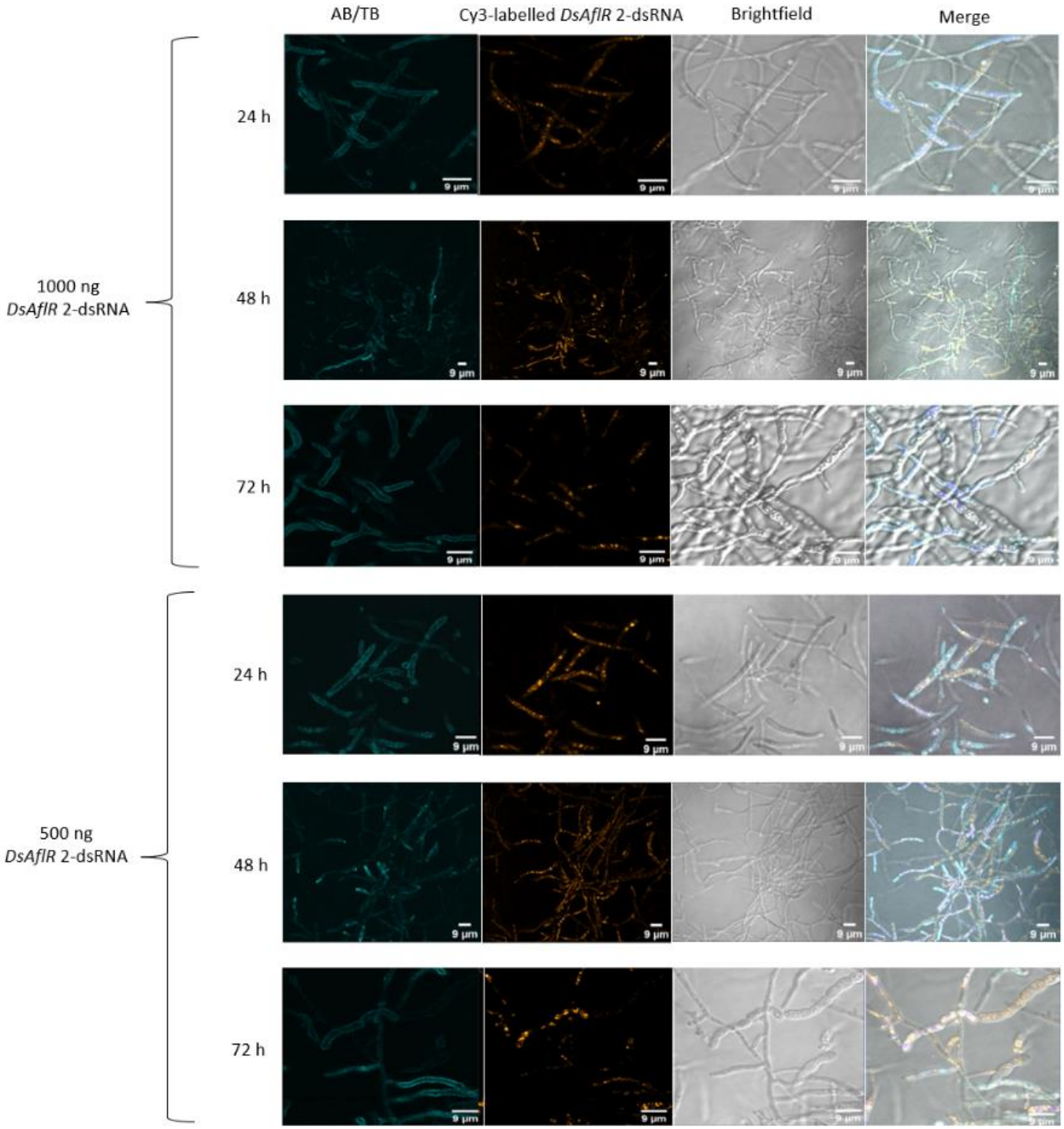

Figure A7.22. Monitoring uptake of fluorescently labelled dothistromin pathway regulatory gene (*DsAflR*) 2-dsRNA in *Dothistroma septosporum* 24, 48 and 72 h post-inoculation with the dsRNA. Hyphae were grown on water agar (WA) with microscope slides and inoculated into liquid cultures as outlined in Section 2.11. Different amounts of *DsAflR* 2-dsRNA were applied as indicated: 2000 ng and 500 ng, in the presence of 0.03% SILWET-L77 and imaged using confocal microscopy. The different colours represent different fluorescence channels, from left to right: cyan fluorescence is representative of Aniline Blue (AB) and Trypan Blue (TB) and orange is Cy3 fluorescence. Grey image is brightfield and the merged image is of all channels. Scale bar is 9 µm.

7.8 Appendices for Chapter 5

7.8.1 Primers used for amplification of target genes for dsRNA synthesis and gene expression determination by quantitative Reverse Transcription Polymerase Chain Reaction (qRT-PCR)

Table A7.5. Primers for dsRNA synthesis of enhanced green fluorescent protein (*eGFP*) and gene expression analyses.

Primer Name	Sequence (5'–3')	Flanks/ Spans intron	cDNA (bp)	gDNA (bp)	Tm (˚C)
Gfp_F_exp1	CGACAACCACTACCTGAGCA	No	82	82	60
Gfp_R_exp1	GAACTCCAGCAGGACCATGT	No	82	82	60
T7_eGFP_fwd_sense_AM	TAATACGACTCACTATAGGGAG AGTGAGCAAGGGCGAGGAGCTG	No	737	737	67.8
eGFP_rev_sense_AM	CTTGTACAGCTCGTCCATGCC	No	737	737	58.2
T7_eGFP_fwd_anti_AM	TAATACGACTCACTATAGGGAG ACTTGTACAGCTCGTCCATGCC	No	737	737	66.0
eGFP_rev_anti_AM	GTGAGCAAGGGCGAGGAGCTG	No	737	737	62.8

T7 promoter sequences are underlined.
qRT-PCR primers are highlighted yellow.
Primers for dsRNA template synthesis are denoted in blue.

ATGGTGAGCAAGGGCGAGGAGCTGTTCACCGGGGTGGTGCCCATCCTGGTCGAGCTGGACGGCG
ACGTAAACGGCCACAAGTTCAGCGTGTCCGGCGAGGGCGAGGGCGATGCCACCTACGGCAAGCT
GACCCTGAAGTTCATCTGCACCACCGGCAAGCTGCCCGTGCCCTGGCCCACCCTCGTGACCACC
CTGACCTACGGCGTGCAGTGCTTCAGCCGCTACCCCGACCACATGAAGCAGCACGACTTCTTCA
AGTCCGCCATGCCCGAAGGCTACGTCCAGGAGCGCACCATCTTCTTCAAGGACGACGGCAACTA
CAAGACCCGCGCCGAGGTGAAGTTCGAGGGCGACACCCTGGTGAACCGCATCGAGCTGAAGGGC
ATCGACTTCAAGGAGGACGGCAACATCCTGGGGCACAAGCTGGAGTACAACTACAACAGCCACA
ACGTCTATATCATGGCCGACAAGCAGAAGAACGGCATCAAGGTGAACTTCAAGATCCGCCACAA
CATCGAGGACGGCAGCGTGCAGCTCGCCGACCACTACCAGCAGAACACCCCCATCGGCGACGGC
CCCGTGCTGCTGCCCGACAACCACTACCTGAGCACCCAGTCCGCCCTGAGCAAAGACCCCAACG
AGAAGCGCGATCACATGGTCCTGCTGGAGTTCGTGACCGCCGCCGGGATCACTCTCGGCATGGA
CGAGCTGTACAAGTAA

Figure A7.23. Nucleotide sequence of enhanced green fluorescent protein (*eGFP*). Colour codes for sequences are shown as follows: Red: coding region (and RNAi target region) (714 bp), yellow highlight: qRT-PCR primers for gene expression determination and blue highlight: primers used for dsRNA template synthesis. No introns are present within this sequence.

Table A7.6. Primers for dsRNA synthesis of dothistromin pathway regulatory gene (*DsAflR*) and gene expression analyses.

Primer Name	Sequence (5'–3')	Flanks/ Spans intron	cDNA (bp)	gDNA (bp)	Tm (˚C)
AflR_F_exp1	ACAAGTCGACGAGCTTCTGG	No	94	94	59.53
AflR_R_exp1	TGCTGCATTTCACCTTCGATG	No	94	94	60.04
AflR_F_exp2	CAGACGGCTCAGACAATGGT	No	88	88	60.32
AflR_R_exp2	TGCGAAAGGAGGTTCACGAG	No	88	88	59.59
DsAflR - RNAi-1-For1	TAATACGACTCACTATAGGGAGAC GGACGGACTTCGCACGCCAC	No	509	509	68.90
DsAflR - RNAi-1-Rev1	CCCATGTCGGACACCGAGG	No	509	509	60.50
DsAflR - RNAi-1-For2	TAATACGACTCACTATAGGGAGAC CCATGTCGGACACCGAGGTG	No	509	509	67.70
DsAflR - RNAi-1-Rev2	CGGACGGACTTCGCACGCCAC	No	509	509	65.50
DsAflR - RNAi-2-For1	TAATACGACTCACTATAGGGAGAC AAACATCGATTTGTCAATG	Yes	408	408	62.0
DsAflR - RNAi-2-Rev1	GTGCGGCTGCGAGGTCGACC	Yes	408	408	66.0
DsAflR - RNAi-2-For2	TAATACGACTCACTATAGGGAGAG TGCGGCTGCGAGGTCGAC	Yes	408	408	68.40
DsAflR - RNAi-2-Rev2	CAAACATCGATTTGTCAATGACC	Yes	408	408	52.80

T7 promoter sequences are underlined.
cDNA and gDNA refer to the amplicon length in base pairs (bp).
qRT-PCR primers are highlighted yellow and green.
Primers for dsRNA template synthesis are denoted in blue and red.

693332 TTCCTGACGGCACTGAGATCCAGGCCCAAGCTTGCAAGCGATGAGGCTTGCTGCAGGCGCCGTGGCGCCA 693263
693262 CACCCGCTGATGGCGCTATCACCCTGTTGGTCGTGCGCATCGGAGTCCTCGAGTAATCCTTCGCGTGGCC 693193
693192 GTGGCTAGCTTGCCCAGCACGTTGTCGGAGCTTATGACTGACTACTACTAATCATGCTGGTCGATCGCTC 693123
693122 CCAACGGGGCCGACCACGCCTCGCCTGTGCTGACCCGCCAGGCTAGCGATCCGCGCAGCTTCATGCAACA 693053
693052 GGGTGCCACCTCTGATCCTTTGAATCGAGCCCCGGGGCATGAAGCTGGCCGACGCAGGAACATTACGGAC 692983
692982 GGTACTCTACACACCTATGAGATCTAGTGTGCCCTCAATCGCCCAGCCCGGCACCTCGTGGCTTTCCTGC 692913
692912 CTATATAGTGGATCACCCGCCTGAAAAGGCTTTCGATGCTCTTGGTCACACCCGGTGGCAGCTGTCATTC 692843
692842 ACTTCCAACCCTACGCGTCTACCAGCGCTTTGGCGGGTTTTGTCTCTTAGCATCGGACGATCCTCCCCTT 692773
692772 CGAGCCTTCGATCACCGTCATCACTATGCCTGAATCACGCGGCTCAGAGTCGAGCGGCTCGACAAGTCGA 692703
692702 CGAGCTTCTGGCACACAACACATCGCAACTCCTAAGCTGAAGGACTCTTGCACTGCTTGTGCAACATCGA 692633
692632 AGGTGAAATGCAGCAAAGATAAGCCAACATGTGCTCGATGCACCCGGCGAGGCTTGACCTGCGATTATGG 692563
692562 CCTTTCGAAGCGGACCGGACGGACTTCGCACGCCACTGCTCAGAAGCAACAGCAACAACGACAGCAACAA 692493
692492 CAACAAAGTCAACAAGAAGCAGCAGATAGGAGGGTCAGCCAGTCCGCAGTCCCTGTGGCCAATATGCTCC 692423
692422 CAGACGTAGATGAGTTCATCTCGCCGATGTCACTGCAAGAGTCTTCGATACTTTCCCCCACGCTCATGCC 692353
692352 AGATCTCAGCACCAGCGGCTCACAAGCTGGCCTGGATCAGTGGAATTCAGATCTGTGGTCGACCATGTTC 692283
692282 GCCCCGAACGAACCAAGCTCAAACAACACTCCAGCAAACACAATGCAGACCCATGGCGGCAATGGCAACG 692213
692212 ACATTGATCATCTATTCAACGACCTCACATCCTACAGCATGCTTGGAGAGCCAACAGACACTGCAATGTC 692143
692142 AAATCAGCATACACATACGTTTTCCGATACTTCATCTTCGATAAGCCCATTCGACCAACTCACCTCGGTG 692073
692072 TCCGACATGGGTAGCCAAGACTTTTCAAACATCGATTTGTCAATGACCAACTGCACACCAGCCATTCAGC 692003
692002 AATCAGTCGAGCCAGCGAACTGCTGCTTGACTGTTGCTCTTGGGTTCATGACGCAGCTGTGTGCCACAGC 691933
691932 ATCATCGTCATGTACCATGCCGGGTAGCCACAATGGTAACACTACTCTTCCAACCATCGACTCTGTTATC 691863
691862 ACAGAGAACAGGCAGATTGTGGACCAGATCGTCAAGATTCTTGAGTGCCCGTGCTCTCATGATGAATATC 691793
691792 TGCTCACCATTGTGCATCTTGTCGTCTTCAAAGTAATGGCTTGGTGAGTTTCGTGCGGCGGACTAATTCT 691723
691722 GGAGGTCAACCACTGACCCCATGTTAGGTACGCAGCAGCAGCTCGCGAGAAGCCCTCTCTGGCGGAAGAG 691653
691652 ATAAACTGGACAGACCAGCAATCCCGTCGACCTCGCAGCCGCACGCACTCGGAGGAAGTCTTGCGATTTC 691583
691582 CTCCTAGTATTGATGGCTACAGCTCAGACGGCTCAGACAATGGTCGCATGGCAGCCCAACTCGTCCTCAG 691513
691512 CGAGTTGCACCGTGTCCAACGACTCGTGAACCTCCTTTCGCAGCGCCTGGAAGGCGTGCGACTGAGGAAC 691443
691442 CACGTCGCAAGCTCCGGTAGCAGTTCTAGCCTGGAGAGCATCGGAGAGGACTCTGTCGTTGGAGTTTCTC 691373
691372 TGTCCGCTACTGCGGGCTCACCTTTGTCTTCGCCAACATTCGATCAGCTTGAAGCTGATCTCAGGAAGCG 691303
691302 TTTGCGTGCAGTCTCTTTTGAGACCATTGACGTTCTGCGTCGTAGTTAGCAAGATCGGAAGTCCTCTTCG 691233
691232 GACCTTGGTTGCATTTCACGGCATCTTCATGACAGATCGACTCGGCATAGAGATACAGGTCGTGCTGTCC 691163
691162 TGTTTTGGTATAGCTGGGGTCTGGGCGCTGGGTTGCGGCGCTGCAACGATGTTTCATAGACTGACGAGAC 691093
691092 GTCACATGTAAATACTAGCATGCCTCAGACTTTCATCGATCCTACAACGAAGTCACTTGATCAGCTCTAC 691023
691022 TGTACTTAGCAAACTGAGTCCCGCCATCTGAGAGGATATCCCATCCGCACAGTGGCACTCAGTCCCGTTG 690953
690952 CAGTGTTCACTTCGATTGGCCACATTCGCGATGTGCTTCTGAATGCCGGCTAAGGAAATCTCCATCCCAC 690883
690882 GTATTGCGGATCCGTGAGGGACTGCTCATCCCGCATCTCGTCATGCTCGCTGCAC 690828

Figure A7.24. Nucleotide sequence of dothistromin pathway regulatory gene (*DsAflR*) (*Ds75566*). Colour codes for sequences: Grey: Upstream or downstream padding, **black:** intron, blue: untranslated region (UTR), **purple:** RNAi-1 (486 bp target region 1 and part of the coding region), **orange:** RNAi-2 (385 bp target region 2 and part of the coding region), red: other parts of the coding region, blue and red: positions of primers for dsRNA template synthesis, yellow and green highlight: qRT-PCR primer positions.

Table A7.7. Primers used for gene expression analyses with the reference gene translation elongation factor 1 alpha (*DsTEF1α*) (*Ds68333*).

Primer Name	Sequence (5'–3')	Flanks/Spans intron	cDNA (bp)	gDNA (bp)	Tm (˚C)
TEF1_F_exp1	ACTATCGACATTGCCCTCTGG	Flanks intron	82	134	59.59
TEF1_R_exp1	TGAAATCACGGTGACCTGGG	Flanks intron	82	134	59.96
TEF1_F_exp2	TTATCGGCCACGTCGACT	Flanks intron	94	152	60
TEF1_R_exp2	TCGAATTTCTCGATGGTACGC	Flanks intron	94	152	60
TEF1_F_exp3	CGTGACATGAGACAGACCG	Flanks intron	102	157	50
TEF1_R_exp3	CTTGGCAGCCTTGACGG	Flanks intron	102	157	60

T7 promoter sequences are underlined.
cDNA and gDNA refer to the amplicon length in base pairs (bp).
Each set of qRT-PCR primers are highlighted either yellow, green, or blue. Primers used for successfully amplify *DsTEF1α* were: TEF1_F_exp3 and TEF1_R_exp3 (Table 2.3).

```
2871106 GCCACACCACTGCCAGTTCGCTTGCCGCTTGTGATGGCTACTATGCCACCAAGTTTTGATGGACCTTCAC 2871175
2871176 CGCAGTTCACAAGCCCCGCCATCCGTTCTCGGACTAGTGTCAGCCCCACCGGCTTGGCGTCTCTCTGCTC 2871245
2871246 ACTTATAATGAAATCTCCGTCCTTTGCAAAACCTTTCTTCGCTTCTGTTGTCCGAAACACCGTAACTCGA 2871315
2871316 GCAGTTGCATCTTTCGTGAGTATCCACAGCATCTGACAACTGCGCGATTGCCACCCGCTGACAGAGCATG 2871385
2871386 CAGAAAAACCCCCCGGTACTTTCCATTTTCCAGAAACCCACCACACAACACCGCCAACACCGACACCATG 2871455
2871456 GGGTACGCCTTCCTCAAACATCACGCTGAAAGAGCCGCGACTGACACATCGTAGTAAGGAAAAGATCCAC 2871525
2871526 ATCAATGTCGTCGTTATCGGGCCACGTCGACTCCGGCAAGTCGACCACCACCGGACGTAAGCGCTCCTCCC 2871595
2871596 TTCCTGCGACCGACACATGATTCTCGGCTCACACAACACACAGACTTGATCTACAAGTGCGGTGGTATCG 2871665
2871666 ACAAGCGTACCATCGAGAAATTCGAGAAGGTGAGTCATCTGGCAACACCGCTTATCGCACGCATTCCTCG 2871735
2871736 ATGCTCGTCAATTCTGTGAGTTGAGGGGCAAAATTTGGTGGGGTGCGAGAATTTTGGCGCCCACTTTTCC 2871805
2871806 TGGGGTTCAACGCCATGATCTCATCCACCACCGCCAAATGCCTTCTCACCGCAATCATGCCCTACTGAAG 2871875
2871876 CACCACGAAACACTAGCCGATTACGTTGCAAACATTTCACATTGAGAACATGACTCTGACAATCTGCCAC 2871945
2871946 AGGAAGCCGCCGAGTTGGGCAAGGGCTCCTTCAAGTACGCATGGGTGCTCGACAAGCTGAAGGCCGAGCG 2872015
2872016 TGAGCGTGGTATCACTATCGACATTGCCCTCTGGAAGTTCGAGACTCCGAAATATTACGTACGGCTTCTT 2872085
2872086 ACTCCCGAAGATGACGGCGCATTGGCTAACGTTCTTGCAGGTCACTGTCATTGACGCCCCAGGTCACCGT 2872155
2872156 GATTTCATCAAGAACATGATCACTGGTACTTCCCAGGCTGACTGCGCCATTCTCATCATCGCCGCTGGTA 2872225
2872226 CTGGTGAGTTCGAGGCCGGTATCTCCAAGGATGGTCAGACTCGTGAGCACGCTCTCCTCGCCTACACCCT 2872295
2872296 AGGCGTGAAGCAGCTCATCGTCGCCATCAACAAGATGGACACCACTAAGTGGTCCGAGGACCGCTTCAAC 2872365
2872366 GAGATCATCAAGGAGACCTCCAACTTCATCAAGAAGGTCGGCTACAACCCAAAGACCGTCCCATTCGTGC 2872435
2872436 CAATCTCCGGTTTCAACGGCGACAACATGATCGACGTTTCCTCCAACTGCCCGTGGTACAAGGGCTGGGA 2872505
2872506 GAAGGAGACCAAGTCCAAGGTGACTGGCAAGACCCTCCTCGAGGCCATCGACGGCATTGACCCACCGTCG 2872575
2872576 CGTCCATCTGACAAGCCACTCCGTCTCCCGCTTCAGGATGTGTACAAGATTGGTGGTATTGGCACGGTCC 2872645
2872646 CAGTCGGTCGTGTTGAGACTGGTGTCATCAAGGCCGGCATGGTCGTCACCTTCGCCCCAGCTGGTGTTAC 2872715
2872716 CACCGAAGTCAAGTCCGTCGAGATGCACCACGAGCAGCTCACCGAGGGTCTACCGGGTGACAACGTCGGC 2872785
2872786 TTCAACGTCAAGAACGTCTCGGTCAAGGAGATCCGTCGTGGCAACGTCGCCGGTGACTCCAAGAACGACC 2872855
2872856 CACCAAAGGGCTGCGACTCCTTCAACGCCCAGGTCATCGTCCTCAACCACCCAGGTCAGGTCGGTGCCGG 2872925
2872926 TTACGCTCCAGTTCTCGACTGCCACACCGCCCACATTGCCTGCAAGTTCTCCGAGCTCCTCGAGAAGATC 2872995
2872996 GACCGTCGTTCCGGCAAGTCCATTGAAGCCTCGCCAAAGTTCATTAAGTCTGGTGACGCTGCCATTGTCA 2873065
2873066 AGATGATTCCATCCAAGCCAATGTGCGTCGAGGCGTTCACCGAGTACCCACCACTTGGTCGTTTCGCTGT 2873135
2873136 CCGTGACATGAGACAGACCGTCGCTGTTGGTGTCATCAAGTCCGTCGTCAAGGCTGACAAGGGCGCTGGC 2873205
2873206 GTACGTACCCTCGACGTCTCTTTGCTTGAATCATGTATGCTGACAAATCTTACAGAAGGTCACCAAGGCC 2873275
2873276 GCCGTCAAGGCTGCCAAGAAGTAAACGAGTGATGACTTTCTTCGGCTTCTGCTTTTGTTTCTTCAAACAA 2873345
2873346 AAAGCGGGTGTTTGTTGGGAGCGGGCGCTTTTTGAGCCTCTTTTTCTCTGCTCTACAGGGAAGATAGCAG 2873415
2873416 GCTTTCCTTCCCTGCCCTCAGCTCCAGTCATACCTTGTTCTAATCTTGCATGACGACGAGCTCGCGTTAG 2873485
2873486 CCTTTGGTCGATTCGGGCAACGACGAGAACTGATCCAACCACGACCACCTTTTCCTTTGTAACGGCATGA 2873555
2873556 GATCACGAAGCGGAGATGATGGCGGTTTTGCGATGGATGGCAAAAGTCTAGAGCAGACTTGGCCTGCCGA 2873625
2873626 TAGCTTAGGTTTCTACTCCTTCAAATGAGAGCAATCAAGGGGTGCATCAAAGGTCTGACGTCTCAAATCT 2873695
2873696 GTTCTGTGCTTTATGACTTCATTCTCATTTGGTGACCATGTGCCGCGGTCTTGCATCAAGCTCGATTTAT 2873765
2873766 ACCTACACAATTTTCTGTCAACTATTTGGTACCTTCATCACCGGCCATGACACCTTCGCACGACCCCAAC 2873835
2873836 AGTATCGCCGGCTGTGTCCTTGACACCTTCGATACATTGCAGCCCAGATA 2873885
```

Figure A7.25. Nucleotide sequence of translation elongation factor 1 alpha (*DsTEF1α*) (*Ds68333*). Colour codes for sequences are shown as follows: Grey: Upstream or downstream padding. Red: coding region, **black:** intron, blue: untranslated region (UTR), yellow, green and blue highlight: qRT-PCR primers.

Table A7.8. Primers used for gene expression analyses to examine if the RNA interference (RNAi) gene, *DCL*, (dicer-like protein; Ds56023) is expressed.

Primer Name	Sequence (5'–3')	Flanks/Spans intron	cDNA (bp)	gDNA (bp)	Tm (˚C)
Dicer_F_exp1	CAAGAACCCGCGAGAGTACC	Flanks intron	87	184	60.46
Dicer_R_exp1	TTGCCAGATCCAGTGTCGAG	Flanks intron	87	184	59.75
Dicer_F_exp2	GCGAGCCAAGAAAGGTAGGT	Spans intron	90	N/A*	60.76
Dicer_R_exp2	TCGATAACCGATCGGAGAAG	Flanks intron	90	N/A*	60.17
Dicer_F_exp3	AGCCCACCACACAAAGAAGA	Flanks intron	81	133	59.45
Dicer_R_exp3	GGTCGGAGCTCTCGTTGTTC	Flanks intron	81	133	60.73

*did not amplify from gDNA.
cDNA and gDNA refer to the amplicon length in base pairs (bp).
Each set of qRT-PCR primers are highlighted green, yellow or blue. Primers used for amplifying *DCL* were: Dicer_F_exp1 and Dicer_R_exp1 (Table 2.3).

```
1361209 CGGCGCGGCGTAGCTGCCGCGCCAAAAAACCGCAAGGTACAAAAGCGCCAAACACAAACGCTGTGACCTG 1361140
1361139 CACACGCAACACAACATGCATGCAAGCTAGCAAGCACCTAGGTTGACCACCTTTTGCTCTTCAAGCACCT 1361070
1361069 CACCACTGCTTGTTTGCTTCAACCCGACTGACTACACCAGCACTGATATCACGCGCCACCATGGGCACGC 1361000
1360999 CAGAACTCCTTCGCGTGCCGGAGACGGGGGAGGATGAGCGCGATGATGGCAATTCCGCCGCATCCGATGA 1360930
1360929 CGAGGACTCCTCTTCGCCAGCGGGTAGTCCTGCCAACACCTGGCAGCTCAAGCGGCGCGCTCAGAAGGCT 1360860
1360859 ATTTTCGAATCGTGGCTCGTCAGTCCCGCTGGTGAGGAAGCACGCAAGCCGCGTACCAAGGACGGCCGGC 1360790
1360789 TCAAGGAAGAGGTTGATGAACAGCAGTCGATCCACTCACTCCTGGCCCAGCAGCAGAAAGGTGCTCCAAT 1360720
1360719 CGTCAAGAACCCGCGAGAGTACCAGCTTGAGCTCTTTGAGCGAGCCAAGAAAGGTAGGTTTGAGGCACGC 1360650
1360649 GCGCGCCTTGCTTCCAACCCATCATGCCTGCTGAGGCACTGGCGCGCTGTTCTGGGACATAGCTGATGTC 1360580
1360579 CTCTGAACAGAGAACACTATCGCCGTTCTCGACACTGGATCTGGCAAGACACTTATAGCCGTGTTACTTC 1360510
1360509 TCCGATCGGTTATCGACGATGAGCTTGAGAAACGAGCGGCTGGTCACGCTCCCAAGATCTCGTTCTTCTT 1360440
1360439 AGTTGCCTCCGTCACCCTGGTCTACCAGCAATTCTCCGTGCTAGACTGCAACCTGGACCATAAAGTGATA 1360370
1360369 CGGCTATGTGGTGCCGACAACGTTGATCGATGGACGGCAGCACACTGGACACAGATCTTCCACGAGAACA 1360300
1360299 AAGTTGTGGTATGCACTGCAGATATCCTATTCCAATGCTTGTCTCGTAGCTTCCTGTCGATGAAGCAGAT 1360230
1360229 CAACCTACTTATCTTTGACGAAGCCCACCACACAAAGAAGAATCATGCCTACGCTAGGTTTGCTGATCAC 1360160
1360159 CCACTCTCTTGACTATGAATTAGTCACTGACTTGTATAGGATCATCAAAGACTTCTATATACCCGAACAA 1360090
1360089 CGAGAGCTCCGACCACGCATCTTTGGCATGACTGCAAGTCCAATTGATGCCAAGGTCGATGTCATACAAG 1360020
1360019 CTGCGTCTGAGCTCGAAAGCCTCCTGGACTGCAAGATTGCAACGACTCAAGACATGAGTCTTGCAGAAGC 1359950
1359949 TATCAAGCGGCCGACCGAGGAGATCCTACGGTACGATGCACTGCCACAGAGATGCTTCGAGACATCACTC 1359880
1359879 TTGCAGGACTTGAAGTCCCGGTATGGGAATATCGAAGTGTTCGCATCGTCGTTCCAGCGCGCTGCCGAAG 1359810
1359809 TGGCTCGTCACCTTGGTCGTTGGTGCGCAGACAACTTTCTTCTTCATGCTTTCTCGCATGAGAAGTCTAG 1359740
1359739 CAAATACTCGGTCGAGGTCGAGAAGAAGTGGCACGCTCGCAAAGGTCGTCAAAAAGTGGCCGAACTTGAC 1359670
1359669 GAAGCTGTAAAGGAGATTCAGGCCGCGACTCATTACATTCAGCAACGATCTCATGTGCTCGACGAGCTCT 1359600
1359599 CGCGGACACAGGATCTGAGCTCCAAGGTACGACAGCTCGACCACTACCTCAGACTGCAGTTCGAGCGCGA 1359530
1359529 GTCGACTCATCGCGCGATTGTGTTTGTCGATAGGCGATACACAGCTCGTCTGCTACACAACCTGTACACC 1359460
1359459 CGACTCAGAGGGCAAGAGGGCTACGAATACCTACGTGGTCATTTCCTGATCGGCTCAAACGGCGGCAGCA 1359390
1359389 TAGACGAGGACTCCTTCTCGTTCCGCCAACAAGTCATGACCCTGATGAAGTTCAGGAAGGGAGAGCTGAA 1359320
1359319 CTGCTTGTTCGCCACATCTGTTGCTGAAGAAGGGCTTGATGTGCCAGACTGCAATCTGGTCATCCGATTC 1359250
1359249 GACATGTATAACACTATGATCCAGTACGTGCAGTCTCGAGGGAGAGCACGAAATCAACACTCCAAATTCA 1359180
1359179 TTCATATGATCGAGAATGGCAACTGTGCCCATCAGCAGACTCTTGGCGAGGTTCGCTGGCAAGAAAATAG 1359110
1359109 CATGCGGAGATTCTGTGACCAATTGCCCGAAGATCGAAAGCTCCAGGGCAACGAAGATCACTTGGAGATG 1359040
1359039 CTCCTGGACAAGGAGAAGAACATCCAAGTGCGCATAGTGCCTTCGACGGGAGCAAAGCTGACCTACGGCA 1358970
1358969 ACGCGCTAGACTACATCGCCAATTTCGTTTCAGCCATCCCGACGGACTGCGACGAGCCTCAGCACCCTAC 1358900
1358899 GTACGAAGTGATGGCTCGCGGTCAGAAGTTCCAAGCAGAGGTAATGTTACCAAACAATGCGCCCCTTCGA 1358830
1358829 TCGGTCATGGGCGCCGTTCACGCCAAGAAAGGGTTAGCGAAGCGCTCTGCGGCGTTCAACGCTTGCATTG 1358760
1358759 AGCTCCTCAAGCTGGGTTACTTCGATGCCTATTTTTTGCCAACGTATACCAAGAAGCTCCCAGCCATGCG 1358690
1358689 CAATGCGTTGCTAGCAGTAGATATGAAGAAGCAGCACGGATACGCAATGTGTCTCAAGCCGAGTATCTGG 1358620
1358619 GCAGAGCAGAGAGGAAGTCTGCCAGGTCAGCTCTACGTCACAGTCATCGACTTTCCCAAAGGTCTCGATC 1358550
1358549 GCCCACACCAGTCGATGGCTTTCCTGACCAGATCACGCATGCCGCACTTCCCGGCGTTCTCGGTTTACTT 1358480
1358479 GAACGACGGACGTAAGACGTCCGTCGTCTCGAAGAGCTTGTCAAAGCCGATAGTGATCTGCGACCACGAG 1358410
1358409 TTGGCTCAGATAACGAAGTTCACTTTCCGTGTCTTCGAGGACGTCTTCAGCAAGACTTATGAAGAAGACA 1358340
1358339 GTGCTCAATTGTCGTACTGGTTAGCACCCGCAAATGTGCAGCTGTCCAGCCAGGATGAAGATAATCAGCA 1358270
1358269 TCTTGCAAATGGCGATCCGGACGCGATGATCGACTGGTCCCTGCTAGATGAAGCATTCACCGTTGGAGAG 1358200
1358199 CGTAAGTGGACGCTCGAGATGCCTGAGTCGTCACTATCAAATATTTTCCTAGTCGATGTCTGGGATGGTA 1358130
1358129 GTCGAAAATTCTATTCCAAGGGAGTGGATCCCTCCAAGAAGGCGACAGATCCGATACCCGAAGGTGTCGC 1358060
1358059 AAAGTCCAAACTCACTGGCACTATCCTTGACTACAGTGTCAGCCTTTGGAAAAAAGCACGACAAGAGCGA 1357990
1357989 GACGCTACTTGGTCCCGAGAACAACCTGTCATCGAAGCAGAGAAGATTTTGACACAACGCAAGAACATGC 1357920
1357919 TTGCACCTCCTGAGCTAAAGGAAGTCAGACAGGATACCAAAGCTTTTCTTTGTGTGCAGCCACTGCGCAT 1357850
1357849 TTCGACTATACCGCCAGAAGTAGCAGCACCATTGTTCATCTGGCCTGCAATCATCTACCGCTTTGAGTCA 1357780
1357779 CATCTGATCAGTCAAGAAGGCTGCAACGTTGTTGGGGTCGACTGTGGACCTGAGTTTGCCCTAGCAGCTT 1357710
1357709 TCACAAAAGACTCTGACAACTCAGGTGAACACGAAGTCGAAGAGCGCGTCAATTTCCAGCGTGGTATGGG 1357640
```

1357639 CGAGAACTACGAAAGATTTGAATTCATCGGCGACACATTTCTCAAGACAGCCACGACGCTGTCGACATTC 1357570
1357569 ATTCTGAATCCAAATGAGAATGAATTTGAATTCCACGTCCGTCGTATGCTGATGCTGTGCAATAAGAACC 1357500
1357499 TCTTCCAGACCGCTATGGGACTCAAGCTATACGAGTACATTCGCAGCTTGCCCTTCAATCGCCGCCTGTG 1357430
1357429 GTATCCAGAAGGCATGAAGCTGTTGGCTGGAACTGGTGTTGTCAAAGGCGAGGAGAAAGTCATGTGGCAC 1357360
1357359 CAACCTCGAGACCATCCCCTTGGTGAGAAGACAATTGCAGATGTCTGCGAAGCGCTCATTGGAGCTGCGT 1357290
1357289 TTATCGCCCACGACTGCCCAGGTGACTGGAAGCCCGAACATTGGGAAAGTGCTATACGGGCTGTGACCAA 1357220
1357219 GCTGGTCAACAACGATGACCACAAAATGCAGACCTGGGAGGACTACAAAGCAGCTTACGCGAAGCCCGCC 1357150
1357149 TACCAGATGCAAGAGGCTACCGCCGTGCAGAAAGACCTGGCGGATAAGGTTGAGCTCGAGCATCTTTATC 1357080
1357079 GCTTTCAGTACCCGCGACTACTCTATTCGGCTTTCGTACACCCTTCGCTGCCGTTCATGTACGAGAAGGT 1357010
1357009 CCCGAACTACCAGCGTCTTGAGTTCTTGGGAGACGCACTTCTCGACATGGCCAGCATCTCCTACCTGTTC 1356940
1356939 TACAAGTATCCAGATAAGGACCCGCAATGGCTCACCGAGCACAAGATGGCCATGGTCTCCAACAAGTTCT 1356870
1356869 TGGGAGCACTTTGTGTGAACATTGGCTTCCACAAGCATCTTCGCCATCACCACGCCAAGCTTGAACATCA 1356800
1356799 AGTCCGCGAGTACGCGATTGAACTGCTGGAAGCCAAGCGCGTCGCCGGCGACAGCAGGGACTACTGGACC 1356730
1356729 ACGGTTAGTGATCCACCAAAGTGCCTCCCTGACATTATCGAGTCATACGTCGGCGCTCTATTCATTGACT 1356660
1356659 CGGACTTCAACTATGCCGAAGTCCAGCGTTTCTTCGACATTCACATCCGCTGGTTCTTCGAAGACATGAA 1356590
1356589 GATCTACGATACATTCGCCAACAATCATCCATGTACGCACTTGCATAACATGCTGCAGACCACGTTCGGA 1356520
1356519 TGCACGGACTATCGGCTGATGGCCAAGGAGTTGCCGAGTGCAGATGGGTTGGAGAGGACGGACGTGGTTG 1356450
1356449 CGGTGGTCATGATCCATGACAAGATCGTGGCTCACAGTAGCGGGAAAAGTGGCAGATATGCTAGGCTTCG 1356380
1356379 TGTTGCAAACAGGGCACTTGCGGTGCTTGATGGACTTGCGCCGTTTGAGTATCGGGCGAGGTTCGAATGC 1356310
1356309 GAATGCAGGGTCGATGAGGAAGGACCGATGAAGATTCTGGAGGGACAGCCGCAGCATGGCGGTATGGTGG 1356240
1356239 ATTGTGCACCGGGTCTGTGCGACGTGTGAACAAGTCACGAGACTCATGAACGTATAATGGACAGAATGAG 1356170
1356169 ACAACACCACATCAGGCAGCGCGGCGACATGCTATCGCCTCGAGCCAAAAGCTACGCTCCCTGCGTTCTG 1356100
1356099 TATGCACGCCGCATGTCTGGAGCTGCAACATTGAACATATATCAAAAACCGAAGTGGTCGGCGGTCAGGA 1356030
1356029 GGTCCGTCAACAGCCCCAG 1356011

Figure A7.26. Nucleotide sequence of *DCL*, (dicer-like protein; Ds56023). Colour codes for sequences are shown as follows: Grey: Upstream or downstream padding. Red: coding region, **black:** intron, blue: untranslated region (UTR), green, yellow and blue highlight: qRT-PCR primers.

7.8.2 Quantitative Polymerase Chain Reaction (qPCR) melt curves and standard curves for relative and absolute quantification

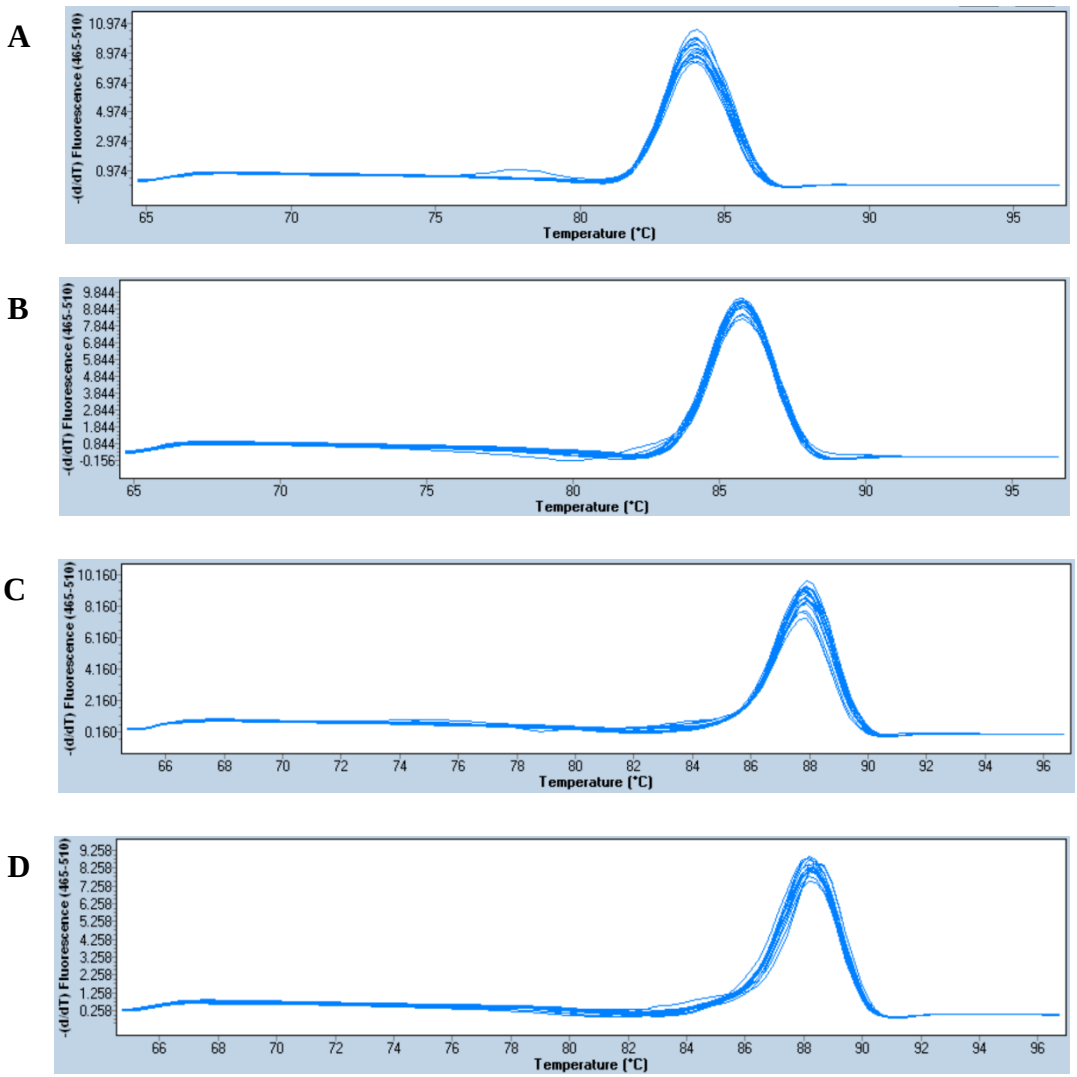

Figure A7.27. Melt curves for quantitative Reverse Transcription Polymerase Chain Reaction (qRT-PCR) gene expression analyses. Wildtype (WT) complementary DNA (cDNA) was used for A, C and D, and eGFP strain cDNA for B. (A) Dothistromin pathway regulatory gene (*DsAflR*). (B) Enhanced green fluorescent protein (*eGFP*). (C) Translation elongation factor 1 alpha (*DsTEF1α*). (D) Dicer-like protein (*DsDCL*). Single peaks were obtained for each gene showing that the primers are specific to their target sequence to be amplified. The melting temperatures for all genes (A–D) are approximately as follows: 84˚C, 86˚C, 88˚C and 88˚C.

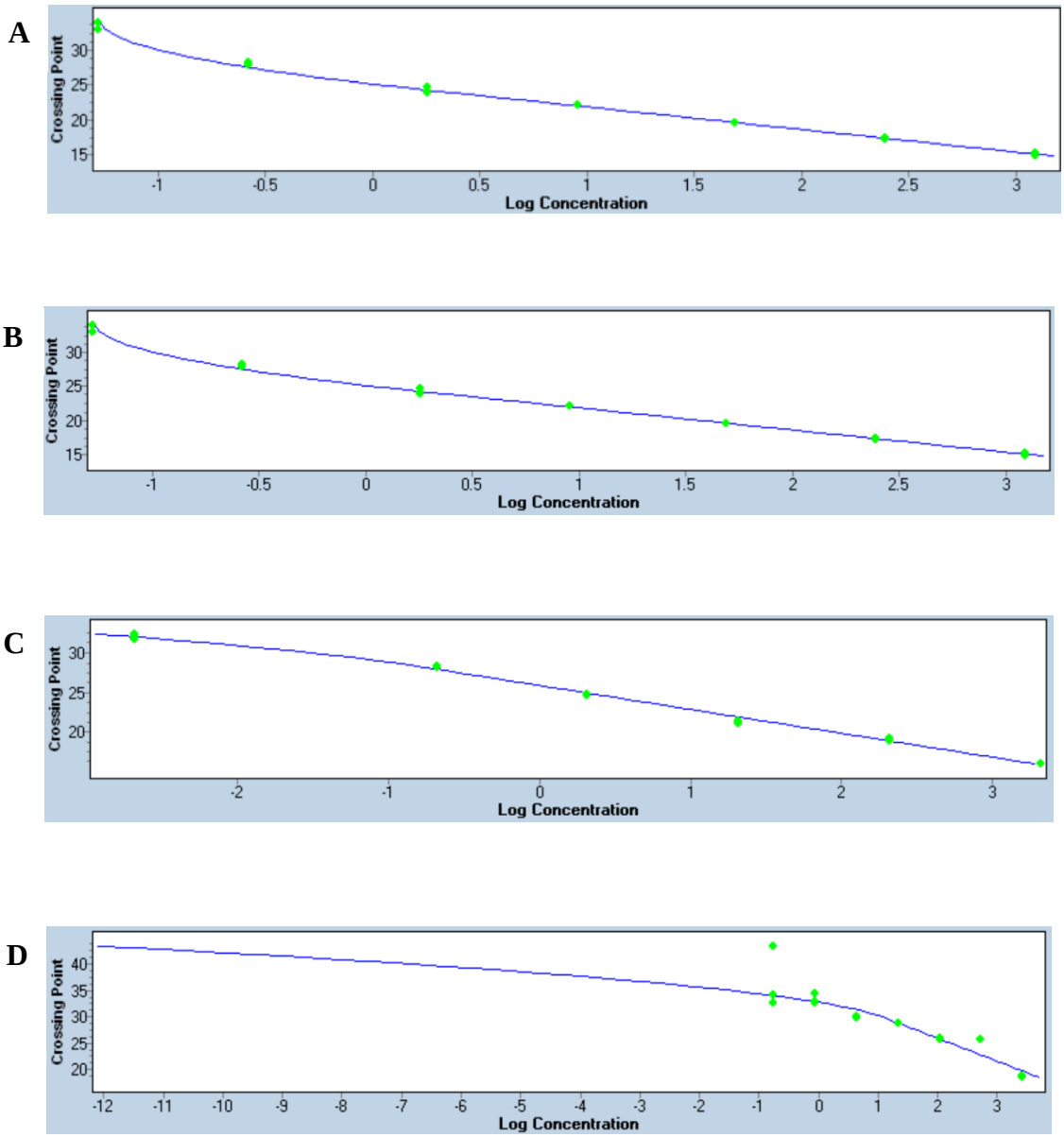

Figure A7.28. Quantitative Reverse Transcription Polymerase Chain Reaction (qRT-PCR) standard curves for *Dothistroma septosporum* target and reference genes for expression analyses. Wildtype (WT) complementary DNA (cDNA) was used for generating standard curves for A, C and D, and eGFP strain cDNA for B. (A) Dothistromin pathway regulatory gene (*DsAflR*). (B) Enhanced green fluorescent protein (*eGFP*). (C) Translation elongation factor 1 alpha (*DsTEF1α*). (D) Dicer-like protein (*DsDCL*).

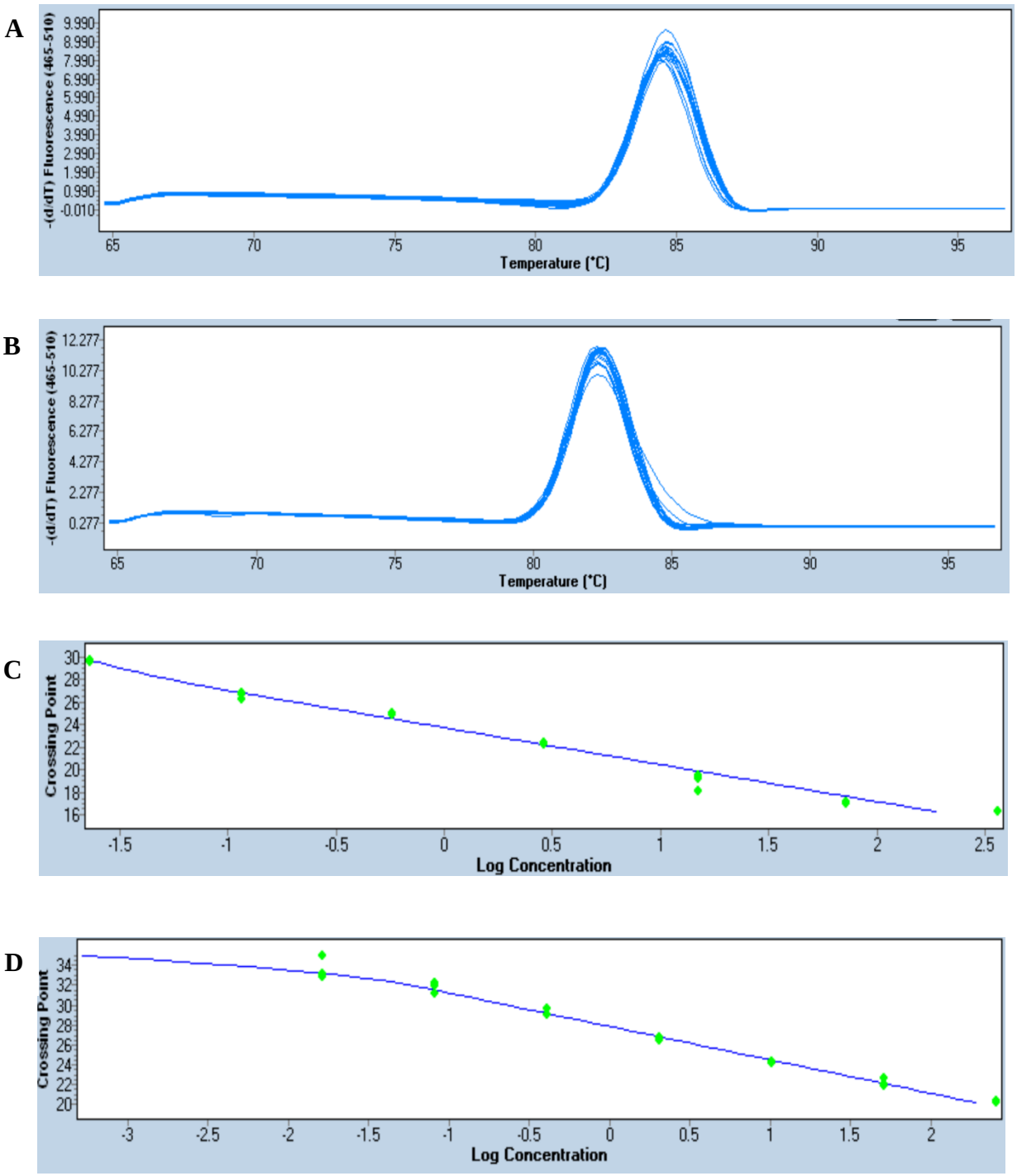

Figure A7.29. Quantitative Polymerase Chain Reaction (qPCR) melt curves and standard curves for biomass estimation for *Dothistroma septosporum* target and reference genes. Genomic DNA (gDNA) was used for generating standard curves. A-B are melting curves for each gene and C-D the standard curves. (A and C) *Dothistroma septosporum* polyketide synthase A (*DsPksA*). (B and D) *Pinus radiata* cinnamyl alcohol dehydrogenase (*CAD*). The melting peaks for *DsPksA* and *CAD* are as follows: 84.5˚C and 82.5˚C.

Table A7.9. Regression line equations, correlation coefficient and efficiency of genes for each standard curve.

	Standard curve (relative quantification)		
Gene	**Regression line[b]**	**R^2 [c]**	**Primer efficiency[d]**
DsTEF1α[a]	Y = -3.027x + 25.86	1.14 (114%)	2.140
DsAflR	Y = -3.198x + 33.22	1.054 (105.4%)	2.054
eGFP	Y = -3.240x + 25.10	1.035 (103.5%)	2.035
DsDCL	Y = -4.339x + 34.60	0.7 (70%)	1.700
	Standard curve (absolute quantification)		
DsPksA	Y = -3.267x + 23.73	1.023 (102.3%)	2.023
CAD	Y = -3.365x + 27.84	0.982 (98.2%)	1.982

[a]Reference gene used to normalise expression of the target genes. A standard curve was generated for a second housekeeping gene, beta-tubulin (*DsTub1*), but the primers were not efficient, therefore only one housekeeping gene was used as a reference for *in vitro* gene expression analyses.
[b]Regression line is the equation for the standard curve, which includes the slope and y-intercept.
[c]R^2 is the correlation coefficient obtained for the standard curve.
[d]Primer efficiency tells you how well the designed primers bind to the target sequence (i.e. whether they are specific) and whether they are efficient. The efficiency of primer pairs is calculated from the slope of the standard curve as: 10^(-1/slope)-1).
Primers are listed in Table 2.3.

A

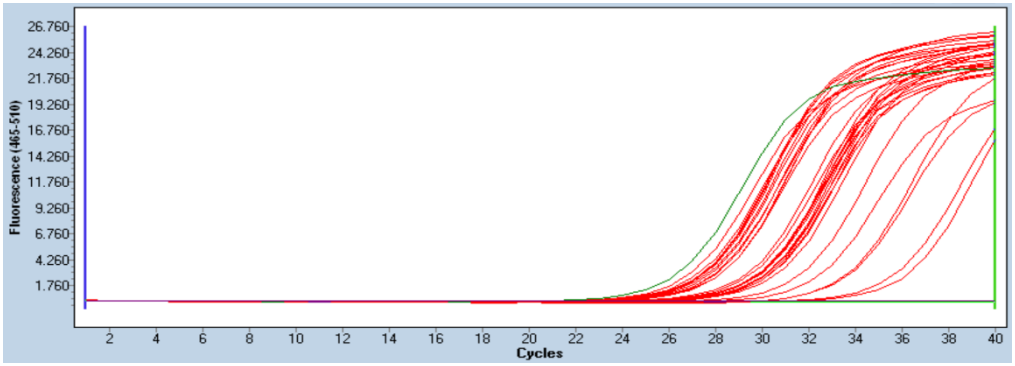

B

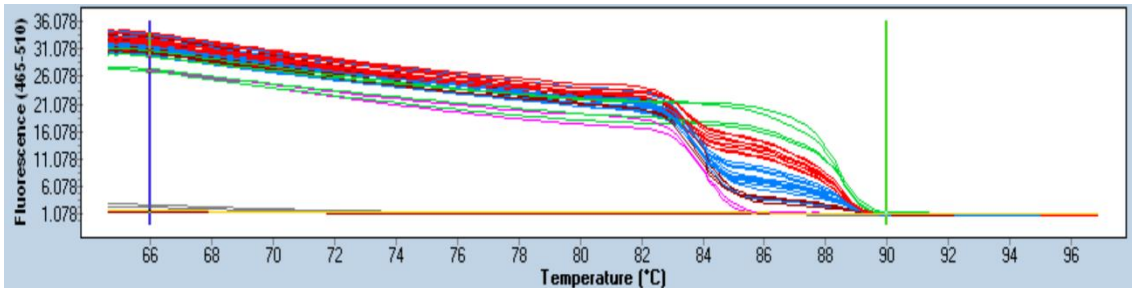

C

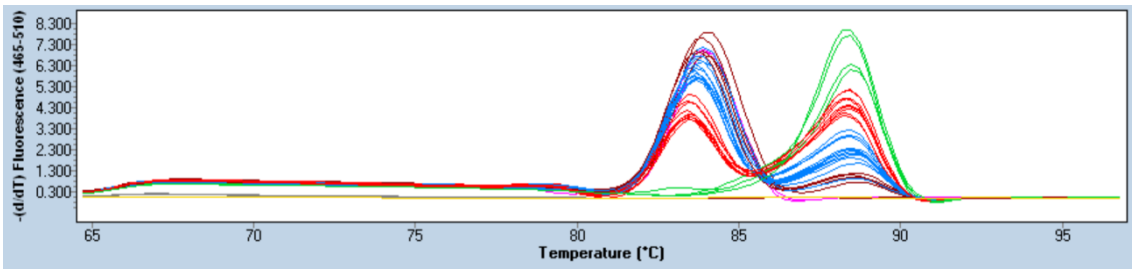

Figure A7.30. Quantitative Reverse Transcription Polymerase Chain Reaction (qRT-PCR) to examine gene expression of Dicer (*DCL*) in *Dothistroma septosporum* mycelium samples treated with dsRNA. (A) Amplification curve. Green line represents the positive calibrator control sample, which a known amount of complementary DNA (cDNA) was quantified using a standard curve assay. (B) Melting curve. (C) Melting peak. Multiple peaks can be seen, indicating there is non-specific amplification using following primers Dicer_F_exp1 and Dicer_R_exp1 (Table 2.3). The primers are not specific to the target sequence even though a primer efficiency of 1.7 (Table A7.9) was obtained, therefore additional primers would need to be designed and ordered for future gene expression analyses.

Table A7.10. Quantitative Reverse Transcription Polymerase Chain Reaction (qRT-PCR) results for *DCL* (dicer-like protein) gene expression analyses with *in vitro* dsRNA-treated *Dothistroma septosporum*.

Treatment	Sample type[a]	dsRNA (ng)[b]	Incubation (h)	Rep[d]	Ct Tar[e]	Ct Ref[f]	2^-ΔΔCt[g]
eGFP-dsRNA	12-well plate	500	72	1	26.62	10.90	0.15
				3	23.52	10.19	0.76
Water	12-well plate	-	72	1	23.55	10.34	1
				3	26.76	14.09	
eGFP-dsRNA	Agar plate	500	72	1	32.90	21.66	0.33
Water	Agar plate	-	72	1	32.44	22.79	1
DsAflR 1-dsRNA	12-well plate	500	72	1	28.91	15.39	0.82
				2	27.07	13.07	0.59
Water	12-well plate	-	72	2	24.60	9.860	1
				3	26.30	14.55	
DsAflR 1-dsRNA	Agar plate	500	72	1	26.67	15.05	0.21
Water	Agar plate	-	72	1	30.69	21.33	1
DsAflR 2-dsRNA	12-well plate	500	24	1	24.63	11.48	1.14
DsAflR 2-dsRNA	12-well plate	500	48	1	25.83	11.67	0.57
DsAflR 2-dsRNA	12-well plate	500	72	1	26.36	11.64	0.39
Water	12-well plate	500	24	1	24.51	10.55	1
			72	2	23.84	11.12	

[a]Sample type refers to the application method used for adding dsRNA. This was either in 12-well plates containing 1–3 mycelium plugs (3 mm^2, grown on DM agar) in each well or dsRNA directly added to the surface of mycelium plugs on DM agar plates.
[b]Amount of dsRNA used in either 2 mL of Potato Dextrose Broth (PDB) in 12-well plates or 5 µL aliquots (mixed with 0.03% SILWET L-77) onto mycelium on agar plates.
[c]Medium was either Dothistroma Medium (DM) or half-strength Potato Dextrose Agar (1/2 x PDA).
[d]Rep is the biological replicate number. Three biological replicates were carried out for each treatment but only two replicates were subjected to qRT-PCR due to lack of time.
[e]Cycle threshold (Ct) for amplification of the target gene (either enhanced green fluorescent protein (*eGFP*) or dothistromin pathway regulatory gene (*DsAflR*), shown as the average of two technical replicates.
[f]Ct for amplification of the reference gene translation elongation factor 1 alpha (*DsTEF1α*), shown as the average of two technical replicates.
[g]2^-ΔΔCt is the formula used to calculate the fold gene expression of target genes relative to reference gene translation elongation factor 1 alpha (*DsTEF1α*).

Evaluation of results: Most of the dsRNA-treated samples had lower *DCL* expression compared to the water controls, which had an expression value of 1.

Next steps: A qRT-PCR assay would need to be repeated with a set of primers that are specific for amplifying *DCL* that have an efficiency of higher than 1.7. The melt curve should give a single peak, indicating one product is amplified.

7.8.3 *In planta* infection assays

Figure A7.31. Example of an empty sampling jar with contaminants growing on the agar. Orange-brown colony growth is most likely *Dothistroma septosporum* growing on the LPch agar media, based on the secretion of dothistromin into the agar. The contaminants are the white fluffy colonies and/or black and grey colonies.

Table A7.11. Summary table of *Pinus radiata* needles inoculated with *Dothistroma septosporum* and treated with dsRNA.

	4.5 weeks incubation[a]				5.5 weeks incubation[a]			
# needles	**Water**	***eGFP*-dsRNA**	***DsAflR* 1-dsRNA**	***DsAflR* 2-dsRNA**	**Water**	***eGFP*-dsRNA**	***DsAflR* 1-dsRNA**	***DsAflR* 2-dsRNA**
Dead needles	44 ± 12.1	37 ± 14.1	46 ± 35.5	47 ± 7.6	60 ± 24.7	40 ± 6.0	5 ± 4.0	9 ± 4.7
Healthy needles	30 ± 12.0	85 ± 27.2	64 ± 35.8	59 ± 5.5	35 ± 9.2	31 ± 18.9	89 ± 49.5	120 ± 24.6
With lesions (non-eGFP)	75 ± 16.2	64 ± 16.1	59 ± 9.6	95 ± 20.1	95 ± 11.7	79 ± 16.8	52 ± 19.1	41 ± 13.7
With eGFP lesions (fluorescent)	39 ± 7.0	35 ± 8.9	34 ± 7.5	48 ± 6.4	29 ± 21.1	37 ± 21.8	19 ± 7.8	30 ± 7.9
Total needles[b]	144 ± 5.5	184 ± 34.4	157 ± 39.5	203 ± 17.4	159 ± 40.4	147 ± 19.7	160 ± 34.6	191 ± 27.0
% needles with eGFP lesions[b]	27 ± 5.3	19 ± 1.2	22 ± 1.7	24 ± 4.2	17 ± 8.4	24 ± 12.3	12 ± 3.6	16 ± 3.0

[a]Microshoots in glass jars containing LPch agar were sprayed with dsRNA (either enhanced green fluorescent protein (*eGFP*), dothistromin pathway regulatory gene (*DsAflR*) 1 or *DsAflR* 2) or water (control) and infected with *Dothistroma septosporum* spores as outlined in Chapter 2, section 2.12. Pine shoots were sampled at 4.5 (jars sealed immediately after spraying) and 5.5 weeks (jars air dried after spraying). The mean ± standard deviation of three biological replicates (shoots) are shown.

[b]Excludes completely dead and dried needles with no eGFP fluorescence but includes needles with lesions that did not appear to fluoresce (needles with non-eGFP lesions).

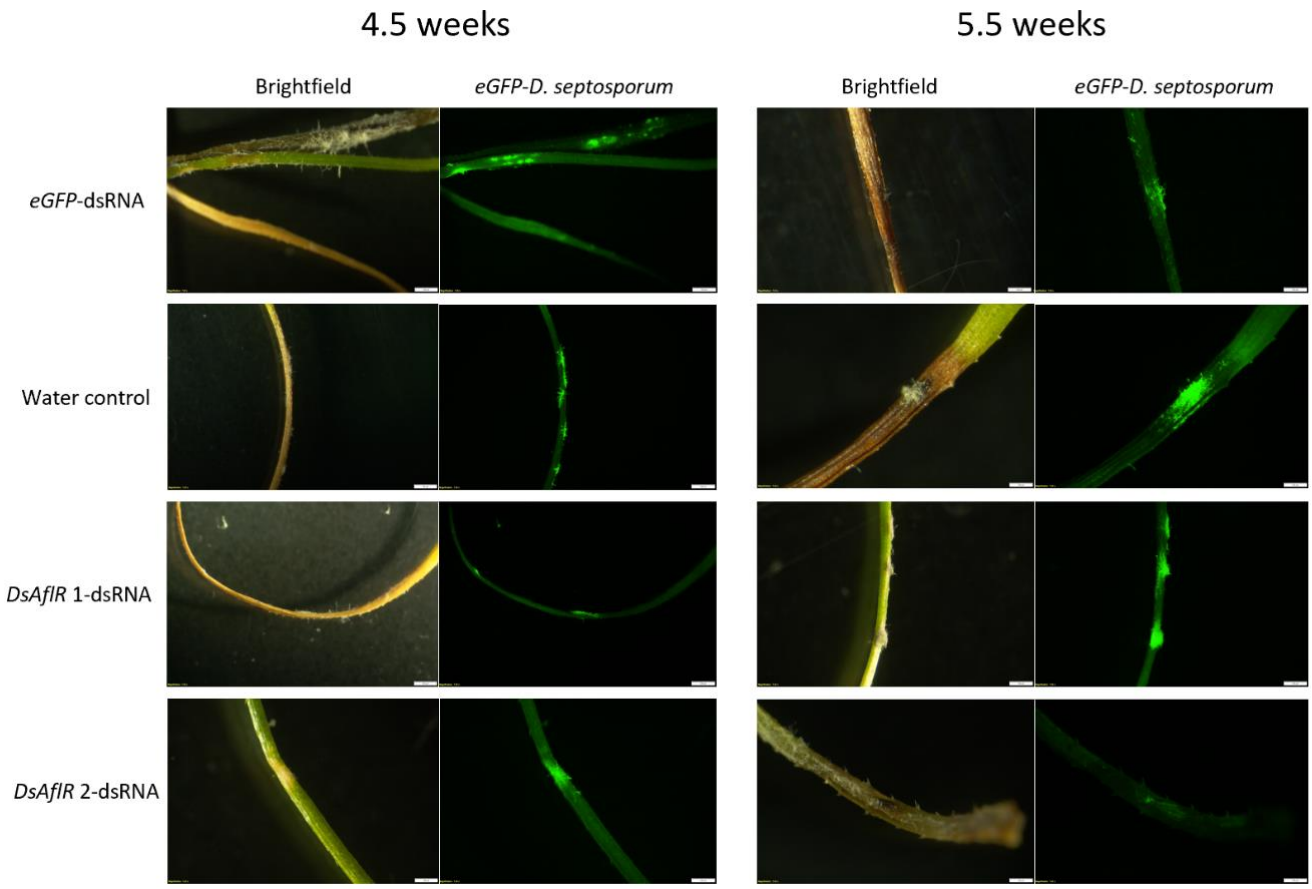

Figure A7.32. Growth of enhanced green fluorescent protein (eGFP)-labelled *Dothistroma septosporum* in *Pinus radiata* needles sprayed with dsRNA. Pine shoots were treated with either *eGFP*-dsRNA, dothistromin pathway regulatory gene (*DsAflR*) 1-dsRNA or *DsAflR* 2-dsRNA, or water (+0.03% SILWET-L77), and infected with *D. septosporum*. Images were captured at 4.5 and 5.5 weeks post-incubation. Growth of *D. septosporum* either in or on the needles can be seen by the GFP fluorescence. In some cases (e.g. eGFP at 4.5 weeks), there appears to be growth of a contaminating fungus (fluffy white-grey appearance) on the needle surface, which is probably a saprophyte. Scale bar is 100 µM.

Table A7.12. Quantitative Polymerase Chain Reaction (qPCR) results for biomass estimation in pine needles at 4.5 weeks post-inoculation.

Test #[a]	Treatment	Sample type[b]	Shoot #[c]	Rep[d]	Ct target (*PksA*)[e]	Ct ref (*CAD*)[f]	Target/Ref[g]
1	*eGFP*-dsRNA	N	2	1	-	-	-
				2			
2	*eGFP*-dsRNA	N	2	1	-	-	-
				2			
1	*eGFP*-dsRNA	N	5	1	-	-	-
				2			
2	*eGFP*-dsRNA	N	5	1	34.34	34.31	0.047
				2	33.56	33.87	0.061
1	*eGFP*-dsRNA	N	7	1	23.94	21.69	0.0128
				2	24.07	21.99	0.0144
2	*eGFP*-dsRNA	N	7	1	29.93	28.5	0.020
				2	29.52	28.27	0.023
1	*DsAflR* 1-dsRNA	N	2	1	-	-	-
				2			
2	*DsAflR* 1-dsRNA	N	2	1	32.5	32.06	0.037
				2	32.29	33.12	0.089
1	*DsAflR* 1-dsRNA	N	5	1	24.33	22.8	0.021
				2	24.62	22.9	0.018
2	*DsAflR* 1-dsRNA	N		1	30.97	32	0.105
			5	2	30.04	31.6	0.153
1	*DsAflR* 1-dsRNA	N	7	1	-	-	-
				2	24.71	32.39	11.276
2	*DsAflR* 1-dsRNA	N	7	1	32.42	33.49	0.105
				2	32.19	33.08	0.093
1	*DsAflR* 2-dsRNA	N	1	1	23.76	21.78	0.015
				2	23.73	21.83	0.016
2	*DsAflR* 2-dsRNA	N	1	1	-	-	-
				2			
1	*DsAflR* 2-dsRNA	N	4	1	-	-	-
				2			
2	*DsAflR* 2-dsRNA	N	4	1	-	-	-
				2			
1	*DsAflR* 2-dsRNA	N	7	1	-	-	-
				2			
2	*DsAflR* 2-dsRNA	N	7	1	-	34.12	0
				2	-	31.73	0
1	Water	N	2	1	22.01	21.46	0.043
				2	22.17	21.18	0.031
2	Water	N	2	1	-	-	-
				2			
1	Water	N	5	1	-	-	-
				2			
2	Water	N	5	1	-	-	-
				2			
1	Water	N	7	1	24.68	22.13	0.010
				2	24.61	22.48	0.014
2	Water	N	7	1	29.88	28.74	0.024
				2	29.22	28.37	0.030

[a]Tests 1 and 2 refer to the experiment number. Test 2 was a repeat of test 1 except the genomic DNA (gDNA) template had undergone an additional purification step (see Chapter 2, section 2.12).
[b]Sample type (N) indicates gDNA was extracted from needles with fluorescent lesions.
[c]Pine shoot number within each jar. gDNA was extracted from three biological replicates (i.e. three different shoots) for each treatment but not all replicates successfully amplified PCR products, as indicated by the dashes (-).
[d]Rep refers to the two technical replicates used for qPCR.
[e]Cycle threshold (Ct) for amplification of polyketide synthase A (*DsPksA*) and cinnamyl alcohol dehydrogenase (*CAD*) as in Table 5.3.
[g]Target/Ref is the ratio of the concentration of *DsPksA* (target gene) to *CAD* (reference gene), calculated from the regression equation.

Table A7.13. Quantitative Polymerase Chain Reaction (qPCR) results for biomass estimation in whole pine shoots at 4.5 weeks post-inoculation.

Test #[a]	Treatment	Sample Type[b]	Shoot #[c]	Rep[d]	Ct target (PksA)[e]	Ct ref (CAD)[f]	Target/Ref[g]
1	*eGFP*-dsRNA	S	1	1	-	-	-
				2			
2	*eGFP*-dsRNA	S	1	1	-	-	-
				2			
1	*eGFP*-dsRNA	S	4	1	-	-	-
				2			
2	*eGFP*-dsRNA	S	4	1	-	-	-
				2			
1	*eGFP*-dsRNA	S	6	1	-	-	-
				2			
2	*eGFP*-dsRNA	S	6	1	-	-	-
				2			
1	*DsAflR* 1-dsRNA	S	1	1	-	-	-
				2			
2	*DsAflR* 1-dsRNA	S	1	1	-	-	-
				2			
1	*DsAflR* 1-dsRNA	S	4	1	-	-	-
				2			
2	*DsAflR* 1-dsRNA	S	4	1	-	-	-
				2			
1	*DsAflR* 1-dsRNA	S	6	1	-	-	-
				2			
2	*DsAflR* 1-dsRNA	S	6	1	-	-	-
				2			
1	*DsAflR* 2-dsRNA	S	1	1	21.35	22.13	0.108
				2	21.06	21.97	0.118
2	*DsAflR* 2-dsRNA	S	1	1	23.6	24.89	0.146
				2	23.9	24.83	0.113
1	*DsAflR* 2-dsRNA	S	3	1	-	-	-
				2			
2	*DsAflR* 2-dsRNA	S	3	1	-	-	-
				2			
1	*DsAflR* 2-dsRNA	S	6	1	-	-	-
				2	26.45	24.48	0.015
2	*DsAflR* 2-dsRNA	S	6	1	28.01	26.35	0.018
				2	27.82	26.03	0.016
1	Water	S	1	1	23.2	21.85	0.024
				2	23.22	22.01	0.027
2	Water	S	1	1	24.92	24.17	0.035
				2	25.62	24.46	0.026
1	Water	S	3	1	23.61	22.08	0.021
				2	23.74	22.17	0.021
2	Water	S	3	1	26.9	25.22	0.018
				2	26.27	24.87	0.022
1	Water	S	6	1	20.88	21.09	0.074
				2	20.93	21.07	0.070
2	Water	S	6	1	24.18	24.89	0.097
				2	23.96	24.91	0.114

[a]Tests 1 and 2 refer to the experiment number. Test 2 was a repeat of test 1 except the genomic DNA (gDNA) template had undergone an additional purification step (see Chapter 2, section 2.12).

[b]Sample type (N) indicates gDNA was extracted from needles with fluorescent lesions.

[c]Pine shoot number within each jar. gDNA was extracted from three biological replicates (i.e. three different shoots) for each treatment but not all replicates successfully amplified PCR products, as indicated by the dashes (-).

[d]Rep refers to the two technical replicates used for qPCR.

[e]Cycle threshold (Ct) for amplification of polyketide synthase A (*DsPksA*) and cinnamyl alcohol dehydrogenase (*CAD*) as in Table 5.4.

[g]Target/Ref is the ratio of the concentration of *DsPksA* (target gene) to *CAD* (reference gene), calculated from the regression equation.